Title
Novel Methodologies for Site-selective Fluorine-18-Labeling of Thiol Containing Molecules via Chemoselective Cysteine Functionalization

Author
McDaniel, James Wells

Publication Date
2022

Peer reviewed|Thesis/dissertation

UNIVERSITY OF CALIFORNIA

Los Angeles

Novel Methodologies for Site-selective Fluorine-18-Labeling of Thiol Containing Molecules via Chemoselective Cysteine Functionalization

A dissertation submitted in partial satisfaction of the

requirements for the degree Doctor of Philosophy

in Chemistry

by

James Wells McDaniel

2022

ABSTRACT OF THE DISSERTATION

Novel Methodologies for Site-selective Fluorine-18-Labeling of Thiol Containing Molecules via Chemoselective Cysteine Functionalization

by

James Wells McDaniel

Doctor of Philosophy in Chemistry

University of California, Los Angeles, 2022

Professor Jennifer M. Murphy, Co-Chair

Professor Michael E. Jung, Co-Chair

This dissertation describes how modern organic chemistry can be used to improve the toolbox of fluorine-18 (^{18}F) labeled prosthetic groups for thiol radiolabeling. Herein, I report two new prosthetic groups (4-[^{18}F]fluorovinylsulfonyl benzene ([^{18}F]FVSB) and a [^{18}F]fluoroaryl gold(III) complex), their syntheses, scope, and stability.

Chapter One provides a popular science background for those currently outside of the synthetic chemistry and radiochemistry communities. This is meant to serve as a broad and brief overview of the work detailed in this dissertation while requiring little background knowledge.

Chapter Two provides a brief overview of positron emission tomography (PET) molecular imaging technology and why fluorine-18 is the radioisotope of choice for clinical applications. This chapter details a variety of radiofluorination methods to prepare ^{18}F-labeled arenes as well as a range of ^{18}F-labeled prosthetic groups and their respective reactivities.

Chapter Three discloses the development of [^{18}F]FVSB, an ^{18}F-labeled vinyl sulfone that is rapidly synthesized via an ^{18}F-deoxyfluorination method. This chapter details the broad scope of [^{18}F]FVSB to radiolabel free thiols in aqueous media while also demonstrating high stability of the ^{18}F-labeled bioconjugates, produced under a variety of conditions.

Chapter Four details the precise operations involved in the manual and fully-automated radiosynthesis of [^{18}F]FVSB and subsequent peptide labeling, including many minute specifics as well as troubleshooting advice for those who may use this method.

Chapter Five demonstrates the design and development of the first gold mediated ^{18}F-arylation reagent for thiol-containing substrates. The robust ^{18}F-gold complex is able to rapidly label free thiols in aqueous environments and furnish stable thioaryl bioconjugates.

The dissertation of James Wells McDaniel is approved

Alexander Michael Spokoyny

Yves F. Rubin

Michael E. Jung, Committee Co-Chair

Jennifer M. Murphy, Committee Co-Chair

University of California, Los Angeles

2022

DEDICATION PAGE

For every student who doesn't feel like they belong,

you make this community all the better.

I hope to be your accomplice.

TABLE OF CONTENTS

LIST OF FIGURES

LIST OF SCHEMES

CHAPTER 2: Introduction

LIST OF TABLES

[^{18}F]FVSB	4-[18F]fluorophenyl vinylsulfone
°C	degrees celsius
^{13}C NMR	carbon-13 nuclear magnetic resonance spectroscopy
18-c-6	1,4,7,10,13,16-hexaoxacyclooctadecane
^{18}F	fluorine-18
^{18}O(p,n)^{18}F	The nuclear reaction whereby oxygen-18 is bombarded with protons, emitting a neutron, to create fluorine-18.
^{19}F NMR	fluorine-19 nuclear magnetic resonance spectroscopy
^{1}H NMR	hydrogen-1 nuclear magnetic resonance spectroscopy
^{13}C-NMR	carbon-13 nuclear magnetic resonance spectroscopy
ABIDO	azadibenzocyclooctyne
Ac	acetyl, acetate
AcOH	acetic acid
aq.	aqueous
Ar	aryl
Boc	*tert*-butyloxycarbonyl
Bpin	pinacol borane
Bq	becquerel
br	broad
Bu	butyl
C	cysteine
cat.	catalytic

$CDCl_3$	deuterated chloroform
$CHCl_3$	chloroform
Ci	curie(s)
CpRu(COD)Cl	Chloro(pentamethylcyclopentadienyl)(cyclooctadiene)ruthenium (II)
CS_NAr	Concerted Nucleophilic Aromatic Substitution
Cu ^{18}F-AAC	copper catalyzed ^{18}F-alkyne-azide cycloaddition
CuAAC	copper catalyzed alkyne-azide cycloaddition
Cys	cysteine
D	aspartic acid
d	doublet
d.c.	decay corrected
DART	direct analysis in real time
DCM	dichloromethane
DFT	density functional theory
DI	deionized
DMF	dimethylformamide
DMSO	dimethylsulfoxide
DMSO-d_6	deuterated dimethylsulfoxide
DOTA	1,4,7,10-Tetraazacyclododecane-1,4,7,10-tetraacetic acid
e^-	Electron
EDG	Electron Donating Group
E_{max}	Maximum Energy

E_{mean}	Mean Energy
equiv	equivalent
ESI-HRMS	high resolution electrospray mass spectromety
Et	ethyl
et al.	et alia (and others)
EtOH	ethanol
EWG	Electron Withdrawing Group
F^-	cluoride
G	glycine
g	gram
g	gram(s)
GBq	gigabecquerel
h	hour(s)
hept	heptet
HPLC	High Pressure Liquid Chromatography
HRMS	high resolution mass spectrometry
i.e.	id est (namely)
IEX	Isotopic Exchange
J	coupling constant
K_{222}	Kryptofix 222
L	liter
LG	Leaving Group
m	multiplet

M	molar
m-	meta-
MA	Molar Activity
mCi	millicurie
Me	methyl
MeCN	acetonitrile
MeOH	methanol
MeV	megaelectron volts
MHz	megahertz
min(s)	minute(s)
mL	mililiter
mp	melting point
n.d.c.	non-decay corrected
NMP	1-Methyl-2-pyrrolidinone
NMR	nuclear magnetic resonance
o-	ortho-
p-	para-
PBS	phosphate buffered saline
PEG	polyethylene glycol
PET	Positron Emission Tomography
Ph	phenyl
pH	measure of acidity
q	quartet

R	arginine
RCP	Radiochemical Purity
RCY	Radiochemical Yield
rt	room temperature
s	singlet
SA	Specific Activity
SFB	N-succinimidyl 4-fluorobenzoate
S_N2	Nucleophilic Substitution Bimolecular
S_NAr	Nucleophilic Aromatic Substitution
t	triplet
TBAF	tetrabutyl ammonium fluoride
t-Bu	*tert*-butyl
TFA	trifluoroacetic acid
THF	tetrahydrofuran
TLC	Thin Layer Chromatography
UV	ultraviolet
α	alpha
β^+	positron
λ	wavelength
μCi	microcurie
μg	microgram
μmol	micromole

ACKNOWLEDGEMENTS

I would like to take some time to thank some of the people who have been helpful through the wild ride that has been the past 6 years. First, thank you to my advisor and mentor Prof. Jennifer Murphy. Your compassion has been endless, and I feel comfortable saying that I have tested it out beyond normal limits. Every depressive episode of mine was only met with kindness and care. When experiments would not work, you always had time to sit down and help troubleshoot. I can say without a doubt that I would not have been able to finish my degree without your aid.

Second, I want to thank my lab members, current and past: Dr. Maruthi Narayanam, Dr. Gaoyuan Ma, Dr. Raymond Gamache, and Mr. Baldwin Liwanag. Each and every one of you has helped me reach this point. Maruthi's interminable zen in the face of my failing experiments and double booked HPLCs. Gaoyuan's willingness to trade handling radioactivity for hours upon hours of HPLC runs. Ray's help in learning how to navigate my qualifying exam. And Baldwin's help in reminding me why I got into this field and this degree program. To each and every one of you, thank you dearly.

To Mr. Jeffrey Collins, thank you for producing what must be hundreds of Curies of activity for my experiments, for dealing with my endless desire to take apart anything broken, and for helping me better understand radiochemistry on a practical level.

I owe my deepest gratitude to Prof. Arlene Russel. Without her help I would have been homeless during the Summer of 2017, after my snap decision to leave my previous lab without even having a new lab to join. She pulled together her resources and was able to find me a last-minute TA appointment that kept me under a roof here in LA. Prof. Russel, truly and dearly thank you so much. Without that help, I would have had to leave UCLA and likely would have never been able to return.

Prof. Jennifer Casey. I don't even know what to say here. I will forever cherish the memory of a highly opinionated second year graduate student, who you had never even met with one-on-one, coming into your office and telling you that your worksheet was terrible and that he had ideas to fix it. You took me seriously despite my naivete, and that charity has been the foundation on which I've built my teaching philosophy, my ideals for education as a field, and our friendship. I hope that one day we'll get to work in the same department, raising Hell for anyone who won't listen and bringing those who will in and always learning and listening to those who do know better.

Dr. Morgan Howe. You have been my partner through the second half of graduate school. Certainly, no part of this process has been easy, but you've inspired me to better myself at every turn and made the terrible parts of this a little bit more tolerable. I'll always be glad that you wore a Games Done Quick shirt to TA meeting to give us a jumping off point for our relationship. Here's to all of the awkward stories of explaining that I am in a relationship with my TA, but we didn't really know each other for a few more years.

I also want to thank my family. I've certainly fallen off a rock for the last, oh…, ten years while I've made my way through my bachelor's and now my doctoral degree. Mom, Dad, Caitlin, Uncle Dick, Mary Jeanne, Suzi, and Pat, thank you all for your patience while I work myself half to death and I promise to call and visit more now that I'm done. (Though that certainly isn't a hard bar to reach.)

Finally, I want to thank everyone who has been my student or mentee, formally or informally, over the last six years. I cannot tell you enough how much inspiration and stability you've provided me. Thank you so much. I hope to make you half as proud of me as I am of all of you, and I hope to continue to make you proud going forward.

BIOGRAPHICAL SKETCH

Education

University of California, Los Angeles • *Los Angeles, CA* 6/2016 – present

Expected Doctor of Philosophy, Organic Chemistry: 9/2022
Candidate of Philosophy, Organic Chemistry: 9/2018
Thesis: Novel Methodologies for Site-selective ^{18}F-labeling of Thiol Containing Molecules via Chemoselective Cysteine Functionalization

University of Florida • *Gainesville, FL* 8/2012 – 5/2016

Bachelor of Science, Chemistry, with an emphasis in Biochemistry, and Zoology: 5/2016
Magna cum laude
Thesis: 4-hydroxyproline Ligations with C-Terminal Salicylicaldehyde

Research Experience

Organic Chemistry • Murphy Group • *UCLA* 7/2017 – present

Chemical Education • Casey Group • *UCLA* 12/2018 – 12/2019

Organic Chemistry • Harran Group • *UCLA* 7/2016 – 6/2017

Materials Chemistry • McElwee-White Group • *University of Florida* 8/2015 – 5/2016

Organic Chemistry • Young Group • *Baylor College of Medicine* 6/2015 – 7/2015

Organic Chemistry • Katritzky Group • *University of Florida* 1/2014 – 12/2014

Teaching Experience

Teaching Fellow • UCLA Department of Chemistry & Biochemistry 7/2016 – present

Awards and Honors

Hanson-Dow Excellence in Teaching Award 2019
The University of California, Los Angeles Summer Research Grant 2016

The Baylor college of Medicine Summer Medical and Research Training (SMART) Program	2015
The Cancer Prevention and Research Institute of Texas (CPRIT) Grant	2015
The University of Florida University Scholars Program Award	2015, 2016
The Howard Hughes Medical Institute Science for Life Undergraduate Intermural Scholarship	2014 – 2015

Peer-Reviewed Publications

1. Halder, R.; Ma, G.; **McDaniel, J.;** Murphy, J.; Neumann, C.; Ritter, T. "Deoxyfluorination of phenols for chemoselective ^{18}F-labeling of peptides." *Nat. Protoc.*, (*manuscript in preparation*)
2. **McDaniel, J. W**., Stauber, J. M., Doud, E. A., Spokoyny, A. M.[*], Murphy, J. M.[*] "An Organometallic Gold(III) Reagent for ^{18}F-Labeling of Unprotected Peptides and Sugars in Aqueous Media" (*Org. Lett.* **2022**, *accepted)*
3. Ma, G.[†], **McDaniel, J.W.**[†], Murphy, J. "One-Step Synthesis of [^{18}F]Fluoro-4-(vinylsulfonyl)benzene (FVSB): a Thiol Reactive Synthon for Selective Radiofluorination of Peptides" *Org. Lett.* **2021** *23* (2), 530-534. DOI: 10.1021/acs.orglett.0c04054
   [†]These authors contributed equally to this work.
4. Nsengiyumva, O., Hamedzadeh, S., **McDaniel, J.**, Macho, J., Simpson, G., Panda, S. S., Katritzky, A. R. "A Benzotriazole-Mediated Route to Protected Marine-Derived Hetero 2,5,-Diketopiperazines Containing Prolines" *Org. Biomol. Chem.*, **2014**, 4399-4403. DOI:10.1039/C5OB00023H

Public Presentations

1. "Development of [^{18}F]Fluoro-4-(vinylsulfonyl)benzene for chemoselective cysteine radiofunctionalization of peptides." eSRS Virtual 2021, May 2021 (*Oral*)
2. "Development of [^{18}F]Fluoro-4-(vinylsulfonyl)benzene for chemoselective cysteine radiofunctionalization of peptides." WMIC Virtual 2020, October 2020 (*Poster*)
3. "Relative Impact of Application-Based and Traditional Videos as Supplementary Resources in a General Chemistry Laboratory." 2020 Biennial Conference of Chemical Education at Oregon State University, July 2020. (*Poster*)
   [*]Because of the global COVID-19 pandemic, the 2020 Biennial Conference on Chemical Education was terminated on April 2, 2020, by the Executive Committee of the Division of Chemical Education, American Chemical Society; and, therefore, this presentation could not be given as intended.
4. "Novel Methodologies for the Site-selective ^{18}F-labeling of Peptides via Chemoselective Cysteine Functionalization." UCLA Molecular and Medical Pharmacology Annual Retreat, November 2019. (*Poster*)
5. "Site-selective ^{18}F-labeleing of proteins via Chemoselective Cysteine Arylation using Organometallic Gold(III) Reagents." UCLA Molecular and Medical Pharmacology Annual Retreat, November 2018. (*Poster*)
6. "Molecular Imaging Diagnostic Tool to Monitor IDO1 Expression *In Vivo*." UCLA Biomedical and Life Science Innovation Day, June 2018. (*Poster*)

CHAPTER 1: Popular Science Background

1.1. Positron Emission Tomography (PET) Imaging

Positron Emission Tomography (PET) imaging is a full-body molecular imaging technology that physicians use to visualize specific tissues within the human body, generally cancers, for diagnostic purposes. PET imaging works by injecting a radioisotope (called PET tracer) which undergoes decay through the release of a positron (β^+), essentially the positive equivalent of an electron, into the body. When a β^+ combines with an electron, two high energy rays (γ rays) are created (***Figure 1.1***).

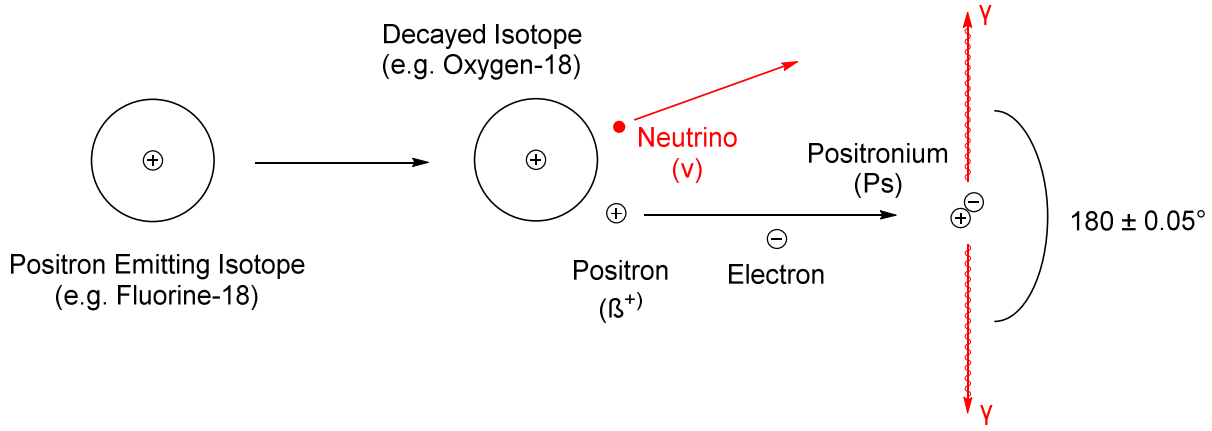

Figure 1.1. Schematic of a positron annihilation.

The signals from the PET tracer can be detected using a specialized PET scanner which allow scientists to determine the location of the PET tracer in the body (***Figure 1.2***). Because these PET tracers are designed to preferentially accumulate in specific tissues, generally cancerous tissues, doctors can identify where the cancer is located within the body.

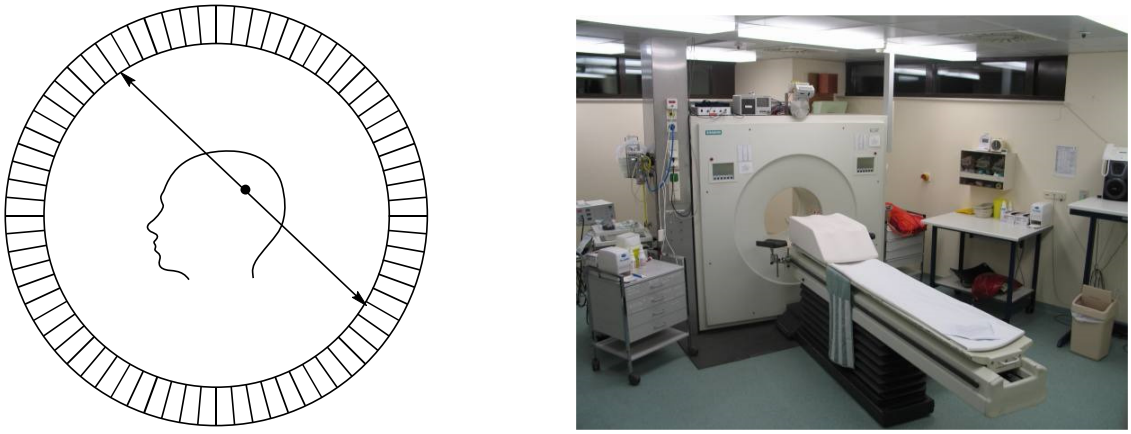

Figure 1.2. Cartoon of a PET imaging detector array (left) and a picture of a clinical PET imaging detector.[1]

1.2. On Fluorine-18

Fluorine-18 is an example of a β^+ emitting isotope. This isotope can be created by bombarding heavy water ($[^{18}O]H_2O$) with protons. This bombardment replaces a neutron with a proton, converting the oxygen atom to a fluorine without changing the mass of the atom, thus creating fluorine-18.

Fluorine-18 is the isotope of choice for PET imaging because of four main properties: 1) it is readily available to research laboratories and hospitals, 2) it almost exclusively undergoes β^+ decay, 3) it has a "Goldilocks" half-life, and 4) the β^+ it emits are *relatively* low energy. Fluorine-18 is produced world-wide at various facilities using a particle accelerator called a cyclotron. This is instrument is responsible for the aforementioned proton bombardment and can be installed in a variety of facilities (UCLA has four cyclotrons). This allows for the on-site radiosynthesis; for facilities which don't have a cyclotron, large quantities of fluorine-18 can be generated offsite and delivered. Because fluorine-18 almost exclusively undergoes β^+ decay, the maximum amount of signal is generated with the minimal amount of radiation exposure to the patient. With a half-life

of ~110 mins, this limits the radiation exposure to the patient (after 24 hours there is essentially no exposure as all of the fluorine-18 has decayed) while still being able to synthesize the PET tracer. For example, the most commonly used PET tracer, [^{18}F]fluorodeoxyglucose ([^{18}F]FDG) (**1.2**), (***Figure 1.3***) can be synthesized in two hours, which means that about half of the initial fluorine-18 will have decayed! Finally, because fluorine-18 emits low energy β^+, the signal cannot travel far through the body which would complicate localizing the PET tracer.

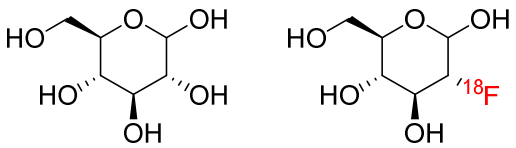

1.1 **1.2**

Figure 1.3. A comparison of glucose (left, **1.1**) and [^{18}F]fluorodeoxyglucose (right, **1.2**).

1.3. Radiofluorination Methods

Because fluorine-18, even when generated in large quantities is still only in the nanomolar amount (10^{-9} m) which is 1,000,000 times less abundant that typical small-scale chemistry which is in millimolar amounts (10^{-3} m), special methods must be developed in order to create fluorine-18 PET tracers. Two of these methods are nucleophilic aromatic substitution (S_NAr) and deoxyfluorination (***Figure 1.4***).

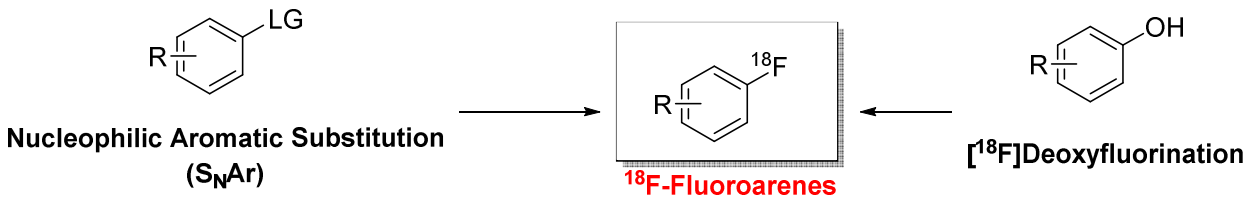

Figure 1.4. Simplified radiofluorination methods with their associated sections in this thesis.

S_NAr can be used to radiofluorinate aromatic rings that are electron deficient. Electron deficiency is needed to stabilize the negative charge created as the [^{18}F]fluoride binds to the ring. Because of this requirement, specialize leaving groups (e.g. iodonium ylides) have been developed to facilitate this transformation, thus mitigating the effects of [^{18}F]fluoride's low concentration. For example, [^{18}F]flortaucipir (**1.5**), a PET tracer used to diagnose and stage Alzheimer's disease, is synthesized using this method (***Figure 1.5***).[2]

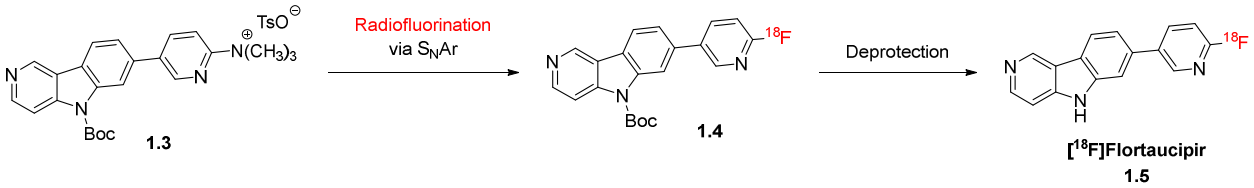

Figure 1.5. The synthesis of [^{18}F]Flortaucipir via S_NAr.

^{18}F-Deoxyfluorination follows a different pathway that allows it to be used to radiofluorinate electron neutral and rich aromatic rings. In this process, a hydroxyl group is replaced with a fluorine-18; however, it does not proceed through the same intermediate as S_NAr. In this reaction a negative charge is not generated on the aromatic ring; as such, ^{18}F-deoxyfluorination can radiofluorinate aromatic rings for which the S_NAr approach would fail. This method was used to synthesize [^{18}F]FPEB (**1.7**). While this compound itself does not preferentially accumulate in a tissue of interest, it can be used to label a biologically relevant molecule with an additional reaction (***Figure 1.6***). Because this method is relatively new (circa 2020), it has not yet had time to be utilized for the development of a PET tracer which has been used in humans.[3, 4]

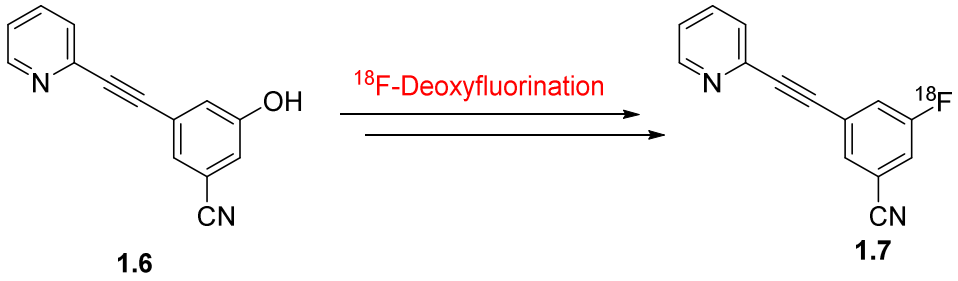

Figure 1.6. The synthesis of [^{18}F]FPEB via ^{18}F-deoxyfluorination

1.4. Labeling Sensitive Molecules

Radiofluorination reactions are harsh and generally incompatible with the biological molecules to be developed into useable PET tracers. The biomolecule is the targeting entity that is responsible for accumulation of the PET tracer in cancerous tissues; without a biomolecule the [^{18}F]fluoride accumulates in bone rather than tissue. The high heat (>100 °C) and organic solvents used in fluorine-18 chemical reactions often cause molecules to decompose. To circumvent this issue, prosthetic groups have been created which can stand up to these harsh reaction conditions and enable the biomolecule of interest to be labeled with fluorine-18 under much milder conditions. Thiols serve as a convenient functional handle to attach these prosthetic groups to (***Figure 1.7***). Because they are relatively rare and have a unique reactivity profile, a single thiol can be selectively labeled without incindentally labeled other reactive groups (like amines and alcohols). This prevents multiple ^{18}F-prosthetic groups from adding to the same biomolecule, generating more molecules of the PET tracer which gives a better signal during PET imaging.

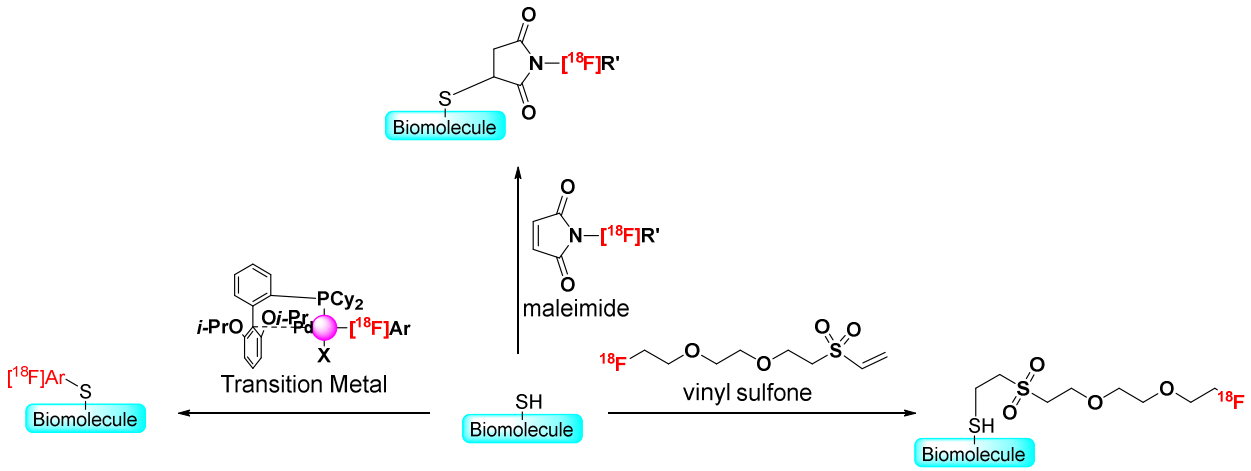

Figure 1.7. Selected examples of thiol-reactive prosthetic groups.

Maleimides are the current gold standard of thiol selective ^{18}F-prosthetic groups. Here the thiol is able to add to the double bond to create a stable covalent bond. A common example of a ^{18}F-maleimide is [^{18}F]FBEM (**1.8**) which has been used to label a variety of thiol containing molecules (***Figure 1.8***). Unfortunately, maleimides are not without limitations. The newly formed thioether linkage can be eliminated from the molecule regenerating the starting materials under physiological conditions; this is made easier by the geometry of the ring. Because of this limitation, alternative ^{18}F-prosthetic groups that are less susceptible to elimination have been created.

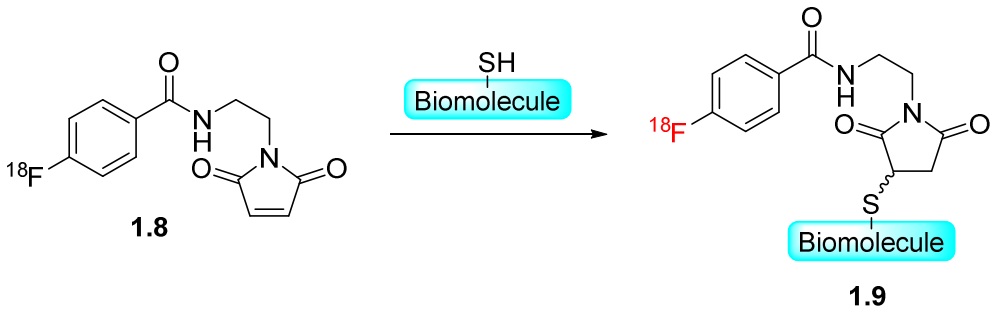

Figure 1.8. Cartoon of [^{18}F]FBEM (**1.8**) thiol labeling.

Unlike ^{18}F-maleimides, ^{18}F-vinyl sulfones are linear and can freely rotate around the new carbon-sulfur bond (***Figure 1.9***). This free rotation slows the elimination process and makes vinyl sulfones comparatively, more stable. At the time of writing, ^{18}F-vinyl sulfones have rarely been used for medical imaging due to the poor yields associated with this chemistry.

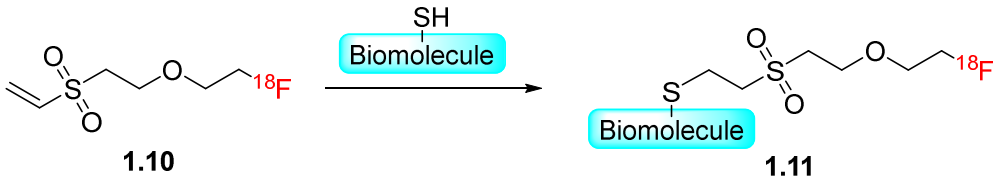

Figure 1.9. Cartoon of ^{18}F-vinyl sulfone thiol labeling.

Another chemical method is ^{18}F-transition-metal mediated arylations. In this case, the carbon-sulfur bond is formed directly between the sulfur atom and the atom of an aromatic ring. These bonds are extremely stable and have not been shown to undergo an elimination process under physiological conditions. The covalent bond between the ^{18}F-aromatic ring and the thiol is created through the use of an ^{18}F-metal complex. Without the ^{18}F-metal complex, this type of covalent bond would be exceptionally difficult to form. At the time of writing, only one such prosthetic group has been reported (***Figure 1.10***); however, this reagent gives poor yields as well.

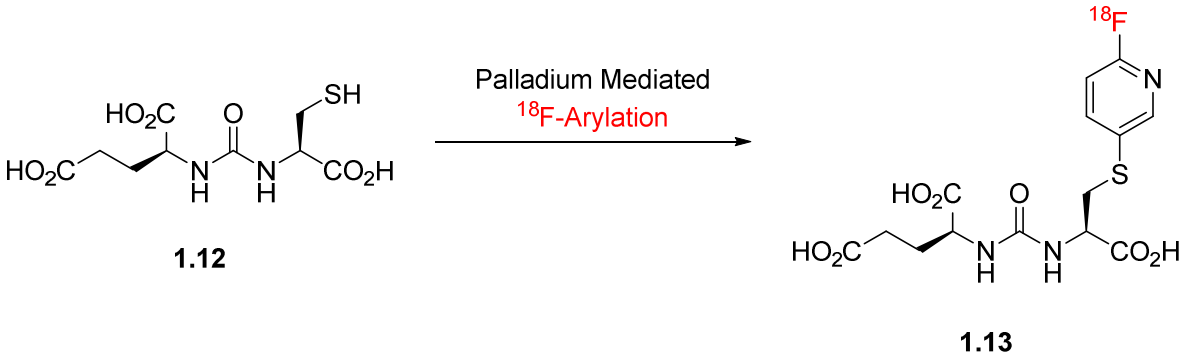

Figure 1.10. An example of palladium mediated ^{18}F-thioarylation.

This dissertation describes the development of a new ^{18}F-vinyl sulfone (4-[^{18}F]fluorovinylsulfonyl benzene ([^{18}F]FVSB)) and a first-in-class ^{18}F-gold complex ([^{18}F]Au(III) complex) that allow for ^{18}F-fluoroarylation, adding to the toolbox of ^{18}F-prosthetic groups for thiol selective labeling (***Figure 1.11***).[5]

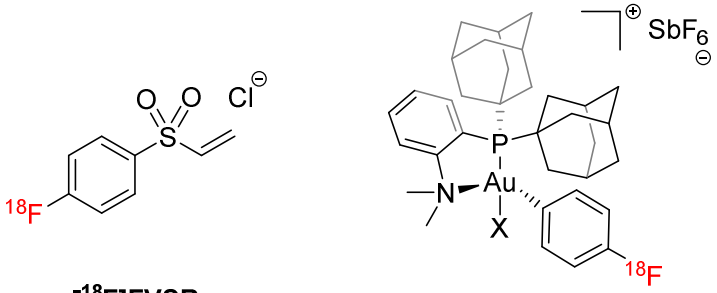

[^{18}F]FVSB
Chapters 3 – 4

[^{18}F]Au(III) Complex
Chapter 5

Figure 1.11. Thiol selective ^{18}F-prothestic groups discussed in this thesis with their associated chapters.

1.5. Notes and References

The citations of this section have been limited for the sake of clarity. For full citations, please see **Chapter 2: Introduction.**

1. Maus, J. This image shows a picture taken from a typical PET facility equipped with an ECAT Exact HR+ PET scanner. PET scanners such as this are steadily being replaced by systems that combine both PET and CT scanners into a single PET/CT imaging device. (accessed 6/3/20222).

2. Jiang, H.; Jain, M. K.; Cai, H., Automated production of [(18)F]Flortaucipir for PET imaging of tauopathies. *Am J Nucl Med Mol Imaging* **2021,** *11* (3), 167-177.

3. Tay, N. E. S.; Chen, W.; Levens, A.; Pistritto, V. A.; Huang, Z.; Wu, Z.; Li, Z.; Nicewicz, D. A., 19F- and 18F-arene deoxyfluorination via organic photoredox-catalysed polarity-reversed nucleophilic aromatic substitution. *Nature Catalysis* **2020,** *3* (9), 734-742.

4. Neumann, C. N.; Hooker, J. M.; Ritter, T., Concerted nucleophilic aromatic substitution with 19F− and 18F−. *Nature* **2016,** *534* (7607), 369-373.

5. Humpert, S.; Omrane, M. A.; Urusova, E. A.; Gremer, L.; Willbold, D.; Endepols, H.; Krasikova, R. N.; Neumaier, B.; Zlatopolskiy, B. D., Rapid 18F-labeling via Pd-catalyzed S-arylation in aqueous medium. *Chemical Communications* **2021,** *57* (29), 3547-3550.

CHAPTER 2: Introduction

2.1. Abstract

An overview of positron emission tomography (PET), a molecular imaging technology, is described. While a variety of radioisotopes are amenable for PET imaging use, fluorine-18 currently stands as the isotope of choice due to its physical properties. With the desire to develop new, facile, and robust PET tracers, a wide range of radiofluorination methods have been developed as well as `^{18}F-prosthetic groups that allow sensitive molecules to be rapidly labeled. This chapter provides a non-exhaustive review of these technologies and methodologies.

2.2. Positron Emission Tomography (PET) Molecular Imaging

The ability to visualize, noninvasively, a patient's homeostasis in a whole-body setting is a relatively recent advent in the larger history of medicine.[1] Many different methods of medical imaging have been developed: magnetic resonance, X-ray, computed tomography, positron emission tomography (PET) imaging, etc. In particular, PET molecular imaging with its high sensitivity provides some of the most detailed images of the internal biochemical processes within patients.[1-4]

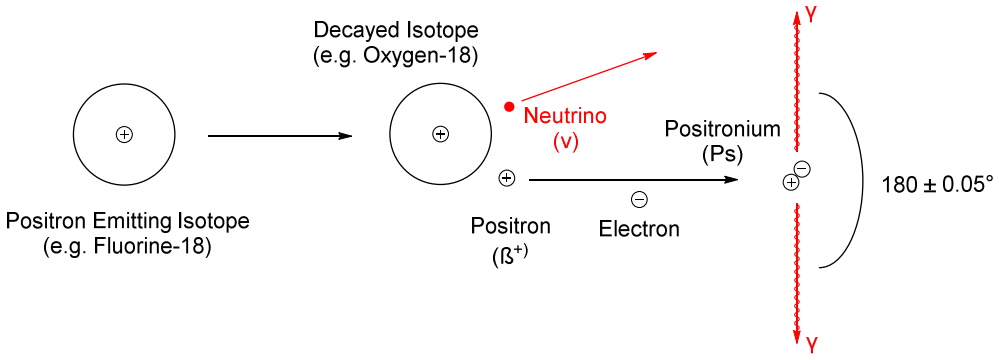

Figure 2.1. Schematic of a positron annihilation.

PET imaging works by injecting a positron (β^+) emitting isotope as part of a relevant targeting construct (e.g. peptide, protein, sugar), called a PET tracer, which will preferentially accumulate in the tissue(s) of interest and consequently reveal the location of the tracer in the body.[2, 4, 5] As the radioisotope undergoes nuclear decay, it emits a positron (β^+) which combines with a nearby electron (e^-) to create a positronium— a highly unstable subatomic particle which undergoes an annihilation event emitting two gamma rays 180° apart (***Figure 2.1***).[2, 4, 5] The two gamma rays are detected in a PET scanner via an enclosed circle of individual detectors with the patient in the center (***Figure 2.2***).[4, 6] The small difference in distance traveled leads to a small difference in the time it takes for the gamma rays to hit their respective detectors.[4, 6] This difference in time is used to calculate the position of the positron/electron annihilation event, thereby determining the location of the PET tracer within the body.[4, 6]

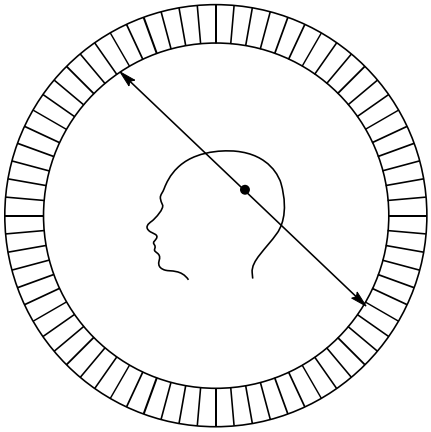

Figure 2.2. Cartoon of a PET imaging detector array.

With the unique properties of this imaging modality, it can be used to perform *in vivo* diagnostics and staging for a variety of diseases, in particular cancers, as well as pharmacokinetic

studies to investigate new drugs.[1, 2, 4, 7] However, before PET imaging can be done, an appropriate radioisotope must be selected.

2.3. Radioisotopes for PET Tracers

A wide range of radioisotopes undergo β^+ decay, but not all of them are ideally suited for PET imaging. An ideal PET radioisotope has four key properties: 1) it is a pure positron emitter, 2) it has a 'Goldilocks' length half-life, 3) the positrons that it emits have low energy, and 4) it is easily available in reasonably large quantities.[3] Pure positron emitters are ideal because they provide the maximum amount of signal per amount of radiation injected and reduce the need for post-processing algorithms for radioisotopes that incidentally release gamma radiation.[4] A 'Goldilocks' half-life is ideal, meaning a half-life which is neither too long that it causes unnecessary radiation exposure to the patient nor too short that it is impractical to chemically manipulate for tracer development and production.[3] A radioisotope with low energy β^+ decay is desirable because the lower energy positrons are less able to travel through space within the patient before combining with an electron, ultimately undergoing annihilation to emit the gamma rays.[8-10] Finally, the radioisotope must be easily available in reasonably large quantities for logistical reasons.[3]

While a wide range of radioisotopes meet these requirements (***Table 2.1***), fluorine-18 is currently preferred among other radioisotopes for clinical PET imaging applications with its half-life of ~110 min, high percentage of β^+ emission (96.9%) and relatively low energy of its emitted positron (E_{max} = 0.634 MeV and E_{mean} = 0.250 MeV).[1-4, 11-13] In addition, nucleophilic fluorine-18 ($[^{18}F]F^-$) can be easily generated on site, through the use of a cyclotron via the $^{18}O(p,n)^{18}F$ nuclear

reaction of [^{18}O]H_2O, providing reliable access to a high radioactivity [^{18}F]fluoride source with a molar activity of up to 4,000 GBq/μmol.[14]

Table 2.1. Properties of radioisotopes used for PET imaging.

Isotope	Half-life	Branching (β^+) in %	E_{max} (MeV)
^{11}C	20.4 min	99.8	0.960
^{13}N	10.0 min	99.8	1.199
^{15}O	2 min	99.9	1.732
^{18}F	**109.7 min**	**96.9**	**0.634**
^{64}Cu	12.7 h	17.5	0.653
^{89}Zr	78.4 h	22.7	0.902
^{68}Ga	67.8 min	87.8, 1.2	1.899, 0.821
^{76}Br	16.2 h	25.8, 6.3	3.382, 0.871
^{82}Rb	1.3 min	81.8, 13.1	3.378, 2.601
^{86}Y	14.7 h	11.9, 5.6	1.221, 1.545
^{124}I	100.2 h	11.7, 10.7	1.535, 2.138

Molar activity (MA), formerly specific activity (SA), is a measure of the ratio between the number of fluorine-18 atoms to the total radiotracer mass in a given sample.[15, 16] In general, high molar activities are required to get high quality PET images. Both ^{19}F- and ^{18}F-functionalized tracers are able to bind to the target yet only the ^{18}F-labeled tracer emits a β^+; therefore, image quality will be reduced if the ^{19}F-tracer occupies the target without providing a positron emitting signal.

While electrophilic ^{18}F-fluorination methods do exist, the presence of carrier added fluorine gas leads to low molar activity electrophilic fluorine-18 sources, namely [^{18}F]F_2, significantly reducing their utility and value in PET tracer development.[14, 16-20] Therefore, electrophilic ^{18}F-fluorination will not be covered in this dissertation.

2.4. Modern Fluorine-18 Chemical Methods to form ^{18}F-Arenes

Modern methods for nucleophilic fluorine-18 incorporation can broadly be separated into two categories: alkyl ^{18}F-fluorination and aryl ^{18}F-fluorination.[11] While alkyl ^{18}F-fluorinations are chemically easier to access through straightforward S_N2 chemistry,[11, 21-23] aryl ^{18}F-fluorinations are preferred as ^{18}F-C(sp^2) are less prone to undergo elimination than their ^{18}F-C(sp^3) counterparts.[11, 14] Additionally, ^{18}F-C(sp^2) bonds have shown greater metabolic stability *in vivo*.[2, 24-26] This stability has garnered intense focus for the development of synthetic methods to install fluorine-18 onto aryl groups (***Figure 2.3***).[14, 27, 28]

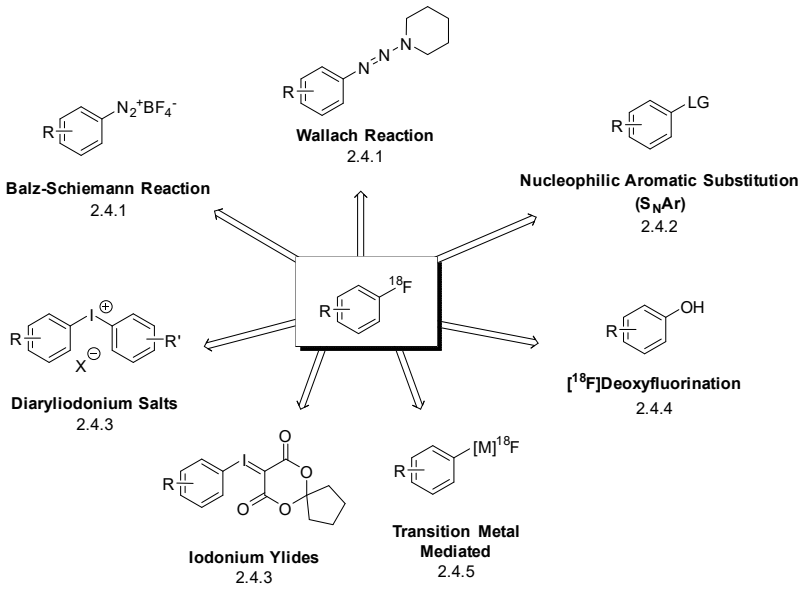

Figure 2.3. Methods for nucleophilic ^{18}F-fluorination with their associated sections.

2.4.1. The Balz-Schiemann and Wallach Reactions

Some of the earliest reports of ^{18}F-fluorination of electron-rich or -neutral arenes utilized Balz-Schiemann chemistry[29] which proceeds via the fluoro-dediazotization of aryldiazonium [^{18}F]tetrafluoroboronates.[30] As each of the four fluorine atoms of the [^{18}F]tetrafluoroboronate have

an equal probability of undergoing the fluoro-dediazotization, the theoretical maximum radiochemical yield (RCY) is limited to 25%. As such, ^{18}F-fluorination via this process results in poor RCYs and low molar activities of the desired [^{18}F]fluoroarene (***Scheme 2.1***).

Scheme 2.1. Radiosynthesis of [^{18}F]fluoroarenes by thermal fluoro-dediazotization.

Despite this limitation, this methodology has been used to label aromatic amino acids[31] such as racemic 3- and 4-[^{18}F]fluorophenylalanine,[32-34] 5- and 6-[^{18}F]fluorotryptophan,[35] and the clinical imaging agent [^{18}F]F-DOPA as both a single enantiomer (24% RCY after chiral HPLC separation) and a racemic mixture (***Scheme 2.2***).[36]

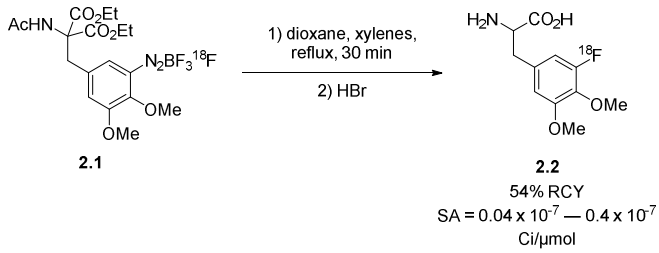

Scheme 2.2. Radiosynthesis of a protected racemic [^{18}F]F-DOPA by fluorodediazotization.

To avoid the possible danger inherent to working with diazo compounds, the Wallach reaction is an alternative method to generate *in situ* aryl diazo compounds from triazines (***Scheme 2.3***).[36-40] With the removal of the [^{18}F]tetrafluoroboronate, the Wallach reaction has been used to synthesize haloperidol (**2.5**) in sufficient MA for use in human PET imaging studies (***Scheme 2.4***).[41]

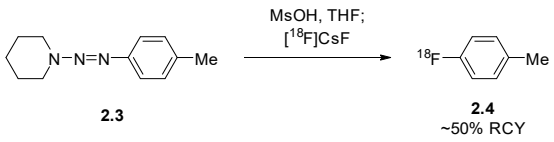

Scheme 2.3. Thermal decomposition of 1-aryl-3,3-dialkyltriazenes for ^{18}F-fluorination.

Both the Balz-Schiemann and Wallach methodologies have not seen wide adoption among the larger fluorine-18 radiochemistry community with the development of more stable and better yielding functional groups amenable to *ipso* ^{18}F-fluorination.[14]

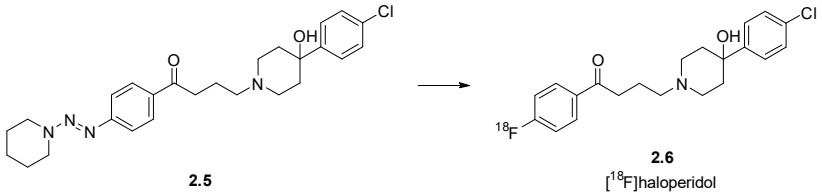

Scheme 2.4. [^{18}F]Haloperidol and its Wallach precursor.

2.4.2. Nucleophilic Aromatic Substitution (S_NAr)

Nucleophilic aromatic substitution (S_NAr) currently stands as the gold standard of radiofluorination.[14] This method is only accessible when a sufficiently electron withdrawing group is present either *ortho*- or *para*- to the leaving group on the arene; the electron withdrawing group is necessary to stabilize the negative charge of the Meisenheimer complex intermediate (***Figure 2.4***).[14, 42] Due to the strict limitation on the scope of arenes amenable to S_NAr, many complex arenes are not suitable for this type of transformation.

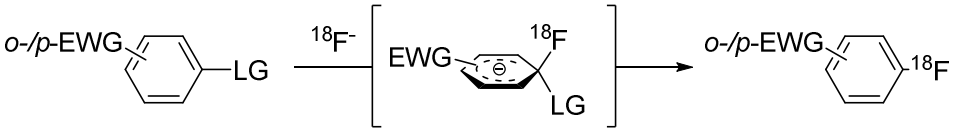

Figure 2.4. General reaction pathway for a radiofluorination via S_NAr.

When designing precursors for S_NAr it is important to consider the electronic properties of both the leaving group as well as the electron withdrawing group. For the leaving group, RCY follows the trend *p*-NO_2 > *p*-CF_3 ≈ *p*-CN > *p*-CHO > *p*-Ac > *m*-NO_2; while for electron withdrawing groups, the trend is -NO_2 ≈ -CHO > -CN ≈ COPh > CO_2Me.[14] It is of note that halides and simple H atoms are incompatible with radiofluorination S_NAr (***Table 2.2***).[14] In cases where suboptimal groups must be used, microwave radiation can be used to increase the RCY (***Table 2.3***).[14, 43]

Table 2.2. Electron Effects in Fluorodeamination Reaction of Trimethylanilinium Triflates

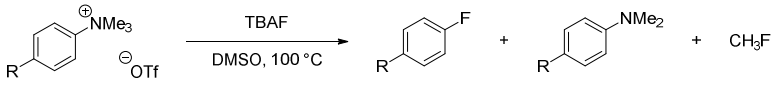

–R	Reaction Time (min)	ArF:CH3F
NO_2	1	>99:1
CHO	1	>99:1
CN	1	99:1
COPh	1	99:1
CO_2Me	2	96:4
Br	10	2:98
H	10	<1:99
Me	10	<1:99
OMe	30	<1:99

Table 2.3. Radiosynthesis of *meta*-Substituted [^{18}F]Fluoroarenes via S_NAr

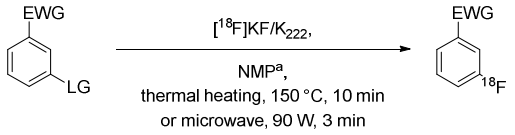

EWG	LG	RCY %	
		Thermal	Microwave
NO_2	NO_2	21	47
CN	NO_2	20	56
Br	F	9	19
Br	NMe_3I	3	17
CF_3	NMe_3I	1	12
NO_2	NMe_3I	4	8

A common means to circumvent the need for an electron-withdrawing substituent on the arene is the use of 2- and 4-substitued pyridines (***Scheme 2.5***). Here, the nitrogen of the pyridine ring is able to stabilize the Meisenheimer intermediate enough that ^{18}F-fluorination can proceed in moderate RCY.[44-46] With an activating group, good RCY can even be achieved on the 3 position of a pyridine ring (***Scheme 2.6***).[47, 48]

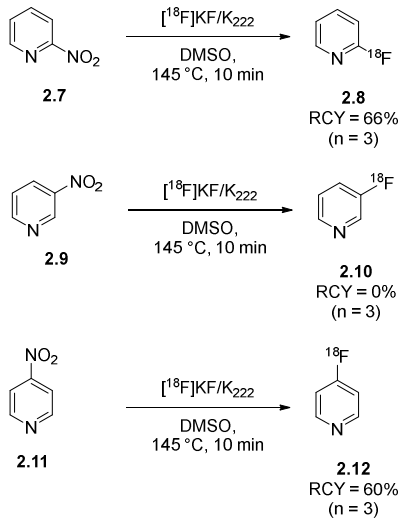

Scheme 2.5. Radiosynthesis of 2-, 3-, and 4-[^{18}F]fluoropyridine.

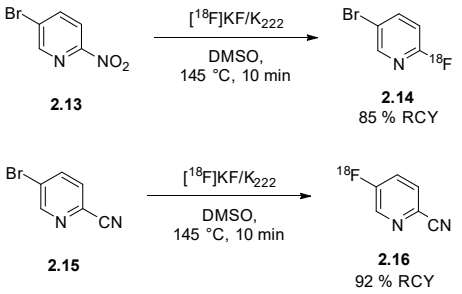

Scheme 2.6. Examples of the radiosynthesis of activated 2- and 3-[^{18}F]fluoropyridine.

2.4.3. ^{18}F-Fluorination of Hypervalent Iodine Species

Diaryliodonium salts are a well-established chemical species with air and moisture tolerance.[49] These salts can be treated with [^{18}F]fluoride to create [^{18}F]fluoroarenes and iodoarenes whose ratios are determined by the electronic properties of the two aryl groups.[50, 51] Under ideal circumstances, a strong bias is incorporated where one ring is electron rich through an electron donating group and the other is electron poor through an electron withdrawing group (***Figure 2.5***).[14]

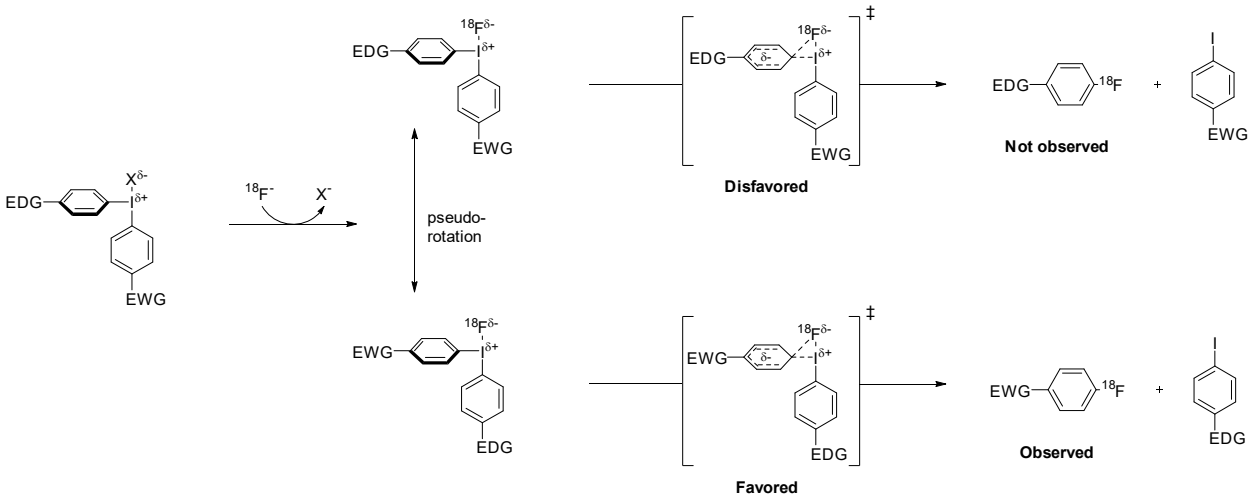

Figure 2.5. Mechanism for the radiofluorination of diaryliodonium salts.

This bias influences the favorability of the radiofluorination transition states and leads to a single observed radiolabeled product with the fluorine-18 installed on the more electron-deficient arene (***Scheme 2.7***).[14]

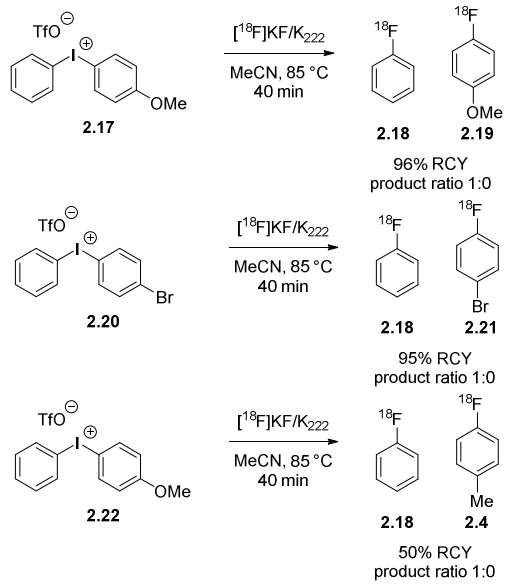

Scheme 2.7. Electronic bias of unsymmetrical diaryliodonium salts.

Despite the need to have an electron withdrawing group to increase the favorability of the radiofluorination, electron rich arenes can be radiofluorinated through the use of electron rich heterocycles such as thiophenes, albeit in modest RCY (***Scheme 2.8***).[51, 52]

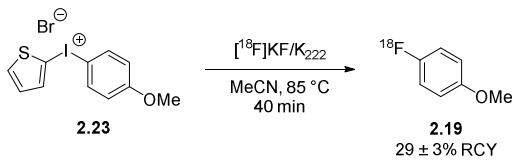

Scheme 2.8. Synthesis of electron-rich 4-[^{18}F]fluoroanisole via diaryliodonium salt.

Building on the success of diaryliodonium salts for radiofluorination, spirocyclic iodonium ylides have been developed.[53] Compared to diaryliodonium constructs, iodonium ylides are more stable and give better RCYs[54] detailed in the optimization studies by Vasdev and Liang (***Figure 2.6***).[53]

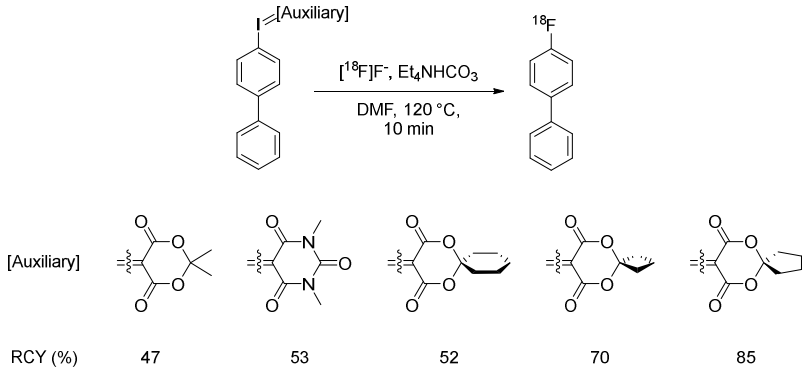

Figure 2.6. Optimization of the dicarbonyl auxiliary spirocyclic iodonium ylides.

Through the use of iodonium ylides, electron rich arenes which would have been largely inaccessible via diaryliodonium salts can be radiofluorinated in modest to good yields (***Figure 2.7***).[55] This method has been used in the large scale production of the radiopharmaceutical [^{18}F]3-fluoro-5-[(pyridin-3-yl)ethynyl]benzonitrile ([^{18}F]FPEB) (**2.33**) in 20% non-decay-corrected yield with a MA of 18 Ci μmol^{-1} (***Scheme 2.9***).[56]

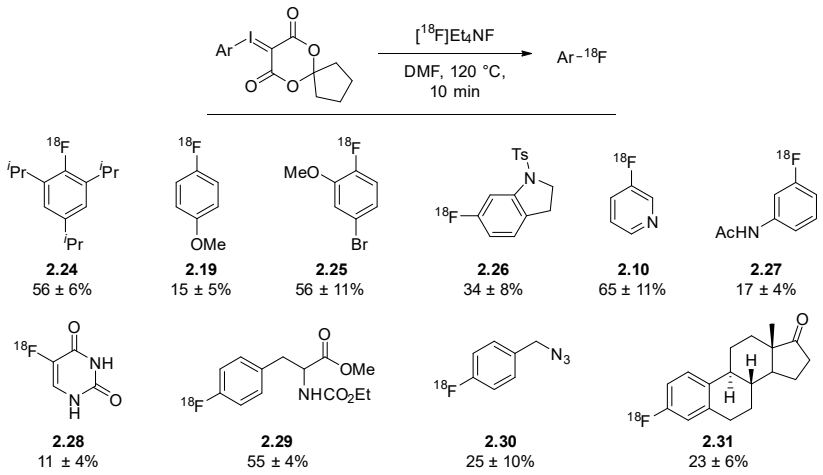

Figure 2.7. Substrate scope of spirocyclic iodonium ylides.

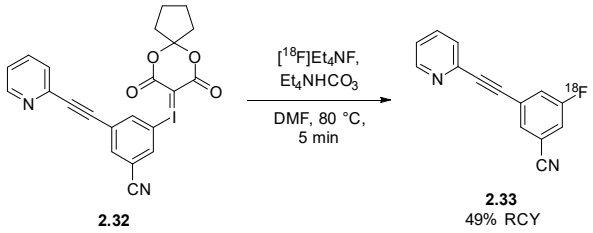

Scheme 2.9. Radiosynthesis of [^{18}F]FPEB (**2.33**) using spirocyclic iodonium ylides.

2.4.4. ^{18}F-Deoxyfluorination

One of the more recent developments in radiofluorination methods is ^{18}F-deoxyfluorination.[57, 58] Broadly, this method directly replaces the hydroxyl group of phenol with [^{18}F]fluoride. This methodology was originally disclosed by Neumann, as a means to access *more* electron-rich [^{18}F]fluoroarenes which are inaccessible through S_NAr methods.[59]

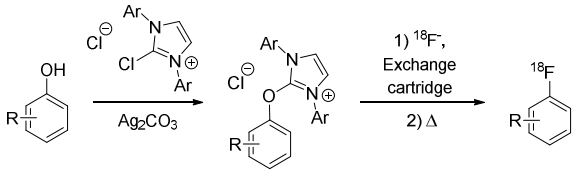

Scheme 2.10. ^{18}F-Deoxyfluorination using a pre-formed imidazolium precursor. Ar = 1,4-diisopropylphenyl.

In its first iteration, an imidazolium precursor is pre-formed before being subjected to radiofluorination conditions (***Scheme 2.10***).[59] In traditional radiofluorination methods, [^{18}F]fluoride is trapped on a quaternary methyl ammonium cartridge and subsequently eluted using an aqueous solution of base (e.g. Et_4NHCO_3) and solvent (e.g. MeCN). Since the eluting solution contains water the mixture must be azeotropically dried to remove the water which can solvate the [^{18}F]fluoride and dramatically reduce its nucleophilicity. This process typically requires 40 minutes or more, which decreases the amount of usable [^{18}F]fluoride as it undergoes radioactive decay. Alternatively, in ^{18}F-deoxyfluorination the uronium precursor in its reaction solvent is used to directly elute the [^{18}F]fluoride from the ion-exchange cartridge, thus removing the lengthy azeotropic drying process that is required in traditional radiofluorination methods.[59] They propose that this reaction is able to occur as a concerted transformation to yield the desired ^{18}F-product (***Scheme 2.11***).[59] Because this method bypasses a Meisenheimer intermediate, it is able to facilitate the radiofluorination of comparatively electron rich systems.[59]

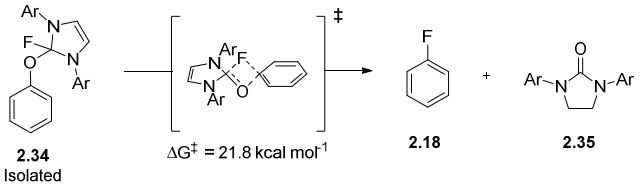

Scheme 2.11. The proposed transition state as determined by DFT calculations (B3LYP/6-31(d), toluene solvent model) (Ar = 2,6-diisopropylphenyl) of deoxyfluorination.

In a subsequent disclosure, Beyzavi, *et al*. demonstrated that highly electron rich phenolic molecules could be directly radiofluorinated with the inclusion of a ruthenium complex that lowers the kinetic barriers, allowing the reaction to proceed (***Figure 2.8***).[58]

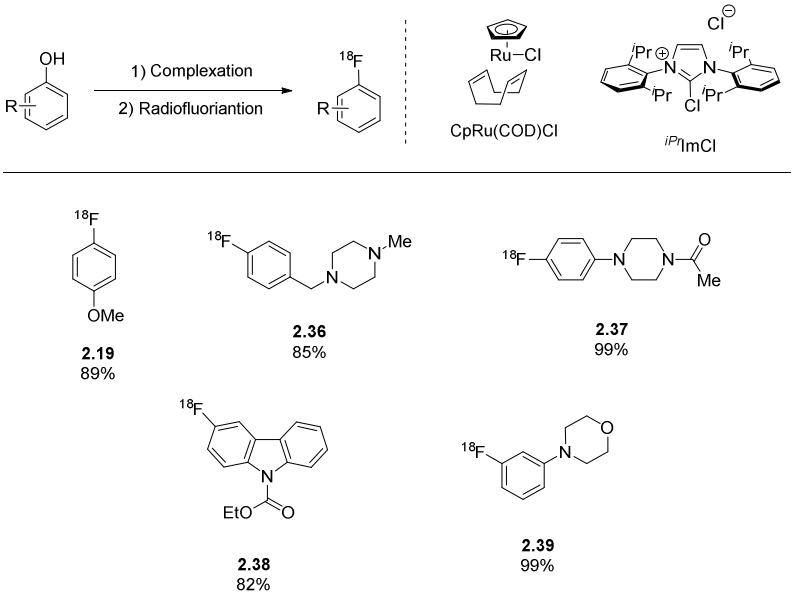

Figure 2.8. ^{18}F-Deoxyfluorination using an *in situ* formed imidazolium complex and selected ^{18}F-products with their RCY_{TLC} (n=1).

This protocol uses CpRu(COD)Cl which is initially complexed to the phenol, followed by chloride displacement to form the imidazolium complex, which is subsequently passed through a

ion-exchange cartridge to elute the [^{18}F]F^{-}.[58] This mixture can be heated to yield the desired [^{18}F]fluoroarene as an η^6 ruthenium complex which is decomplexed to yield the final ^{18}F-tracer.[58] Based on DFT calculations, the inclusion of the ruthenium allows for the formation of an η^6 π coordination which decreases the kinetic barrier of forming intermediate **2.44** and allows for the final concerted S_NAr (CS_NAr) to take place (***Scheme 2.12***).[58] Even with highly electron rich arenes, good to excellent RCY are achieved, including the functionalization of β-lactam **2.46** (***Figure 2.9***).[58]

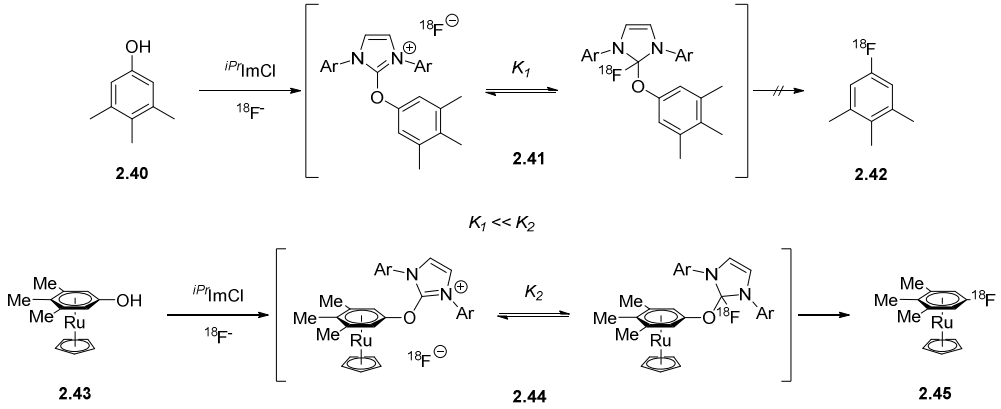

Scheme 2.12. A comparison of different ^{18}F-deoxyfluorination pathways.

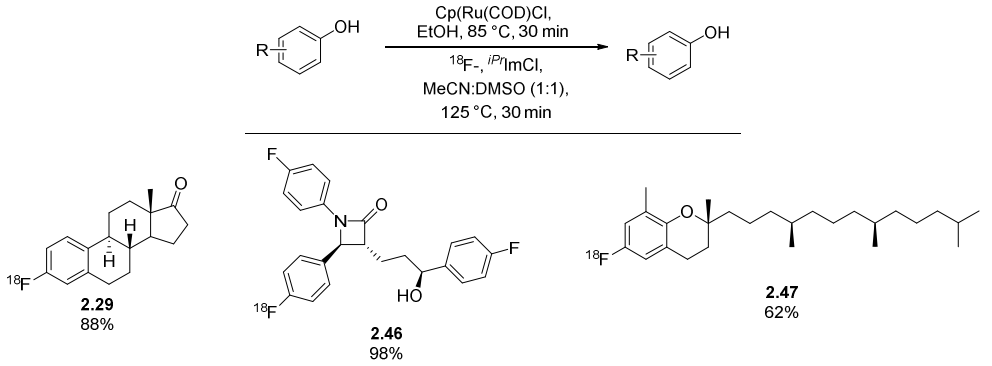

Figure 2.9. Selected substrates for ruthenium-mediated ^{18}F-deoxyfluorination of phenols.

2.4.5. Transition Metal Mediated ^{18}F-Fluorination

Palladium, nickel, and copper have seen wide use in the [^{18}F]fluorination of arenes.[14] Beginning with palladium C-H fluorination, chemists have been able to adapt this chemistry to make it amenable for fluorination and radiofluorination with a $Pd^{(II/IV)}$ catalytic cycle.[60, 61] Ritter *et al.* developed a methodology to oxidize [^{18}F]fluoride to an electrophilic ^{18}F-umpolung agent (**2.49**) via a high valent Pd(IV)-[^{18}F]fluoride species (***Scheme 2.13***).[62] Complex **2.49** provides an elegant method to overcome the low molar activity of traditional electrophilic fluorine-18 sources. This high valent Pd(IV)-[^{18}F]fluoride complex (**2.49**) was formed in 90% RCY from [^{18}F]KF/18-crown-6 and could subsequently be used as an electrophilic fluorine-18 source as well as oxidant in the formation of [^{18}F]fluoroarenes (***Scheme 2.14***).[63, 64]

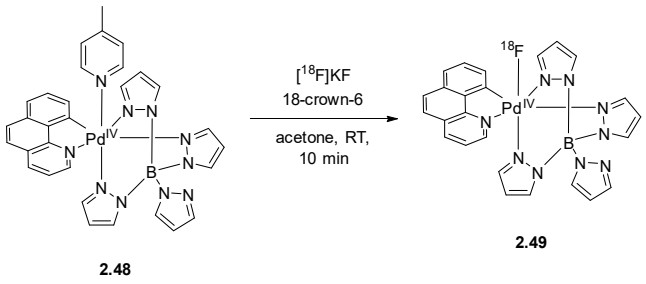

Scheme 2.13. Synthesis of [^{18}F]Pd(IV)F complex **2.49**.

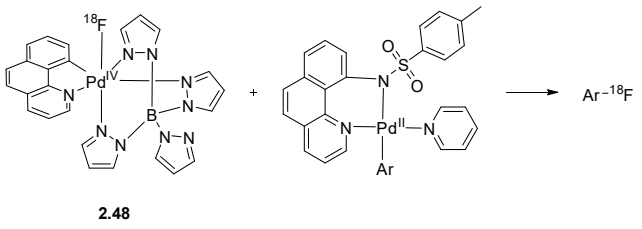

Scheme 2.14. Synthesis of [^{18}F]fluoroarenes from palladium organometallic complexes.

An alternative that has been investigated also by the Ritter group is organometallic ^{18}F-nickel complexes. These nickel complexes can incorporate small amounts of fluoride-18 (0.1 – 0.5 mCi) in aqueous media (removing the need for lengthy azeotropic drying) and subsequently label a series of aryl groups (***Figure 2.10***).[65] Increasing the scale of this method to larger amounts of radioactivity was non-trivial. Increases to the volume of aqueous [^{18}F]fluoride above 1% v/v with respect to the reaction solvent led to the complete degradation of the Ni(II)-aryl complex.[66] Even with azeotropic drying, the reaction could not proceed as the ^{18}F solutions became incompatible with the Ni(II)-aryl complex. Through optimization, Ritter *et al.* were able to prepare [^{18}F]MDL100907 (**2.55**) on 37 mCi scale (3% n.d.c. RCY) with a specific activity of 1.5 Ci/μmol (***Scheme 2.15***).[66] Since then this method has been used to synthesize a range of PET tracers: 6-[^{18}F]FDOPA, 6-[^{18}F]FMT, 6-[^{18}F]FDA, among others.[67]

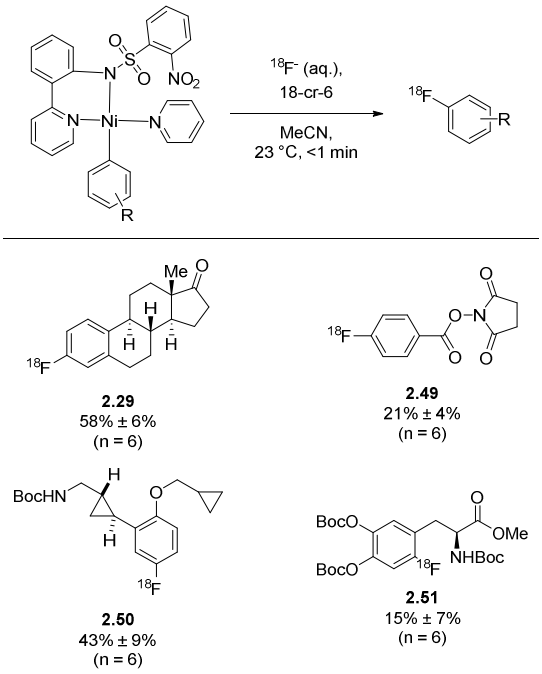

Figure 2.10. One-step Ni-mediated radiofluorination with aqueous [^{18}F]fluoride and oxidant utilizing small aliquots of target water.

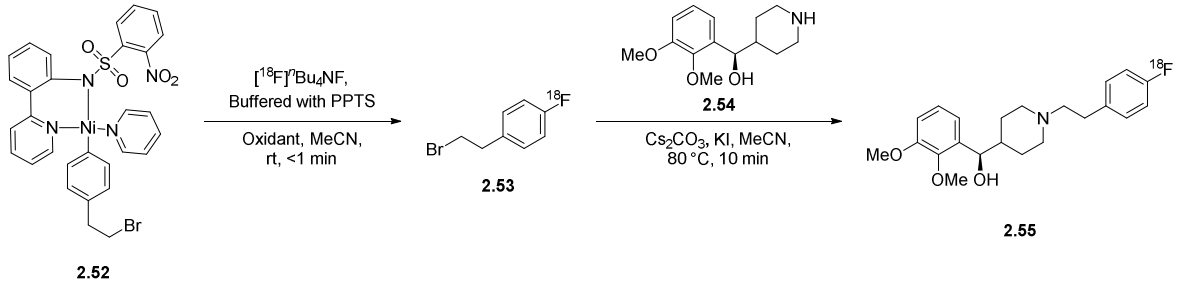

Scheme 2.15. Radiosynthesis of [^{18}F]MDL100907 (**2.55**) utilizing Ni-mediated [^{18}F]fluorination methodology.

These organometallic complexes are not the only means by which transition metals have been used for ^{18}F-aryl fluorination. Palladium and copper have both seen use, though to vastly different degrees. The reductive elimination of a Pd(II)Ar(F) intermediate remains a challenge as undesired reactions between the fluoride and ancillary ligands can occur.[68] With this and other challenges, the practical adaptation of this procedure to [^{18}F]fluoride remains difficult. One example of a palladium mediated aryl radiofluorination is 1-[^{18}F]-fluoronaphthalene, which has been synthesized in 32% RCY. In order to achieve this RCY, CsF carrier had to be added, limiting the final MA.[69] Further, electron rich arenes resulted in poor RCY and electron deficient arenes are more easily accessed using the methods described elsewhere in this section.[69] For these reasons, the scope of this methodology is limited.

Copper mediated radiofluorination is quite a different story. Chan-Lam coupling has a broad scope in its ability to form C-heteroatom bonds from accessible and shelf stable reagents.[70] Following the development of direct C-F coupling reactions of arylboronate esters using only nucleophilic fluoride,[71, 72] Gouverneur *et al.* developed a n.c.a. ^{18}F-based carbon-fluorine Chan-Lam cross-coupling reaction.[73] This method was the first to reveal copper-mediated

radiofluorination using nucleophilic [^{18}F]fluoride and readily available pinacol boranes. Using this method, PET ligands [^{18}F]DAA1106 (**2.58**) and *N*,*N*-diBoc protected 6-[^{18}F]fluoro-*m*-tyrosine (**2.59**) were synthesized from their arylBpin precursor in 59% and 58% RCY respectively (***Figure 2.11***).[73] The work of the Sanford group has also been a boon to this methodology. In their work, they were able to synthesize [^{18}F]FPEB in a single step.[74] This methodology has since been optimized to use minimal amounts of base making it amenable to more sensitive PET tracers.[75]

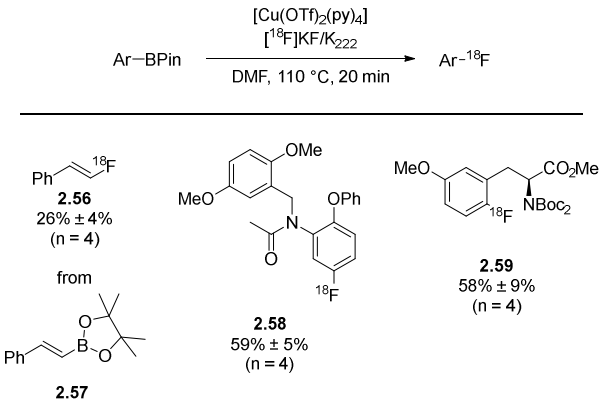

Figure 2.11. Radiosynthesis of (2-[^{18}F]fluoroethenyl)benzene (**2.56**), [^{18}F]DAA1106 (**2.58**), and a protected 6-[^{18}F]fluoro-*m*-tyrosine (**2.59**).

2.5. Prosthetic Groups for [^{18}F]Fluorine Incorporation onto Biomolecules

Chemical methodologies for direct ^{18}F-fluorination require harsh conditions (organic solvents and high temperatures) and are generally incompatible with most biologically relevant molecules, such as peptides and proteins.[7, 76] As such, prosthetic groups which can withstand the harsh reaction conditions of ^{18}F-fluorination but contain functional handles for bioconjugation chemistry have been developed to radiolabel sensitive biomolecules under milder conditions.

While this section may be lengthy it is by no means exhaustive; many reviews have been written about the variety of fluorine-18 containing prosthetic groups.[7, 76-81]

2.5.1. B-, Si-, Al-^{18}F Labeled Prosthetic Groups

A direct and elegant method to incorporate fluorine-18 into sensitive molecules is the isotope exchange (IEX) of fluorine-19 with fluorine-18 to form stable B- or Si-^{18}F bonds (***Figure 2.12***). In these processes, the relevant metal contains a fluorine-19 atom that can be replaced with a fluorine-18 atom and is also covalently bonded to the targeting molecule of interest.[7, 76] Alternatively, chelation chemistry can be used to incorporate an aluminum-[^{18}F]fluoride ([^{18}F]AlF) complex to a pendant chelating group (***Figure 2.12***).[7, 76]

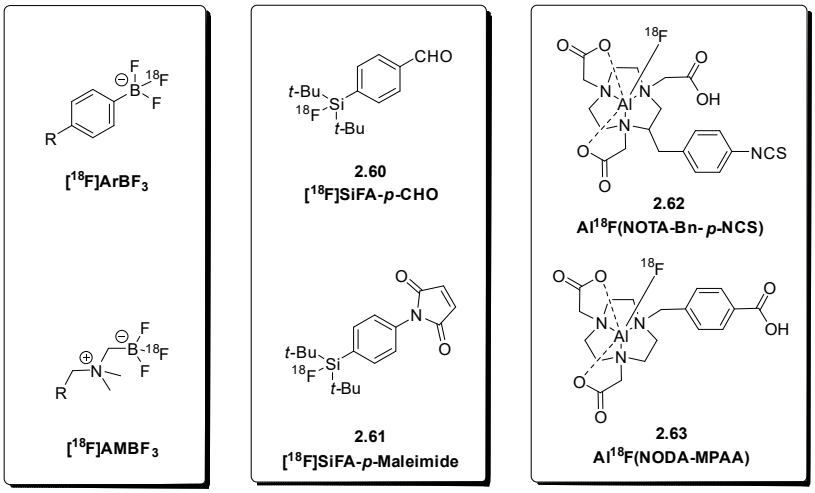

Figure 2.12. Prominent B-, Si-, and Al-^{18}F building blocks.

Boron based radiofluorination is documented as early as the 1960s[82, 83] but did not gain notoriety until 2005.[84, 85] In their work, Ting and Perrin *et al.* reported the first example of B-^{18}F bond formation in aqueous media using a biotinylated arylboronic ester and [^{18}F]KHF_2.[85] With

concerns about hydrolytic degradation, the authors sought to verify the stability of [^{18}F]arylfluoroboronates at pH 7.5, mimicking physiological conditions, and found that there was no significant release of fluorine-18 from their labeled compounds.[85]

Many other tracers utilizing B-^{18}F have been developed over the past 17 years.[86-92] Of note is the kit-like synthesis of an [^{18}F]RGD peptide where RGD-ArBF_3 is treated with [^{18}F]fluoride under acidic conditions.[89] Following HPLC purification, the RGD-[^{18}F]ArBF_3 was isolated in good RCY (65 % n.d.c.) with exceptional molar activity for isotopic exchange (14 Ci μmol^{-1}).[89]

The first Si-^{18}F bond formation was reported in 1985 by Rosenthal *et al*.[93] They were able to synthesize [^{18}F]fluorotrimethylsilane; however it was subsequently discovered that [^{18}F]fluorotrimethylsilane underwent rapid hydrolysis, releasing the [^{18}F]fluoride.[93] With the ease with which Si-^{18}F bonds form, efforts have been made to disrupt the hydrolytic cleavage that was previously demonstrated.[94, 95] A robust means to increase Si-^{18}F stability is the inclusion of flanking *tert*-butyl groups on the silicon atom, creating substantial steric bulk near the Si-^{18}F bond, thereby hindering hydrolysis.[94, 95] ^{18}F-Tracers utilizing this structural motif have been demonstrated to be stable *in vitro* in human serum for over 60 mins.[94, 95] These developments have led to the creation of a variety of Si-^{18}F PET tracers such as [^{18}F]BMPPSiF, a bivalent homodimeric SiF–dipropargyl glycerol derivatized radioligand, (synthesized in 52% RCY (d.c.) with 12.9 Ci μmol^{-1}) which is used to image serotonin receptors.[96]

Unlike the B- and Si-^{18}F, [^{18}F]AlF complexes use chelation chemistry. In this case, the complex is formed first and then chelated into either a NOTA or DOTA chelating group pendant to the molecule of interest.[7, 76] This methodology is of particular interest as it takes advantage of the fast kinetics of chelation and, in some circumstances, can avoid the use of HPLC purification.[7, 76] Noteworthy examples of [^{18}F]AlF tracers are dimeric cyclic RGDyK peptide (synthesized in 5–

25% RCY) which targets $\alpha\beta_3$ integrin receptor[97] and folate-NOTA-Al^{18}F radiotracer (synthesized in 19% RCY with 1.9 Ci/μmol) used for the diagnosis of folate-receptor expressing cancers.[98]

All of these isotope exchange methods are not without problems. In particular, they all require acidic conditions which leaves them vulnerable to degradation under physiological conditions unless care is taken to develop tracers that minimize this problem.[7, 76] Additionally, some tracers in this category (in particular [^{18}F]AlF complexes) require high temperatures to form, meaning they can only be used with biomolecules which can withstand high temperatures (>100 °C) [7, 76]. Finally, the major limitation to these methods is that isotope exchange (like those utilized in some B- and Si-^{18}F) tend to give low molar activities (<1 Ci μmol^{-1}). [7, 76] This characteristic is caused by the inseparability of the abundant ^{19}F-precursor from the ^{18}F-tracer product, which have identical chemical compositions.

2.5.2. Cycloaddition ^{18}F-Labeled Prosthetic Groups

Much like the field of chemical biology, radiosynthesis has benefited from the advent of biorthogonal chemistry— most prominently in the form of the Huisgen cycloaddition.[76, 81] In this dipolar cycloaddition, azides undergo a 3 + 2 cycloaddition with alkynes to afford the resulting 1,2,3-triazoles which are robust under physiological conditions.[99] Traditionally this reaction, in a radiofluorination setting, requires elevated temperatures to compensate for sluggish kinetics; however, the incorporation of a copper catalyst, as discovered independently by Sharpless[100] and Meldal[101] in 2001 and further developed in the time since, has provided a means to make this chemistry more compatible with fluorine-18.

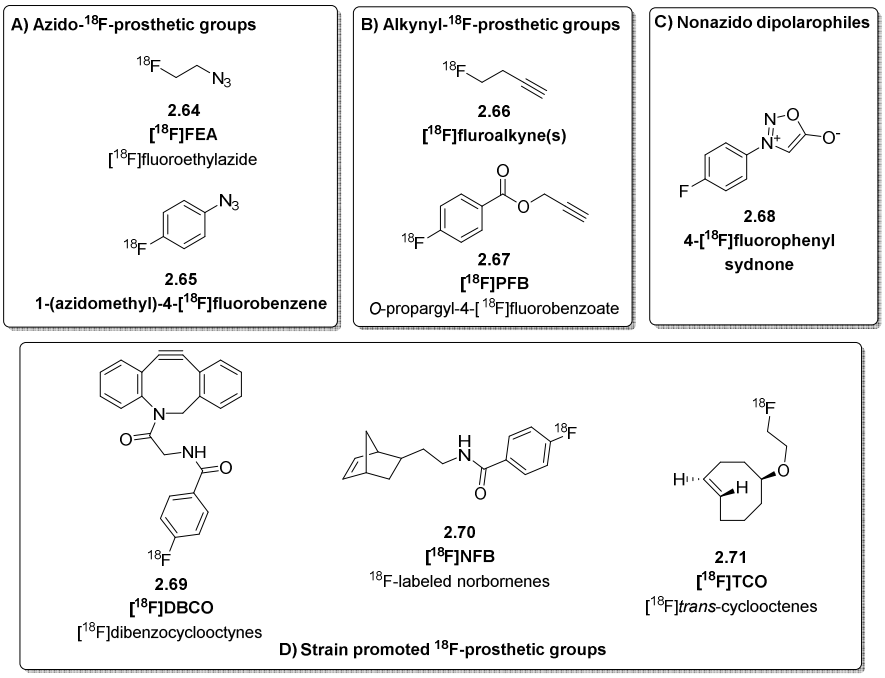

Figure 2.13. Selected ^{18}F-prosthetic groups used in cycloaddition chemistries.

The first use of copper catalyzed ^{18}F-alkyne-azide cycloaddition (Cu ^{18}F-AAC) was demonstrated in 2006 by Maruik and Sutcliffe who synthesized a trio of fluorine-18 containing alkynes which were subsequently reacted with azide-functionalized peptides.[102] The volatility of ^{18}F-labeled azides has limited their broad use as prosthetic groups; as a result, interest in alternative ^{18}F-labeled cycloaddition moieties has notably increased, such as the development of ^{18}F-PEGylated alkynes.[103] The incorporation of the PEG chains not only decreases the volatility of the ^{18}F-labeled compounds but also increases their thermal stability and the renal clearance of the ^{18}F-labeled tracer.[103] Despite further development of ^{18}F-azides, their use has been limited in clinical PET imaging studies.[7] [^{18}F]fluoroethylazide (**2.64**)[104, 105] and [^{18}F]fluorobenzylazide (**2.65**)[106-109] are exception to this (***Figure 2.13A***), having been used in a variety of PET tracers despite their variable RCYs (largely attributed to the reduction of the azide in the presence of copper wire in acidic conditions as reported by Glaser et al.[110]).

^{18}F-Alkynyl precursors have also seen use in radiolabeling biomolecules (***Figure 2.13B***).[7, 76, 81] With the number of reactions available to radiofluorinate aryl compounds (see **Section 2.4**) in combination with improved metabolic stability of aromatic C_{sp2}-F bond, this class of compounds is very attractive for radiolabeling biomolecules.[2, 24-26] The first ^{18}F-alkynyl precursor disclosed is [^{18}F]fluoro-*N*-(prop-2-ynyl)benzamide (**2.72**) (***Figure 2.14***).[111] This ^{18}F-labeled alkyne was used to radiolabel an azide functionalized neurotensin, human serum albumin,[112] a phosphopeptide and an L-oligonucleotide.[113] Since then, pyridine-based fluorine-18 alkynyl precursors have been developed and successfully used to radiolabel a DNA analogue among other biomolecules functionalized with an azido handle.[114]

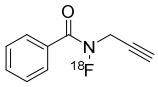

2.72
[^{18}F]fluoro-N-(prop-2-ynyl)benzamide

Figure 2.14. The structure of [^{18}F]fluoro-*N*-(prop-2-ynyl)benzamide.

While Huisegen cyclizations and CuAAC require either high temperature or toxic copper catalysts, both of these can be avoided with the use of strain promoted azide-alkyne cyclization (SPAAC), first demonstrated by Blomquist *et al*.[115] By increasing the strain of the dipolarophile, rapid kinetics can be achieved without high temperatures or metal catalysts.[116] Bouvet *et al*. reported the synthesis of a fluorine-18 labeled azadibenzocyclooctyne (ABIDO) derivative using the conventional prosthetic group [^{18}F]SFB (**2.86**) in 85% RCY (d.c.) based on [^{18}F]SFB.[117] Upon reaction of the [^{18}F]ABIDO derivative with a corresponding azide-terminated biomolecule they isolated tracers **2.73** and **2.74** in 69–98% RCY. In addition, Arumugan *et al*. fully automated the synthesis of an ^{18}F-ABIDO prosthetic group and subsequent reaction with N-terminal azido-

modified peptides.[117] Because this reaction was carried out in ethanol, it was developed into a "kit-like" peptide labeling approach.[118]

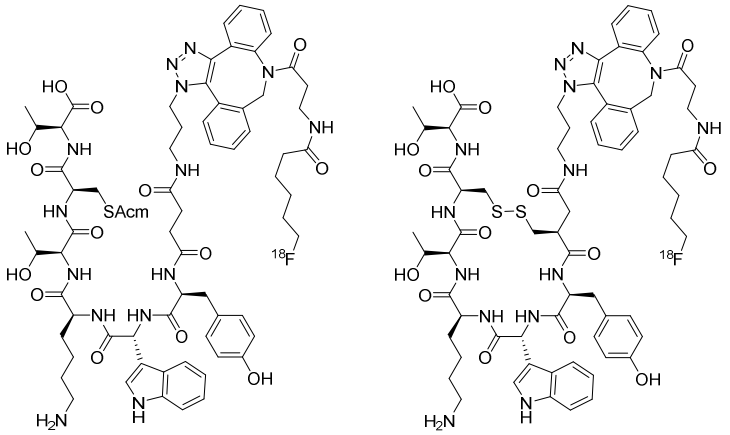

Figure 2.15. Radiolabeled peptides synthesized from azido-functionalized peptides and [^{18}F]ABIDO. Only one regioisomer is shown for simplicity.

This field has seen continued development through the advent of strained alkenes such as ^{18}F-functionalized norbornenes (**2.70**)[119] and *trans*-cyclooctenes (**2.71**)[120, 121] (***Figure 2.13D***) as well as non-azido dipoles, such as 4-[^{18}F]-fluorophenyl sydnone (**2.68**) (***Figure 2.13C***).[122] The development of 4-[^{18}F]-fluorophenyl sydnone (**2.68**) is actually one of serendipity.[122] The Murphy group originally sought to generate 4-[^{18}F]-fluorophenyl sydnone (**2.68**) from [^{18}F]fluoride displacement of a 4-nitrophenyl sydnone precursor. However, rather than nucleophilic displacement occurring at the nitro substituent, the [^{18}F]fluoride displaced the sydnone as the preferred leaving group, affording [^{18}F]fluoro-4-nitrobenzenes (***Scheme 2.16***). Unlike the nitro group, the sydnone is unable to participate in resonance with the aromatic ring due to steric interactions that result in a 40° angle between the planes of each respective ring. To access the

desired 4-[^{18}F]-fluorophenyl sydnone (**2.68**), the symmetric precursor 1,4-disydnonyl benzene was prepared which underwent efficient radiofluorination to afford the desired ^{18}F-prosthetic group in 58% RCY with a MA of 1.3 Ci μmol^{-1} (***Scheme 2.17***). **2.68** was used to label a DBCO-functionalized neuropeptide ([$_{D}$-Ala^{2}, $_{D}$-Leu^{5}]-enkephalin in >97% RCY at 50 °C in 8 mins via strain-promoted sydnone-alkyne cycloaddition (SPSAC). Recently, the Murphy group has successfully used 4-[^{18}F]-fluorophenyl sydnone (**2.68**), via a ^{18}F-deoxyfluorination reaction, to radiolabeled peptides targeting human CD8α with nanomolar affinity via SPSAC (***Figure 2.16***).[123]

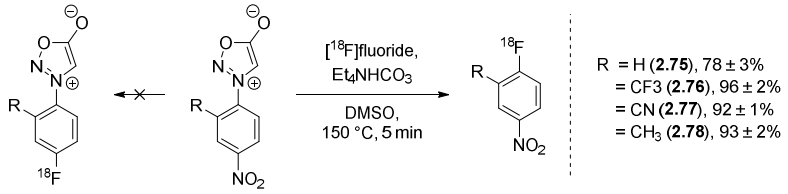

Scheme 2.16. Radiofluorination of *para*-nitro substituted *N*-arylsydnones.

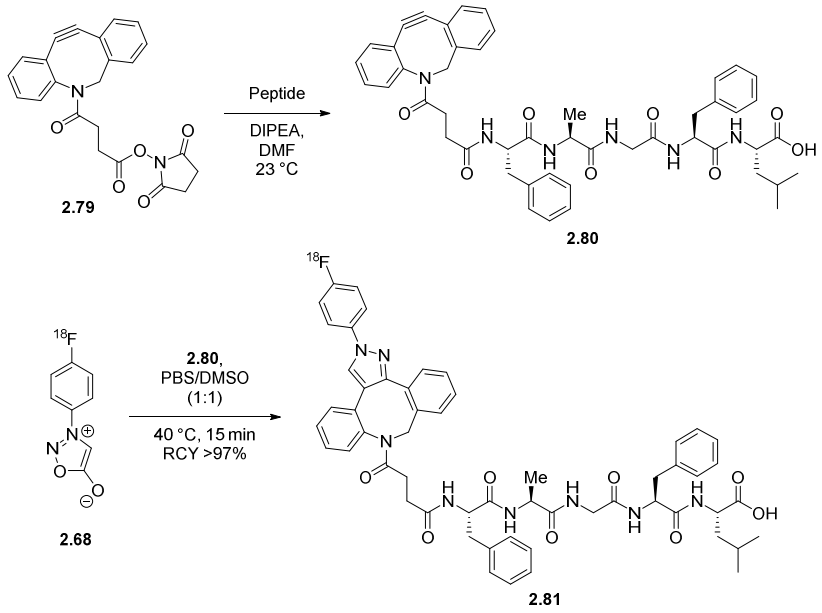

Scheme 2.17. Preparation and application of 4-[^{18}F]-fluorophenylsydnone (**2.68**) toward ^{18}F-labeling of neuropeptide [$_{D}$-Ala^{2}, $_{D}$-Leu^{5}]-enkephalin.

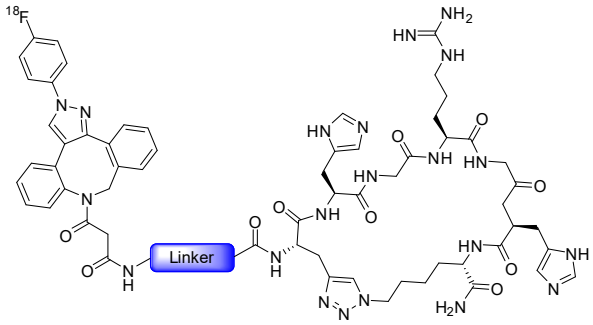

Figure 2.16. Radiolabeled peptides targeting human CD8α.

2.5.3. Amine-reactive ^{18}F-Labeled Prosthetic Groups

While the prosthetic group methods discussed above all require the introduction of functional handles, biomolecules already contain many native handles that can be used for the incorporation of ^{18}F-prosthetic groups.[99] Amines serve as the obvious functional handle given their prominence in lysine residues as well as the N-terminus of non-terminally functionalized peptides and proteins.[99] Amine-reactive ^{18}F-labeled prosthetic groups can be divided into two subclasses: 1) acylating agents and 2) oxime forming agents.

^{18}F-acylating agents contain one of the most commonly used amine reactive ^{18}F-labeled prosthetic group (***Figure 2.17***)— [^{18}F]-*N*-succinimidyl-4-fluorobenzoate ([^{18}F]SFB) (**2.86**).[124] This molecule, and those like it ([^{18}F]-*N*-succinimidyl *o*-(di-*tert*-butylfluorosilyl)-benzoate ([^{18}F]SiFB),[125, 126] [^{18}F]fluoronicotinic acid tetrafluorophenyl ester ([^{18}F]-Py-TFP),[127] etc.) can be synthesize from [^{18}F]fluorobenzoic acid or in one step from a trimethyl ammonium precursor. Each of these activated esters can be used to form amide bonds from reactive amines.

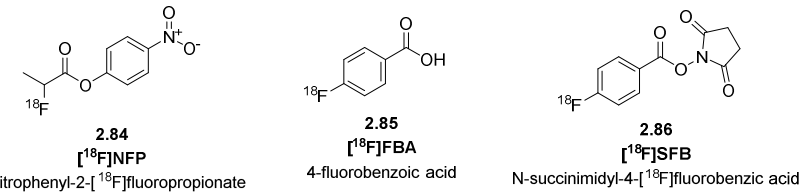

Figure 2.17. Selected examples of amine-reactive prosthetic groups containing an activated ester.

Returning to [^{18}F]SFB (**2.86**), the most common ^{18}F-acylating agent, its first reported synthesis was by Zalutsky and Vaidyanathan in 1992.[124] Though this process required many steps, they were able to isolate the desired product in 25% RCY (d.c.) with a synthesis time of only 100 minutes.[124] They were then able to label a monoclonal antibody F(ab')$_2$ fragment, obtaining the radiotracer in 40–60% RCY (d.c., based on [^{18}F]SFB activity) with an additional 20 minutes.[124] Since its initial synthesis, [^{18}F]SFB's (**2.86**) synthesis has been optimized and fully automated with RCY (d.c.) up to 55%, and still sees regular use.[128] In 2019, a collaboration at UCLA utilized [^{18}F]SFB (**2.86**) to label GA101 cys-diabody (GAcDb) and test the ability to image B cell lymphomas with the resulting PET tracer ([^{18}F]FB-GAcDb).[129] [^{18}F]FB-GAcDb was prepared in 37% RCY with a molar activity of 12.8 μCi/μg and specifically targets human CD20-expressing B cells in transgenic mice.

^{18}F-Oxime formation has also been a proven robust radiolabeling method and has seen wide use for labeling aminooxy-functionalized peptides with fluorine-18.[7, 76] These prosthetic groups contain a variety of fluorine-18 labeled aldehydes and hemi-acetals. A noteworthy example of their use can be found in the work of Glaser *et al.*[130] They reported the radiosynthesis of [^{18}F]fluciclatide (**2.88**) using [^{18}F]fluorobenzaldehyde ([^{18}F]FBA) (**2.85**) with a hydroxyl amine

derived-RGD peptide (**2.87**) (***Scheme 2.18***).[130] The desired ^{18}F-labeled product (**2.88**) was obtained in 23% RCY (d.c.) in 3 hours with a MA of 2.0–4.6 Ci μmol^{-1}.[130]

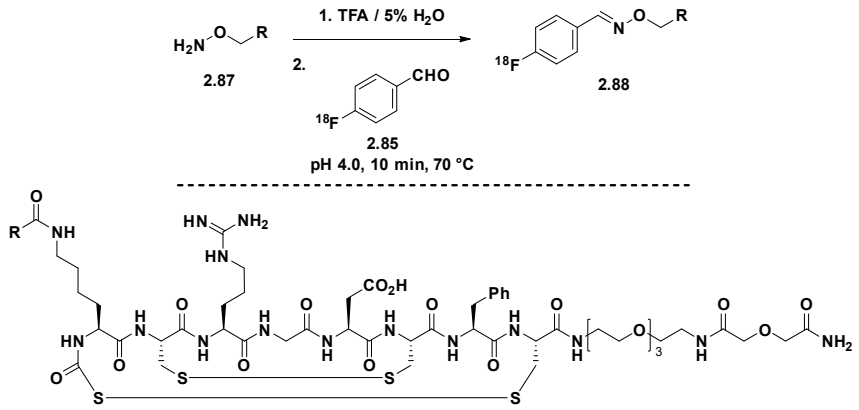

Scheme 2.18. Oxime condensation reaction to form [^{18}F]fluciclatide.

2.5.4. Thiol-reactive ^{18}F-Labeled Prosthetic Groups

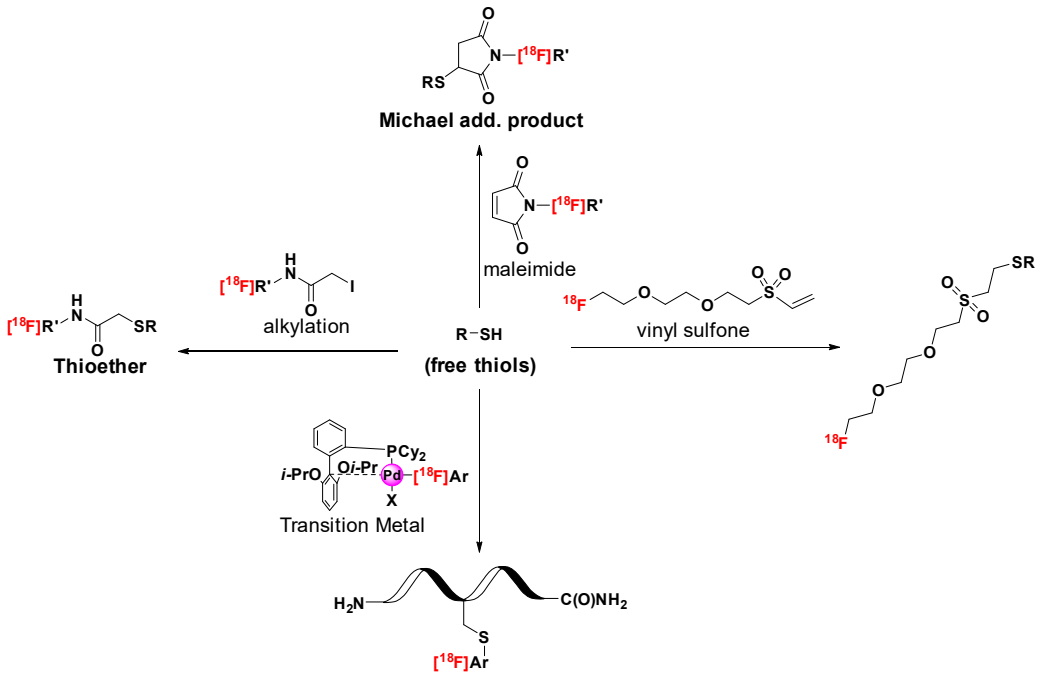

Figure 2.18. Select examples of thiol-reactive prosthetic groups.

While some ^{18}F-acylating agents, like [^{18}F]SFB (**2.86**), can be used to radiolabel thiols, a separate class of prosthetic groups has been created in order to increase regioselectivity.[7, 76] Unlike other nucleophilic groups in biomolecules, thiols possess two unique properties: (1) they are much rarer and only occur on one of the least abundant natural amino acids, cysteine (Cys), or can be installed, either through site selective mutagenesis or other synthetic processes, and (2) they are soft nucleophiles, giving them a unique reactivity profile among other naturally occurring nucleophiles (e.g. amines, hydroxyls).[131]

The best known and most widely used thiol-reactive ^{18}F-prosthetic groups are ^{18}F-maleimides (***Figure 2.18***).[7] This class of prosthetic group contains an α,β-unsaturated carbonyl moiety that is amenable to Michael addition of a free thiol.[7] Because of the high chemoselectivity of this class of compound, a variety of derivatives have been created.[130, 132-139] Despite their popularity though, the primary drawback of ^{18}F-maleimides is that they can undergo retro-Michael addition, releasing the ^{18}F-labeled synthon from the biomolecule of interest.[7, 140-144] This is most commonly seen in compounds that contain maleimides, rather than other α,β-unsaturated carbonyls, because the geometry of the five membered ring primes the system to undergo elimination.

Even with the dominant success of ^{18}F-maleimides, other thiol selective prosthetic groups exist such as ^{18}F-labeled α-bromo- or iodoacetamides and ^{18}F-labeled vinyl sulfones (***Figure 2.18***), though their collective use remains limited. Due to the lengthy syntheses of ^{18}F-labeled α-bromo- or iodoacetamides, resulting in poor isolated yields, broad utility for these prosthetic groups remains to be seen.[145-147] In the case of ^{18}F-labeled vinyl sulfones, it is largely due to their recent discovery and ongoing development. In a 2014 publication, Wu *et al*. synthesized 2-(2-(2-

([^{18}F]fluoroethyoxy)ethoxy)-ethylfulsonyl)-ethane ([^{18}F]F-DEG-VS) and labeled a neurotensin analogue in moderate yield (95% RCY d.c.).[148] Since then, additional work has been done to synthesize a small array of alkyl vinyl sulfones from the Li and Ma research groups.[149]

A final class of thiol-reactive ^{18}F-labeled prosthetic groups are transition metal mediated ^{18}F-arylative agents (***Figure 2.18***). At the time of writing, only one publication has been disclosed demonstrating ^{18}F-labeling via a palladium catalyzed system.[150] In their 2021 work, Humpert *et al*. synthesized 5-iodo-2-[^{18}F]fluoropyridine, and using Xantphos Pd G3, labeled several small peptides. This included a prostate-specific membrane antigen imaging agent which stands to be a possible candidate for prostate carcinoma imaging.[150] This area remains ripe for development.

2.6. Conclusion

PET molecular imaging is a valuable tool for disease diagnostics and staging as well as the development and improved understanding of drug-like molecules and biomolecules. Through the use of nucleophilic fluorine-18 chemical methods a wide range of ^{18}F-labeled arenes, from electron rich to electron poor, can be constructed. Despite the fact that many biomolecules are not amenable to direct radiofluorination conditions, the development of ^{18}F-prosthetic groups has allowed the radiolabeling of a wide range of sensitive biomolecules with fluorine-18 through native and chemically installed functional handles. The work detailed above has generated a wide range of PET tracers to date; however, robust chemical methods are needed to increase the availability of diverse ^{18}F-prosthetic groups and to provide efficient routes towards the production of valuable PET radiotracers.

2.7. Notes and References

1. Al-Sharify, Z. T.; Al-Sharify, T. A.; Al-Sharify, N. T.; Yahya naser, H., A critical review on medical imaging techniques (CT and PET scans) in the medical field. *IOP Conference Series: Materials Science and Engineering* **2020,** *870* (1), 012043.

2. Ametamey, S. M.; Honer, M.; Schubiger, P. A., Molecular Imaging with PET. *Chemical Reviews* **2008,** *108* (5), 1501-1516.

3. Conti, M.; Eriksson, L., Physics of pure and non-pure positron emitters for PET: a review and a discussion. *EJNMMI Physics* **2016,** *3* (1).

4. Shukla, A. K.; Kumar, U., Positron emission tomography: An overview. *J Med Phys* **2006,** *31* (1), 13-21.

5. Jones, T., The role of positron emission tomography within the spectrum of medical imaging. *European Journal of Nuclear Medicine* **1996,** *23* (2), 207-211.

6. Phelps, M. E.; Hoffman, E. J.; Mullani, N. A.; Ter-Pogossian, M. M., Application of annihilation coincidence detection to transaxial reconstruction tomography. *J Nucl Med* **1975,** *16* (3), 210-24.

7. Krishnan, H. S.; Ma, L.; Vasdev, N.; Liang, S. H., ¹⁸F-Labeling of Sensitive Biomolecules for Positron Emission Tomography. *Chemistry - A European Journal* **2017,** *23* (62), 15553-15577.

8. Jødal, L.; Le Loirec, C.; Champion, C., Positron range in PET imaging: non-conventional isotopes. *Physics in Medicine and Biology* **2014,** *59* (23), 7419-7434.

9. Levin, C. S.; Hoffman, E. J., Calculation of positron range and its effect on the fundamental limit of positron emission tomography system spatial resolution. *Physics in Medicine and Biology* **1999,** *44* (3), 781-799.

10. Laforest, R.; Liu, X., Image quality with non-standard nuclides in PET. *Q J Nucl Med Mol Imaging* **2008,** *52* (2), 151-8.

11. Deng, X.; Rong, J.; Wang, L.; Vasdev, N.; Zhang, L.; Josephson, L.; Liang, S. H., Chemistry for Positron Emission Tomography: Recent Advances in ^{11}C-, ^{18}F-, ^{13}N-, and ^{15}O-Labeling Reactions. *Angewandte Chemie* **2019,** *58* (9), 2580-2605.

12. Schirrmacher, R.; Wangler, C.; Schirrmacher, E., Recent Developments and Trends in 18F-Radiochemistry: Syntheses and Applications. *Mini-Reviews in Organic Chemistry* **2007,** *4* (4), 317-329.

13. Wester, H. J.; Schottelius, M., Fluorine-18 Labeling of Peptides and Proteins. Springer Berlin Heidelberg: pp 79-111.

14. Preshlock, S.; Tredwell, M.; Gouverneur, V., 18F-Labeling of Arenes and Heteroarenes for Applications in Positron Emission Tomography. *Chemical Reviews* **2016,** *116* (2), 719-766.

15. Grieken, R. v.; Bruin, M. d., Nomenclature for radioanalytical chemistry (IUPAC Recommendations 1994). *Pure and Applied Chemistry* **1994,** *66* (12), 2513-2526.

16. De Goeij, J. J. M.; Bonardi, M. L., How do we define the concepts specific activity, radioactive concentration, carrier, carrier-free and no-carrier-added? *Journal of Radioanalytical and Nuclear Chemistry* **2005,** *263* (1), 13-18.

17. Allyson, B.; Satyamurthy, N.; Gerald, B.; Michael, P.; Jorge, R. B., Identification and quantitation of gaseous compounds of fluorine generated in 18F F2 target systems. *Nuclear Medicine and Biology* **1996,** *23* (4), 391-405.

18. James, P. O. N.; Henry, F. V., Preparation of fluorine-18 gas from an 11MeV cyclotron: a target system for the CTI RDS 111 cyclotron. *Nuclear Instruments and Methods in Physics*

Research Section A: Accelerators, Spectrometers, Detectors and Associated Equipment **1999,** *438* (1), 166-172.

19. Strijckmans, K., The isochronous cyclotron: principles and recent developments. *Computerized Medical Imaging and Graphics* **2001,** *25* (2), 69-78.

20. Roberts, A. D.; Barnhart, T. E.; Nickles, R. J., *Isotope Production For Medical Applications*. 2005.

21. Kniess, T.; Laube, M.; Brust, P.; Steinbach, J., 2-[^{18}F]Fluoroethyl tosylate – a versatile tool for building ^{18}F-based radiotracers for positron emission tomography. *Med Chem Comm* **2015,** *6* (10), 1714-1754.

22. van der Born, D.; Pees, A.; Poot, A. J.; Orru, R. V. A.; Windhorst, A. D.; Vugts, D. J., Fluorine-18 labelled building blocks for PET tracer synthesis. *Chemical Society Reviews* **2017,** *46* (15), 4709-4773.

23. Zhang, M.-R.; Suzuki, K., [18F]Fluoroalkyl Agents: Synthesis, Reactivity and Application for Development of PET Ligands in Molecular Imaging. *Current Topics in Medicinal Chemistry* **2007,** *7* (18), 1817-1828.

24. Miller, P. W.; Long, N. J.; Vilar, R.; Gee, A. D., Synthesis of 11C, 18F, 15O, and 13N Radiolabels for Positron Emission Tomography. *Angewandte Chemie International Edition* **2008,** *47* (47), 8998-9033.

25. Campbell, M. G.; Ritter, T., Modern Carbon–Fluorine Bond Forming Reactions for Aryl Fluoride Synthesis. *Chemical Reviews* **2015,** *115* (2), 612-633.

26. O'Hagan, D., Understanding organofluorine chemistry. An introduction to the C–F bond. *Chemical Society Reviews* **2008,** *37* (2), 308-319.

27. Brooks, A. F.; Topczewski, J. J.; Ichiishi, N.; Sanford, M. S.; Scott, P. J. H., Late-stage [18F]fluorination: new solutions to old problems. *Chem. Sci.* **2014,** *5* (12), 4545-4553.

28. Halder, R.; Ritter, T., 18F-Fluorination: Challenge and Opportunity for Organic Chemists. *The Journal of Organic Chemistry* **2021,** *86* (20), 13873-13884.

29. Arbusow, A. E.; Dunin, A. A., Über Phosphon-carbonsäuren. *Berichte der deutschen chemischen Gesellschaft (A and B Series)* **1927,** *60* (2), 291-295.

30. Anbar, M.; Guttmann, S., The Isotopic Exchange of Fluoroboric Acid with Hydrofluoric Acid. *The Journal of Physical Chemistry* **1960,** *64* (12), 1896-1899.

31. Palmer, A. J.; Clark, J. C.; Goulding, R. W., The preparation of fluorine-18 labelled radiopharmaceuticals. *The International Journal of Applied Radiation and Isotopes* **1977,** *28* (1), 53-65.

32. Goulding, R.; Gunasekera, S., Fluorine-18 labelled Lp-fluorophenylalanine. *The International Journal of Applied Radiation and Isotopes* **1975,** *26* (9), 561-564.

33. Goulding, R.; Palmer, A., The preparation of fluorine-18 labelled p-fluorophenylalanine for clinical use. *The International Journal of Applied Radiation and Isotopes* **1972,** *23* (3), 133-137.

34. Hoyte, R. M.; Christman, D. R.; Atkins, H. L.; Hauser, W.; Wolf, A. P., Organic radiopharmaceuticals labeled with short-lived nuclides. III. ^{18}F-labeled phenylalanines. *Journal of Nuclear Medicine* **1971,** *12* (6), 280-286.

35. Atkins, H.; Christman, D.; Fowler, J. *Organic Radiopharamceuticals Labeled with Isotopes of Short Half-life. V.* ^{18}F-Labeled 5-and 6-Fluorotryptophan; Brookhaven National Lab., Upton, NY; and others: 1972.

36. Firnau, G.; Nahmias, C.; Garnett, S., Synthesis of 3, 4-dihydroxy-5-fluoro-DL-phenylalanine and 3, 4-dihydroxy-5-[fluorine-18] fluoro-DL-phenylalanine. *Journal of medicinal chemistry* **1973,** *16* (4), 416-418.

37. Rosenfeld, M. N.; Widdowson, D. A., A mild and efficient method of aromatic fluorination. *Journal of the Chemical Society, Chemical Communications* **1979,** (20), 914-916.

38. Ng, J. S.; Katzenellenbogen, J. A.; Kilbourn, M. R., Aromatic fluorinations suitable for fluorine-18 labeling of estrogens. *The Journal of Organic Chemistry* **1981,** *46* (12), 2520-2528.

39. Satyamurthy, N.; Barrio, J. R.; Schmidt, D. G.; Kammerer, C.; Bida, G. T.; Phelps, M. E., Acid-catalyzed thermal decomposition of 1-aryl-3, 3-dialkyltriazenes in the presence of nucleophiles. *The Journal of Organic Chemistry* **1990,** *55* (15), 4560-4564.

40. Pages, T.; Langlois, B. R., Fluorination of aromatic compounds from 1-aryl-3, 3-dimethyltriazenes and fluoride anions in acidic medium: 1. A model for ^{18}F labelling. *Journal of Fluorine Chemistry* **2001,** *107* (2), 321-327.

41. Kilbourn, M. R.; Welch, M. J.; Dence, C. S.; Tewson, T. J.; Saji, H.; Maeda, M., Carrier-added and no-carrier-added syntheses of [^{18}F]spiroperidol and [^{18}F]haloperidol. *The International Journal of Applied Radiation and Isotopes* **1984,** *35* (7), 591-598.

42. Adams, D.; Clark, J., Nucleophilic routes to selectively fluorinated aromatics. *Chemical Society Reviews* **1999,** *28* (4), 225-231.

43. Lazarova, N.; Siméon, F. G.; Musachio, J. L.; Lu, S.; Pike, V. W., Integration of a microwave reactor with Synthia to provide a fully automated radiofluorination module. *Journal of Labelled Compounds and Radiopharmaceuticals* **2007,** *50* (5-6), 463.

44. Illuminati, G., Nucleophilic heteroaromatic substitution. In *Advances in Heterocyclic Chemistry*, Elsevier: 1964; Vol. 3, pp 285-371.

45. Illuminati, G.; Stegel, F., The formation of anionic σ-adducts from heteroaromatic compounds: structures, rates, and equilibria. In *Advances in heterocyclic chemistry*, Elsevier: 1983; Vol. 34, pp 305-444.

46. Schlosser, M.; Ruzziconi, R., Nucleophilic substitutions of nitroarenes and pyridines: new insight and new applications. *Synthesis* **2010,** *2010* (13), 2111-2123.

47. Malik, N.; Solbach, C.; Voelter, W.; Machulla, H.-J., Nucleophilic aromatic substitution by [^{18}F] fluoride at substituted 2-nitropyridines. *Journal of radioanalytical and nuclear chemistry* **2010,** *283* (3), 757-764.

48. Angelini, G.; Margonelli, A.; Sparapani, C.; Ursini, O.; Salvadori, P.; Di Sacco, S.; Riva, A.; Fusari, L., ^{18}F-nucleophilic heteroaromatic substitution: some data on the reactivity and selectivity of the ^{18}F-fluorination reaction. *Journal of Labelled Compounds and Radiopharmaceuticals* **1994,** *35*, 562-564.

49. Merritt, E. A.; Olofsson, B., Diaryliodonium Salts: A Journey from Obscurity to Fame. *Angewandte Chemie International Edition* **2009,** *48* (48), 9052-9070.

50. Pike, V. W.; Aigbirhio, F. I., Reactions of cyclotron-produced [^{18}F]fluoride with diaryliodonium salts—a novel single-step route to no-carrier-added [^{18}F]fluoroarenes. *Journal of the Chemical Society, Chemical Communications* **1995,** (21), 2215-2216.

51. Pike, V.; Widdowson, D., The synthesis of [^{18}F]fluoroarenes from the reaction of cyclotron-produced [^{18}F]fluoride ion with diaryliodonium salts. *Journal of the Chemical Society, Perkin Transactions 1* **1998,** (13), 2043-2046.

52. Carroll, M. A.; Jones, C.; Tang, S. L., Fluoridation of 2-thienyliodonium salts. *Journal of Labelled Compounds and Radiopharmaceuticals* **2007,** *50* (5-6), 450-451.

53. Rotstein, B. H.; Stephenson, N. A.; Vasdev, N.; Liang, S. H., Spirocyclic hypervalent iodine(III)-mediated radiofluorination of non-activated and hindered aromatics. *Nature Communications* **2014,** *5* (1).

54. Hill, D. E.; Holland, J. P., Computational studies on hypervalent iodonium (III) compounds as activated precursors for ^{18}F-radiofluorination of electron-rich arenes. *Computational and Theoretical Chemistry* **2015,** *1066*, 34-46.

55. Cardinale, J.; Ermert, J.; Humpert, S.; Coenen, H. H., Iodonium ylides for one-step, no-carrier-added radiofluorination of electron rich arenes, exemplified with 4-(([^{18}F]fluorophenoxy)-phenylmethyl) piperidine NET and SERT ligands. *Rsc Advances* **2014,** *4* (33), 17293-17299.

56. Stephenson, N. A.; Holland, J. P.; Kassenbrock, A.; Yokell, D. L.; Livni, E.; Liang, S. H.; Vasdev, N., Iodonium ylide–mediated radiofluorination of ^{18}F-FPEB and validation for human use. *Journal of Nuclear Medicine* **2015,** *56* (3), 489-492.

57. Neumann, C. N.; Hooker, J. M.; Ritter, T., Concerted nucleophilic aromatic substitution with ^{19}F− and ^{18}F−. *Nature* **2016,** *534* (7607), 369-373.

58. Beyzavi, H.; Mandal, D.; Strebl, M. G.; Neumann, C. N.; D'Amato, E. M.; Chen, J.; Hooker, J. M.; Ritter, T., ^{18}F-Deoxyfluorination of Phenols via Ru π-Complexes. *ACS Central Science* **2017,** *3* (9), 944-948.

59. Tay, N. E. S.; Chen, W.; Levens, A.; Pistritto, V. A.; Huang, Z.; Wu, Z.; Li, Z.; Nicewicz, D. A., ^{19}F- and ^{18}F-arene deoxyfluorination via organic photoredox-catalysed polarity-reversed nucleophilic aromatic substitution. *Nature Catalysis* **2020,** *3* (9), 734-742.

60. Hull, K. L.; Anani, W. Q.; Sanford, M. S., Palladium-Catalyzed Fluorination of Carbon−Hydrogen Bonds. *Journal of the American Chemical Society* **2006,** *128* (22), 7134-7135.

61. Wang, X.; Mei, T.-S.; Yu, J.-Q., Versatile Pd(OTf)₂·2H₂O-Catalyzed *ortho*-Fluorination Using NMP as a Promoter. *Journal of the American Chemical Society* **2009,** *131* (22), 7520-7521.

62. Lee, E.; Kamlet, A. S.; Powers, D. C.; Neumann, C. N.; Boursalian, G. B.; Furuya, T.; Choi, D. C.; Hooker, J. M.; Ritter, T., A Fluoride-Derived Electrophilic Late-Stage Fluorination Reagent for PET Imaging. *Science* **2011,** *334* (6056), 639-642.

63. Furuya, T.; Ritter, T., Carbon−Fluorine Reductive Elimination from a High-Valent Palladium Fluoride. *Journal of the American Chemical Society* **2008,** *130* (31), 10060-10061.

64. Furuya, T.; Benitez, D.; Tkatchouk, E.; Strom, A. E.; Tang, P.; Goddard, W. A.; Ritter, T., Mechanism of C−F Reductive Elimination from Palladium(IV) Fluorides. *Journal of the American Chemical Society* **2010,** *132* (11), 3793-3807.

65. Lee, E.; Hooker, J. M.; Ritter, T., Nickel-Mediated Oxidative Fluorination for PET with Aqueous [^{18}F]Fluoride. *Journal of the American Chemical Society* **2012,** *134* (42), 17456-17458.

66. Ren, H.; Wey, H.-Y.; Strebl, M.; Neelamegam, R.; Ritter, T.; Hooker, J. M., Synthesis and Imaging Validation of [^{18}F]MDL100907 Enabled by Ni-Mediated Fluorination. *ACS Chemical Neuroscience* **2014,** *5* (7), 611-615.

67. Zlatopolskiy, B. D.; Zischler, J.; Urusova, E. A.; Endepols, H.; Kordys, E.; Frauendorf, H.; Mottaghy, F. M.; Neumaier, B., A Practical One-Pot Synthesis of Positron Emission Tomography (PET) Tracers via Nickel-Mediated Radiofluorination. *ChemistryOpen* **2015,** *4* (4), 457-462.

68. Grushin, V. V., Palladium Fluoride Complexes: One More Step toward Metal-Mediated C−F Bond Formation. *Chemistry - A European Journal* **2002,** *8*, 1006-1014

69. Cardinale, J.; Ermert, J.; Kügler, F.; Helfer, A.; Brandt, M. R.; Coenen, H. H., Carrier-effect on palladium-catalyzed, nucleophilic^{18}F-fluorination of aryl triflates. *Journal of Labelled Compounds and Radiopharmaceuticals* **2012,** *55* (12), 450-453.

70. Qiao, J.; Lam, P., Copper-Promoted Carbon-Heteroatom Bond Cross-Coupling with Boronic Acids and Derivatives. *Synthesis* **2011,** *2011* (06), 829-856.

71. Fier, P. S.; Luo, J.; Hartwig, J. F., Copper-Mediated Fluorination of Arylboronate Esters. Identification of a Copper(III) Fluoride Complex. *Journal of the American Chemical Society* **2013,** *135* (7), 2552-2559.

72. Ye, Y.; Sanford, M. S., Mild Copper-Mediated Fluorination of Aryl Stannanes and Aryl Trifluoroborates. *Journal of the American Chemical Society* **2013,** *135* (12), 4648-4651.

73. Tredwell, M.; Preshlock, S. M.; Taylor, N. J.; Gruber, S.; Huiban, M.; Passchier, J.; Mercier, J.; Génicot, C.; Gouverneur, V., A General Copper-Mediated Nucleophilic ^{18}F-Fluorination of Arenes. *Angewandte Chemie International Edition* **2014,** *53* (30), 7751-7755.

74. Mossine, A. V.; Brooks, A. F.; Makaravage, K. J.; Miller, J. M.; Ichiishi, N.; Sanford, M. S.; Scott, P. J. H., Synthesis of [^{18}F]Arenes via the Copper-Mediated [^{18}F]Fluorination of Boronic Acids. *Organic Letters* **2015,** *17* (23), 5780-5783.

75. Zlatopolskiy, B. D.; Zischler, J.; Krapf, P.; Zarrad, F.; Urusova, E. A.; Kordys, E.; Endepols, H.; Neumaier, B., Copper-Mediated Aromatic Radiofluorination Revisited: Efficient Production of PET Tracers on a Preparative Scale. *Chemistry - A European Journal* **2015,** *21* (15), 5972-5979.

76. Richter, S.; Wuest, F., 18F-Labeled Peptides: The Future Is Bright. *Molecules* **2014,** *19* (12), 20536-20556.

77. Okarvi, S., Recent progress in fluorine-18 labelled peptide radiopharmaceuticals. *European journal of nuclear medicine* **2001,** *28* (7), 929-938.

78. Nerella, S. G.; Bhattacharya, A.; Thacker, P. S.; Tulja, S., Synthetic methodologies and PET imaging applications of fluorine-18 radiotracers: a patent review. *Expert Opinion on Therapeutic Patents* **2022,** (just-accepted).

79. Jacobson, O.; Kiesewetter, D. O.; Chen, X., Fluorine-18 radiochemistry, labeling strategies and synthetic routes. *Bioconjugate chemistry* **2015,** *26* (1), 1-18.

80. L Cole, E.; N Stewart, M.; Littich, R.; Hoareau, R.; JH Scott, P., Radiosyntheses using fluorine-18: the art and science of late stage fluorination. *Current topics in medicinal chemistry* **2014,** *14* (7), 875-900.

81. Kettenbach, K.; Schieferstein, H.; Ross, T. L., ^{18}F-Labeling Using Click Cycloadditions. *BioMed Research International* **2014,** *2014*, 1-16.

82. HM, A.; IZ, K., The localization of intracranial space-occupying lesions by fluoroborate ions labelled with fluorine 18. *The American Journal of Roentgenology, Radium Therapy, and Nuclear Medicine* **1962,** *88*, 350-354.

83. Entzian, W.; Aronow, S.; Soloway, A.; Sweet, W., A preliminary evaluation of F18-labeled tetrafluoroborate as a scanning agent for intracranial tumors. *Journal of Nuclear Medicine* **1964,** *5* (7), 542-550.

84. Perrin, D. M., [^{18}F]-Organotrifluoroborates as radioprosthetic groups for PET imaging: from design principles to preclinical applications. *Accounts of Chemical Research* **2016,** *49* (7), 1333-1343.

85. Ting, R.; Adam, M. J.; Ruth, T. J.; Perrin, D. M., Arylfluoroborates and alkylfluorosilicates as potential PET imaging agents: high-yielding aqueous biomolecular 18F-labeling. *Journal of the American Chemical Society* **2005,** *127* (38), 13094-13095.

86. Ting, R.; Harwig, C.; auf dem Keller, U.; McCormick, S.; Austin, P.; Overall, C. M.; Adam, M. J.; Ruth, T. J.; Perrin, D. M., Toward [18F]-labeled aryltrifluoroborate radiotracers: in vivo positron emission tomography imaging of stable aryltrifluoroborate clearance in mice. *Journal of the American Chemical Society* **2008,** *130* (36), 12045-12055.

87. auf dem Keller, U.; Bellac, C. L.; Li, Y.; Lou, Y.; Lange, P. F.; Ting, R.; Harwig, C.; Kappelhoff, R.; Dedhar, S.; Adam, M. J., Novel matrix metalloproteinase inhibitor [^{18}F]marimastat-aryltrifluoroborate as a probe for in vivo positron emission tomography imaging in cancer. *Cancer research* **2010,** *70* (19), 7562-7569.

88. Li, Y.; Liu, Z.; Lozada, J.; Wong, M. Q.; Lin, K.-S.; Yapp, D.; Perrin, D. M., Single step ^{18}F-labeling of dimeric cycloRGD for functional PET imaging of tumors in mice. *Nuclear Medicine and Biology* **2013,** *40* (8), 959-966.

89. Liu, Z.; Li, Y.; Lozada, J.; Wong, M. Q.; Greene, J.; Lin, K.-S.; Yapp, D.; Perrin, D. M., Kit-like ^{18}F-labeling of RGD-^{19}F-arytrifluroborate in high yield and at extraordinarily high specific activity with preliminary in vivo tumor imaging. *Nuclear medicine and biology* **2013,** *40* (6), 841-849.

90. Liu, Z.; Pourghiasian, M.; Radtke, M. A.; Lau, J.; Pan, J.; Dias, G. M.; Yapp, D.; Lin, K. S.; Bénard, F.; Perrin, D. M., An organotrifluoroborate for broadly applicable one-step ^{18}F-labeling. *Angewandte Chemie* **2014,** *126* (44), 12070-12074.

91. Liu, Z.; Lin, K.-S.; Bénard, F.; Pourghiasian, M.; Kiesewetter, D. O.; Perrin, D. M.; Chen, X., One-step 18F labeling of biomolecules using organotrifluoroborates. *Nature protocols* **2015,** *10* (9), 1423-1432.

92. Liu, Z.; Chen, H.; Chen, K.; Shao, Y.; Kiesewetter, D. O.; Niu, G.; Chen, X., Boramino acid as a marker for amino acid transporters. *Science advances* **2015,** *1* (8), e1500694.

93. Rosenthal, M.; Bosch, A.; Nickles, R.; Gatley, S., Synthesis and some characteristics of no-carrier added [^{18}F]fluorotrimethylsilane. *The International journal of applied radiation and isotopes* **1985,** *36* (4), 318-319.

94. Schirrmacher, R.; Bradtmöller, G.; Schirrmacher, E.; Thews, O.; Tillmanns, J.; Siessmeier, T.; Buchholz, H. G.; Bartenstein, P.; Wängler, B.; Niemeyer, C. M., ^{18}F-labeling of peptides by means of an organosilicon-based fluoride acceptor. *Angewandte Chemie International Edition* **2006,** *45* (36), 6047-6050.

95. Schirrmacher, R.; Bradtmöller, G.; Schirrmacher, E.; Thews, O.; Tillmanns, J.; Siessmeier, T.; Buchholz, H. G.; Bartenstein, P.; Wängler, B.; Niemeyer, C. M., ^{18}F-Markierung von Peptiden mithilfe eines Organosilicium-Fluoridacceptors. *Angewandte Chemie* **2006,** *118* (36), 6193-6197.

96. Hazari, P. P.; Schulz, J.; Vimont, D.; Chadha, N.; Allard, M.; Szlosek-Pinaud, M.; Fouquet, E.; Mishra, A. K., A new SiF–dipropargyl glycerol scaffold as a versatile prosthetic group to design dimeric radioligands: Synthesis of the [^{18}F]BMPPSiF tracer to image serotonin receptors. *Chem Med Chem* **2014,** *9* (2), 337-349.

97. Lang, L.; Li, W.; Guo, N.; Ma, Y.; Zhu, L.; Kiesewetter, D. O.; Shen, B.; Niu, G.; Chen, X., Comparison study of [^{18}F]FAl-NOTA-PRGD2, [^{18}F]FPPRGD2, and [^{68}Ga]Ga-NOTA-PRGD2 for PET imaging of U87MG tumors in mice. *Bioconjugate chemistry* **2011,** *22* (12), 2415-2422.

98. Chen, Q.; Meng, X.; McQuade, P.; Rubins, D.; Lin, S.-A.; Zeng, Z.; Haley, H.; Miller, P.; González Trotter, D.; Low, P. S., Synthesis and preclinical evaluation of folate-NOTA-Al^{18}F for PET imaging of folate-receptor-positive tumors. *Molecular pharmaceutics* **2016,** *13* (5), 1520-1527.

99. Sletten, E. M.; Bertozzi, C. R., Bioorthogonal Chemistry: Fishing for Selectivity in a Sea of Functionality. *Angewandte Chemie International Edition* **2009,** *48* (38), 6974-6998.

100. Rostovtsev, V. V.; Green, L. G.; Fokin, V. V.; Sharpless, K. B., A stepwise huisgen cycloaddition process: copper (I)-catalyzed regioselective "ligation" of azides and terminal alkynes. *Angewandte Chemie* **2002,** *114* (14), 2708-2711.

101. Tornøe, C. W.; Christensen, C.; Meldal, M., Peptidotriazoles on solid phase:[1, 2, 3]-triazoles by regiospecific copper (I)-catalyzed 1, 3-dipolar cycloadditions of terminal alkynes to azides. *The Journal of organic chemistry* **2002,** *67* (9), 3057-3064.

102. Marik, J.; Sutcliffe, J. L., Click for PET: rapid preparation of [^{18}F]fluoropeptides using CuI catalyzed 1, 3-dipolar cycloaddition. *Tetrahedron Letters* **2006,** *47* (37), 6681-6684.

103. Sirion, U.; Kim, H. J.; Lee, J. H.; Seo, J. W.; Lee, B. S.; Lee, S. J.; Oh, S. J.; Chi, D. Y., An efficient F-18 labeling method for PET study: Huisgen 1, 3-dipolar cycloaddition of bioactive substances and F-18-labeled compounds. *Tetrahedron letters* **2007,** *48* (23), 3953-3957.

104. Glaser, M.; Årstad, E., "Click labeling" with 2-[^{18}F]fluoroethylazide for positron emission tomography. *Bioconjugate chemistry* **2007,** *18* (3), 989-993.

105. Kobus, D.; Giesen, Y.; Ullrich, R.; Backes, H.; Neumaier, B., A fully automated two-step synthesis of an 18F-labelled tyrosine kinase inhibitor for EGFR kinase activity imaging in tumors. *Applied Radiation and Isotopes* **2009,** *67* (11), 1977-1984.

106. Thonon, D.; Kech, C.; Paris, J.; Lemaire, C.; Luxen, A., New strategy for the preparation of clickable peptides and labeling with 1-(azidomethyl)-4-[^{18}F]-fluorobenzene for PET. *Bioconjugate chemistry* **2009,** *20* (4), 817-823.

107. Chun, J.-H.; Pike, V. W., Single-Step Radiosynthesis of "18F-Labeled Click Synthons" from Azide-Functionalized Diaryliodonium Salts. *European Journal of Organic Chemistry* **2012,** *2012* (24), 4541-4547.

108. Mercier, F.; Paris, J.; Kaisin, G.; Thonon, D.; Flagothier, J.; Teller, N.; Lemaire, C.; Luxen, A., General Method for Labeling siRNA by Click Chemistry with Fluorine-18 for the Purpose of PET Imaging. *Bioconjugate Chemistry* **2011,** *22* (1), 108-114.

109. Jacobson, O.; Weiss, I. D.; Wang, L.; Wang, Z.; Yang, X.; Dewhurst, A.; Ma, Y.; Zhu, G.; Niu, G.; Kiesewetter, D. O.; Vasdev, N.; Liang, S. H.; Chen, X., ^{18}F-Labeled Single-Stranded DNA Aptamer for PET Imaging of Protein Tyrosine Kinase-7 Expression. *Journal of Nuclear Medicine* **2015,** *56* (11), 1780.

110. Glaser, M.; Årstad, E.; Gaeta, A.; Nairne, J.; Trigg, W.; Robins, E. G., Copper-mediated reduction of 2-[^{18}F]fluoroethyl azide to 2-[^{18}F]fluoroethylamine. *Journal of Labelled Compounds and Radiopharmaceuticals* **2012,** *55* (9), 326-331.

111. Ramenda, T.; Bergmann, R.; Wuest, F., Synthesis of ^{18}F-labeled neurotensin (8-13) via copper-mediated 1, 3-dipolar [3+2] cycloaddition reaction. *Letters in Drug Design & Discovery* **2007,** *4* (4), 279-285.

112. Ramenda, T.; Kniess, T.; Bergmann, R.; Steinbach, J.; Wuest, F., Radiolabelling of proteins with fluorine-18 via click chemistry. *Chemical communications* **2009,** (48), 7521-7523.

113. Ramenda, T.; Steinbach, J.; Wuest, F., 4-[^{18}F] Fluoro-N-methyl-N-(propyl-2-yn-1-yl) benzenesulfonamide ([^{18}F] F-SA): a versatile building block for labeling of peptides, proteins and

oligonucleotides with fluorine-18 via Cu (I)-mediated click chemistry. *Amino Acids* **2013,** *44* (4), 1167-1180.

114. Inkster, J. A.; Guérin, B.; Ruth, T. J.; Adam, M. J., Radiosynthesis and bioconjugation of [^{18}F] FPy5yne, a prosthetic group for the ^{18}F labeling of bioactive peptides. *Journal of Labelled Compounds and Radiopharmaceuticals: The Official Journal of the International Isotope Society* **2008,** *51* (14), 444-452.

115. Blomquist, A. T.; Liu, L. H., Many-Membered Carbon Rings .7. Cyclooctyne. *Journal of the American Chemical Society* **1953,** *75* (9), 2153-2154.

116. Dommerholt, J.; Rutjes, F. P. J. T.; Van Delft, F. L., Strain-Promoted 1,3-Dipolar Cycloaddition of Cycloalkynes and Organic Azides. Springer International Publishing: 2016; 57-76.

117. Arumugam, S.; Chin, J.; Schirrmacher, R.; Popik, V. V.; Kostikov, A. P., F-18 Azadibenzocyclooctyne (F-18 ADIBO): A biocompatible radioactive labeling synthon for peptides using catalyst free [3+2] cycloaddition. *Bioorganic & Medicinal Chemistry Letters* **2011,** *21* (23), 6987-6991.

118. Hausner, S. H.; Abbey, C. K.; Bold, R. J.; Gagnon, M. K.; Marik, J.; Marshall, J. F.; Stanecki, C. E.; Sutcliffe, J. L., Targeted In vivo Imaging of Integrin αβ with an Improved Radiotracer and Its Relevance in a Pancreatic Tumor Model. *Cancer Research* **2009,** *69* (14), 5843-5850.

119. Knight, J. C.; Richter, S.; Wuest, M.; Way, J. D.; Wuest, F., Synthesis and evaluation of an ^{18}F-labelled norbornene derivative for copper-free click chemistry reactions. *Organic & Biomolecular Chemistry* **2013,** *11* (23), 3817.

120. Selvaraj, R.; Liu, S.; Hassink, M.; Huang, C.-W.; Yap, L.-P.; Park, R.; Fox, J. M.; Li, Z.; Conti, P. S., Tetrazine-trans-cyclooctene ligation for the rapid construction of integrin αvβ3 targeted PET tracer based on a cyclic RGD peptide. *Bioorganic & Medicinal Chemistry Letters* **2011,** *21* (17), 5011-5014.

121. Devaraj, N. K.; Thurber, G. M.; Keliher, E. J.; Marinelli, B.; Weissleder, R., Reactive polymer enables efficient in vivo bioorthogonal chemistry. *Proceedings of the National Academy of Sciences* **2012,** *109* (13), 4762-4767.

122. Narayanam, M. K.; Ma, G.; Champagne, P. A.; Houk, K. N.; Murphy, J. M., Synthesis of [^{18}F]Fluoroarenes by Nucleophilic Radiofluorination ofN-Arylsydnones. *Angewandte Chemie International Edition* **2017,** *56* (42), 13006-13010.

123. Narayanam, M. K.; Lai, B. T.; Loredo, J. M.; Wilson, J. A.; Eliasen, A. M.; Laberge, N. A.; Nason, M.; Cantu, A. L.; Luton, B. K.; Xu, S.; Agnew, H. D.; Murphy, J. M., Positron Emission Tomography Tracer Design of Targeted Synthetic Peptides via ^{18}F-Sydnone Alkyne Cycloaddition. *Bioconjugate Chemistry* **2021,** *32* (9), 2073-2082.

124. Vaidyanathan, G.; Zalutsky, M. R., Labeling proteins with fluorine-18 using N-succinimidyl 4-[^{18}F]fluorobenzoate. *International Journal of Radiation Applications and Instrumentation. Part B. Nuclear Medicine and Biology* **1992,** *19* (3), 275-281.

125. Zeng, J.-L.; Wang, J.; Ma, J.-A., New Strategies for Rapid ^{18}F-Radiolabeling of Biomolecules for Radionuclide-Based In Vivo Imaging. *Bioconjugate Chemistry* **2015,** *26* (6), 1000-1003.

126. Kostikov, A. P.; Chin, J.; Orchowski, K.; Schirrmacher, E.; Niedermoser, S.; Jurkschat, K.; Iovkova-Berends, L.; Wängler, C.; Wängler, B.; Schirrmacher, R., Synthesis of [^{18}F]SiFB: a

prosthetic group for direct protein radiolabeling for application in positron emission tomography. *Nature Protocols* **2012,** *7* (11), 1956-1963.

127. Olberg, D. E.; Arukwe, J. M.; Grace, D.; Hjelstuen, O. K.; Solbakken, M.; Kindberg, G. M.; Cuthbertson, A., One Step Radiosynthesis of 6-[^{18}F]Fluoronicotinic Acid 2,3,5,6-Tetrafluorophenyl Ester ([^{18}F]F-Py-TFP): A New Prosthetic Group for Efficient Labeling of Biomolecules with Fluorine-18. *Journal of Medicinal Chemistry* **2010,** *53* (4), 1732-1740.

128. Tang, G.; Zeng, W.; Yu, M.; Kabalka, G., Facile synthesis of N-succinimidyl 4-[^{18}F]fluorobenzoate ([^{18}F]SFB) for protein labeling. *Journal of Labelled Compounds and Radiopharmaceuticals* **2008,** *51* (1), 68-71.

129. Zettlitz, K. A.; Tavaré, R.; Tsai, W.-T. K.; Yamada, R. E.; Ha, N. S.; Collins, J.; Van Dam, R. M.; Timmerman, J. M.; Wu, A. M., ^{18}F-labeled anti-human CD20 cys-diabody for same-day immunoPET in a model of aggressive B cell lymphoma in human CD20 transgenic mice. *European Journal of Nuclear Medicine and Molecular Imaging* **2019,** *46* (2), 489-500.

130. Glaser, M.; Morrison, M.; Solbakken, M.; Arukwe, J.; Karlsen, H.; Wiggen, U.; Champion, S.; Kindberg, G. M.; Cuthbertson, A., Radiosynthesis and Biodistribution of Cyclic RGD Peptides Conjugated with Novel [^{18}F]Fluorinated Aldehyde-Containing Prosthetic Groups. *Bioconjugate Chemistry* **2008,** *19* (4), 951-957.

131. Ochtrop, P.; Hackenberger, C. P. R., Recent advances of thiol-selective bioconjugation reactions. *Current Opinion in Chemical Biology* **2020,** *58*, 28-36.

132. Toyokuni, T.; Walsh, J. C.; Dominguez, A.; Phelps, M. E.; Barrio, J. R.; Gambhir, S. S.; Satyamurthy, N., Synthesis of a New Heterobifunctional Linker, N-[4-(Aminooxy)butyl]maleimide, for Facile Access to a Thiol-Reactive ^{18}F-Labeling Agent. *Bioconjugate Chemistry* **2003,** *14* (6), 1253-1259.

133. Berndt, M.; Pietzsch, J.; Wuest, F., Labeling of low-density lipoproteins using the ^{18}F-labeled thiol-reactive reagent N-[6-(4-[^{18}F]fluorobenzylidene)aminooxyhexyl]maleimide. *Nuclear Medicine and Biology* **2007,** *34* (1), 5-15.

134. Li, X.; Link, J. M.; Stekhova, S.; Yagle, K. J.; Smith, C.; Krohn, K. A.; Tait, J. F., Site-Specific Labeling of Annexin V with F-18 for Apoptosis Imaging. *Bioconjugate Chemistry* **2008,** *19* (8), 1684-1688.

135. de Bruin, B.; Kuhnast, B.; Hinnen, F.; Yaouancq, L.; Amessou, M.; Johannes, L.; Samson, A.; Boisgard, R.; Tavitian, B.; Dollé, F., 1-[3-(2-[^{18}F]Fluoropyridin-3-yloxy)propyl]pyrrole-2,5-dione: Design, Synthesis, and Radiosynthesis of a New [^{18}F]Fluoropyridine-Based Maleimide Reagent for the Labeling of Peptides and Proteins. *Bioconjugate Chemistry* **2005,** *16* (2), 406-420.

136. Denholt, C. L.; Kuhnast, B.; Dollé, F.; Hinnen, F.; Hansen, P. R.; Gillings, N.; Kjær, A., Fluorine-18 labelling of a series of potential EGFRvIII targeting peptides with a parallel labelling approach using [^{18}F]FPyME. *Journal of Labelled Compounds and Radiopharmaceuticals* **2010,** *53* (13), 774-778.

137. Yue, X.; Kiesewetter, D. O.; Guo, J.; Sun, Z.; Zhang, X.; Zhu, L.; Niu, G.; Ma, Y.; Lang, L.; Chen, X., Development of a New Thiol Site-Specific Prosthetic Group and Its Conjugation with [Cys40]-exendin-4 for in Vivo Targeting of Insulinomas. *Bioconjugate Chemistry* **2013,** *24* (7), 1191-1200.

138. Yue, X.; Yan, X.; Wu, C.; Niu, G.; Ma, Y.; Jacobson, O.; Shen, B.; Kiesewetter, D. O.; Chen, X., One-Pot Two-Step Radiosynthesis of a New 18F-Labeled Thiol Reactive Prosthetic Group and Its Conjugate for Insulinoma Imaging. *Molecular Pharmaceutics* **2014,** *11* (11), 3875-3884.

139. Inkster, J. A. H.; Liu, K.; Ait-Mohand, S.; Schaffer, P.; Guérin, B.; Ruth, T. J.; Storr, T., Sulfonyl Fluoride-Based Prosthetic Compounds as Potential 18F Labelling Agents. *Chemistry – A European Journal* **2012,** *18* (35), 11079-11087.

140. Ravasco, J. M. J. M.; Faustino, H.; Trindade, A.; Gois, P. M. P., Bioconjugation with Maleimides: A Useful Tool for Chemical Biology. *Chemistry – A European Journal* **2019,** *25* (1), 43-59.

141. Koniev, O.; Wagner, A., Developments and recent advancements in the field of endogenous amino acid selective bond forming reactions for bioconjugation. *Chem. Soc. Rev.* **2015,** *44* (15), 5495-5551.

142. Eaton, W. D.; Hulett, J.; Brunson, R.; True, K., The First Isolation in North America of Infectious, Hematopoietic Necrosis Virus (IHNV) and Viral Hemorrhagic Septicemia Virus (VHSV) in Coho Salmon from the Same Watershed. *Journal of Aquatic Animal Health* **1991,** *3* (2), 114-117.

143. Shen, B.-Q.; Xu, K.; Liu, L.; Raab, H.; Bhakta, S.; Kenrick, M.; Parsons-Reponte, K. L.; Tien, J.; Yu, S.-F.; Mai, E.; Li, D.; Tibbitts, J.; Baudys, J.; Saad, O. M.; Scales, S. J.; McDonald, P. J.; Hass, P. E.; Eigenbrot, C.; Nguyen, T.; Solis, W. A.; Fuji, R. N.; Flagella, K. M.; Patel, D.; Spencer, S. D.; Khawli, L. A.; Ebens, A.; Wong, W. L.; Vandlen, R.; Kaur, S.; Sliwkowski, M. X.; Scheller, R. H.; Polakis, P.; Junutula, J. R., Conjugation site modulates the in vivo stability and therapeutic activity of antibody-drug conjugates. *Nature Biotechnology* **2012,** *30* (2), 184-189.

144. Adumeau, P.; Davydova, M.; Zeglis, B. M., Thiol-Reactive Bifunctional Chelators for the Creation of Site-Selectively Modified Radioimmunoconjugates with Improved Stability. *Bioconjugate Chemistry* **2018,** *29* (4), 1364-1372.

145. Dolle, F.; Hinnen, F.; Vaufrey, F.; Tavitian, B.; Crouzel, C., A general method for labeling oligodeoxynucleotides with ^{18}F for in vivo PET imaging. *Journal of Labelled Compounds and Radiopharmaceuticals* **1997,** *39* (4), 319-330.

146. Kuhnast, B.; de Bruin, B.; Hinnen, F.; Tavitian, B.; Dollé, F., Design and Synthesis of a New [^{18}F]Fluoropyridine-Based Haloacetamide Reagent for the Labeling of Oligonucleotides: 2-Bromo-N-[3-(2-[^{18}F]fluoropyridin-3-yloxy)propyl]acetamide. *Bioconjugate Chemistry* **2004,** *15* (3), 617-627.

147. Shangguan, D.; Li, Y.; Tang, Z.; Cao, Z. C.; Chen, H. W.; Mallikaratchy, P.; Sefah, K.; Yang, C. J.; Tan, W., Aptamers evolved from live cells as effective molecular probes for cancer study. *Proceedings of the National Academy of Sciences* **2006,** *103* (32), 11838-11843.

148. Wu, Z.; Li, L.; Liu, S.; Yakushijin, F.; Yakushijin, K.; Horne, D.; Conti, P. S.; Li, Z.; Kandeel, F.; Shively, J. E., Facile Preparation of a Thiol-Reactive ^{18}F-Labeling Agent and Synthesis of ^{18}F-DEG-VS-NT for PET Imaging of a Neurotensin Receptor–Positive Tumor. *Journal of Nuclear Medicine* **2014,** *55* (7), 1178-1184.

149. Zhang, T.; Cai, J.; Wang, H.; Wang, M.; Yuan, H.; Wu, Z.; Ma, X.; Li, Z., RXH-Reactive ^{18}F-Vinyl Sulfones as Versatile Agents for PET Probe Construction. *Bioconjugate Chemistry* **2020,** *31* (11), 2482-2487.

150. Tilden, J. A. R.; Lubben, A. T.; Reeksting, S. B.; Kociok-Köhn, G.; Frost, C. G., Pd(II)-Mediated C−H Activation for Cysteine Bioconjugation. *Chemistry – A European Journal* **2022**.

CHAPTER 3: One-Step Synthesis of [^{18}F]Fluoro-4-(vinylsulfonyl)benzene: A Thiol Reactive Synthon for Selective Radiofluorination of Peptides

Gaoyuan Ma,[§] James W. McDaniel,[§] and Jennifer M. Murphy

Org. Lett. **2021**, *23*, 2, 530–534.

[§] G.M. and J.W.M. contributed equally to this work.

3.1. Abstract

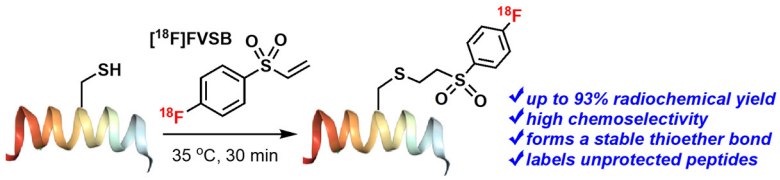

Radiolabeled peptide-based molecular imaging probes exploit the advantages of large biologics and small molecules, providing both exquisite selectivity and favorable pharmacokinetic properties. Here, we report an operationally simple and broadly applicable approach for the ^{18}F-fluorination of unprotected peptides via a new radiosynthon, [^{18}F]fluoro-4-(vinylsulfonyl)benzene. This reagent demonstrates excellent chemoselectivity at the cysteine residue and rapid ^{18}F-labeling of a diverse scope of peptides to generate stable thioether constructs.

3.2. Introduction

Radiolabeled peptides are important positron emission tomography (PET) imaging tools due to their selectivity toward overexpressed cell surface receptors of many cancers, which can be exploited for targeting purposes.[1-5] Critical to the continued development of valuable PET probes

is the availability of chemical methods to access diverse radiolabeled peptides. Remarkable breakthroughs in ^{18}F-chemistry to afford ^{18}F-labeled peptides with minimal perturbation have unveiled direct synthetic paths toward previously inaccessible radiolabeled peptides.[6-10] Despite recent advances in site-specific radiofluorination, ^{18}F-labeling of peptides is most frequently conducted via conjugation with prosthetic groups.[11-16]

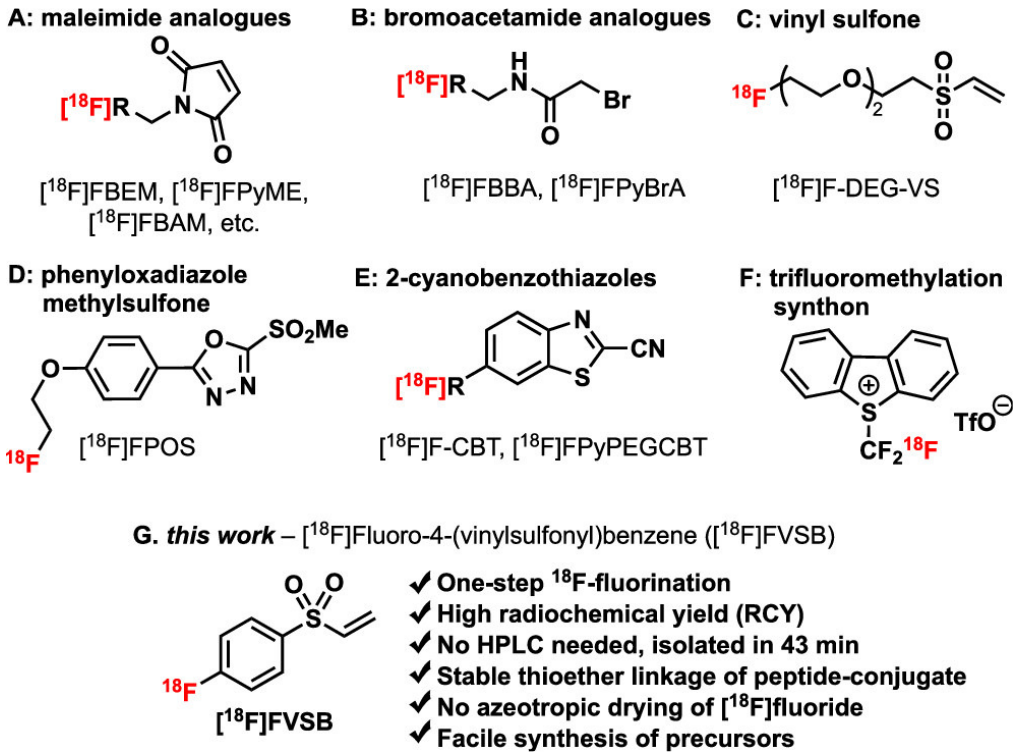

Figure 3.1. Thiol reactive radiosynthons for ^{18}F-labeling of cysteine containing peptides.

Selective bioconjugation reactions for ^{18}F-labeling of peptides have largely focused around modification of lysine and cysteine side chains.[17, 18] Site-selective conjugation via thiol-based chemistry is more desirable when compared to unselective modification of lysine residues, which can produce poorly defined, heterogeneous mixtures of labeled products.[19, 20] A powerful tool for site-specific bioconjugation to cysteine and perhaps the most utilized prosthetic group for selective

^{18}F-labeling of peptides is the maleimide-based synthon.[13, 21-25] Maleimide-based prosthetic groups (***Figure 3.1A***) have garnered persistent popularity due to their fast kinetics and remarkable cysteine chemoselectivity; however, significant limitations exist, the most notable being susceptibility of the succinimidyl thioether linkage to hydrolysis via a retro-Michael reaction.[18, 26-28] Furthermore, bioconjugation with maleimide-based prosthetic groups creates stereoisomeric mixtures of *exo*- and *endo*-isomers.[29] In addition, many of these synthons involve three-step syntheses, are obtained in <20% radiochemical yield (RCY), and expend 95–115 min to obtain the HPLC-purified prosthetic group.[21-23]

Several other radiosynthons have been reported for site-selective cysteine conjugation via thiol alkylation (***Figure 3.1***). Despite moderate success, bromoacetamides require three step syntheses, azeotropic drying of [^{18}F]fluoride and HPLC purification, resulting in a lengthy production process.[30-32] Reported in 2014, [^{18}F]-(2-(2-(2-fluoroethoxy)ethoxy)ethylsulfonyl)-ethane ([^{18}F]F-DEG-VS) was utilized to label a neurotensin analogue in moderate yield and maintained *in vivo* stability with no [^{18}F]fluoride release.[33] More recently, prosthetic groups based on heteroaromatic derivatives provide an alternative class of thiol-reactive synthons with improved stability over maleimides (***Figure 3.1D,E***).[34-37] In addition, a new reagent for ^{18}F-trifluoromethylation has demonstrated chemoselective ^{18}F-labeling of cysteine-containing peptides, including a [^{18}F]CF_3-amyloid-β fragment (***Figure 3.1F***).[9] Despite remarkable advancements, preparation of current thiol-reactive radiosynthons require azeotropic drying of [^{18}F]fluoride and nearly all protocols involve HPLC purification prior to cysteine conjugation. In addition, multistep syntheses or the use of unstable precursors and reagents pose further challenges, resulting in low yields. A robust thiol-reactive synthon that produces a selective and

stable linkage while overcoming these limitations offers an attractive alternative approach for peptide ^{18}F-labeling applications.

Here, we report the synthesis and development of [^{18}F]fluoro-4-(vinylsulfonyl)benzene ([^{18}F]FVSB), a new prosthetic group for site-specific conjugation to cysteine residues to afford stable ^{18}F-labeled peptides for applications in PET molecular imaging (***Figure 3.1G***). This radiosynthon is prepared in one step, enabled by the deoxyfluorination of a highly stable uronium precursor via a tetrahedral intermediate, and is utilized without azeotropic drying or HPLC purification. Our objective was to provide a readily accessible thiol-reactive synthon for the facile construction of stable, site-specific ^{18}F-labeled peptide conjugates. Critical advantages of a vinyl sulfone motif for cysteine conjugation include the high reactivity with free thiols and the formation of aqueous-stable thioether linkages.[18, 38-42] Although reports of vinyl sulfone-functionalized tags toward bioconjugation of peptides and proteins exist, the versatility of this synthon has not been fully explored in the context of ^{18}F-labeling.[41] We designed a vinyl sulfonyl phenol substrate and opted to employ the ^{18}F-deoxyfluorination method reported by Neumann *et al*.[6] This methodology was chosen due to its robust scope, high radiochemical conversion, use of a stable and accessible precursor, as well as the ability to eliminate azeotropic drying. We anticipated this approach would provide a direct path to a vinyl sulfonyl ^{18}F-arene in a rapid manner.

3.3. Results and Discussion

Preparation of the precursor, uronium **3.6**, consists of a five-step synthesis and began with commercial thiophenol **3.1**, which underwent alkylation with bromoethanol followed by oxidation with Oxone to afford sulfone **3.3** (***Scheme 3.1***). Treatment with thionyl chloride and pyridine supplied the chloro intermediate which subsequently underwent elimination under basic conditions

to furnish vinyl sulfone **3.4** in 81% yield. Uronium precursor **3.6** was obtained upon treatment of phenol **3.4** with chloroimidazolium chloride and Ag_2CO_3 in chloroform and used after simple filtration with no additional purification.[6]

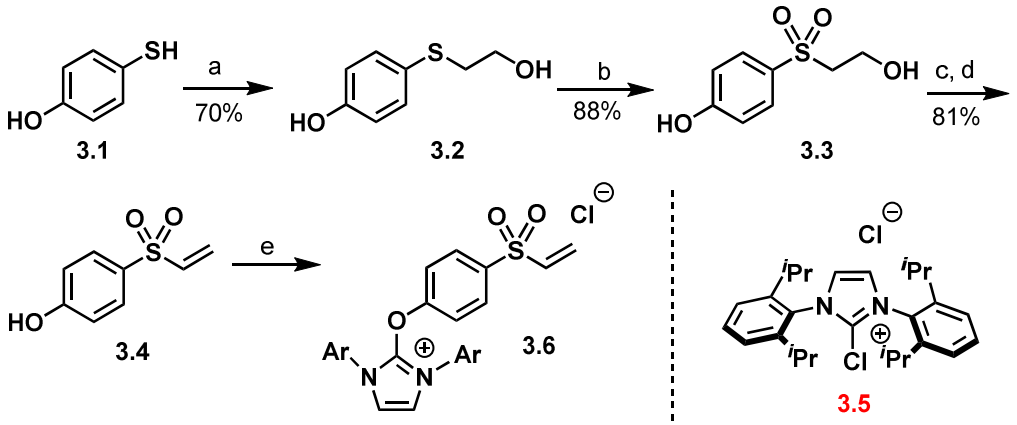

Scheme 3.1. Reagents and conditions: a) 2-bromoethanol, 1.0 N aq. NaOH, MeOH, 23 °C, 21 h; b) OXONE®, MeOH, 23 °C, 2 h; c) $SOCl_2$, pyridine, CH_2Cl_2, 23 °C, 20 h; d) Et_3N, THF, 23 °C, 24 h; e) Ag_2CO_3, **3.5**, $CHCl_3$, 60 °C, 4.5 h.

The ^{18}F-deoxyfluorination to produce [^{18}F]FVSB **3.7** began with direct elution of aqueous [^{18}F]fluoride from the anion-exchange cartridge, forgoing the azeotropic drying step of conventional radiofluorination approaches (***Table 3.1***). In this method, aqueous [^{18}F]fluoride was trapped on the cartridge and residual water was removed by flushing with 2-butanone/ethanol (10:1, v/v) and N_2 gas through the cartridge. Uronium complex **3.6** in a solution of 2-butanone:ethanol was directly passed through the cartridge, without base or additives, to elute the [^{18}F]fluoride. The reaction mixture was directly heated to 130 °C for 30 min and afforded crude [^{18}F]FVSB **3.7**. Initial optimization focused on the type of anion exchange cartridge and the uronium **3.6** precursor amounts. [^{18}F]Fluoride elution using a Sep-Pak Accell Plus QMA plus light

cartridge was poor, presumably due to excess resin. Improvement in the elution was observed with a custom-made cartridge using 1/16″ PTFE tubing containing 4 mg Biorad MP-1 resin in between two polyethylene frits. Despite moderate elution, inconsistency in the custom cartridges led us to identify a more practical approach that would use a commercial cartridge. Chromafix 30-PS-HCO_3 cartridges were employed which gave sufficiently high elution efficiency using 5 mg of uronium **3.6** with 94 ± 2% RCY, determined by radio-TLC (***Table 3.1*** entry 2). While 3 mg of uronium **3.6** gave poor [^{18}F]fluoride elution, no improvement in elution efficiency and comparable RCY was obtained when >5 mg of **3.6** was used (***Table 3.1.*** entries 1, 3, and 4).

Table 3.1. Reaction Optimization to Afford **[^{18}F]FVSB**[a]. Product identity was confirmed by radio-HPLC coinjection with the verified reference standard **^{19}F-3.7**. Ar = 2,6-diisopropylphenyl.

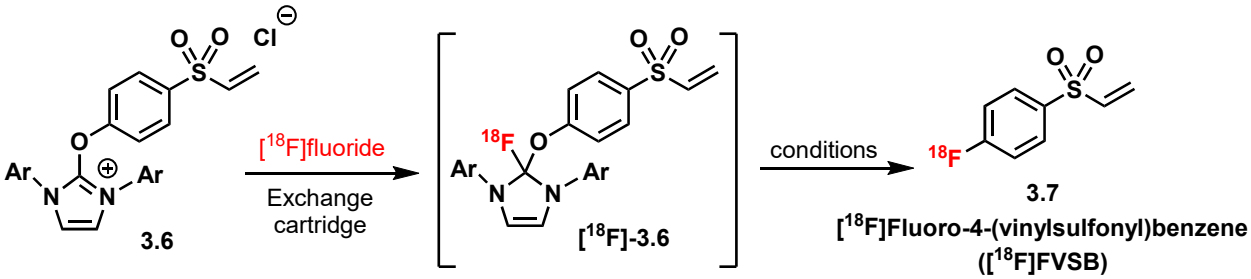

entry[a]	precursor (mg)	elution efficiency[b]	RCY[c]
1	3	60 ± 3%	88 ± 4%[d]
2	5	84 ± 3%	94 ± 2%[e]
3	7	84 ± 2%	97 ± 1%[e]
4	9	83 ± 1%	96 ± 2%[d]

[a] Conditions: precursor, [^{18}F]fluoride (~500 μCi), 10:1 butanone:EtOH (1 mL), 130 °C, 30 min. [b] determined by dividing the activity eluted from the cartridge by the initial activity loaded on the cartridge. [c] determined by radio-TLC. [d] n = 2. [e] n = 5.

We hypothesized that HPLC purification could be avoided and that [^{18}F]FVSB may be promptly utilized for peptide conjugation. We next focused on cartridge purification of [^{18}F]FVSB

and screened various commercial cartridges (***Table 3.6***). Purification by Oasis HLB plus short LP cartridges resulted in removal of unreacted [^{18}F]fluoride and enabled isolation of [^{18}F]FVSB within 43 min in 46 ± 4% decay-corrected RCY with 85% radiochemical purity (RCP) (***Table 3.3***, ***Table 3.4***, ***Figure 3.13***, and ***Figure 3.14***). The molar activity was calculated for HPLC-purified [^{18}F]FVSB and determined to be >2.87 Ci·μmol^{-1} (106.2 GBq·μmol^{-1}). Notably, precursor **3.6** could be stored at −4 °C for up to 12 months or at room temperature for up to 6 months and used with no discernible loss in quality or RCY.

Peptides containing the Arg-Gly-Asp (RGD) sequence display high affinity for integrin $\alpha_v\beta_3$ and are useful for PET molecular imaging of angiogenesis.[43] As such, we initially investigated the bioconjugation of cysteine-containing peptides with [^{18}F]FVSB **3.7** using the linear tetramer **3.8**, Arg-Gly-Asp-Cys (RGDC) (***Table 3.2***). Conjugate addition of 5 mg of peptide **3.8** to [^{18}F]FVSB **3.7** proceeded in sodium borate (pH 8.5) buffer in 30 min in 65 ± 4% RCY, as determined by radio-HPLC (entry 1). Bioconjugation in HEPES (pH 7.3) buffer afforded peptide conjugate **3.9** in 59 ± 4% RCY (entry 2). Optimization of the reaction temperature revealed that mild temperatures (23–35 °C) gave highest RCYs and heating to 45 °C decreased the RCY to 47 ± 5% (entries 1, 3, 4 and ***Table 3.8***).

In many cases, unreacted [^{18}F]FVSB **3.7** was present after 30 min yet increasing the reaction time is undesirable for PET applications. We sought to push the thiol conjugation to completion by exploring a solvent additive, such as DMF or MeOH, which may enhance peptide solubility (***Table 3.9***). With 25% MeOH, ^{18}F-labeled conjugate **3.9** was obtained in 86 ± 7% RCY in sodium borate buffer (entry 5). Too much methanol was detrimental to the reaction (entry 6), yet 50% MeOH in either buffer afforded ^{18}F-labeled conjugate **3.9** in 90 ± 0% RCY (entry 7). Comparable RCYs were obtained by lowering the peptide precursor amount to 3 mg (entry 8 and

Table 3.7). Lastly, for labeling precious peptides with limited supply, 1 mg of precursor was sufficient to afford the radiolabeled peptide conjugate in high RCY (entry 9). Although DMF could be used, we opted to employ MeOH because the peptide solubility appeared better in MeOH over DMF and, due to its lower boiling point, MeOH can be readily removed by evaporation.

Table 3.2. Bioconjugation Optimization[a]

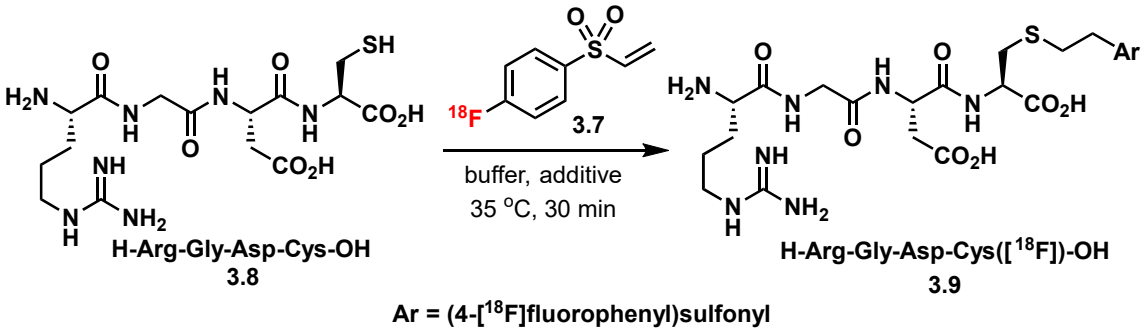

entry[a]	precursor (mg)	buffer	additive	RCY (%)[b]
1	5	borate (pH 8.5)	—	65 ± 4
2	5	HEPES (pH 7.3)	—	59 ± 4
3	5	borate (pH 8.5)	—	70 ± 7[c]
4	5	borate (pH 8.5)	—	47 ± 5[d]
5	5	borate (pH 8.5)	25% MeOH	86 ± 7
6	5	HEPES (pH 7.3)	75% MeOH	27 ± 1
7	5	borate (pH 8.5)	50% MeOH	90 ± 0
8	**3**	**borate (pH 8.5)**	**50% MeOH**	**89 ± 6**
9	1	borate (pH 8.5)	50% MeOH	79 ± 11

[a] Conditions: ~400 - 700 μCi **7** per reaction, solvent (500 μL). Reactions performed in duplicate. [b] non-isolated RCY is estimated by radio-HPLC analysis of crude peptide **9**. [c] Reaction temp. = 23 °C. [d] Reaction temp. = 45 °C. Ar = 4-[^{18}F]fluorophenyl.

The optimized bioconjugation conditions were applied to a series of thiol-containing peptides to examine the versatility of [^{18}F]FVSB toward complex substrates which mimic potential PET tracers (***Figure 3.2***). The unprotected, linear RGDC peptide **3.8** readily delivered ^{18}F-construct **3.9** in 84 ± 8% decay-corrected RCY with exclusive reactivity at the cysteine residue. An analogue of the gastrin-releasing peptide receptor (GRPR) tracer MG11 was successfully

conjugated to [^{18}F]FVSB **3.7** to afford octamer **3.10** as the single radioactive product in 83 ± 10% RCY.[44] Of note, competitive reactivity with tryptophan was not observed by radio-HPLC, verifying the indole ring of tryptophan is compatible with the labeling protocol (***Figure 3.22***).

Cyclic RGD peptides have also garnered sufficient interest as PET tracers prompting us to synthesize cyclic RGDfC analogue **3.11** which was achieved in 87 ± 2% RCY.[44, 45] Due to the recent success in targeting prostate specific membrane antigen (PSMA) for PET imaging of prostate cancer, we applied the approach toward radiolabeling of a PSMA analogue which gave construct **3.12** in 80 ± 3% RCY.[46] Synthesis of an ^{18}F-labeled neuromedin B analogue **3.13** was accomplished in 93 ± 1% RCY. Additionally, larger peptides, such as the bombesin analogue **3.14** containing 14 amino acids was successfully radiolabeled in 55 ± 11% RCY.[47] The presence of unreacted [^{18}F]FVSB in the HPLC trace for analogue **3.14** suggests that cosolvent systems to increase solubility for larger peptides could remedy the incomplete conversion for specific cases.

To reinforce the compatibility of [^{18}F]FVSB in the presence of other nucleophilic residues, such as histidine or lysine, competition studies were conducted (***Figures 3.27 – 31***). Competition between *N*-Boc-cysteine and *N*-Boc-lysine with [^{18}F]FVSB yielded, exclusively, the desired cysteine-conjugate addition product in 85 ± 0% RCY, while the lysine-conjugate addition product was not observed (***Figure 3.29***). Similarly, competition between *N*-Boc-cysteine and *N*-Boc-histidine afforded the cysteine-conjugate addition product in 88 ± 2% RCY and the histidine-conjugate addition product in only 1 ± 2% RCY (***Figure 3.31***). Importantly, these studies reveal the overwhelming predominance for bioconjugation to occur at the cysteine residue, even when histidine or lysine residues are present. Lastly, reactivity toward *N*-terminal amines was evaluated with an RGD peptide lacking a cysteine residue. In this case, with no available thiol, amine conjugation toward [^{18}F]FVSB proceeded in only 6% RCY; therefore, the presence of *N*-terminal

free amines is well tolerated and does not impede generation of the desired thiol-conjugated product (***Figure 3.32***).

To evaluate the peptide conjugates for stability against elimination of the vinyl sulfone and loss of the radiolabel, peptide **3.9** was incubated for 1 h at 35 °C in various conditions and the remaining conjugate was calculated by HPLC analysis (***Figures 3.33 – 3.36***). In aqueous glutathione or in pH 2.6 acetic acid buffer, 97% of conjugate **3.9** and 0% of [^{18}F]FVSB were observed. In pH 9.5 sodium borate buffer, 82% of conjugate **3.9** and 5% of [^{18}F]FVSB were observed. These results suggest that, after 1 h, 5% elimination of the vinyl sulfone occurs under basic conditions and no observable elimination occurs under neutral or acidic conditions.

Preliminary attempts at automation were conducted using the ELIXYS FLEX/CHEM radiochemical synthesis module (Sofie Biosciences). Starting with 21 mCi of [^{18}F]fluoride, the automated protocol resulted in an elution efficiency of 82 ± 0% and afforded [^{18}F]FVSB in 63 ± 1% RCY, determined by radio-TLC (n = 2, unoptimized), demonstrating the process can successfully be automated for PET applications.

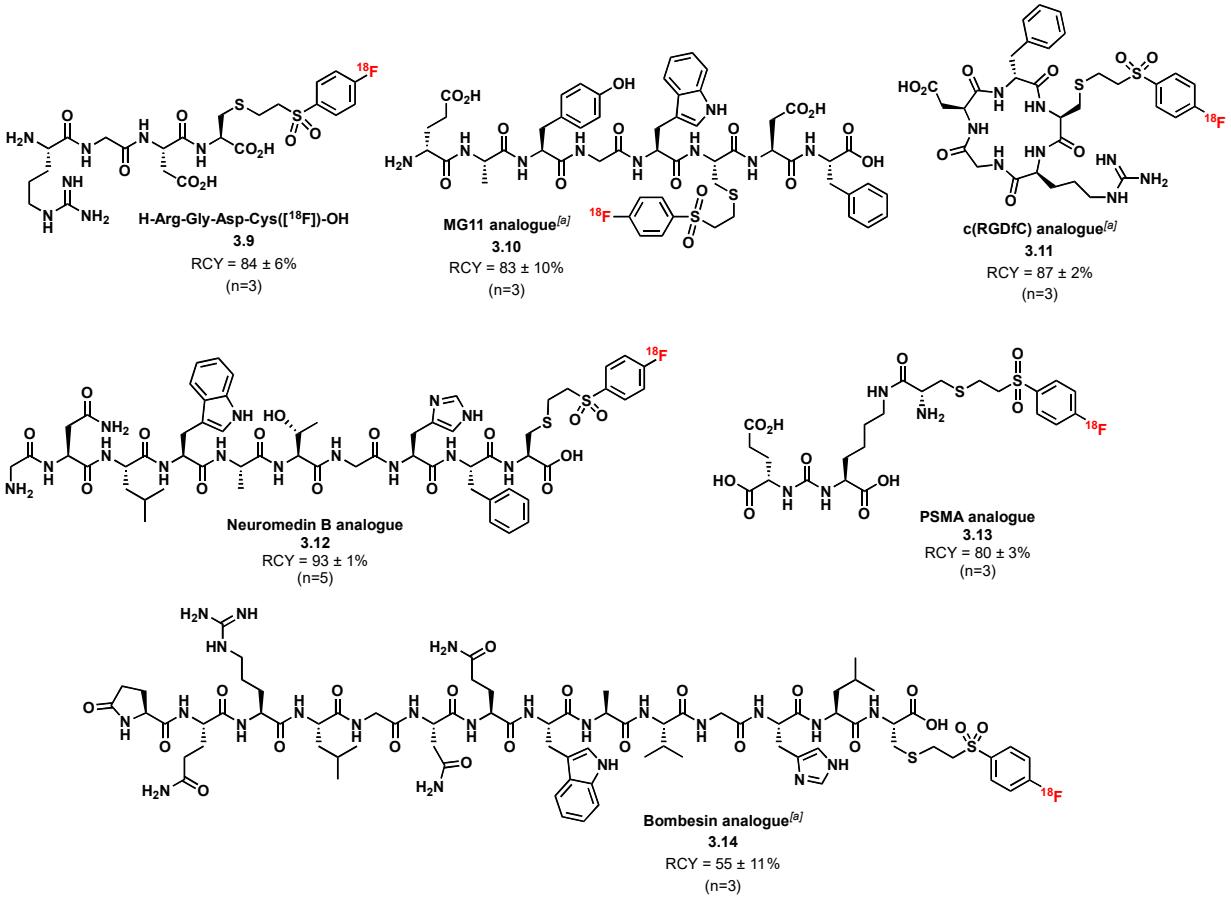

Figure 3.2. Site-selective ^{18}F-labeling of peptides via cysteine bioconjugation with [^{18}F]fluoro-4-(vinylsulfonyl)benzene. Reaction conditions: peptide (3 mg), **3.**7 (0.5−1.5 mCi), sodium borate buffer pH 8.5 (250 μL), MeOH (250 µL), 35 °C, 30 min. Radiochemical purity (RCP) was determined by radio-HPLC and was calculated by dividing the integrated area of the ^{18}F-labeled product peak by the total integrated area of all ^{18}F-labeled peaks. Identity of each labeled product was confirmed by coinjection with the authentic ^{19}F-reference standard. The decay-corrected radiochemical yield (RCY) was calculated by dividing the final activity of the labeled product by starting [^{18}F]FVSB activity, multiplied by the RCP. [a]5 mg peptide, HEPES buffer pH 7.3 (250 μL), DMF (250 μL).

3.4. Conclusions

In summary, we developed a simple, metal-free approach for ^{18}F-labeling of cysteine containing peptides via a novel prosthetic group, [^{18}F]FVSB. To our knowledge this is the first

aryl vinyl sulfone radiosynthon to be reported which can be produced in 43 min in high molar activity and directly used for peptide conjugation without HPLC purification. The robustness of our method is highlighted by the diversity of peptide conjugates that were successfully ^{18}F-labeled in up to 93% RCY. We contend that the [^{18}F]FVSB radiosynthon will offer significant improvement over current strategies for multiple reasons. First, its simplicity—our method is a one-step radiofluorination of a stable precursor that is facile to synthesize and provides [^{18}F]FVSB in high RCY. Second, conjugation to [^{18}F]FVSB yields a highly stable thioether linkage using 2 μmol peptide. Third, and perhaps most crucial, our method eliminates the time-consuming azeotropic drying and HPLC purification steps—a noteworthy benefit for fluorine-18 methodology. Additionally, exclusive reactivity at the cysteine residue in the presence of other nucleophilic residues was demonstrated, confirming the high chemoselectivity of our approach.

3.5. Experimental Section

3.5.1. Materials and Methods

All chemicals and reagents were purchased from commercial sources and used without further purification. Chloroimidazolium chloride **3.5** was purchased from Strem Chemicals, Inc. (Product No. 07-0620) and used as received. Peptides were purchased from Bachem Americas, Inc. and used as received. Silicon oil bath was used as the heating source for all non-radioactive reactions. All deuterated solvents were purchased from Cambridge Isotope Laboratories. Unless otherwise noted, reactions were carried out in oven-dried glassware using commercially available anhydrous solvents. Solvents used for extractions and chromatography were not anhydrous. Reactions and chromatography fractions were analyzed by thin-layer chromatography (TLC) using Merck precoated silica gel 60 F254 glass plates (250 μm) and visualized by ultraviolet irradiation or by staining with *para*-anisaldehyde solution. Flash column chromatography was performed using E. Merck silica gel 60 (230−400 mesh) with compressed air. NMR spectra were recorded on a Bruker ARX 400 (400 MHz for ^{1}H; 100 MHz for ^{13}C, 376 MHz for ^{19}F) or a Bruker ARX 500 (500 MHz for ^{1}H; 126 MHz for ^{13}C, 471 MHz for ^{19}F) spectrometer. Chemical shifts are reported in parts per million (ppm, δ) using the residual solvent peak as the reference. The coupling constants, , are reported in Hertz (Hz), and the multiplicity identified as the following: br (broad), s (singlet), d (doublet), t (triplet), q (quartet), hept (heptet) and m (multiplet). High-resolution electrospray mass spectrometry (ESI-HRMS) data were acquired with a Thermo Scientific™ Q-Exactive Plus Spectrometer with a quadrupole mass filter and Orbitrap mass analyzer. For some samples, high resolution mass spectra were obtained on Thermo ScientificTM Exactive Mass Spectrometer with DART ID-CUBE. Fluorine-19 reference standards were synthesized from the commercial peptides. Melting points were recorded on a Büchi melting point apparatus B-545.

3.5.2. Experimental Procedure and Characterization Data

3.5.2.1. Preparation of phenol substrate for deoxyfluorination[48, 49]

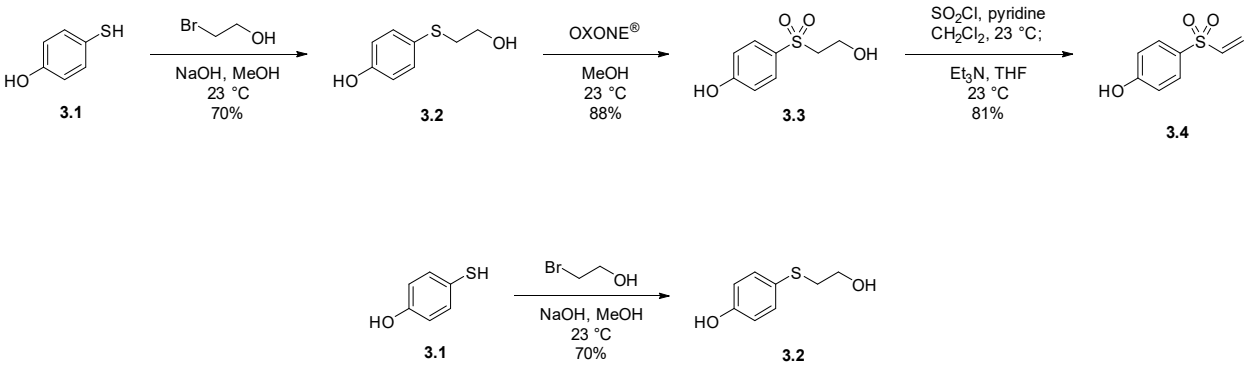

To a solution of 4-mercaptophenol **3.1** (2.0 g, 15.8 mmol) in methyl alcohol (10 mL) was added dropwise aqueous NaOH (1 N, 17.3 mL) at -5 °C over a period of 30 min. After stirring at -5 °C for 1 h, a solution of 2-bromoethanol (2.3 mL, 17.3 mmol) in methyl alcohol (7 mL) was added dropwise at -5 °C over a period of 15 min. The reaction mixture was stirred for 21 h at room temperature then concentrated to remove methanol. The crude residue was dissolved in ether (20 mL) and extracted with water (5 mL). After extraction and phase separation, the organic layer was washed with saturated $NaHCO_3$ (10 mL) and brine (10 mL). The combined organic layers were dried over Na_2SO_4, concentrated and purified by flash column chromatography (10-30% EtOAc in n-hexane) to afford 4-((2-hydroxyethyl)thio)phenol **3.2** (1.87 g, 11 mmol, 70% yield) as a white solid. ^{1}H NMR (400 MHz, DMSO-d_6, δ): 9.5 (s, 1H), 7.18 (d, J = 8.8 Hz, 2H), 6.68 (d, J = 8.4 Hz, 2H), 4.77 (t, J = 6 Hz, 1H), 3.43 (m, 2H), 2.8 (t, J = 6.8 Hz, 2H). ^{13}C NMR (100 MHz, DMSO-d_6, δ): 157.1, 133.3, 124.1, 116.5, 60.5, 37.9. HRMS (ESI-TOF) m/z: [M+Na] + Calc'd for $C_8H_{10}O_2SNa$ 193.0299; Found 193.0293. Melting point: 72 – 73 °C.

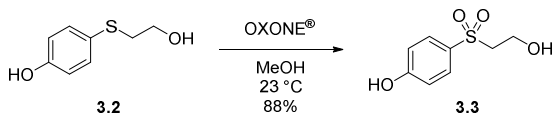

To a solution of 4-((2-hydroxyethyl)thio)phenol **3.2** (1.0 g, 5.87 mmol) in methyl alcohol (5 mL) was added slowly, OXONE® (5.43 g, 8.82 mmol) at 10 °C over 20 min. The suspension was stirred at room temperature (exothermic reaction) for 2 h and filtered. The filtrate was washed with a 38-40% (v/v) aqueous sodium hydrogen sulfite solution (0.5 mL) and the pH of the reaction mixture was adjusted to ~7.0 with 1.0 M aqueous NaOH. The suspension was filtered and the filtrate was concentrated *in vacuo*. The crude residue was purified by flash column chromatography (20-60% EtOAc in *n*-hexane) to afford 4-((2-hydroxyethyl)sulfonyl)phenol **3.3** (1.0 g, 5.20 mmol, 88% yield) as a white solid. ^{1}H NMR (400 MHz, DMSO-d$_6$, δ): 10.53 (s, 1H), 7.65 (d, J = 8.8 Hz, 2H), 6.9 (d, J = 8.8 Hz, 2H), 4.8 (t, J = 5.2 Hz, 1H), 3.6 (m, 2H), 3.29-3.27 (m, 2H). ^{13}C NMR (100 MHz, DMSO-d$_6$, δ): 162.5, 130.5, 130.1, 116.1, 58.4, 55.6. HRMS (ESI-TOF) m/z: [M+Na] + Calc'd for $C_8H_{10}O_4SNa$ 225.0197; Found 225.0190. Melting point: 106 – 109 °C.

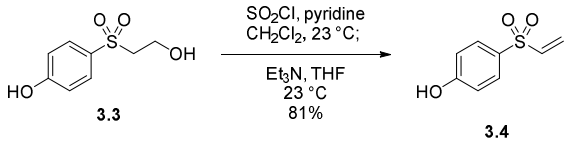

To a solution of 4-((2-hydroxyethyl)sulfonyl)phenol **3.3** (1.0 g, 5.19 mmol) in CH_2Cl_2 (6 mL) was added pyridine (0.8 mL, 10 mmol) at room temperature. The reaction mixture was cooled to 0 °C and a solution of thionyl chloride (0.64 mL, 8.8 mmol) in CH_2Cl_2 (5 mL) was added dropwise over 15 min. After stirring at room temperature for 20 h the reaction mixture was diluted with 1 mL brine and the suspension was extracted. The combined organic layers were washed with brine (2 x 2 mL), dried over Na_2SO_4 and concentrated *in vacuo* to afford 4-((2-chloroethyl)sulfonyl)phenol which was used directly without purification. To a solution of 4-((2-chloroethyl)sulfonyl)phenol

(0.8 g, 3.6 mmol) in THF (8 mL) was added triethylamine (0.76 mL, 5.4 mmol) in THF (5 mL) at room temperature. The reaction mixture was stirred for 24 h at room tempterature and a precipitate formed**.** Triethylamine hydrochloride salt was filtered and the colorless filtrate was concentrated *in vacuo*. The crude solid was purified by flash column chromatography (5-30% EtOAc in *n*-hexane) to give 4-(vinylsulfonyl)phenol **3.4** (0.53 g, 2.90 mmol, 81% yield) as a white solid. ^{1}H NMR (400 MHz, DMSO-d_6, δ): 10.62 (s, 1H), 7.63 (d, *J* = 8.8 Hz, 2H), 6.97 (dd, *J* = 16.4, 9.6 Hz, 2H), 6.92 (d, *J* = 8.8 Hz, 1H), 6.17 (d, *J* = 16.8 Hz, 1H), 6.04 (d, *J* = 9.6 Hz, 1H). ^{13}C NMR (100 MHz, DMSO-d_6, δ): 162.7, 139.9, 130.4, 129.5, 127.2, 116.5. HRMS (ESI-TOF) m/z: [M+Na] + Calc'd for $C_8H_8O_3SNa$ 207.0092; Found 207.0084. Melting point: 64 – 66 °C.

3.5.2.2. Preparation of vinyl sulfone uronium precursor 3.6 for radiolabeleing[50]

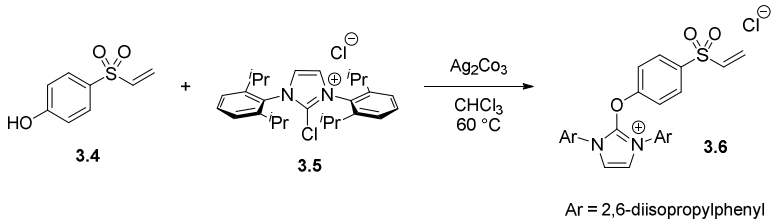

To a 4 ml vial containing 4-(vinylsulfonyl)phenol **3.4** (0.2 mmol, 36 mg), chloroimidazolium chloride **3.5** (0.2 mmol, 90 mg) and silver carbonate (0.1 mmol, 26 mg), was added chloroform (1.5 mL) and the resulting suspension left to stir at 60 °C for 4.5 hours. The precipitate was removed by filtration and the filtrate was concentrated to obtain the labeling precursor **3.6** (0.16 mmol, 95 mg, 80%) as a white solid. Precursor **3.6** was used for ^{18}F-deoxyfluorination without further purification. ^{1}H NMR (500 MHz, $CDCl_3$, δ): 8.43 (s, 2H), 7.70 (d, *J* = 9 Hz, 2H), 7.56 (t, *J* = 7.5 Hz, 2H), 7.30 (d, *J* = 7.5 Hz, 4H), 6.67 (d, *J* = 9 Hz, 2H), 6.51-6.40 (m, 2H), 6.08 (d, *J* = 9 Hz, 1H), 2.49 (hept, *J* = 6.5 Hz, 4H), 1.30 (d, *J* = 6.5 Hz, 12H), 1.18 (d, *J* = 6.5 Hz, 12H). ^{13}C NMR (100 MHz, $CDCl_3$, δ): 156.4, 145.3, 143.0, 139.0, 137.4, 132.8, 130.9, 129.6, 127.0, 125.3,

124.1, 118.4, 29.6, 25.8, 22.9. HRMS (ESI-TOF) m/z: [M-Cl] + Calc'd for $C_{35}H_{43}N_2O_3S$ 571.2994; Found 571.2986.

3.5.2.3. Preparation of ^{19}F-fluroinated reference standards

Synthesis of 1-fluoro-4-(vinylsulfonyl)benzene 3.7-ref[48, 49]

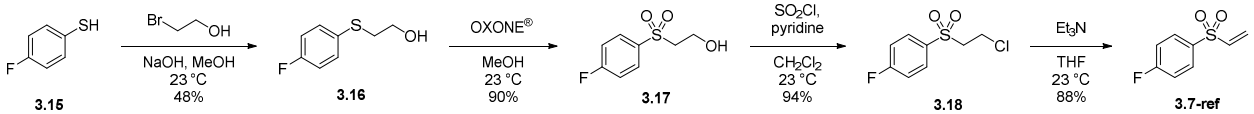

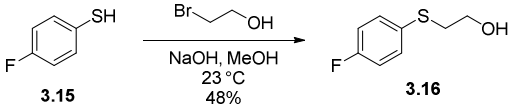

To a solution of 4-fluorobenzenethiol **3.15** (280 mg, 2.19 mmol) in methyl alcohol (3 mL) was added dropwise aqueous NaOH (1N, 2.4 mL) at -5 ºC over a period of 15 min and the reaction was stirred for 1 h at -5 °C. To the reaction mixture was added dropwise a solution of 2-bromoethanol (0.3 mL, 2.4 mmol) in methyl alcohol (1 mL) at -5 ºC over a period of 10 min. The reaction mixture was allowed to warm to room temperature and was stirred for 21 h. The methyl alcohol was removed under reduced pressure and water (5 mL) and ether (20 mL) were added to the crude residue. The phases were separated and the aqueous layer was extracted with ether. The combined organic layers were washed with saturated $NaHCO_3$ and brine. The combined organic layers were dried over Na_2SO_4, concentrated and purified by flash column chromatography (5-20% EtOAc in *n*-hexane) to afford 2-((4-fluorophenyl)thio)ethanol **3.16** (0.18 g, 1.05 mmol, 48% yield) as a light yellow oil. ^{1}H NMR (400 MHz, $CDCl_3$, δ): 7.41-7.36 (m, 2H), 6.99 (t, J = 8.8 Hz, 2H), 3.7 (t, J = 6 Hz, 2H), 3.04 (t, J = 6 Hz, 2H), 2.22 (s, 1H). ^{13}C NMR (100 MHz, $CDCl_3$, δ): 162.2 (d, J = 245.8 Hz), 133.3 (d, J = 8.1 Hz), 129.6 (d, J = 3.4 Hz), 116.2 (d, J = 21.7 Hz), 60.2,

38.6. ^{19}F NMR (376 MHz, $CDCl_3$, δ): -114.5. HR-APCI (EI) m/z: [M] + Calc'd for C_8H_9FOS 172.0358; Found 172.0364.

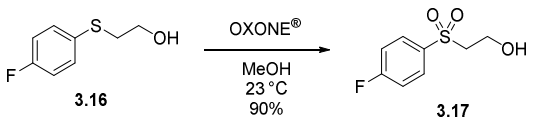

To a solution of 2-((4-fluorophenyl)thio)ethanol **3.16** (181 mg, 1.05 mmol) in methyl alcohol (4 mL) was added slowly, OXONE® (972 mg, 1.58 mmol) at 10 °C over 20 min. The suspension was stirred at room temperature (exothermic reaction) for 2 h and filtered. The filtrate was washed with a 38-40% (v/v) aqueous sodium hydrogen sulfite solution (0.5 mL), dried over Na_2SO_4 and concentrated *in vacuo* to afford crude 2-((4-fluorophenyl)sulfonyl)ethanol **3.17** (0.19 g, 0.95 mmol, 90% yield) as a light yellow oil which was used without further purification. ^{1}H NMR (400 MHz, $CDCl_3$, δ): 7.88 (dd, J = 8.8, 5.2 Hz, 2H), 7.18 (t, J = 8.8 Hz, 2H), 3.91 (t, J = 5.6 Hz, 2H), 3.32 (t, J = 5.6 Hz, 2H), 3.26 (s, 1H). ^{13}C NMR (100 MHz, $CDCl_3$, δ): 165.9 (d, J = 254.9 Hz), 135.2 (d, J = 3.2 Hz), 130.9 (d, J = 9.7 Hz), 116.7 (d, J = 89.6 Hz), 58.4, 56.1. ^{19}F NMR (376 MHz, $CDCl_3$, δ): -103.0 HRMS (ESI-TOF) m/z: [M+Na] + Calc'd for $C_8H_9FO_3SNa$ 227.0154; Found 227.0146.

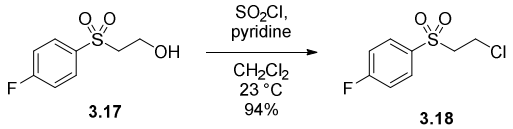

To a solution of 2-((4-fluorophenyl)sulfonyl)ethanol **3.17** (190 mg, 0.95 mmol) in CH_2Cl_2 (3 mL) was added pyridine (0.15 mL, 1.86 mmol) at room temperature. The reaction mixture was cooled to 0 °C and a solution of thionyl chloride (119 μL, 1.61 mmol) in CH_2Cl_2 (1 mL) was added dropwise over 15 min. After stirring at room temperature for 20 h the reaction mixture was diluted

with brine (1 mL) and the suspension was extracted. The combined organic layers were washed with brine (2 x 2 mL), dried over Na_2SO_4 and concentrated *in vacuo* to afford 1-((2-chloroethyl)sulfonyl)-4-fluorobenzene **3.18** (0.20 g, 0.90 mmol, 94% yield) as a yellow solid. Compound **3.18** is slightly unstable and undergoes spontaneous elimination to afford vinyl sulfone **3.7-ref**. For this reason, intermediate **3.18** was taken on to the next step without further purification. ^{1}H NMR (400 MHz, $CDCl_3$, δ): 7.93 (dd, *J* = 8.8, 5.2 Hz, 2H), 7.26 (t, *J* = 8.8 Hz, 2H), 3.75 (t, *J* = 8 Hz, 2H), 3.52 (t, *J* = 7.6 Hz, 2H). ^{13}C NMR (100 MHz, $CDCl_3$, δ): 166.2 (d, *J* = 255.8 Hz), 134.8 (d, *J* = 3.2 Hz), 131.1 (d, *J* = 9.6 Hz), 116.9 (d, *J* = 22.5 Hz), 58.2, 35.6. ^{19}F NMR (376 MHz, $CDCl_3$, δ): -102.3. HRMS (ESI-TOF) m/z: [M+Na] + Calc'd for $C_8H_8ClFO_2SNa$ 244.9815; Found 244.9809.

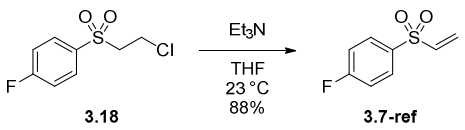

3.18 **3.7-ref**

To a solution of 1-((2-chloroethyl)sulfonyl)-4-fluorobenzene **3.18** (202 mg, 0.9 mmol) in THF (3 mL) was added dropwise triethylamine (187 μL, 1.35 mmol) in THF (1 mL) at room temperature. The reaction mixture was stirred for 1 h at room tempterature and quenched with aqueous HCl (1.0 M, 1.0 mL)**.** Ethyl acetate (4 mL) was added, the phases were separated and the aqueous phase was extracted with ethyl acetate (2 x 3 mL). The combined organic layers were washed with brine (2 x 2 mL), dried over Na_2SO_4, concentrated *in vacuo* and purified by flash column chromatography (10-30% EtOAc in *n*-hexane) to afford fluoro-4-(vinylsulfonyl)benzene **3.7-ref** (0.15 g, 0.79 mmol, 88% yield) as a light yellow oil. ^{1}H NMR (400 MHz, $CDCl_3$, δ): 7.91 (dd, *J* = 8.8, 4.8 Hz, 2H), 7.26-7.2 (m, 2H), 6.6 (dd, *J* = 16.4, 10 Hz, 2H), 6.46 (d, *J* = 16.4 Hz, 1H), 6.05 (d, *J* = 10 Hz, 1H). ^{13}C NMR (100 MHz, $CDCl_3$, δ): 165.8 (d, *J* = 254.8 Hz), 138.4, 135.6 (d, *J* =

3.2 Hz), 130.8 (d, J = 9.7 Hz), 127.9, 116.8 (d, J = 22.6 Hz). ^{19}F NMR (376 MHz, $CDCl_3$, δ): -103.4. HRMS (ESI-TOF) m/z: [M+Na] + Calc'd for $C_8H_7FO_2SNa$ 209.0049; Found 209.0041.

General procedure for the preparation of peptide ^{19}F-reference standards:

A vial (4 mL) equipped with a Teflon-coated magnetic stirring bar was charged with fluoro-4-(vinylsulfonyl)benzene (1.1 equiv), peptide (1.0 equiv), sodium borate buffer (pH 8.5, 500 μL), and methanol (500 μL). The reaction mixture was stirred at room temperature for 0.5 – 1.5 hr. The reference compound was purified by semi-preparative HPLC on a Phenomenex reverse-phase Luna column (10 × 250 mm, 5 μm, flow rate = 3 mL/min, 254 nm) with an isocratic mixture of 5:95 (MeCN:water, 0.1% TFA, v:v) for 3 minutes, followed by a linear gradient to 80:20 (MeCN:water, 0.1% TFA, v:v) over 30 minutes and a linear gradient to 95:5 (MeCN:water, 0.1% TFA, v:v) over 10 minutes. For the purification of **3.12-ref**, **3.19-ref** and **3.21-ref**, TFA was omitted from the mobile phase. The collected fractions containing the product were combined and concentrated *in vacuo* to dryness to afford the desired product. Analytical HPLC analysis of the purified compound was performed via UV absorbance at 254 nm, with a Phenomenex reverse-phase Luna column (4.6 × 250 mm, 5 μm) with a flow rate of 1 mL/min.

H-Arg-Gly-Asp-Cys-OH analogue (3.9-ref)

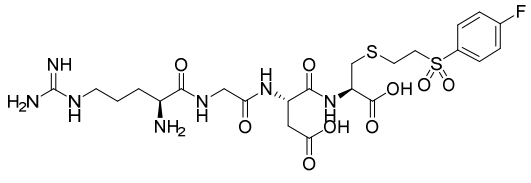

3.9-ref

The reaction mixture was purified by semi-preparative HPLC and concentrated *in vacuo* to afford **3.9-ref** (5.8 mg, 69% yield) as a white solid. ^{1}H NMR (400 MHz, DMSO-d_6, δ): 8.67 (t, J = 5.6

Hz, 1H), 8.42 (d, J = 8.0 Hz, 1H), 8.01 (d, J = 7.2 Hz, 1H), 7.95 (dd, J = 8.8, 5.2 Hz, 2H), 7.47 (dd, J = 8.8, 8.8 Hz, 2H), 7.28 (m, 3H), 4.54-4.49 (m, 1H), 4.11 (dd, J = 12.8, 6.4 Hz, 1H), 3.91-3.71 (m, 3H), 3.57-3.53 (m, 2H), 3.13 (s, 2H), 3.09- 3.02 (m, 2H), 2.88 (dd, J = 13.6, 5.2 Hz, 1H), 2.73-2.60 (m, 4H), 1.73 (m, 2H), 1.58-1.45 (m, 2H). ^{13}C NMR (125 MHz, DMSO-d_6, δ): 172.45, 172.36, 170.9, 169.2, 168.6, 165.6 (C-F, 1JC-F = 251.4 Hz), 157.3, 135.5 (C-F, 4JC-F = 2.8 Hz), 131.6 (C-F, 3JC-F = 9.8 Hz), 117.2 (C-F, 2JC-F = 22.4 Hz), 55.4, 53.0, 52.3, 50.1, 42.2, 36.6, 33.5, 29.5, 29.0, 24.7, 24.3 ^{19}F NMR (376 MHz, DMSO-d_6, δ): -104.6. HRMS (ESI-TOF) m/z: [M+H] + Calc'd for $C_{23}H_{35}FN_7O_9S_2$ 636.1922; Found 636.1902.

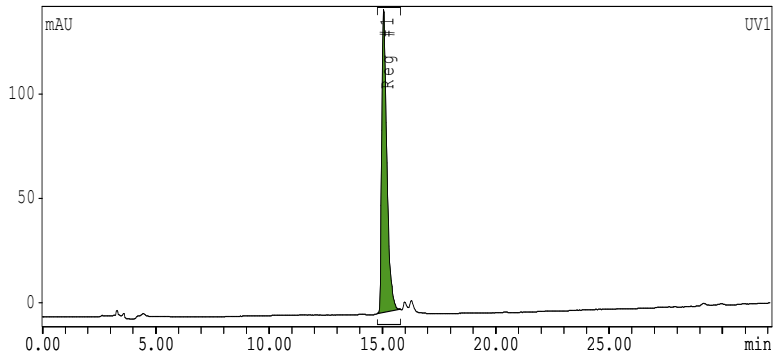

Figure 3.3. Analytical HPLC trace for **3.9-ref**. HPLC mobile phase: isocratic mixture of 5:95 (MeCN:water, 0.1% TFA, v:v) for 3 minutes, followed by a linear gradient to 80:20 (MeCN:water, 0.1% TFA, v:v) over 30 minutes.

H-*D*-Glu-Ala-Tyr-Gly-Trp-Cys-Asp-Phe-OH (MG11 analogue) (3.10-ref)

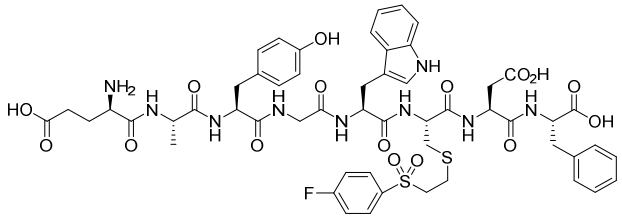

3.10-ref

The reaction mixture was purified by semi-preparative HPLC and concentrated *in vacuo* to afford **3.10-ref** (1.5 mg, 68% yield) as a white solid. HRMS (ESI-TOF) m/z: [M+H] + Calc'd for $C_{54}H_{63}FN_9O_{16}S_2$ 1176.3818; Found 1176.3809.

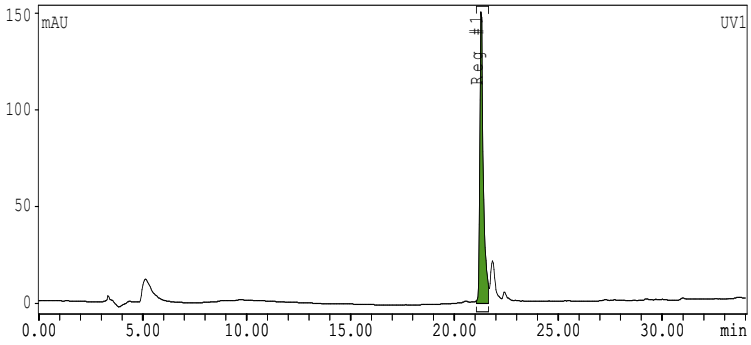

Figure 3.4. Analytical HPLC trace for **3.10-ref.** HPLC mobile phase: isocratic mixture of 5:95 (MeCN:water, 0.1% TFA, v:v) for 3 minutes, followed by a linear gradient to 80:20 (MeCN:water, 0.1% TFA, v:v) over 30 minutes.

c(Arg-Gly-Asp-Phe-Cys) analogue (3.11-ref)

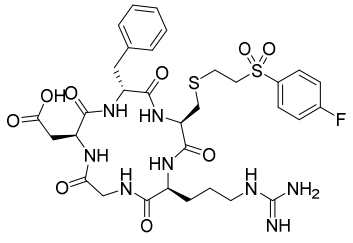

3.11-ref

The reaction mixture was purified by semi-preparative HPLC and concentrated *in vacuo* to afford **3.11-ref** (1.7 mg, 72% yield) as a white solid. HRMS (ESI-TOF) m/z: [M+H] + Calc'd for $C_{32}H_{42}FN_8O_9S_2$ 765.2500; Found 765.2485.

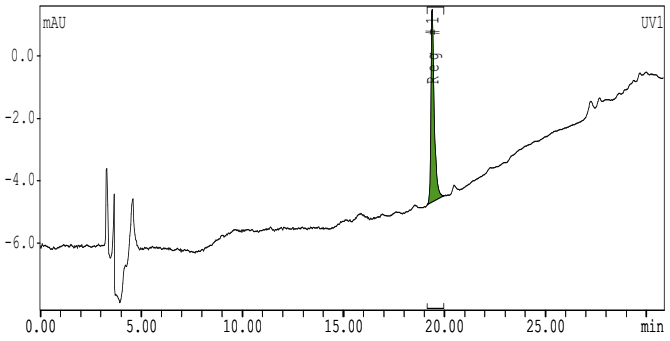

Figure 3.5. Analytical HPLC trace for **3.11-ref**. HPLC mobile phase: isocratic mixture of 5:95 (MeCN:water, 0.1% TFA, v:v) for 3 minutes, followed by a linear gradient to 80:20 (MeCN:water, 0.1% TFA, v:v) over 30 minutes.

PSMA analogue (3.12-ref)

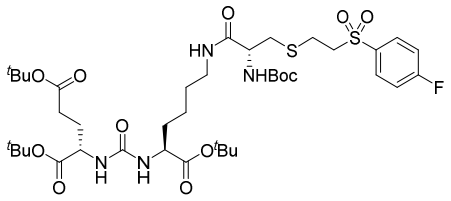

3.12-ref

The reaction mixture was purified by semi-preparative HPLC and concentrated *in vacuo* to afford **3.12-ref** (3.5 mg, 73% yield) as a white solid. HRMS (ESI-TOF) m/z: [M+Na] + Calc'd for $C_{40}H_{65}FN_4O_{12}S_2Na$ 899.3922; Found 899.3904. ^{1}H NMR (400 MHz, $CDCl_3$, δ): 7.96 (dd, *J* = 8.8, 5.2 Hz, 2H), 7.28-7.24 (m, 2H), 6.94 (s, 1H), 5.76 (d, *J* = 8 Hz, 1H), 5.7 (d, *J* = 8 Hz, 1H), 5.47 (d, *J* = 7.2 Hz, 1H), 4.38-4.27 (m, 3H), 3.49-3.33 (m, 3H), 3.11-3.06 (m, 1H), 2.92-2.82 (m, 4H), 2.38-2.25 (m, 2H), 2.12-2.03 (m, 1H), 1.87-1.72 (m, 2H), 1.46 (s, 9H), 1.44 (s, 9H), 1.43 (s, 18H), 0.88-0.83 (m, 2H). ^{13}C NMR (126 MHz, $CDCl_3$, δ): 173.3, 172.4, 171.0, 166.0 (d, *J* = 257.3 Hz), 157.2, 155.9, 134.9 (d, *J* = 3.4 Hz), 131.1 (d, *J* = 9.6 Hz), 116.8 (d, *J* = 22.7 Hz), 82.2, 81.4, 80.5, 56.3, 53.9, 53.0, 52.9, 38.7, 34.4, 31.7, 31.5, 31.0, 29.7, 28.4, 28.3, 28.09, 28.06, 28.02, 24.8, 21.6. ^{19}F NMR (376 MHz, $CDCl_3$, δ): -102.8. HRMS (ESI-TOF) m/z: [M+Na] + Calc'd for $C_{40}H_{65}FN_4O_{12S2}Na$ 899.3922; Found 899.3904.

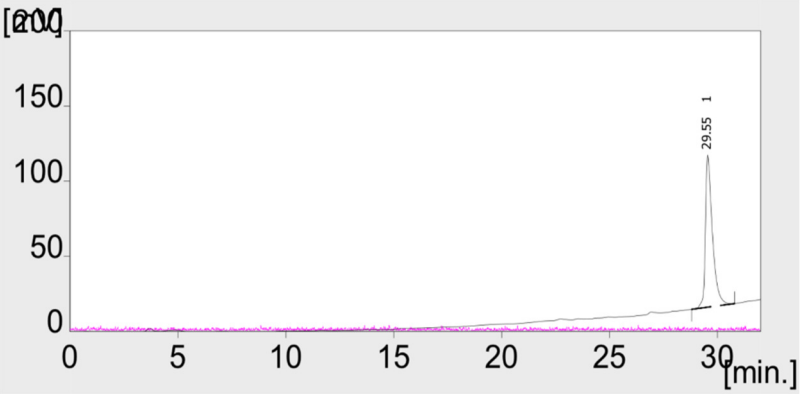

Figure 3.6. Analytical HPLC trace for **3.12-ref**. HPLC mobile phase: isocratic mixture of 5:95 (MeCN:water, 0.1% TFA, v:v) for 3 minutes, followed by a linear gradient to 80:20 (MeCN:water, 0.1% TFA, v:v) over 30 minutes and 95:5 (MeCN:water, 0.1% TFA, v:v) over 5 minutes.

H-Gly-Asn-Leu-Trp-Ala-Thr-Gly-His-Phe-Cys-OH (Neuromedin B analogue) (3.13-ref)

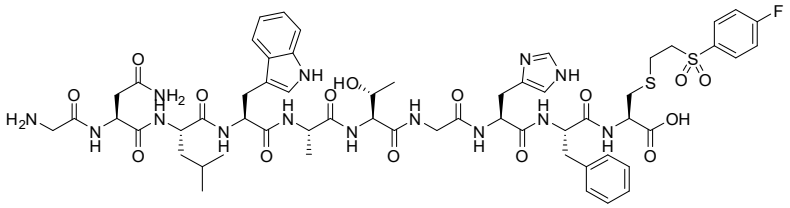

3.13

The reaction mixture was purified by semi-preparative HPLC and concentrated *in vacuo* to afford **3.13-ref** (2 mg, 87% yield) as a white solid. HRMS (ESI-TOF) m/z: [M+H] + Calc'd for $C_{58}H_{76}FN_{14}O_{15}S_2$ 1291.5040; Found 1291.5035.

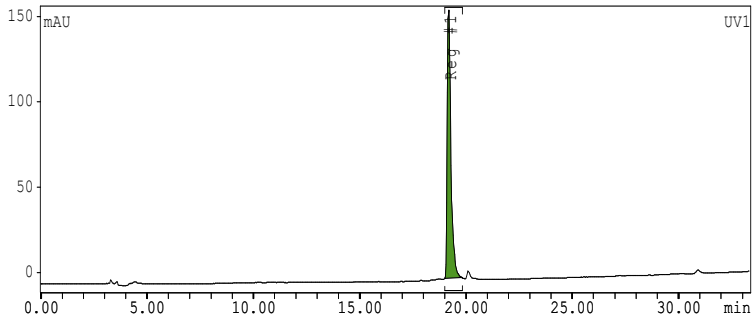

Figure 3.7. Analytical HPLC trace for **3.13-ref**. HPLC mobile phase: isocratic mixture of 5:95 (MeCN:water, 0.1% TFA, v:v) for 3 minutes, followed by a linear gradient to 80:20 (MeCN:water, 0.1% TFA, v:v) over 30 minutes.

Pyr-Gln-Arg-Leu-Gly-Asn-Gln-Trp-Ala-Val-Gly-His-Leu-Cys-OH (Bombesin analogue) (3.14-ref)

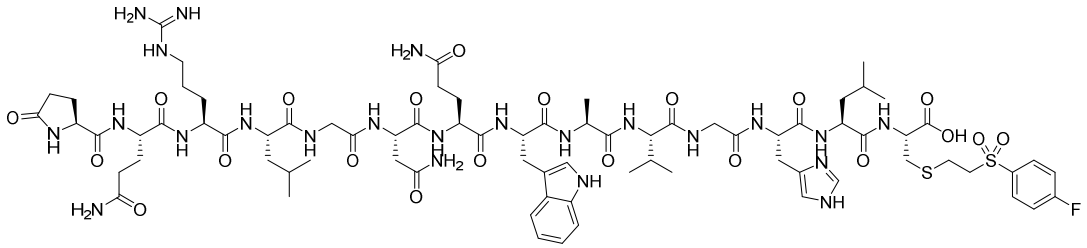

3.14-ref

The reaction mixture was purified by semi-preparative HPLC and concentrated *in vacuo* to afford **3.14-ref** (2.2 mg, 81% yield) as a white solid. HRMS (ESI-TOF) m/z: [M+H] + Calc'd for $C_{77}H_{113}FN_{23}O_{21}S_2$ 1778.7907; Found 1778.7977.

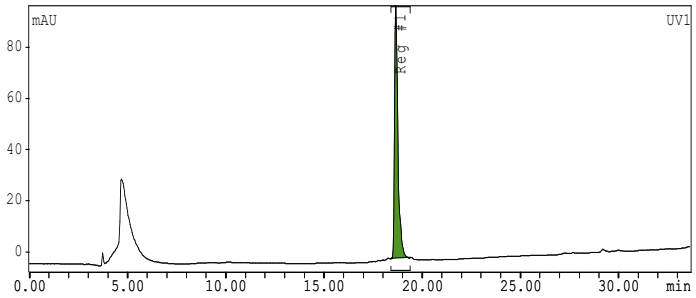

Figure 3.8. Analytical HPLC trace for **3.14-ref**. HPLC mobile phase: isocratic mixture of 5:95 (MeCN:water, 0.1% TFA, v:v) for 3 minutes, followed by a linear gradient to 80:20 (MeCN:water, 0.1% TFA, v:v) over 30 minutes.

Preparation of amino acid ^{19}F-reference standards:

FVSB-conjugated *N*-Boc-Cys-OH (3.19-ref)

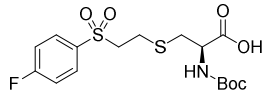

3.19-ref

A vial (4 mL) equipped with a Teflon-coated magnetic stirring bar was charged with fluoro-4-(vinylsulfonyl)benzene **3.7-ref** (1 equiv), *N*-Boc-cysteine (1 equiv), sodium borate buffer (pH 8.5, 500 μL), and methanol (500 μL). The reaction mixture was stirred at room temperature for 1.5 h. The reaction mixture was purified by semi-preparative HPLC and concentrated *in vacuo* to afford **3.19-ref** (11.4 mg, 69% yield) as a white solid. ^{1}H NMR (400 MHz, DMSO-d_6, δ): 7.94 (dd, J = 8.8, 5.2 Hz, 2H), 7.46 (t, J = 8.8 Hz, 2H), 5.96 (d, J = 5.6 Hz, 1H), 3.59-3.44 (m, 4H), 2.86 (dd, J = 13.2, 4 Hz, 1H), 2.73 (dd, J = 13.2, 5.2 Hz, 1H), 2.67-2.53 (m, 2H), 1.31 (s, 9H). ^{13}C NMR (100 MHz, DMSO-d_6, δ): 171.9, 165.6 (d, J = 251.2 Hz), 155.1, 135.6 (d, J = 2.7 Hz), 131.5 (d, J = 10 Hz), 117.1 (d, J = 22.6 Hz), 77.9, 55.8, 55.3, 35.9, 28.6, 25.0. ^{19}F NMR (376 MHz, DMSO-d_6, δ): -104.8. HRMS (ESI-TOF) m/z: [M+Na] + Calc'd for $C_{16}H_{22}FNO_6S_2Na$ 430.0770; Found 430.0758.

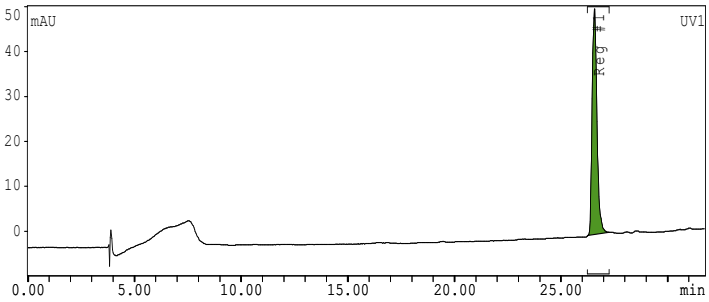

Figure 3.9. Analytical HPLC trace for **3.19-ref**. HPLC mobile phase: isocratic mixture of 5:95 (MeCN:water, 0.1% TFA, v:v) for 3 minutes, followed by a linear gradient to 80:20 (MeCN:water, 0.1% TFA, v:v) over 30 minutes.

FVSB-conjugated *N*-Boc-Lys-OH (3.20-ref)

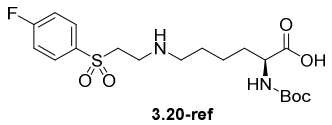

3.20-ref

A vial (4 mL) equipped with a Teflon-coated magnetic stir bar was charged with fluoro-4-(vinylsulfonyl)benzene **3.7-ref** (1 equiv), *N*-Boc-lysine (1 equiv), sodium borate buffer (pH 9.5, 500 μL), and methanol (500 μL). The reaction mixture was stirred at 50 °C overnight. The reaction mixture was purified by semi-preparative HPLC and concentrated *in vacuo* to afford **3.20-ref** (5 mg, 28% yield) as a white solid. ^{1}H NMR (400 MHz, DMSO-d_6, δ): 8.0-7.97 (m, 2H), 7.55-7.51 (m, 2H), 7.02 (d, J = 8 Hz, 1H), 3.82-3.56 (m, 4H), 3.15-3.11 (m, 2H), 2.86-2.83 (m, 2H), 1.7-1.17 (m, 4H), 1.33 (s, 9H). ^{13}C NMR (100 MHz, DMSO-d_6, δ): 174.6, 165.9 (d, J = 252.2 Hz), 156.1, 134.9 (d, J = 2.4 Hz), 131.7 (d, J = 10.1 Hz), 117.5 (d, J = 22.8 Hz), 78.5, 53.7, 51.6, 47.2, 30.6, 28.7, 25.7, 23.1, 22.1. ^{19}F NMR (376 MHz, DMSO-d_6, δ): -103.8. HRMS (ESI-TOF) m/z: [M+H] + Calc'd for $C_{19}H_{30}FN_2O_6S$ 433.1809; Found 433.1806.

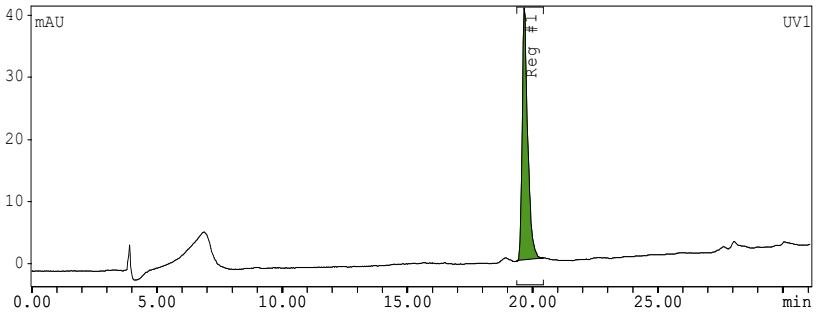

Figure 3.10. Analytical HPLC trace for **3.20-ref**. HPLC mobile phase: isocratic mixture of 5:95 (MeCN:water, 0.1% TFA, v:v) for 3 minutes, followed by a linear gradient to 80:20 (MeCN:water, 0.1% TFA, v:v) over 30 minutes.

FVSB-conjugated *N*-Boc-His-OH (3.21-ref)

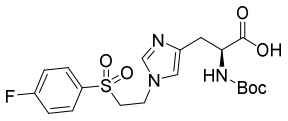

3.21-ref

A vial (4 mL) equipped with a Teflon-coated magnetic stirring bar was charged with fluoro-4-(vinylsulfonyl)benzene **3.7-ref** (1 equiv), *N*-Boc-histidne (1 equiv), sodium borate buffer (pH 8.5, 500 μL), and methanol (250 μL). The reaction mixture was stirred at 35 °C for 12 h. The reaction mixture was purified by semi-preparative HPLC and concentrated *in vacuo* to afford **3.21-ref** (14 mg, 81% yield) as a white solid. ^{1}H NMR (400 MHz, DMSO-d_6, δ): 7.94-7.82 (m, 2H), 7.41 (t, *J* = 8.4 Hz, 2H), 7.27 (s, 1H), 6.66 (s, 1H), 5.83 (d, *J* = 7.2 Hz, 1H), 4.14 (dt, *J* = 6.4, 2.8 Hz, 2H), 3.83 (t, *J* = 6.4 Hz, 2H), 3.64 (dd, *J* = 11.2, 6.4 Hz, 4H), 2.7 (dd, *J* = 14.8, 4.4 Hz, 4H), 2.6 (dd, *J* = 14.8, 6.4 Hz, 4H), 1.29 (s, 9H). ^{13}C NMR (126 MHz, DMSO-d_6, δ): 174.0, 165.5 (d, *J* = 253.1 Hz), 155.2, 139.9, 136.3, 135.7 (d, *J* = 2.9 Hz), 131.3 (d, *J* = 9.9 Hz), 117.0 (d, *J* = 22.8 Hz), 116.4, 77.4, 55.4, 38.0, 32.2, 31.2, 28.7. ^{19}F NMR (376 MHz, DMSO-d_6, δ): -104.8. HRMS (ESI-TOF) m/z: [M+H] + Calc'd for $C_{19}H_{25}FN_3O_6S$ 442.1448; Found 442.1448.

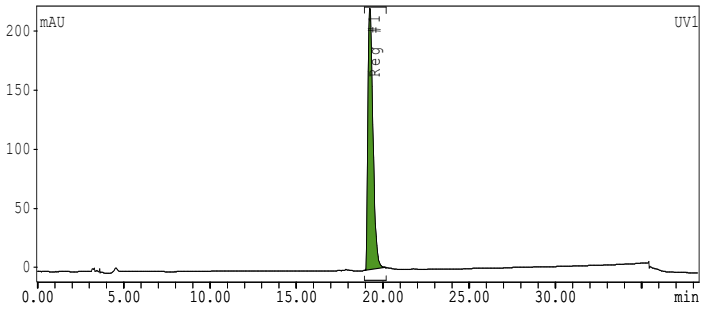

Figure 3.11. Analytical HPLC trace for **3.21-ref**. HPLC mobile phase: isocratic mixture of 5:95 (MeCN:water, 0.1% TFA, v:v) for 3 minutes, followed by a linear gradient to 80:20 (MeCN:water, 0.1% TFA, v:v) over 30 minutes.

FVSB-conjugated H-Arg-Gly-Asp-OH (3.22-ref)

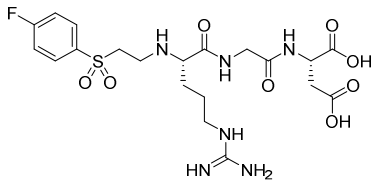

3.22

A vial (4 mL) equipped with a Teflon-coated magnetic stirring bar was charged with fluoro-4-(vinylsulfonyl)benzene **3.7-ref** (1.5 equiv), peptide (1 equiv), sodium borate buffer (pH 9.5, 500 μL), and methanol (500 μL). The reaction mixture was stirred at 50 °C overnight. The reaction mixture was purified by semi-preparative HPLC and concentrated *in vacuo* to afford **3.22-ref** (3.1 mg, 55% yield) as a white solid. ^{1}H NMR (500 MHz, DMSO-d_6, δ): 8.71 (brs, 2H), 8.40-8.38 (m, 1H), 7.99 (d, J = 5 Hz, 2H), 7.64-7.63 (m, 1H), 7.52 (d, J = 4.5 Hz, 2H), 4.55 (t, J = 6.5 Hz, 1H), 4.01 (t, J = 6.5 Hz, 1H), 3.82-3.78 (m, 2H), 3.62 (s, 2H), 3.10-3.02 (m, 4H), 2.71-2.57 (m, 2H), 1.98-1.97 (m, 1H), 1.63 (m, 2H), 1.48-1.43 (m, 2H), 1.22-1.14 (m, 2H). ^{13}C NMR (125 MHz, DMSO-d_6, δ): 172.7, 172.1, 170.8, 168.4, 165.9 (d, J = 252.0 Hz), 157.2, 135.0 (d, J = 2.9 Hz), 131.7 (d, J = 9.9 Hz), 117.4 (d, J = 22.4 Hz), 60.2, 49.1, 41.9, 36.6, 24.7, 21.2, 14.6. ^{19}F NMR

(376 MHz, DMSO-d_6, δ): -103.9. HRMS (ESI-TOF) m/z: [M+H] + Calc'd for $C_{20}H_{30}FN_6O_8S$ 533.1830; Found 533.1811.

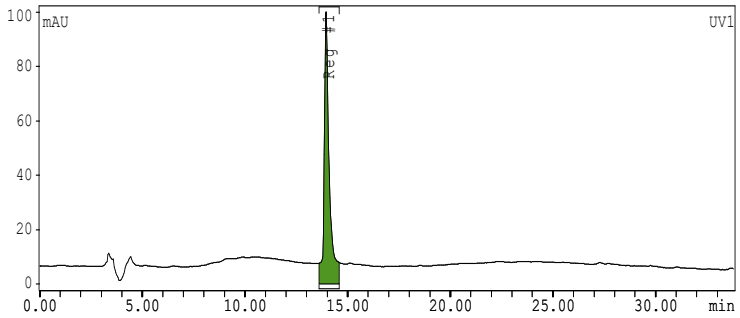

Figure 3.12. Analytical HPLC trace for **3.22-ref**. HPLC mobile phase: isocratic mixture of 5:95 (MeCN:water, 0.1% TFA, v:v) for 3 minutes, followed by a linear gradient to 80:20 (MeCN:water, 0.1% TFA, v:v) over 30 minutes.

3.5.2.4. Preparation of Glu-Urea-Lys-Cys precursor 3.24 for PSMA analogue

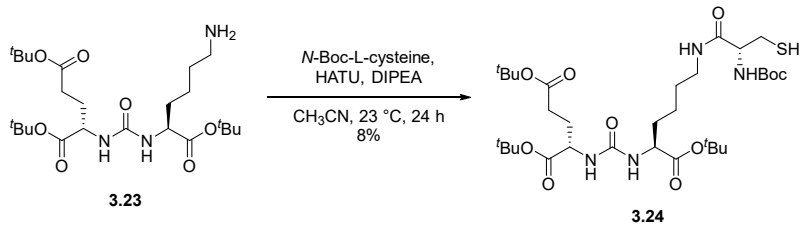

Glu-Urea-Lys **3.23** was synthysized according to literature procedure.[51] The ^{1}H and ^{13}C NMR spectroscopic data were consistent with previously reported values. To a solution of *N*-Boc-L-cysteine (36.3 mg, 0.164 mmol) in CH_3CN (10 mL) at 0 °C was added HATU (66 mg, 0.174 mmol), Glu-Urea-Lys **3.23** (79.9 mg, 0.164 mmol) and diisopropylethylamine (30 µL, 0.174 mmol). The reaction was stirred for 24 h at room temperature. The solvent was removed under reduced pressure and the crude residue was dissolved in CH_2Cl_2 (5 mL) and extracted with saturated aqueous NH_4Cl (5 mL). The phases were separated and the aqueous layer was extracted

with CH_2Cl_2 (3 x 5 mL). The combined organic layers were dried over Na_2SO_4, concentrated, and purified by flash column chromatography (30-50% EtOAc in *n*-hexane) to afford **3.24** (9 mg, 0.013 mmol, 8% yield) as a white solid.[52] ^{1}H NMR (400 MHz, $CDCl_3$, δ): 7.16 (brs, 1H), 6.02-5.96 (m, 2H), 5.63 (d, *J* = 8.4 Hz, 1H), 4.43- 4.37 (m, 2H), 4.31 (ddd, *J* = 8.0, 8.0, 4.0 Hz, 1H), 3.53-3.45 (m, 1H), 3.10-3.05 (m, 1H), 2.94-2.87 (m, 1H), 2.83-2.76 (m, 1H), 2.41-2.26 (m, 3H), 2.13-2.04 (m, 1H), 1.88-1.70 (m, 4H), 1.63-1.54 (m, 3H), 1.47 (s, 9H), 1.43-1.42 (m, 27H). ^{13}C NMR (100 MHz, $CDCl_3$, δ): 173.64, 173.63, 172.39, 172.36, 171.5, 157.30, 82.3, 81.2, 80.5, 80.4, 60.4, 56.3, 52.93, 52.85, 38.8, 31.66, 31.60, 28.6, 28.4, 28.10, 28.08, 28.03, 27.0, 21.7. HRMS (ESI-TOF) m/z: [M+Na] + Calc'd for $C_{32}H_{58}N_4O_{10}SNa$ 713.3771; Found 713.3775.

3.5.3. Radiochemistry

3.5.3.1. General materials and methods

No-carrier-added [^{18}F]fluoride was produced by the $^{18}O(p,n)^{18}F$ nuclear reaction in a Siemens RDS-112 cyclotron at 11 MeV using a 1 mL tantalum target with havar foil. Unless otherwise stated, reagents and solvents were commercially available and used without further purification. HPLC grade acetonitrile and trifluoroacetic acid were purchased from Fisher Scientific. 2-Butanone (ACS reagent, ≥99.0%) and Ethyl alcohol (200 proof, anhydrous, ≥99.5%) were purchased from Sigma-Aldrich® and used as received. DI water was obtained from a Water Purification System. Sodium oxalate salt (≥99%) was purchased from Sigma-Aldrich and used as received. Anhydrous dimethylformamide was purchased from Acros Organics and used as received. Reaction glass vials were purchased from Chemglass. Oasis® HLB plus short (Part No. 186000132), Sep-pak C18 plus short (Part No. WAT020515) and Sep-Pak tC18 plus short cartridges (Part No. WAT036810) were purchased from Waters Corporation. Chromafix 30-PS-

HCO_3^- cartridges (Part No. 00260110) were purchased from ABX advanced biochemical compounds GmbH. An aluminum heating block was used as the heating source for all reactions. Radio-TLCs were analyzed using a miniGITA* TLC scanner. HPLC purifications were performed on a Knauer Smartline HPLC system with inline Knauer UV (254 nm) detector and gamma-radiation coincidence detector and counter (Bioscan Inc.). Semi-preparative HPLC was performed using Phenomenex reverse-phase Luna column (10 × 250 mm, 5 μm) with a flow rate of 4.0 mL/min. Final purity and identity of compounds were determined by analytical HPLC analysis performed with a Phenomenex reverse-phase Luna column (4.6 × 250 mm, 5 μm) with a flow rate of 1.0 mL/min. All chromatograms were collected by a GinaStar (Raytest) analog to digital converter and GinaStar software.

HPLC Eluents

Eluent A

Solvent A = H_2O + 0.1% TFA, Solvent B = CH_3CN + 0.1% TFA Flow rate = 1 mL/min

0 – 3 min = 5% B

3 – 30 min = 5% B to 80% B

30 – 60 min = 80% B to 95% B

Eluent B

Solvent A = H_2O + 0.1% TFA, Solvent B = CH_3CN + 0.1% TFA, Flow rate = 1 mL/min

0 – 60 min = 60% B

Eluent C

Solvent A = H_2O + 0.1% TFA, Solvent B = CH_3CN + 0.1% TFA, Flow rate = 4 mL/min

0 – 10 min = 15% B

10 – 25 min = 15% B to 35% B

25+ min = 35% B

Cartridge Preconditioning:

Oasis® HLB plus short LP, Sep-Pak C18 plus short, and Sep-Pak tC18 plus short cartridges were preconditioned by sequentially pushing absolute ethanol (5 mL) and H_2O (10 mL) through the cartridge. Chromafix 30-PS-HCO_3 cartridges were preconditioned by sequentially pushing a potassium oxalate monohydrate solution (3 mL, 10 mg/mL in H_2O) and H_2O (2 mL) through the cartridge.

3.5.3.2. Preparation of [^{18}]Ffluoro-4-(vinylsulfonyl)benzene ([^{18}F]FVSB)

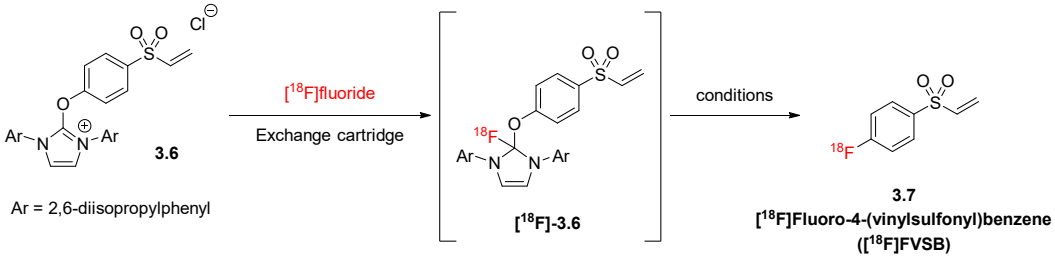

[^{18}F]Fluoride solution in H_2O was passed through a preconditioned Chromafix 30-PS-HCO_3 cartridge and excess water was removed by pushing air (36 mL), via syringe, through the cartridge. The cartridge was washed with a mixture of 2-butanone and ethanol (2 mL, 10:1) followed by air (36 mL). Subsequently, the [^{18}F]fluoride was eluted into a 4 mL borosilicate glass reaction vial

using a solution of uronium precursor **3.6** (5 mg) in 2-butanone and ethanol (1 mL, 10:1). The reaction vial was sealed with a Teflon lined cap and heated to 130 °C for 30 min with stirring.

Note: Formation of **[^{18}F]FVSB** is presumed to occur via intermediate **[^{18}F]-3.6**, however evidence of this intermediate was not confirmed here. Extensive mechanistic studies were conducted in the seminal ^{18}F-deoxyfluorination report (*Nature* **2016**, *534*, 369-373) that provide strong evidence that the reaction proceeds through a tetrahedral intermediate such as **[^{18}F]-3.6**.

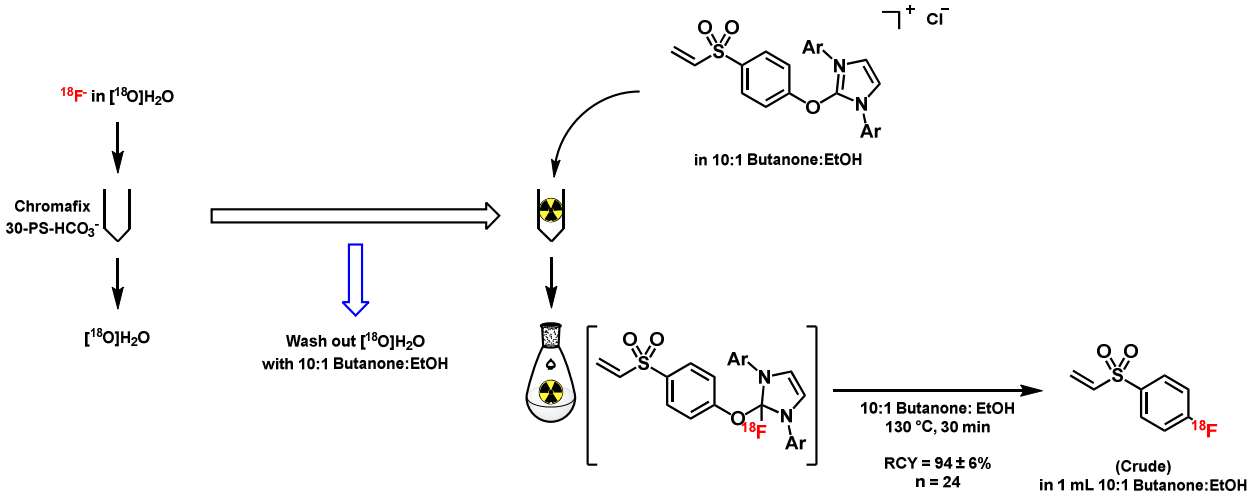

The vial was allowed to cool to room temperature for 1 – 2 minutes before its contents were transferred into a centrifuge tube (50 mL) containing 20 mL of H_2O. The contents were subjected to cartridge purification and passed through an Oasis HLB plus short cartridge, followed by pushing air (36 mL) through the cartridge. The trapped [^{18}F]Fluoro-4-(vinylsulfonyl)benzene ([^{18}F]FVSB) was washed with water (5 mL), dried with air (36 mL) and subsequently eluted from the cartridge into a 20 mL borosilicate scintillation vial with diethyl ether (2 mL).

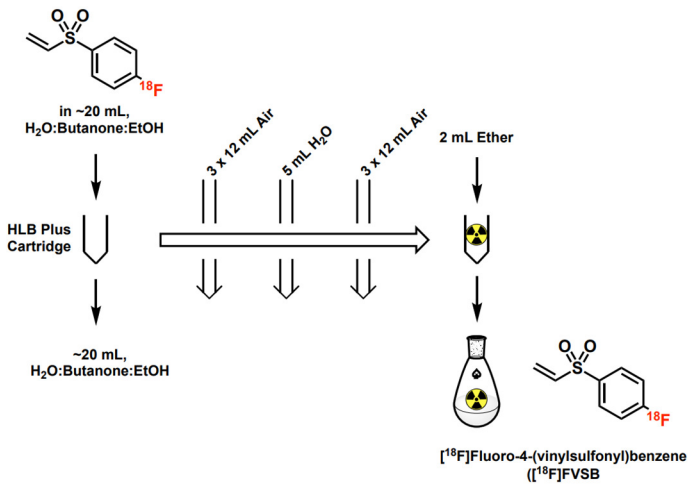

An aliquot of the purified [^{18}F]FVSB was spotted on a silica gel coated TLC plate, developed in a glass chamber with acetonitrile:water (95:5) as the eluent and analyzed using a miniGITA* TLC scanner. The radiochemical yield (RCY) was determined by radio-TLC and was calculated by dividing the integrated area of the ^{18}F-fluorinated product peak by the total integrated area of all peaks and multiplying by 100 to convert to percentage units. Isolated RCY was determined by dividing the final activity of the isolated, cartridge-purified [^{18}F]FVSB by the starting [^{18}F]fluoride activity, and is decay-corrected. Analytical HPLC (eluent A) was used to confirm product identity and purity via UV absorbance at 254 nm by coinjection with the ^{19}F-reference standard. An aliquot of the crude reaction mixture (10 µL) was added to the ^{19}F-reference standard (1 mg/mL) in acetonitrile (10 µL) and the sample was injected into the analytical HPLC.

Table 3.3. Preparation of [^{18}F]Fluoro-4-(vinylsulfonyl)benzene ([^{18}F]FVSB)

Entry	**Starting Activity (mCi)**	**Isolated Activity after HLB cartridge purification (mCi)**	**Synthesis Time (min)[a]**	**RCY (%)[b]**	**Isolated RCY (%)[c]**
1	19.3	5.87 (9.05 d.c.)	68	98	47
2	21.9	7.43 (10.34 d.c.)	52	97	47
3	17.0	5.76 (8.12 d.c.)	54	94	48
4	19.4	4.86 (6.68 d.c.)	50	95	34
5	23.0	7.37 (11.14 d.c.)	65	95	48
6	17.9	5.63 (7.84 d.c.)	52	94	44
7	25.5	8.67 (12.22 d.c.)	54	73	48
8	35.1	11.81 (16.86 d.c.)	56	94	48
9	26.4	7.95 (11.50 d.c.)	58	97	44
10	33.3	11.59 (16.76 d.c.)	58	98	50
mean ± SD			**56 ± 6**	**94 ± 7**	**46 ± 4**

[a]Calculated as the time to obtain cartridge purified [^{18}F]FVSB relative to aqueous [^{18}F]fluoride. Unoptimized and includes time taken for intermediate measurements throughout the process. [b]RCY was determined by radio-TLC analysis of the crude product. [c]Isolated RCY was determined by measuring the final activity of the cartridge-purified [^{18}F]FVSB versus starting [^{18}F]fluoride activity and is decay-corrected.

Table 3.4. Optimized synthesis time for preparation of [^{18}F]FVSB

Entry	1	2	3	4	5	6	7	8	9	10	**mean ± SD**
Synthesis Time (min)[a]	40	39	47	45	47	49	43	43	40	39	**43 ± 3**

[a]Calculated as the time to obtain cartridge purified [^{18}F]FVSB relative to aqueous [^{18}F]fluoride. Uninterrupted process without taking intermediate measurements.

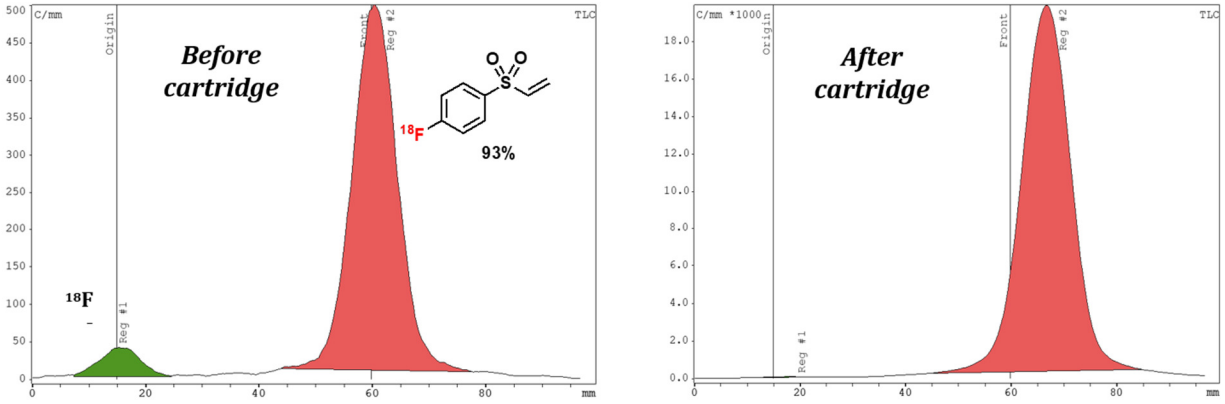

Figure 3.13. Example of integrated radio-TLC scan of crude [^{18}F]FVSB (left panel) and cartridge purified [^{18}F]FVSB (right panel). TLC plate mobile phase = acetonitrile/water 95:5.

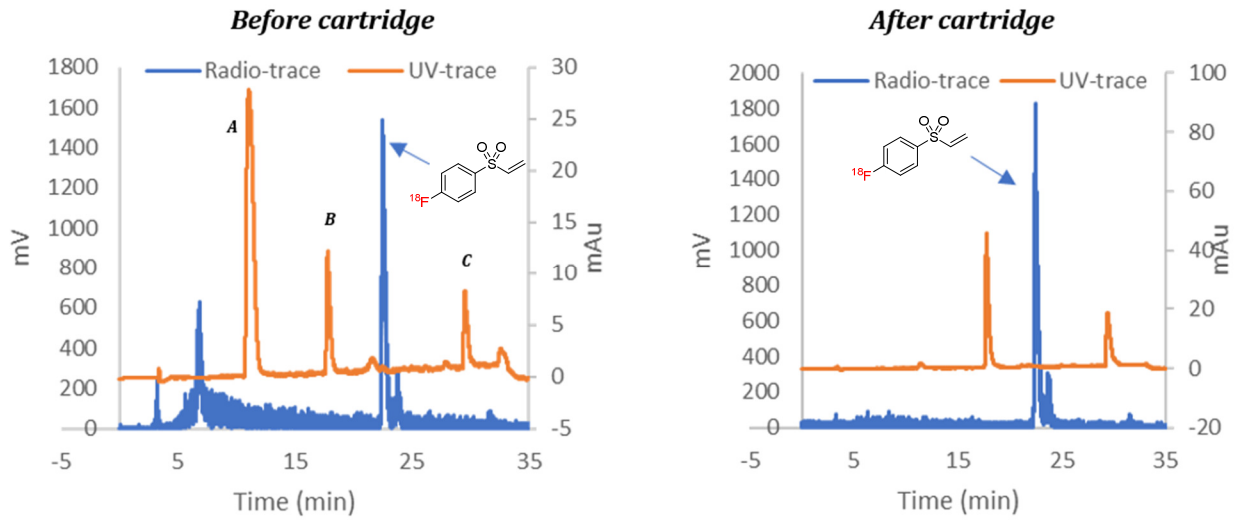

Figure 3.14. Radio-HPLC with 254 nm UV trace (upper, orange) and radioactive trace (lower, blue) of crude [^{18}F]FVSB (left panel) and cartridge purified [^{18}F]FVSB (right panel), obtained in 85% radiochemical purity (RCP). Peaks in UV trace identified as: (**A**) 2-butanone; (**B**) phenol **3.4**; (**C**) uronium precursor **3.6**. HPLC mobile phase: Eluent A.

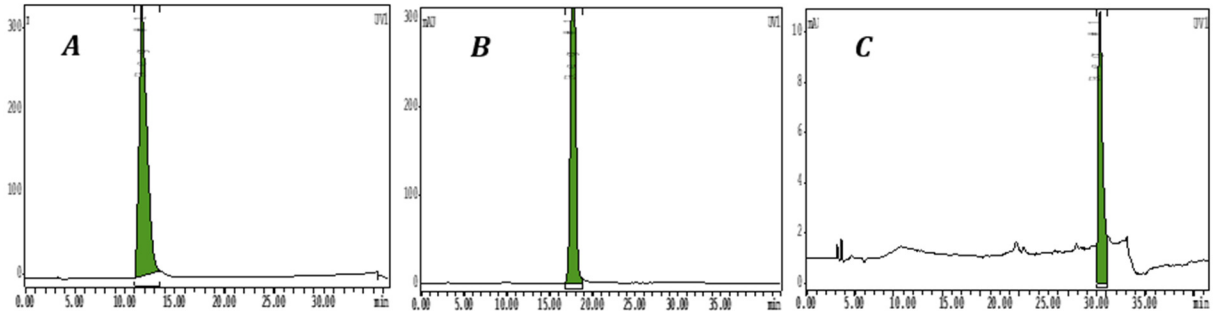

Figure 3.15. UV trace of pure (A) 2-butanone, 11.6 min; (B) phenol 3.4, 17.7 min; (C) uronium precursor 3.6, 30.2 min. HPLC mobile phase: Eluent A.

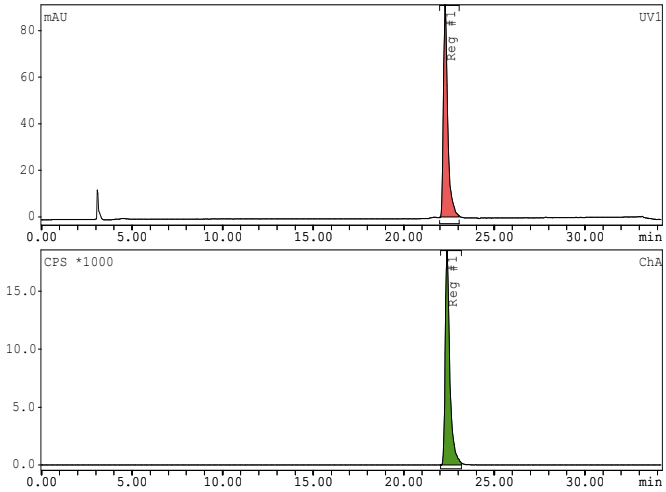

Figure 3.16. Coinjection of semi-preparative HPLC purified [^{18}F]FVSB spiked with an aliquot of [^{19}F]FVSB reference standard. Semi-preparative HPLC mobile phase: Eluent C. Radioactive trace (lower) and 254 nm UV trace (upper). Analytical HPLC mobile phase: Eluent A.

3.5.3.3. ^{18}F-Deoxyfluorination optimization

Table 3.5. Optimization of precursor mass for ^{18}F-deoxyfluorination[a]

Entry	Precursor amount (mg)	Elution efficiency[b] (%)	Elution efficiency[b] (%) mean ± SD	RCY (%)	RCY (%) mean ± SD
1	3	58	60 ± 3	85	88 ± 2
2	3	63		91	
3	5	84	**84 ± 3**	94	**94 ± 2**
4	5	85		90	
5	5	85		96	
6	5	79		96	
7	5	87		94	
8	7	84	84 ± 2	97	97 ± 1
9	7	87		97	
10	7	84		97	
11	7	84		98	
12	7	81		96	
13	9	84	83 ± 1	97	96 ± 2
14	9	83		94	

[a]Reaction conditions: [^{18}F]fluoride (~500 μCi), 10:1 butanone:EtOH (1 mL), 130 °C, 30 min. RCY was determined by radio-TLC analysis of the crude product. [b]determined by dividing the activity eluted from the cartridge by the initial activity loaded on the cartridge, non-decay-corrected.

3.5.3.4. Cartridge purification and optimization

Table 3.6. Optimization of precursor mass for ^{18}F-deoxyfluorination[a]

Cart-ridge	Dilu-tion Volume (mL H_2O)	Water Wash Volume (mL H_2O)	Elution Solvent	Elution Volume (mL)	Trapping Efficiency[b] (%)	Elution Efficiency[c] (%)	RCY[d] (%)	Count
C18	10	0	MeOH	2.5	97 ± 2	63 ± 5	35 ± 5	2
tC18	10	0	MeOH	2.5	52 ± 2	50 ± 3	47 ± 1	2
tC18	10	0	MeOH	1	70 ± 5	87 ± 0	35 ± 3	2
tC18	10	5	MeOH	1	61 ± 6	63 ± 0	55 ± 7	2
HLB	5	0	MeOH	2.5	35 ± 1	78 ± 3	44 ± 1	2
tC18	10	5	DCM	1	74 ± 3	67 ± 1	95 ± 1	2
tC18	10	5	Ether	1	75 ± 5	66 ± 3	98 ± 1	2
tC18	15	5	Ether	1	70 ± 1	65 ± 17	89 ± 1	2
tC18	5	5	Ether	1	88 ± 1	83 ± 3	100 ± 1	2
HLB	15	5	Ether	1	91 ± 0	59 ± 5	100 ± 0	2
HLB	15	5	Ether	2	89 ± 1	79 ± 1	100 ± 1	2

[a]Aliquots of crude [^{18}F]FVSB were added to a centrifuge tube (50 mL) containing H_2O. The contents were passed through a purification cartridge, followed by pushing air (36 mL) through the cartridge. The trapped [^{18}F]FVSB was washed with water, dried with air (36 mL) and subsequently eluted from the cartridge into a 20 mL borosilicate scintillation vial with an organic solvent. An aliquot of the purified [^{18}F]FVSB was spotted on a silica gel coated TLC plate, developed in a glass chamber with acetonitrile:water (95:5) as the eluent and analyzed via radio-TLC. [b]determined by dividing the activity trapped on the cartridge by the initial activity loaded on the cartridge, non-decay-corrected. [c]determined by dividing the activity eluted from the cartridge by the initial activity trapped on the cartridge, non-decay-corrected. [d]RCY was determined by radio-TLC, calculated by dividing the integrated area of the ^{18}F-fluorinated product peak by the total integrated area of all peaks and multiplying by 100 to convert to percentage units.

3.5.3.5. Molar activity of [^{18}F]FVSB

A calibration curve was generated from the authentic [^{19}F]FVSB reference standard, by measuring the integration of the UV absorbance signal at 240 nm for nine different concentrations (***Figure 3.17***). To determine the molar activity of [^{18}F]FVSB, semi-preparative HPLC was performed to obtain pure [^{18}F]FVSB (using eluent C). A 330 µCi of HPLC-purified [^{18}F]FVSB was injected into an analytical HPLC (using eluent B). The UV absorption corresponding to the radio-peak was measured and was determined to be below the signal of detection for analysis (***Figure 3.18***). It was determined that the lowest measurable UV absorption of 9.4741 mAu*s corresponds to 1.15 x 10^{-4} µmol of [^{19}F]FVSB (***Figure 3.19***). As the UV absorption of 330 µCi of [^{18}F]FVSB was below this measurement by comparison, the molar activity of [^{18}F]FVSB was estimated to be at or greater than 2.87 Ci · µmol^{-1} (106.2 GBq · µmol^{-1}).

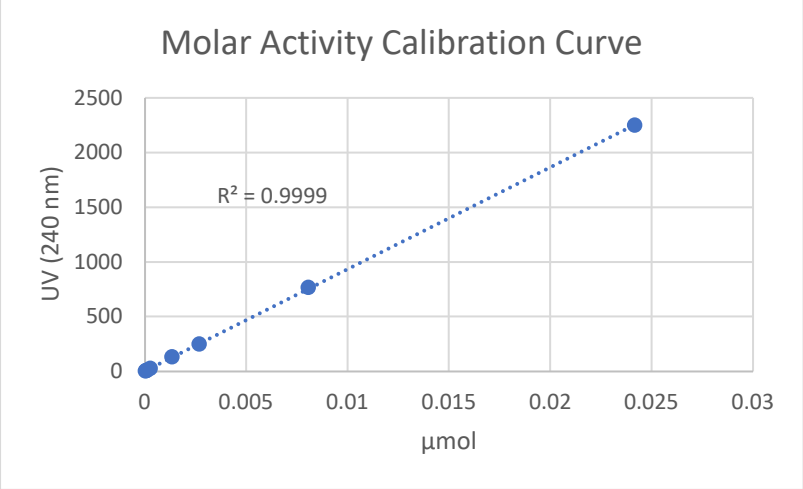

Figure 3.17. Standard curve measuring the UV absorbance of different amounts of authentic reference standard [^{19}F]FVSB.

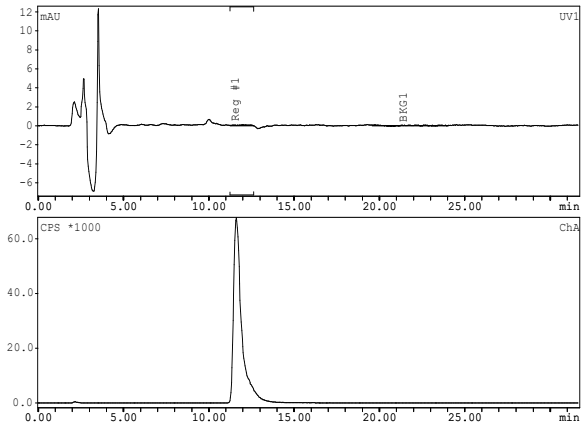

Figure 3.18. Analytical HPLC radio-trace (lower) and UV-trace (upper) of purified [^{18}F]FVSB. HPLC mobile phase: Eluent B.

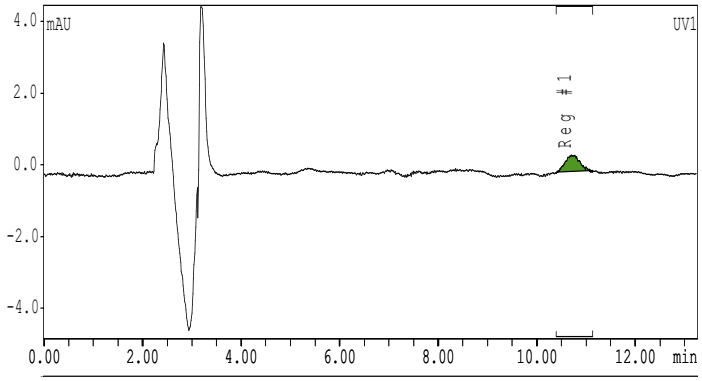

Figure 3.19. Analytical HPLC UV-trace of reference standard [^{19}F]FVSB used for molar activity calculation. HPLC mobile phase: Eluent B.

3.5.4. Bioconjugation

3.5.4.1. General materials and methods

Following cartridge purification of [^{18}F]Fluoro-4-(vinylsulfonyl)benzene (**[^{18}F]FVSB**), the diethyl ether was removed via mild heating (55 ºC) to afford pure dry [^{18}F]FVSB for peptide bioconjugation. To this vial, was added, a solution of peptide in buffer:organic solvent. The contents were sealed with a Teflon lined cap and stirred at 23–45 °C for 20–30 min. An aliquot of

the crude reaction mixture was diluted in buffer (500 µL) and subjected to HPLC analysis. Product identity and purity was determined by HPLC, comparing the radio-trace of ^{18}F-labeled peptide with the UV-trace of the ^{19}F-reference standard, via coinjection. An aliquot of the crude reaction mixture was added to the ^{19}F-reference standard and the sample was subjected to analytical HPLC analysis.

3.5.4.2. Optimization of bioconjugations

Commercial RGDC peptide (Product No. 4030602, Bachem Americas Inc.) was used for all optimization screens, unless otherwise stated. The tables in each section describe the reaction conditions used, with the variable being tested denoted in the table title.

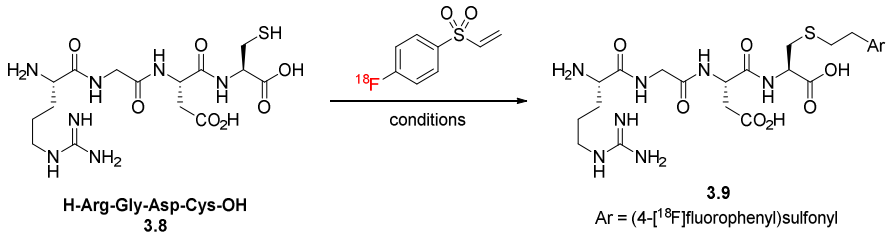

Table 3.7. Optimization of peptide mass[a]

Entry	Peptide mass (mg)	RCY (%)
1	3	59
2	**3**	**74**
3	5	62
4	5	68
5	7	51
6	7	31

[a]Reaction conditions: [^{18}F]FVSB (~500 µCi), RGDC peptide **3.8**, sodium borate buffer (500 µL, pH 8.5), 35 °C, 30 min. RCY was determined by radio-HPLC analysis of the crude product.

Table 3.8. Optimization of reaction temperature[a]

Entry	Reaction Temperature (°C)	RCY (%)
1	23	75
2	23	65
3	35	62
4	35	68
5	45	50
6	45	43

[a]Reaction conditions: [^{18}F]FVSB (~500 μCi), RGDC peptide **3.8** (5 mg), sodium borate buffer (500 μL, pH 8.5), 30 min. RCY was determined by radio-HPLC analysis of the crude product.

Table 3.9. Optimization of solvent system[a]

Entry	Solvent System	RCY (%)
1	HEPES (pH 7.3)	56
2	HEPES (pH 7.3)	61
3	Sodium Borate (pH 8.5)	62
4	Sodium Borate (pH 8.5)	68
5	Sodium Borate (pH 8.5) 75%, MeOH 25%	91
6	Sodium Borate (pH 8.5) 75%, MeOH 25%	81
7	HEPES (pH 7.3) 75%, MeOH 25%	84
8	HEPES (pH 7.3) 75%, MeOH 25%	80
9	**HEPES (pH 7.3) 50%, MeOH 50%**	**90**
10	**HEPES (pH 7.3) 50%, MeOH 50%**	**90**
11	**HEPES (pH 7.3) 50%, MeOH 50%**	**89**
12	**Sodium Borate (pH 8.5) 50%, MeOH 50%**	**90**
13	**Sodium Borate (pH 8.5) 50%, MeOH 50%**	**90**
14	HEPES (pH 7.3) 25%, MeOH 75%	28
15	HEPES (pH 7.3) 25%, MeOH 75%	26
16	Sodium Borate (pH 9.5) 50%, MeOH 50%	93
17	Sodium Borate (pH 9.5) 50%, MeOH 50%	94

[a]Reaction conditions: [^{18}F]FVSB (~500 μCi), RGDC peptide **3.8** (5 mg), solvent (500 μL), 35 °C, 30 min. RCY was determined by radio-HPLC analysis of the crude product.

3.5.4.3. Preparation of ^{18}F-labeled peptides

A solution of peptide (3 mg) and solvent (sodium borate buffer pH 8.5, 250 μL: methanol, 250 μL) was thoroughly mixed via sonication at room temperature for 5 minutes. To a vial containing cartridge-purified, isolated [^{18}F]FVSB **3.7**, was added, the peptide solution. The combined contents were sealed with a Teflon lined cap and the vial was heated on a hot plate to 35 °C for 30 min. An aliquot of the crude reaction mixture was diluted in buffer (500 μL) and subjected to

HPLC analysis. The radiochemical purity (RCP) was calculated by diving the integrated area of the ^{18}F-labeled product peak by the total integrated area of all ^{18}F-labeled peaks, as determined by radio-HPLC, and multiplied by 100 to convert to percentage units. The decay-corrected (d.c.) RCY is relative to [^{18}F]FVSB and was determined by dividing the final activity (d.c.) of the crude ^{18}F-labeled peptide by the starting activity of isolated [^{18}F]FVSB, multiplied by the RCP. Product identity and purity was determined by analytical HPLC, comparing the radio-trace of ^{18}F-labeled peptide with the UV-trace of the authentic ^{19}F-reference standard, via coinjection.

Analytical HPLC Eluent for all ^{18}F-labeled peptide substrates: **Eluent A**.

*Semi-preparative HPLC Eluent for purification of peptide **3.9**:*

Solvent A = H_2O + 0.1% TFA, Solvent B = CH_3CN + 0.1% TFA, Flow rate = 4 mL/min

0 – 5 min = 5% B

5 – 20 min = 5% B to 55% B

30+ min = 55% B

Radiochemical Yield (RCY)

$$= \frac{\text{measured activity of crude 18F labeled product}}{\text{starting activity of isolated [18F]FVSB}} \times (\text{RCP}) \times 100\%$$

^{18}F-labeled RGDC Analogue (3.9)

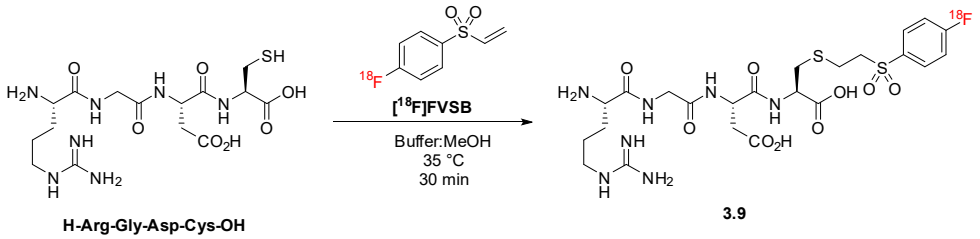

Table 3.10. Bioconjugation of Arg-Gly-Asp-Cys to [^{18}F]FVSB

Entry	Starting Activity (mCi)	Crude Product Activity (mCi)	RCP (%)	RCY (d.c.) (%)
1	0.463	0.319 (0.406 d.c.)	87	76
2	0.545	0.428 (0.521 d.c.)	96	92
3	0.377	0.294 (0.372 d.c.)	86	85
Average			**89 ± 6**	**84 ± 8**

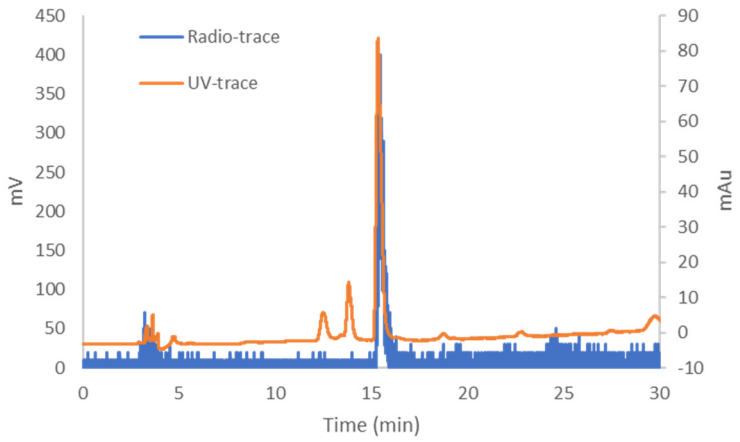

Figure 3.20. Analytical HPLC trace. Coinjection of crude ^{18}F-labeled peptide **3.9** (radio-HPLC trace = blue) with the purified peptide reference standard (UV trace = orange).

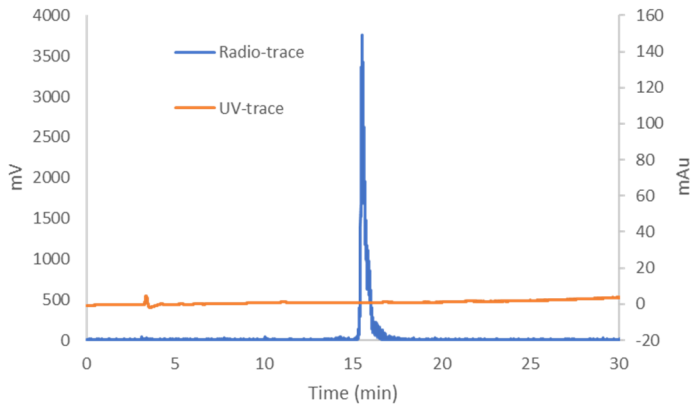

Figure 3.21. Analytical HPLC trace of HPLC-purified ^{18}F-labeled peptide **3.9**.

^{18}F-labeled MG11 analogue (3.10)

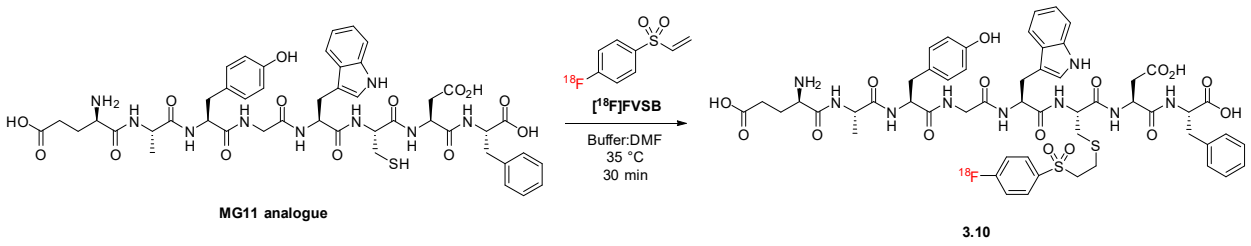

Table 3.11. Bioconjugation of MG11 analogue to [^{18}F]FVSB

Entry	Starting Activity (mCi)	Crude Product Activity (mCi)	RCP (%)	RCY (d.c.) (%)
1	1.515	1.240 (1.510 d.c.)	88	88
2	0.457	0.377 (0.456 d.c.)	90	90
3	0.495	0.401 (0.493 d.c.)	72	72
Average			**83 ± 10**	**83 ± 10**

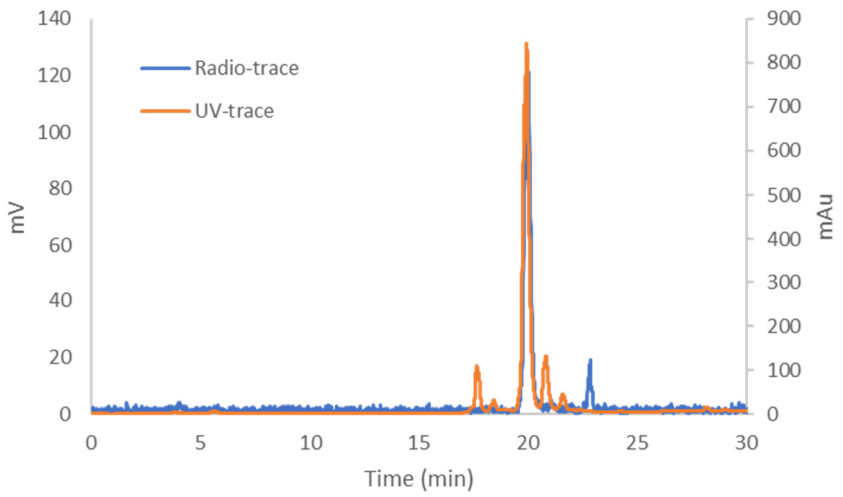

Figure 3.22. Analytical HPLC trace. Coinjection of crude ^{18}F-labeled peptide **3.10** (radio-HPLC trace = blue) with the purified peptide reference standard (UV trace = orange).

^{18}F-labeled c(RGDfC) analogue (3.11)

Note: For c(RGDfC) analogue **3.11, 5 mg of peptide precursor and 1.0 M HEPES buffer pH 7.3, 250 µL: dimethylformamide, 250 µL were used.

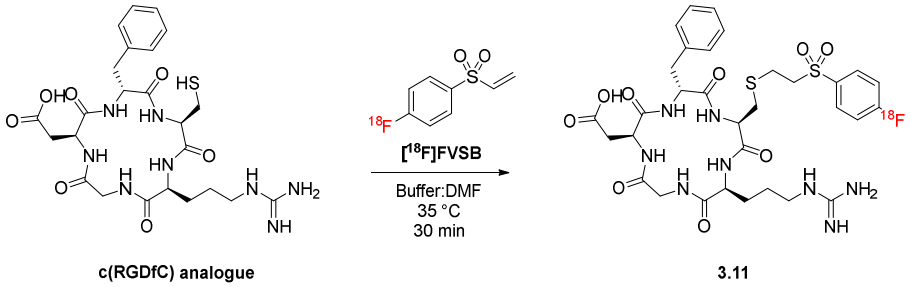

Table 3.12. Bioconjugation of c(RGDfC) analogue to [^{18}F]FVSB

Entry	Starting Activity (mCi)	Crude Product Activity (mCi)	RCP (%)	RCY (d.c.) (%)
1	0.475	0.393 (0.474 d.c.)	84	84
2	0.643	0.532 (0.640 d.c.)	88	88
3	0.811	0.671 (0.808 d.c.)	88	88
Average			**87 ± 2**	**87 ± 2**

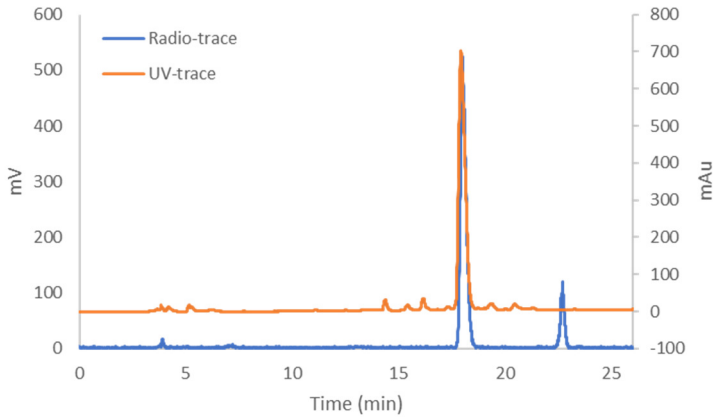

Figure 3.23. Analytical HPLC trace. Coinjection of crude ^{18}F-labeled peptide **3.11** (radio-HPLC trace = blue) with the purified peptide reference standard (UV trace = orange).

^{18}F-labeled PSMA analogue (3.12)

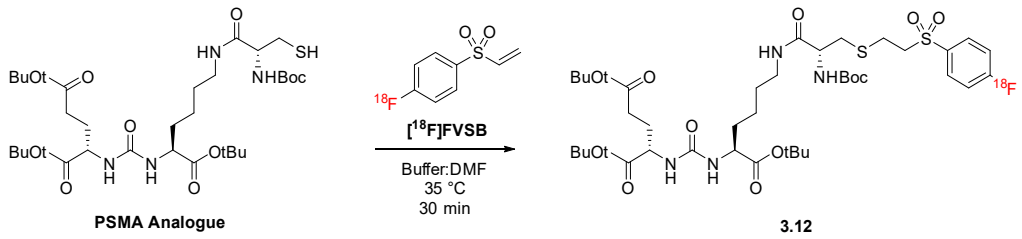

Table 3.13. Bioconjugation of PSMA analogue to [^{18}F]FVSB

Entry	Starting Activity (mCi)	Crude Product Activity (mCi)	RCP (%)	RCY (d.c.) (%)
1	1.508	1.113 (1.501 d.c.)	78	78
2	0.319	0.264 (0.318 d.c.)	79	79
3	1.473	1.147 (1.397 d.c.)	88	83
Average			**82 ± 6**	**80 ± 3**

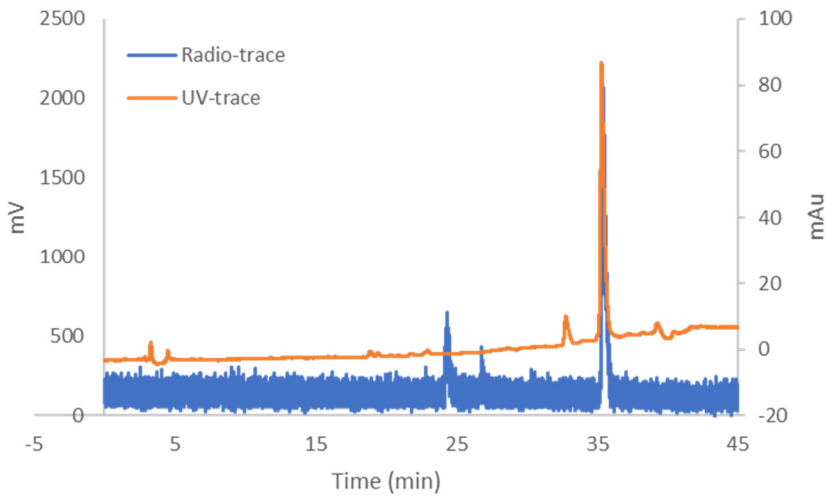

Figure 3.24. Analytical HPLC trace. Coinjection of crude ^{18}F-labeled peptide **3.12** (radio-HPLC trace = blue) with the purified peptide reference standard (UV trace = orange).

^{18}F-labeled Neuromedin B analogue (3.13)

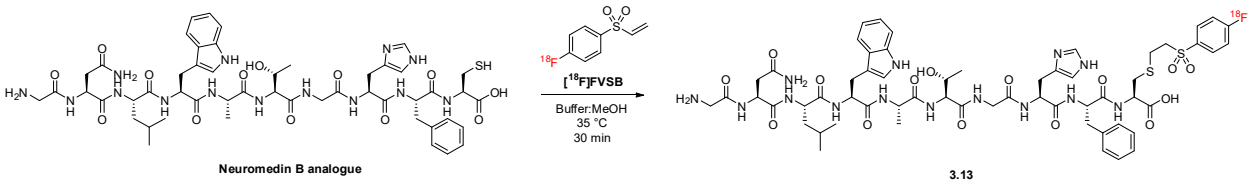

Table 3.14. Bioconjugation of Neuromedin B analogue to [^{18}F]FVSB

Entry	Starting Activity (mCi)	Crude Product Activity (mCi)	RCP (%)	RCY (d.c.) (%)
1	0.517	0.386 (0.511 d.c.)	93	92
2	1.779	1.448 (1.752 d.c.)	95	94
3	0.391	0.320 (0.389 d.c.)	92	92
Average			**93 ± 2**	**93 ± 1**

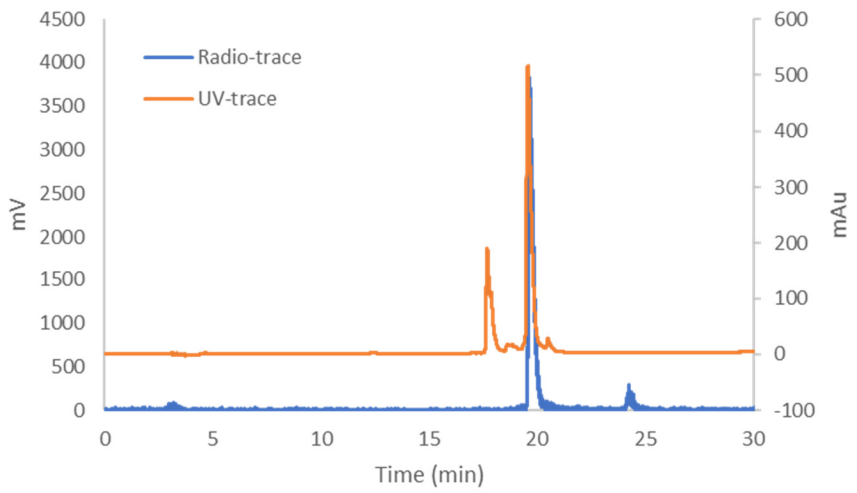

Figure 3.25. Analytical HPLC trace. Coinjection of crude ^{18}F-labeled peptide **3.13** (radio-HPLC trace = blue) with the purified peptide reference standard (UV trace = orange).

^{18}F-labeled Bombesin analogue (3.14)

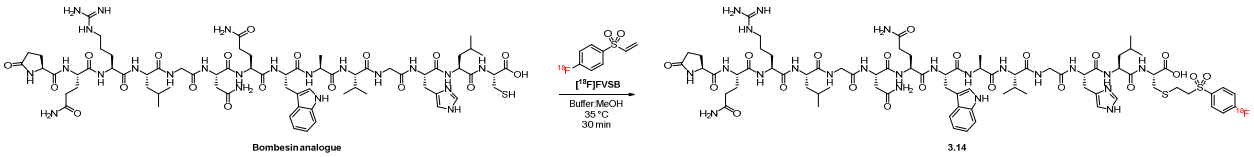

Table 3.15. Bioconjugation of Bombesin analogue to [^{18}F]FVSB. [a]5 mg peptide, HEPES buffer pH 7.3 (250 µL), DMF (250 µL)

Entry	Starting Activity (mCi)	Crude Product Activity (mCi)	RCP (%)	RCY (d.c.) (%)
1	0.753	0.591 (0.723 d.c.)	55	53
2	0.630	0.416 (0.526 d.c.)	80	67
3	0.431	0.332 (0.423 d.c.)	46	45
Average			**60 ± 18**	**55 ± 11**
4[a]	1.172	0.936 (1.162 d.c.)	50	50
5[a]	0.807	0.650 (0.797 d.c.)	42	41
6[a]	0.627	0.508 (0.623 d.c.)	43	43
Average[a]			**45 ± 4**	**45 ± 4**

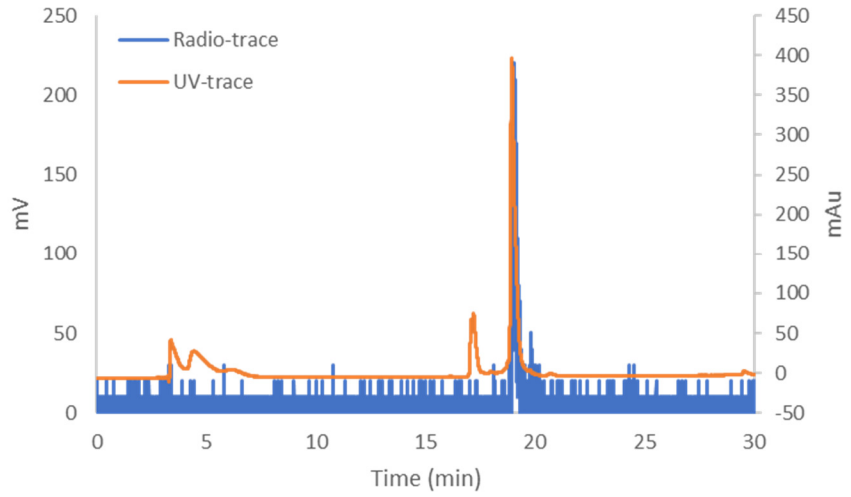

Figure 3.26. Analytical HPLC trace. Coinjection of crude ^{18}F-labeled peptide **3.14** (radio-HPLC trace = blue) with the purified peptide reference standard (UV trace = orange).

3.5.4.4. Competition experiments

Chemoselectivity towards cysteine bioconjugation in the presence of other nucleophilic amino acid residues was examined. Amino acid residues were added either alone (5 mg) or in parallel with cysteine (3 mg each) to a solution of cartridge purified [^{18}F]FVSB (500 µL, 1:1, 1.0 M HEPES buffer pH 7.3: methanol). The contents were sealed with a Teflon lined cap and heated to 35 °C for 30 min. An aliquot of the crude reaction mixture was diluted in buffer (500 µL) and analyzed using analytical HPLC. HPLC Mobile Phase: Eluent A.

Cysteine conjugation

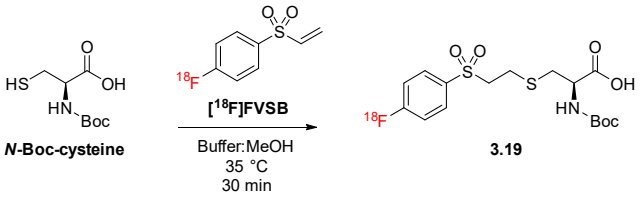

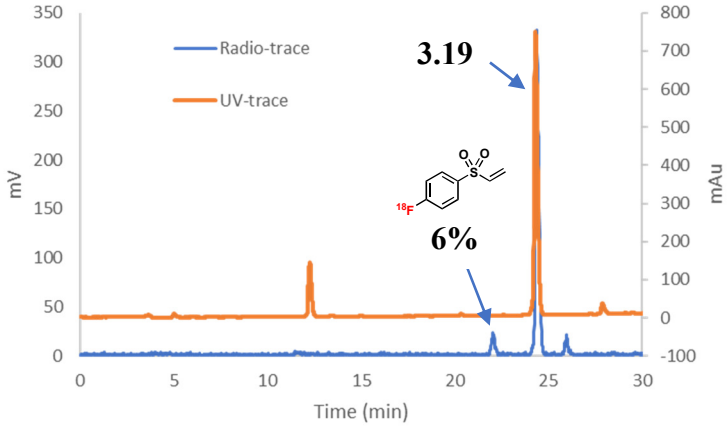

Figure 3.27. Radio-HPLC trace (blue) of the crude ^{18}F-labeled *N*-Boc-cysteine **3.19** coinjected with the ^{19}F authentic reference standard (UV trace = orange). Reaction between *N*-Boc-cysteine and [^{18}F]FVSB **3.7** afforded cysteine-conjugate addition product **3.19** in 84 ± 4% RCY and unreacted [^{18}F]FVSB **3.7** in 6 ± 2% RCY, determined via analytical radio-HPLC (n = 3).

Lysine conjugation

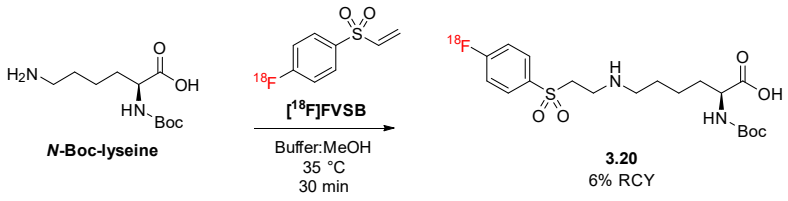

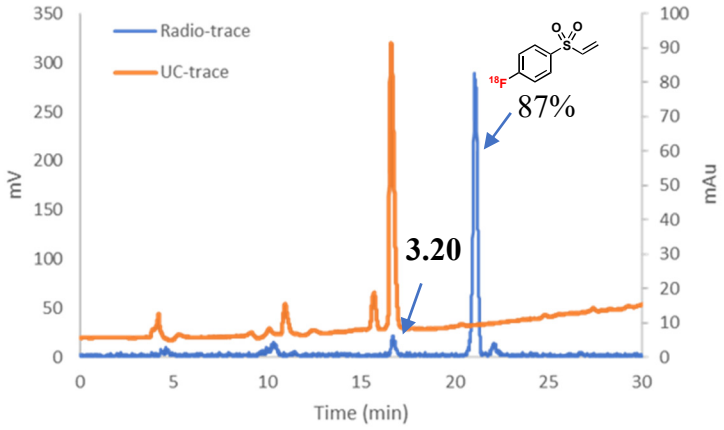

Figure 3.28. Radio-HPLC trace (blue) of the crude ^{18}F-labeled *N*-Boc-lysine **3.20** coinjected with the ^{19}F authentic reference standard (UV trace = orange). Reaction between *N*-Boc-lysine and [^{18}F]FVSB **3.7** afforded lysine-conjugate addition product **3.20** in 6 ± 2% RCY and unreacted [^{18}F]FVSB **3.7** in 87 ± 8% RCY, determined via analytical radio-HPLC (n = 3).

Lysine versus Cysteine conjugation

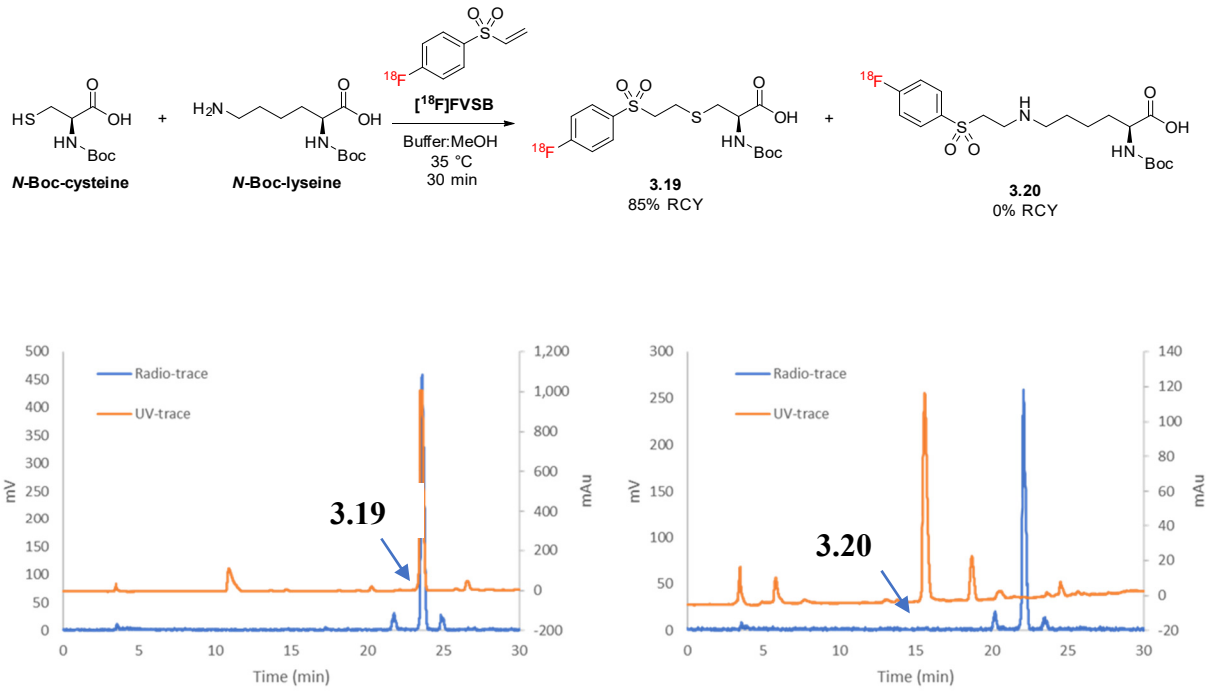

Figure 3.29. Competition experiment between *N*-Boc-lysine and *N*-Boc-cysteine. Radio-HPLC trace (blue) of the crude reaction mixture coinjected with the ^{19}F authentic reference standards (UV trace = orange). Reaction with [^{18}F]FVSB **3.7** afforded cysteine-conjugate addition product **3.19** in 85 ± 0% RCY, determined via analytical radio-HPLC with ^{19}F-*N*-Boc-cysteine coinjection (left). Lysine-conjugate addition product **3.20** was not observed via analytical radio-HPLC with ^{19}F-*N*-Boc-lysine coinjection (right). Experiments were conducted in triplicate.

Histidine conjugation

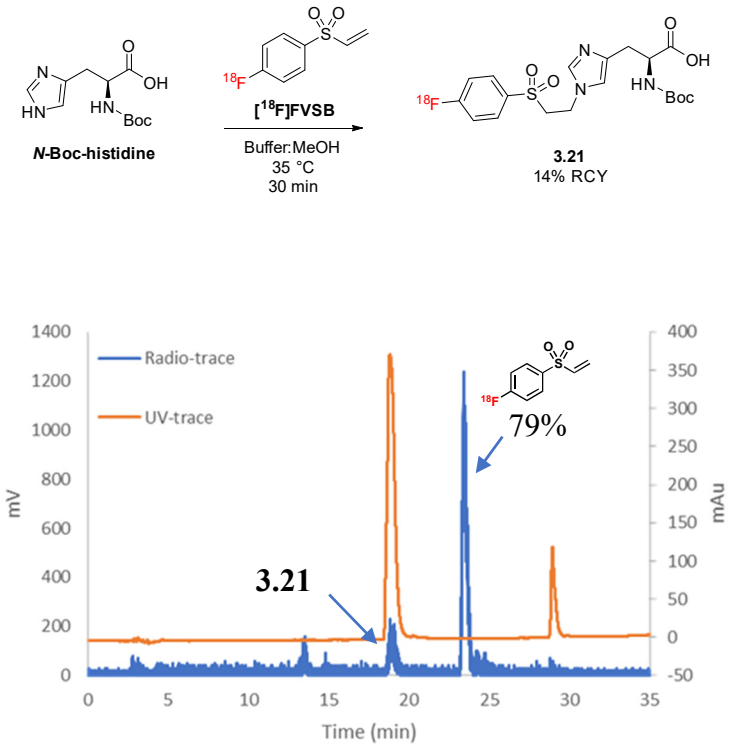

Figure 3.30. Radio-HPLC trace (blue) of the crude ^{18}F-labeled *N*-Boc-histidine **3.21** coinjected with the ^{19}F authentic reference standard (UV trace = orange). Reaction between *N*-Boc-histidine and [^{18}F]FVSB **3.7** afforded histidine-conjugate addition product **3.21** in 14 ± 1% RCY and unreacted [^{18}F]FVSB **7** in 79 ± 3% RCY, determined via analytical radio-HPLC (n = 3).

Histidine versus Cysteine conjugation

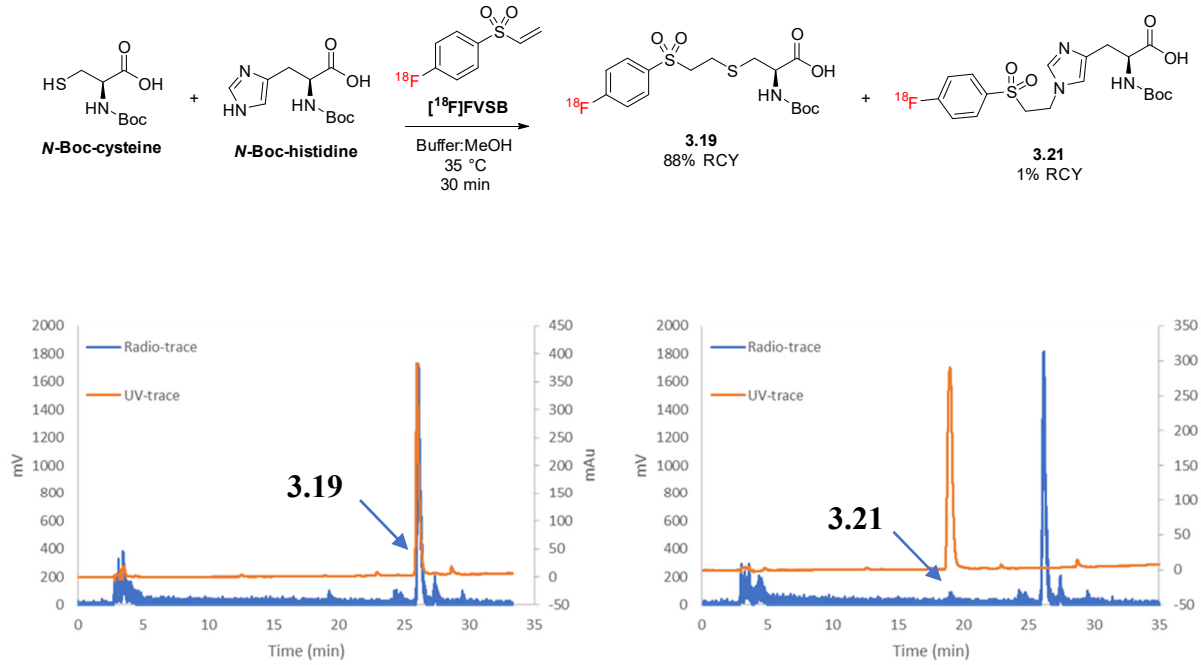

Figure 3.31. Competition experiment between *N*-Boc-histidine and *N*-Boc-cysteine. Radio-HPLC trace (blue) of the crude reaction mixture coinjected with the ^{19}F authentic reference standards (UV trace = orange). Reaction with [^{18}F]FVSB **3.7** afforded cysteine-conjugate addition product **3.19** in 88 ± 2% RCY, determined via analytical radio-HPLC with ^{19}F-*N*-Boc-cysteine coinjection (upper panel). Histidine-conjugate addition product **3.21** was formed in 1 ± 2% RCY, determined via analytical radio-HPLC with ^{19}F-*N*-Boc-histidine coinjection (lower panel). Experiments were conducted in triplicate.

N-terminal amine conjugation to [^{18}F]FVSB

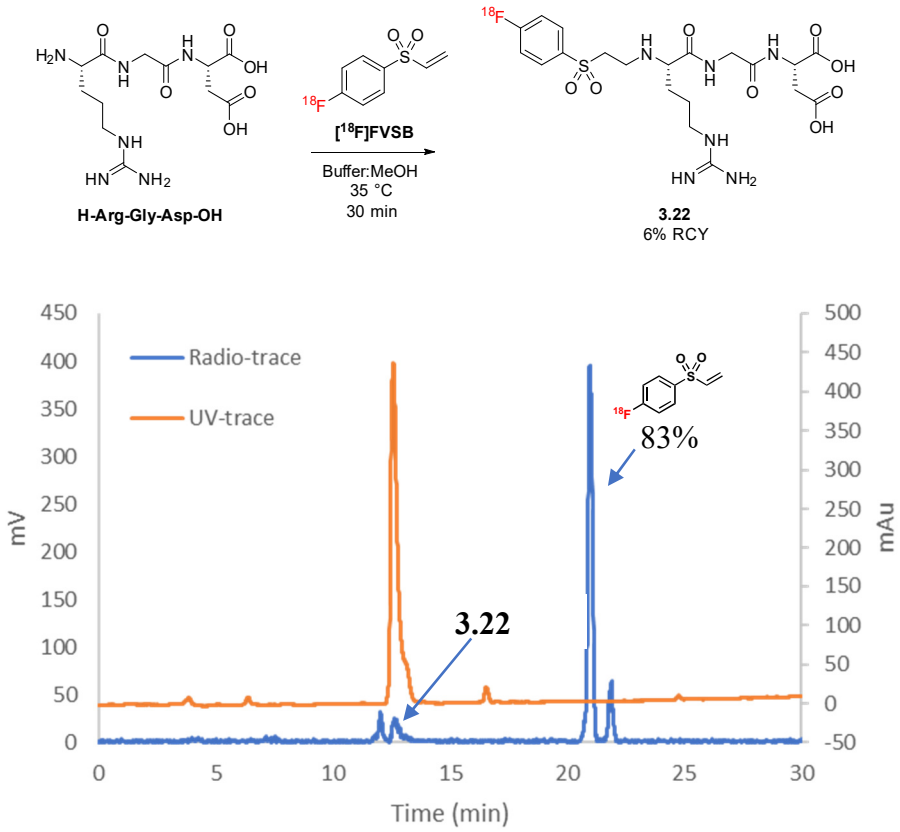

Figure 3.32. Radio-HPLC trace (blue) of the crude ^{18}F-labeled RGD construct **3.22** coinjected with the ^{19}F authentic reference standard (UV trace = orange). Reaction between the *N*-terminal amine of H-Arg-Gly-Asp-OH and [^{18}F]FVSB **3.7** afforded the conjugate addition product **3.22** in 6 ± 1% RCY and unreacted [^{18}F]FVSB **3.7** in 83 ± 1% RCY, determined via analytical radio-HPLC (n = 3).

3.5.4.5. Peptide conjugate stability studies

The stability of the thioether bond formed via Michael addition to [^{18}F]FVSB was evaluated under various conditions to identify if the retro-Michael reaction readily occurs with the peptide conjugates. To HPLC-purified, ^{18}F-labeled RGDC peptide **3.9** (40-60 μCi) was added the appropriate acid/base/glutathione buffer solution (500 μL) in a borosilicate glass reaction vial. The reaction vial was sealed with a Teflon lined cap and stirred for 1 h at 35 °C, using a heating block on a hot plate. An aliquot of the crude reaction mixture (175 μL) was analyzed by HPLC and the remaining amounts of peptide **3.9** were analyzed at 0 h and 1 h time points.

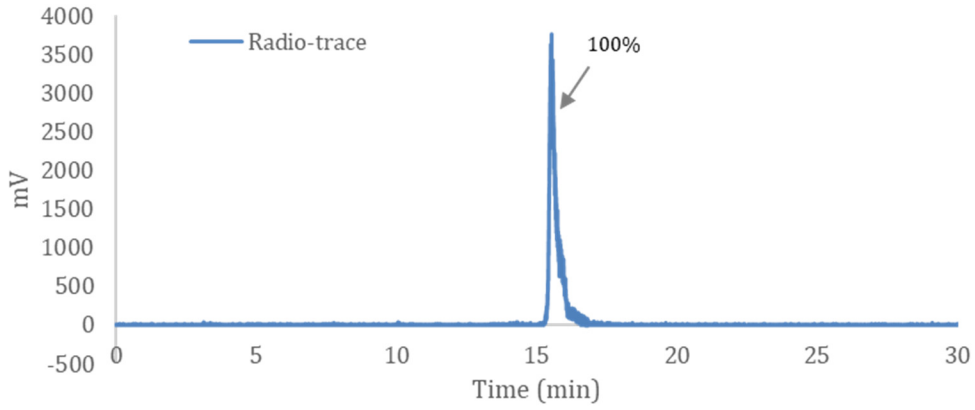

Figure 3.33. Initial analytical radio-HPLC trace of the purified ^{18}F-labeled RGDC construct **3.9**.

Stability in acidic media: 0.5 M acetic acid buffer, pH 2.6

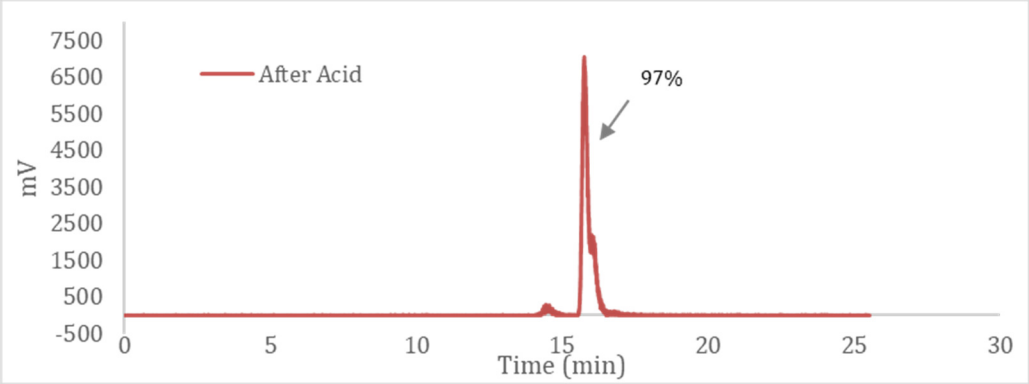

Figure 3.34. Analytical radio-HPLC trace of the purified ^{18}F-labeled RGDC construct **3.9** in acidic media after 1 h.

Stability in basic media: 0.5 M sodium borate buffer, pH 9.5

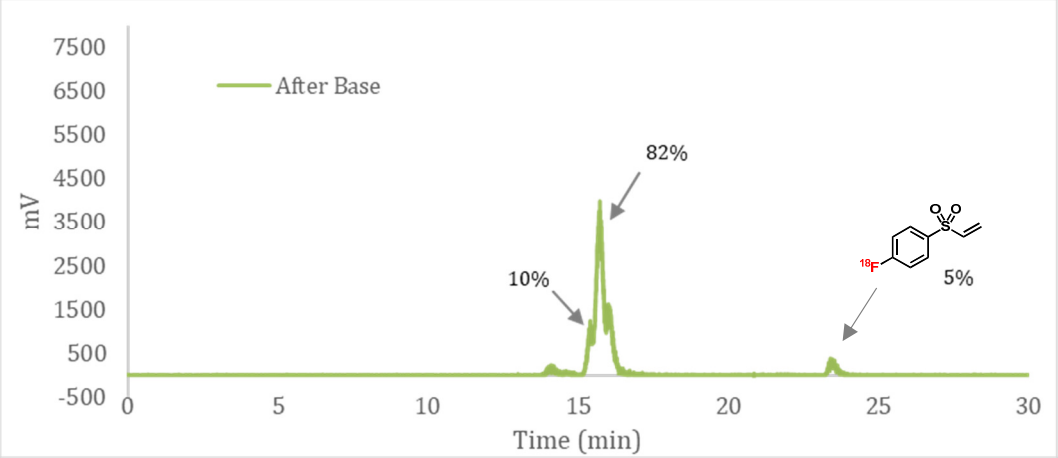

Figure 3.35. Analytical radio-HPLC trace of the purified ^{18}F-labeled RGDC construct **3.9** in basic media after 1 h.

Stability in neutral media with glutathione: 3.3 mM glutathione in water, pH 7.0

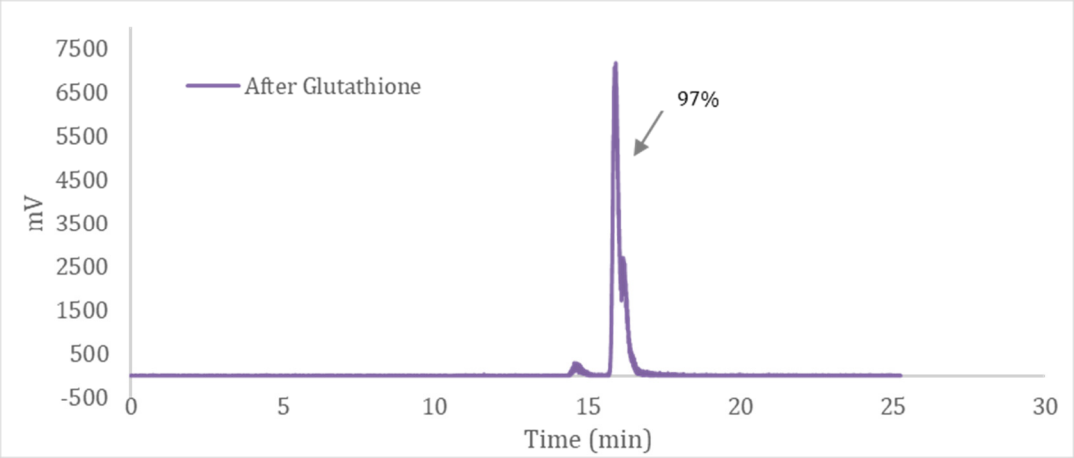

Figure 3.36. Analytical radio-HPLC trace of the purified ^{18}F-labeled RGDC construct **3.9** in neutral media with glutathione after 1 h.

3.6. Appendix

3.6.1. ^{1}H, ^{13}C, ^{19}F NMR Spectra

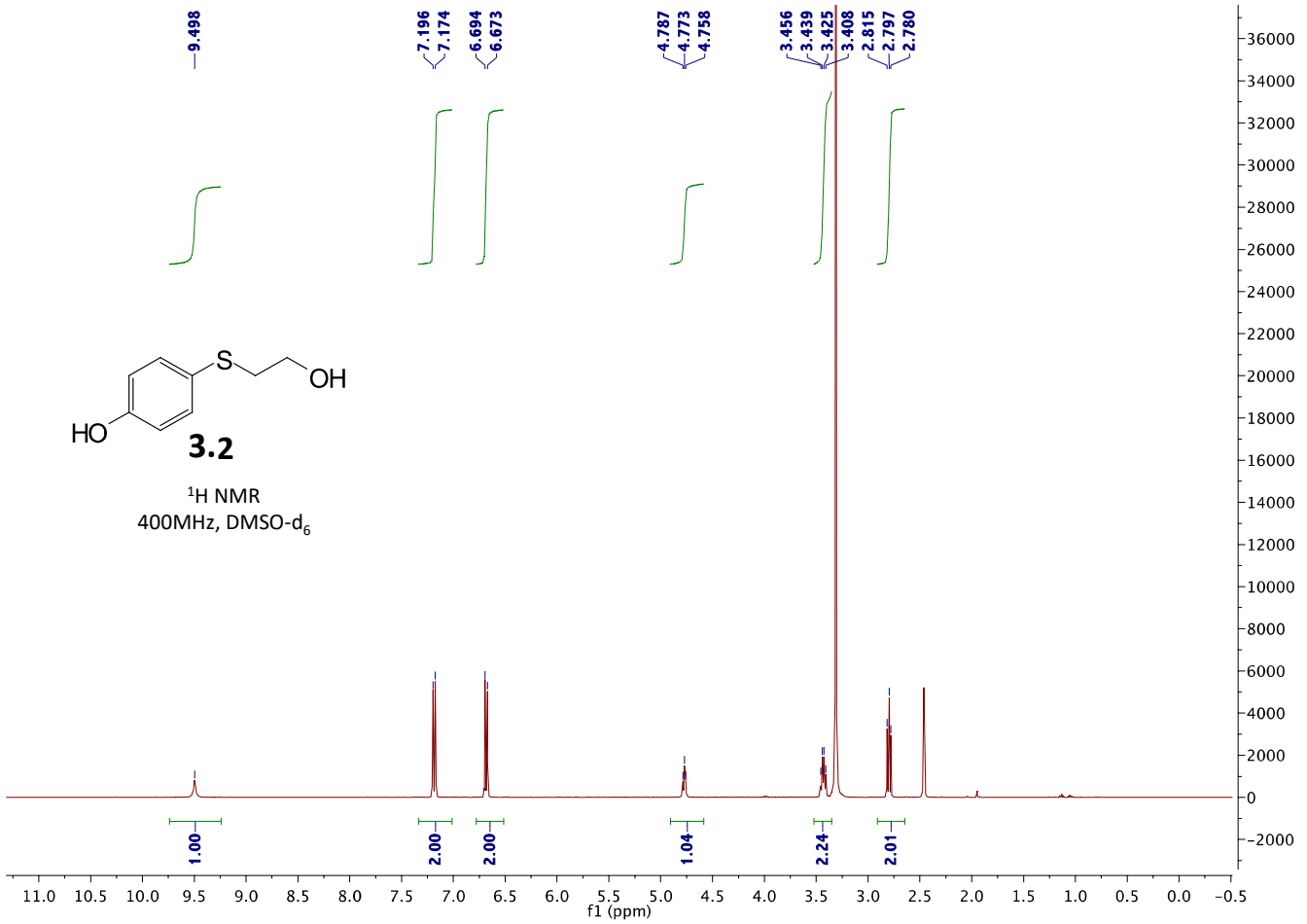

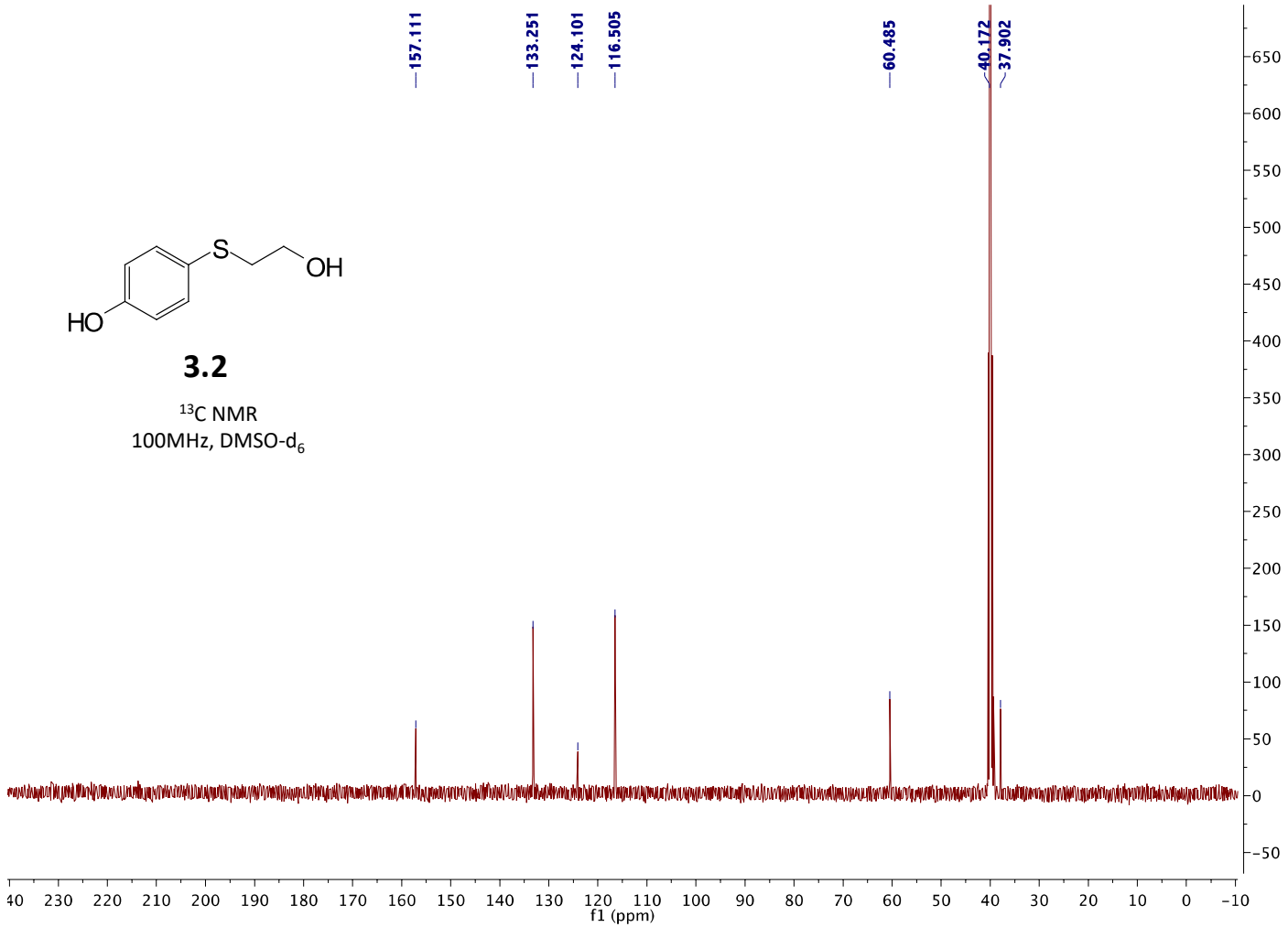
157.111
133.251
124.101
116.505
60.485
40.172
37.902
S
OH
HO
3.2
13C NMR
100MHz, DMSO-d6
f1 (ppm)

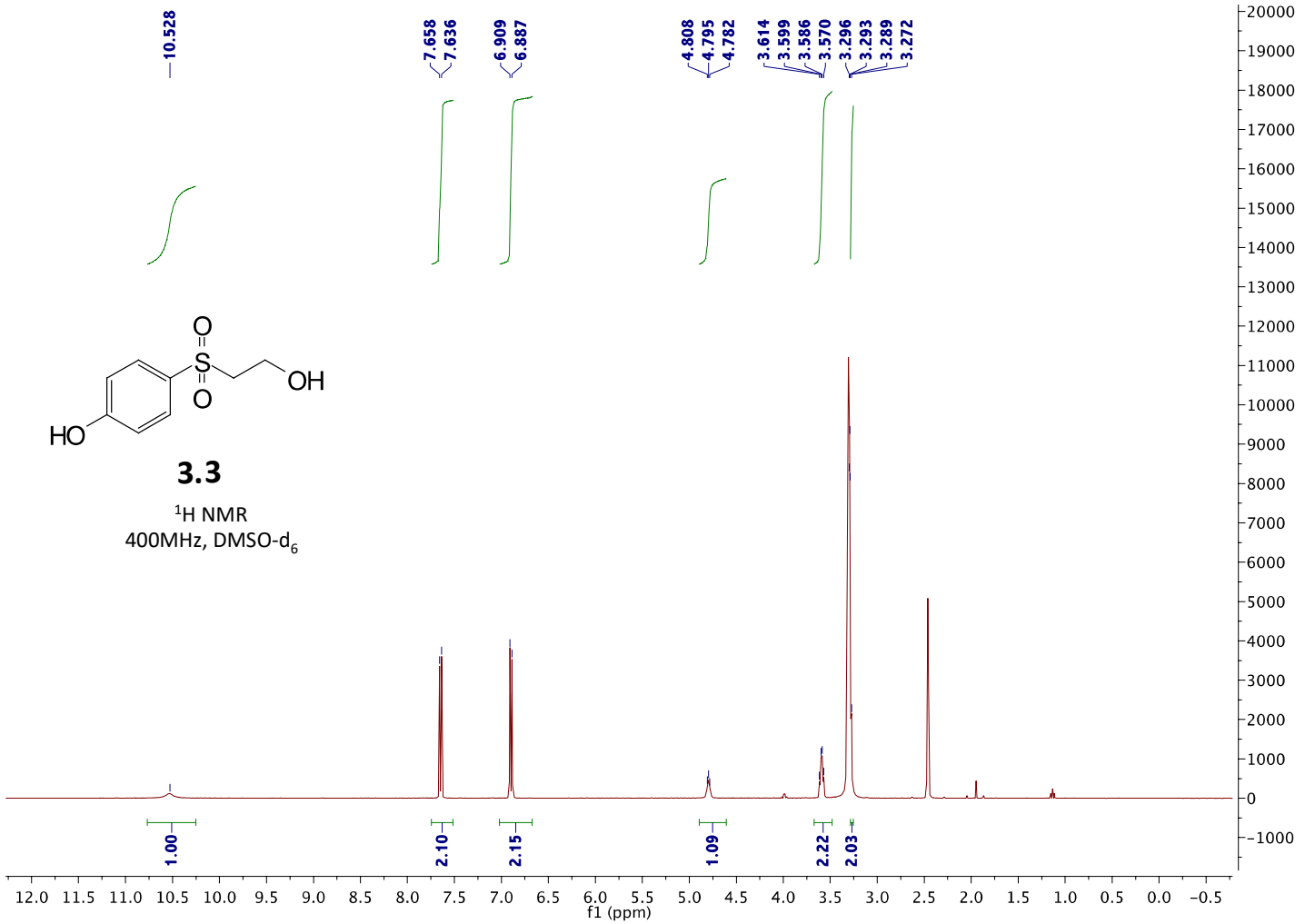
10.528
7.658
7.636
6.909
6.887
4.808
4.795
4.782
3.614
3.599
3.586
3.570
3.296
3.293
3.289
3.272
HO
S
O
O
OH
3.3
1H NMR
400MHz, DMSO-d6
1.00
2.10
2.15
1.09
2.22
2.03
f1 (ppm)

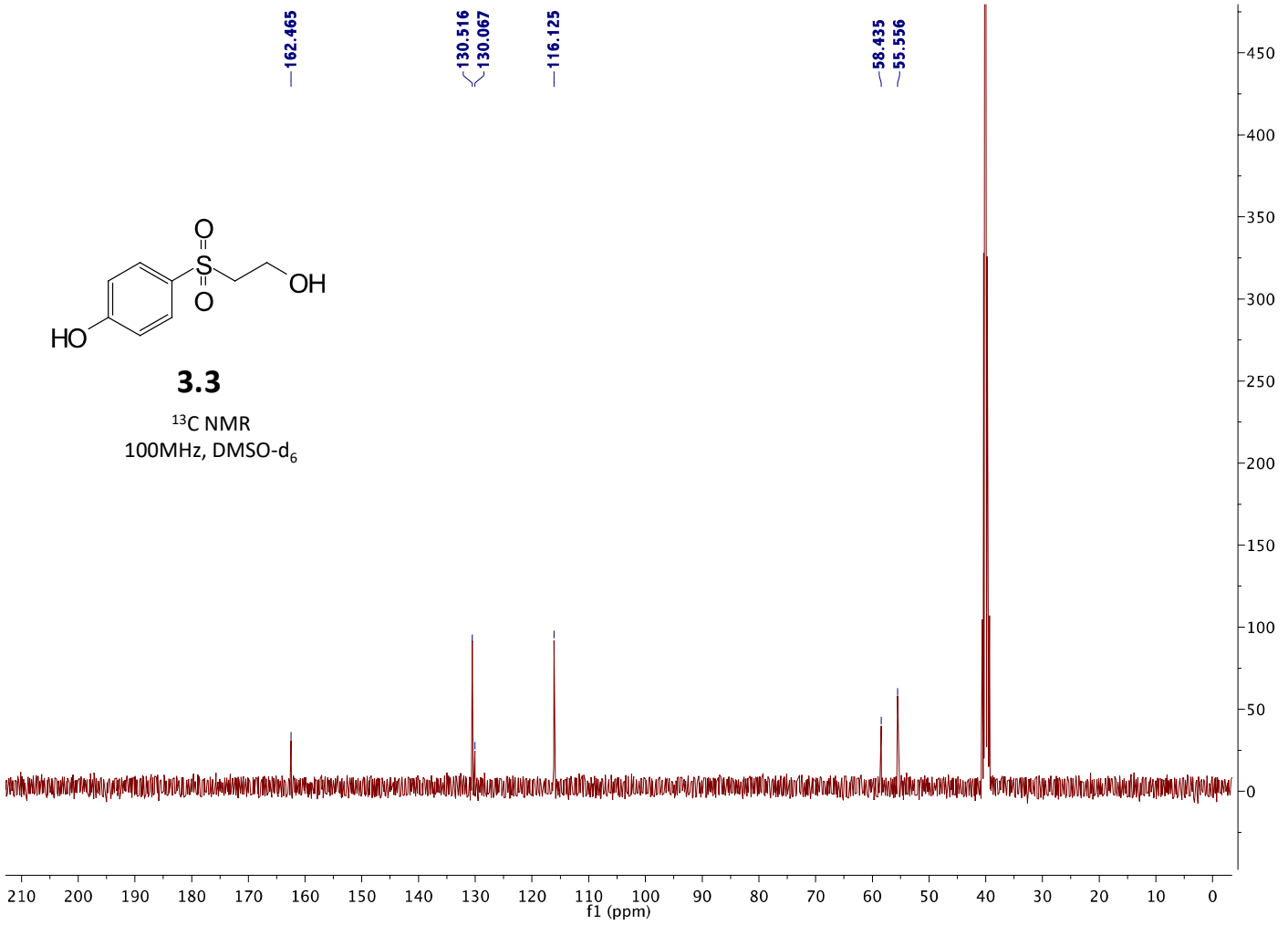
162.465
130.516
130.067
116.125
58.435
55.556
HO
OH
O
S
O
3.3
13C NMR
100MHz, DMSO-d6
f1 (ppm)

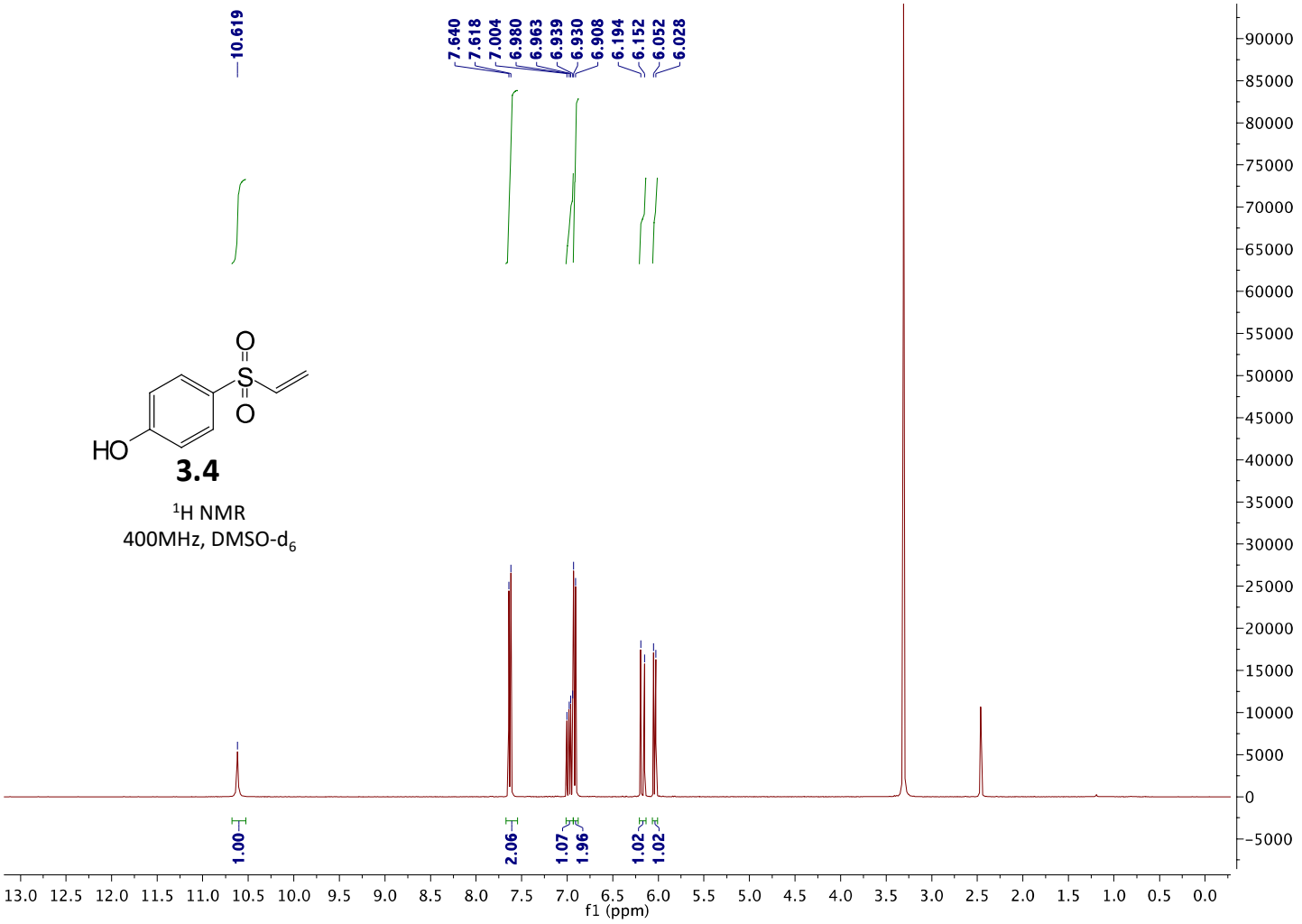
10.619
7.640
7.618
7.004
6.980
6.963
6.939
6.930
6.908
6.194
6.152
6.052
6.028
HO
3.4
1H NMR
400MHz, DMSO-d6
1.00
2.06
1.07
1.96
1.02
1.02
f1 (ppm)

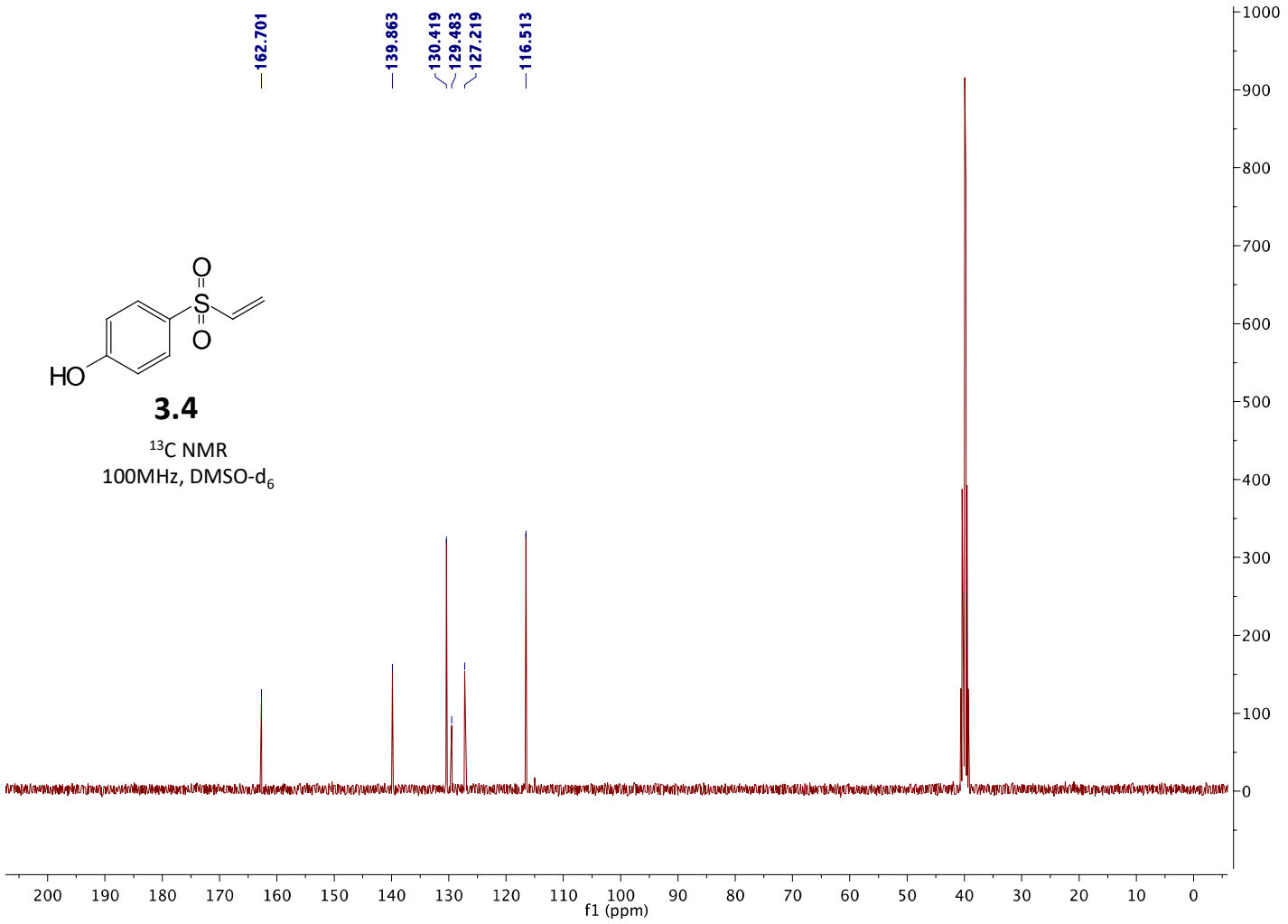
162.701
139.863
130.419
129.483
127.219
116.513
HO
O
S
O
3.4
13C NMR
100MHz, DMSO-d6
1000
900
800
700
600
500
400
300
200
100
0
200 190 180 170 160 150 140 130 120 110 100 90 80 70 60 50 40 30 20 10 0
f1 (ppm)

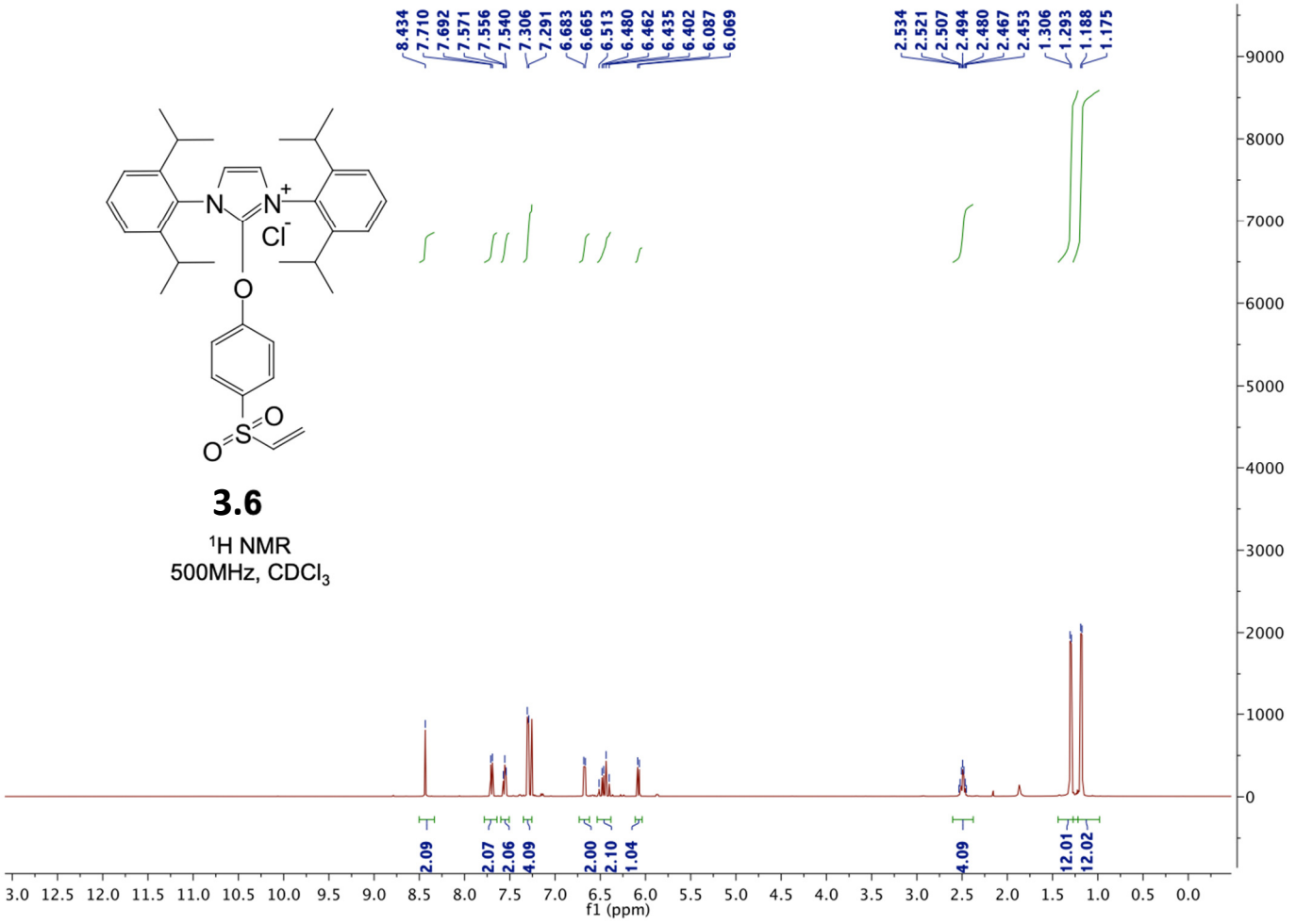
8.434
7.710
7.692
7.571
7.556
7.540
7.306
7.291
6.683
6.665
6.513
6.480
6.462
6.435
6.402
6.087
6.069
2.534
2.521
2.507
2.494
2.480
2.467
2.453
1.306
1.293
1.188
1.175
Cl-
O
O
O
S
3.6
1H NMR
500MHz, CDCl3
2.09
2.07
2.06
4.09
2.00
2.10
1.04
4.09
12.01
12.02
f1 (ppm)

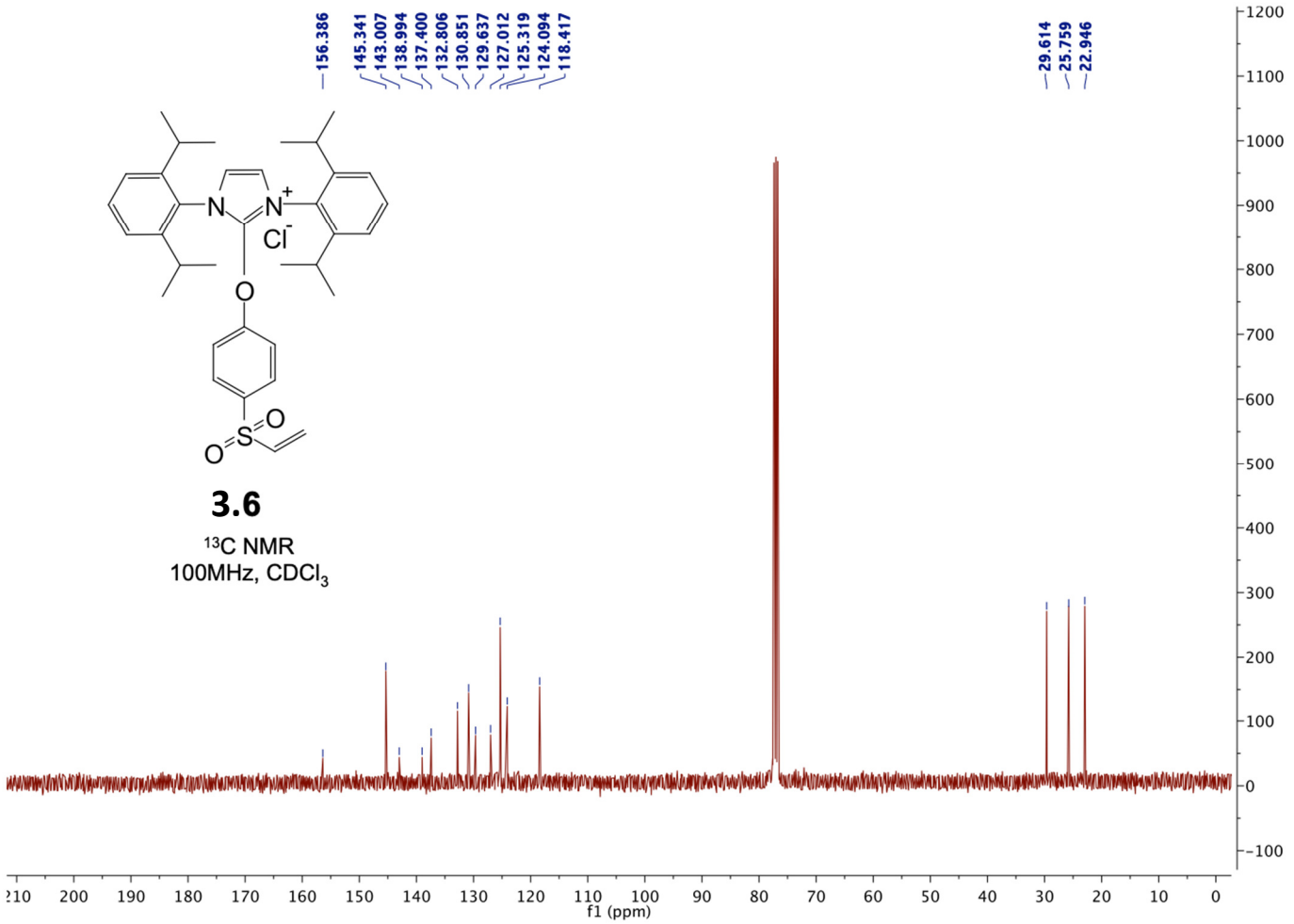
156.386
145.341
143.007
138.994
137.400
132.806
130.851
129.637
127.012
125.319
124.094
118.417
29.614
25.759
22.946
N
N+
Cl-
O
O
S
O
O
3.6
13C NMR
100MHz, CDCl3
f1 (ppm)

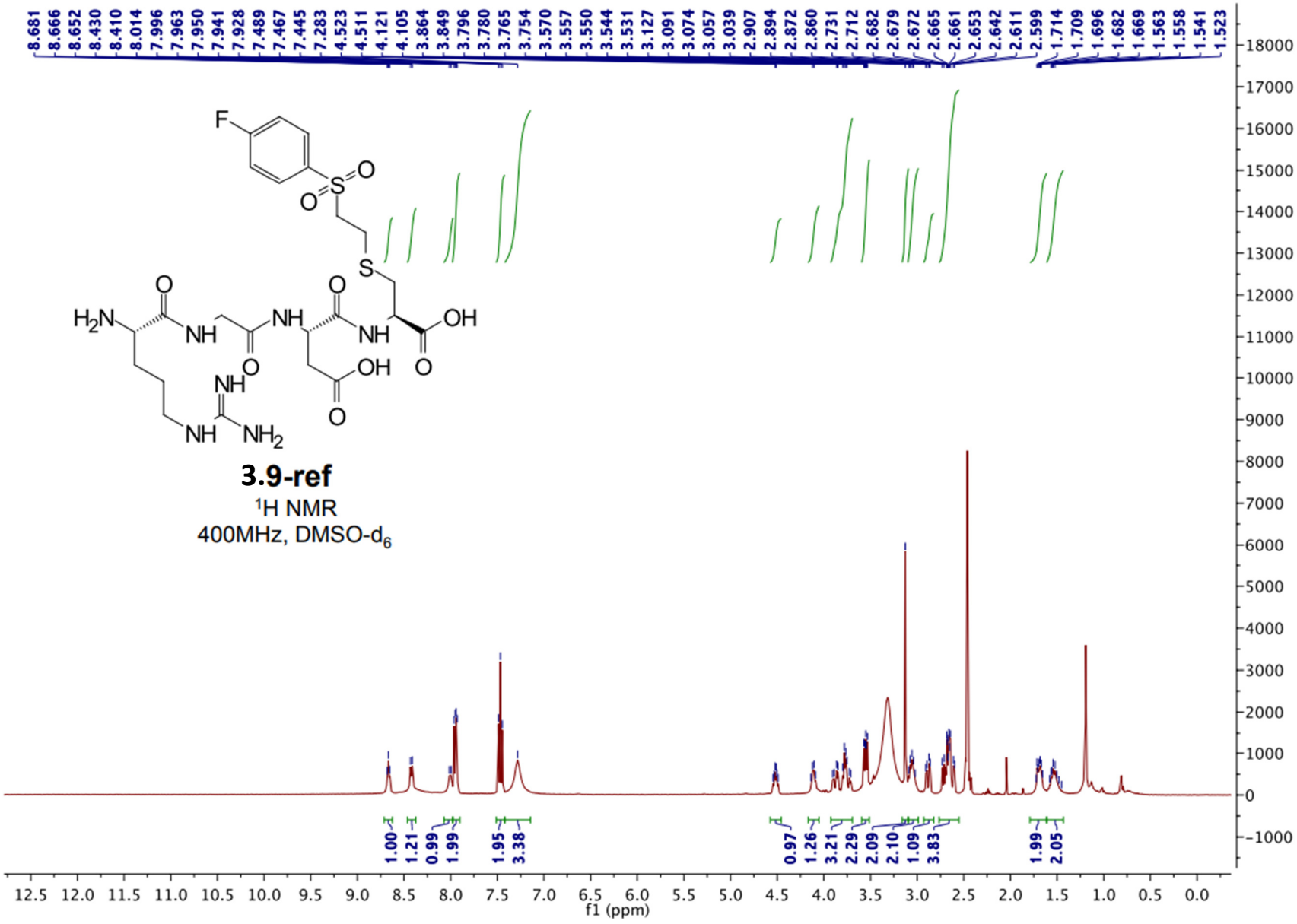
3.9-ref
1H NMR
400MHz, DMSO-d6
f1 (ppm)

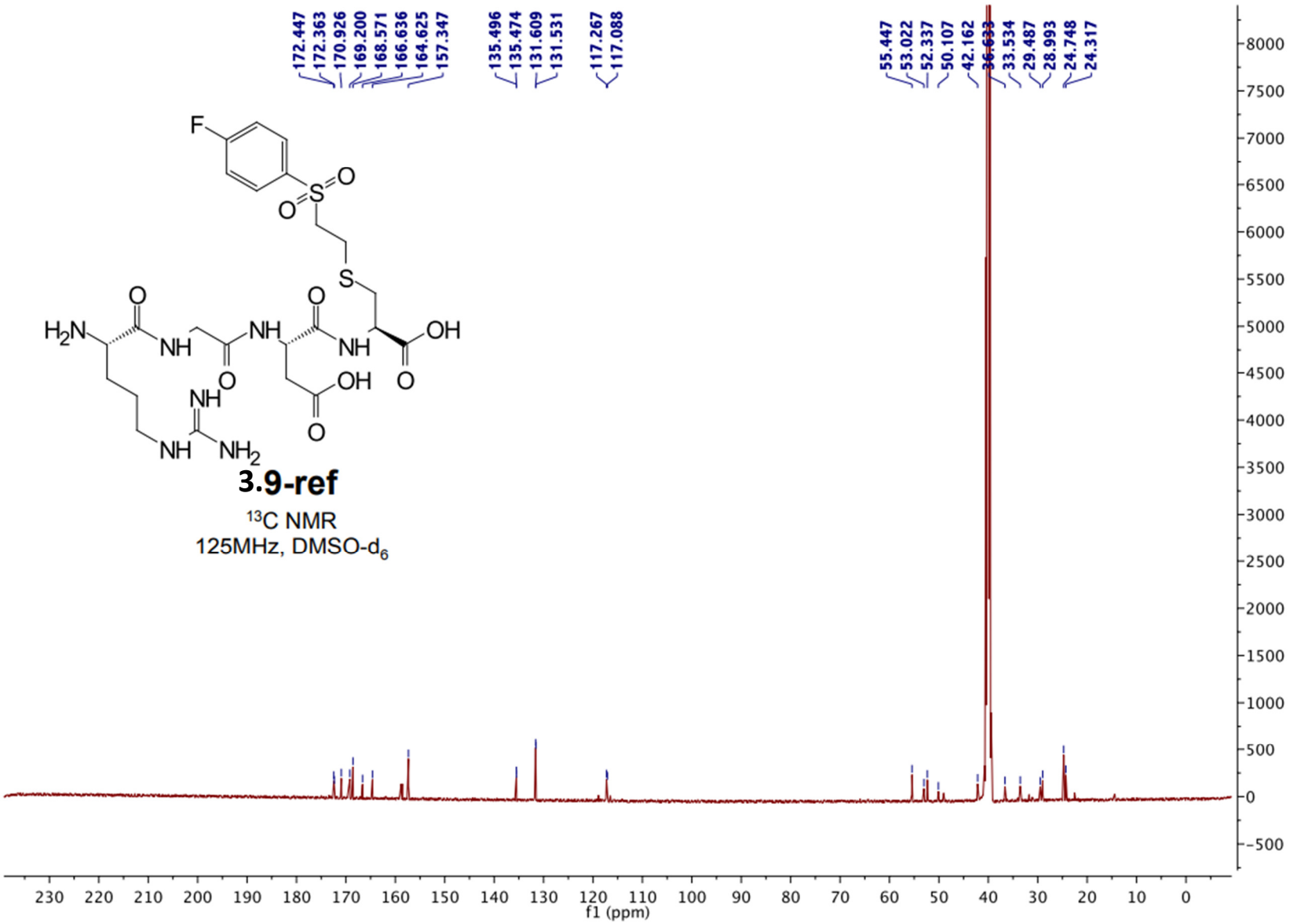
172.447
172.363
170.926
169.200
168.571
166.636
164.625
157.347
135.496
135.474
131.609
131.531
117.267
117.088
55.447
53.022
52.337
50.107
42.162
36.633
33.534
29.487
28.993
24.748
24.317
F
O
O
S
S
O
NH
NH
NH
OH
O
O
O
O
NH
NH
NH2
3.9-ref
13C NMR
125MHz, DMSO-d6
f1 (ppm)

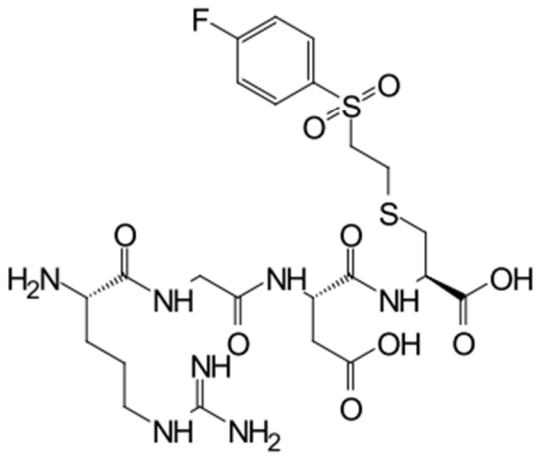

3.9-ref

^{19}F NMR
376MHz, DMSO-d_6

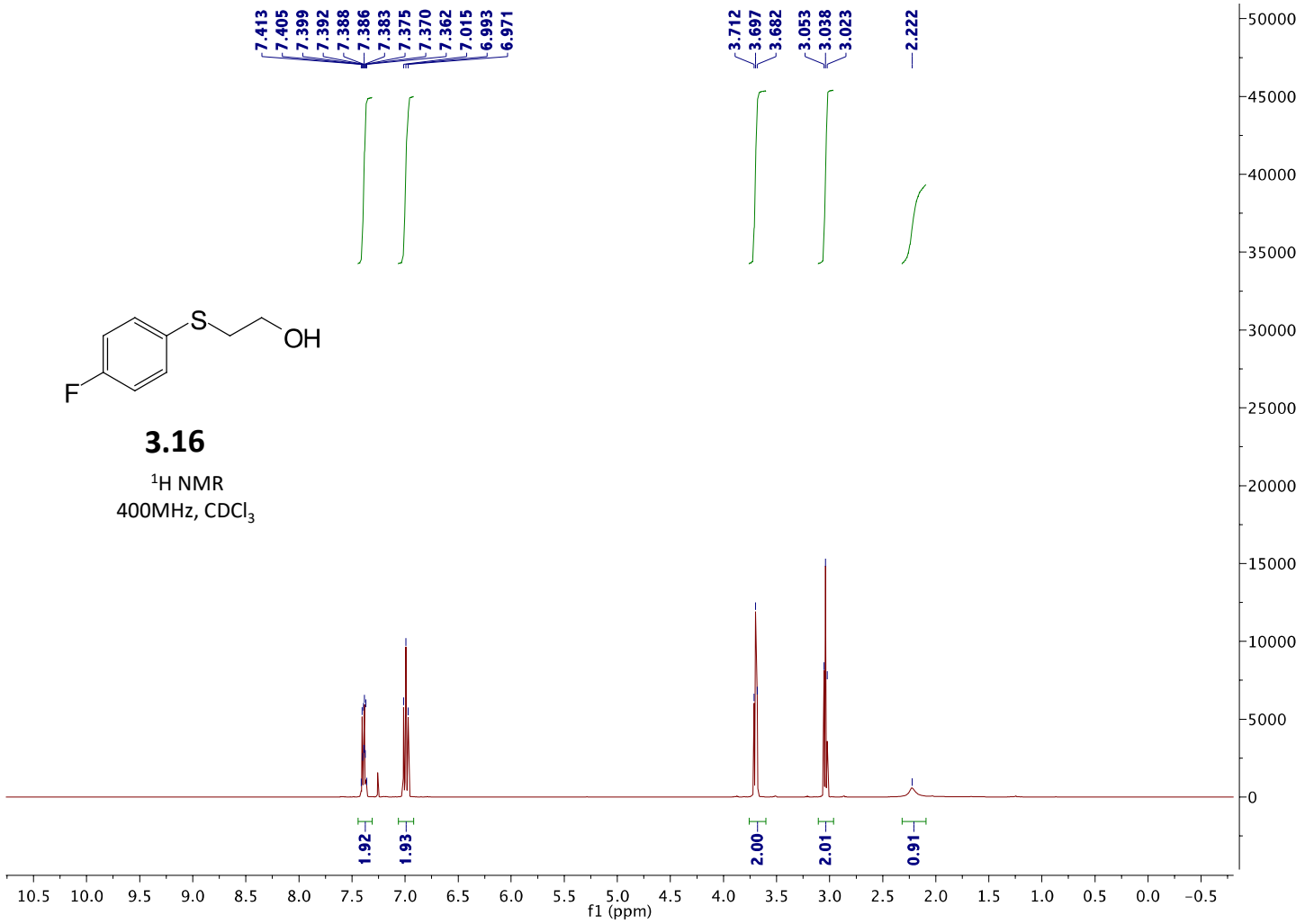
7.413
7.405
7.399
7.392
7.388
7.386
7.383
7.375
7.370
7.362
7.015
6.993
6.971
3.712
3.697
3.682
3.053
3.038
3.023
2.222
S
OH
F
3.16
1H NMR
400MHz, CDCl3
1.92
1.93
2.00
2.01
0.91
f1 (ppm)

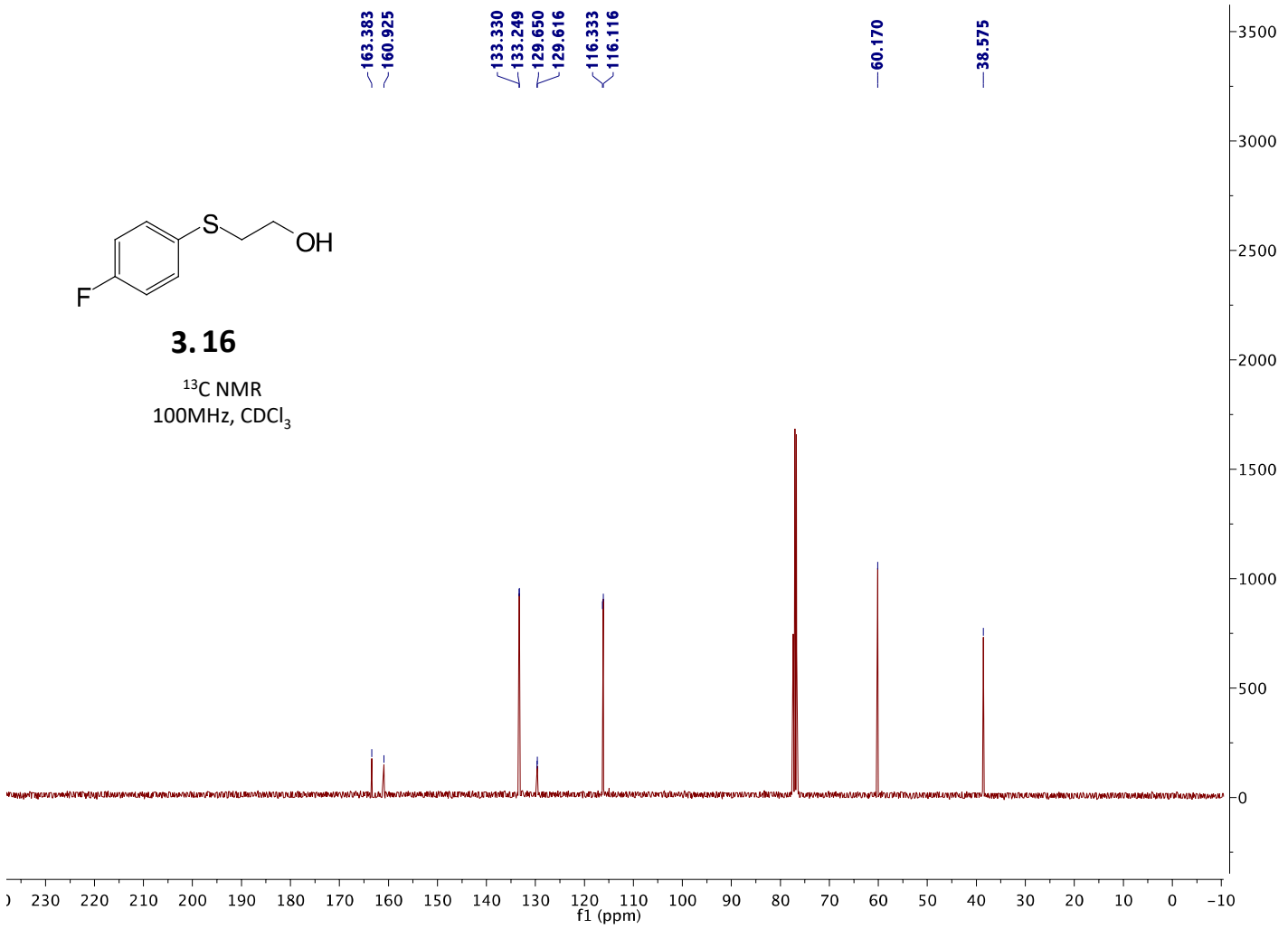
163.383
160.925
133.330
133.249
129.650
129.616
116.333
116.116
60.170
38.575
S
OH
F
3.16
13C NMR
100MHz, CDCl3
f1 (ppm)

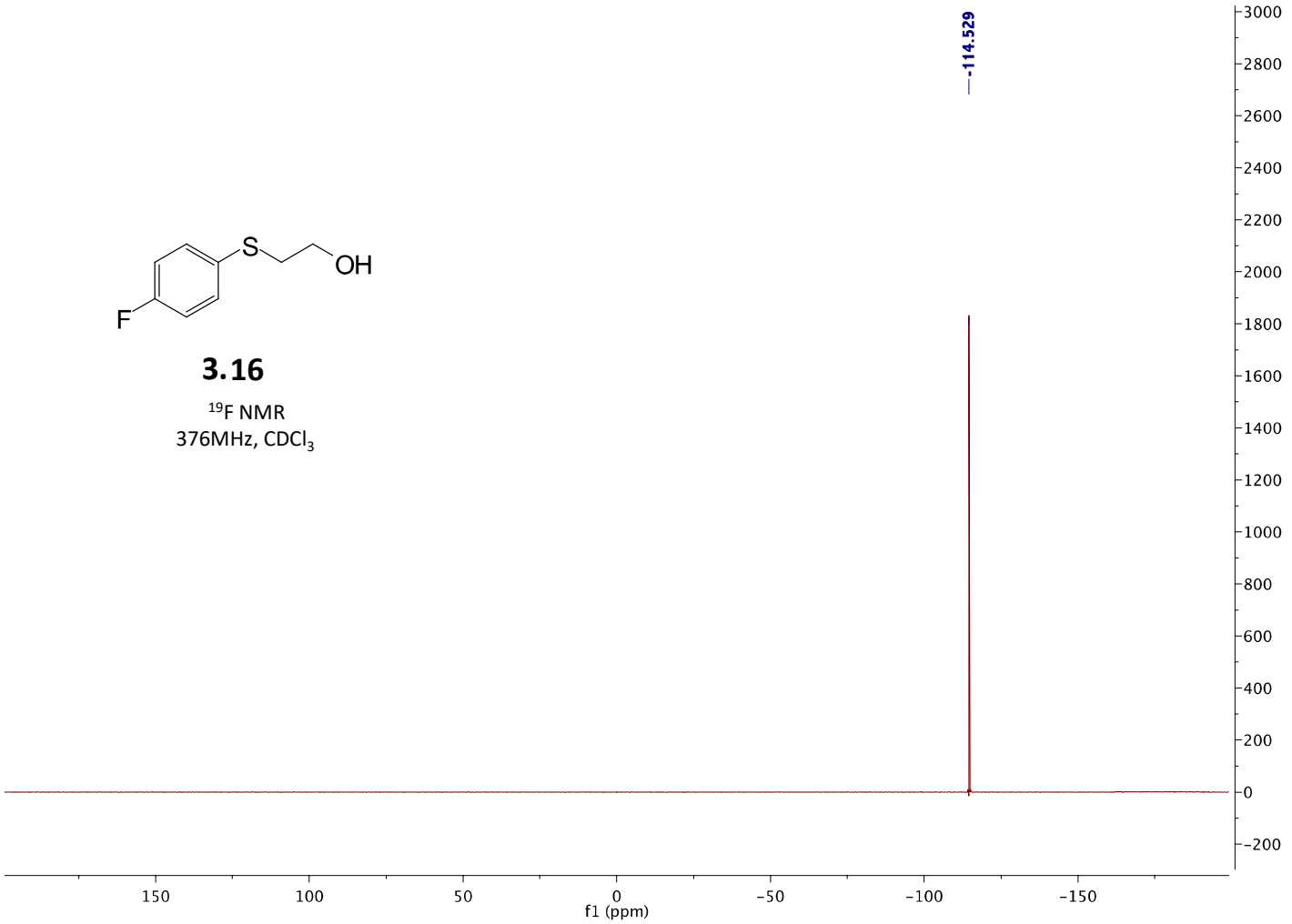

3.16

^{19}F NMR
376MHz, $CDCl_3$

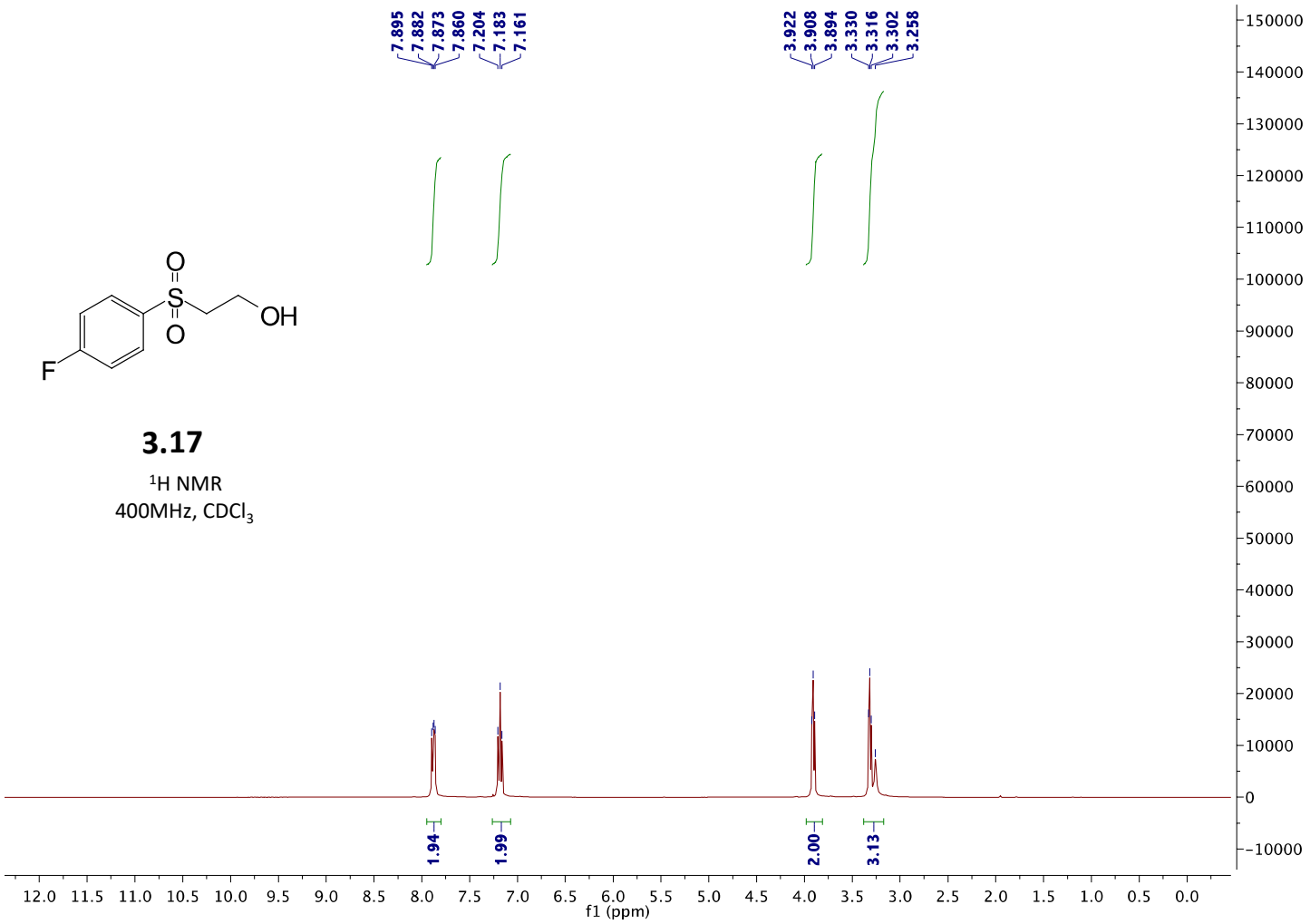

3.17

^{1}H NMR

400MHz, $CDCl_3$

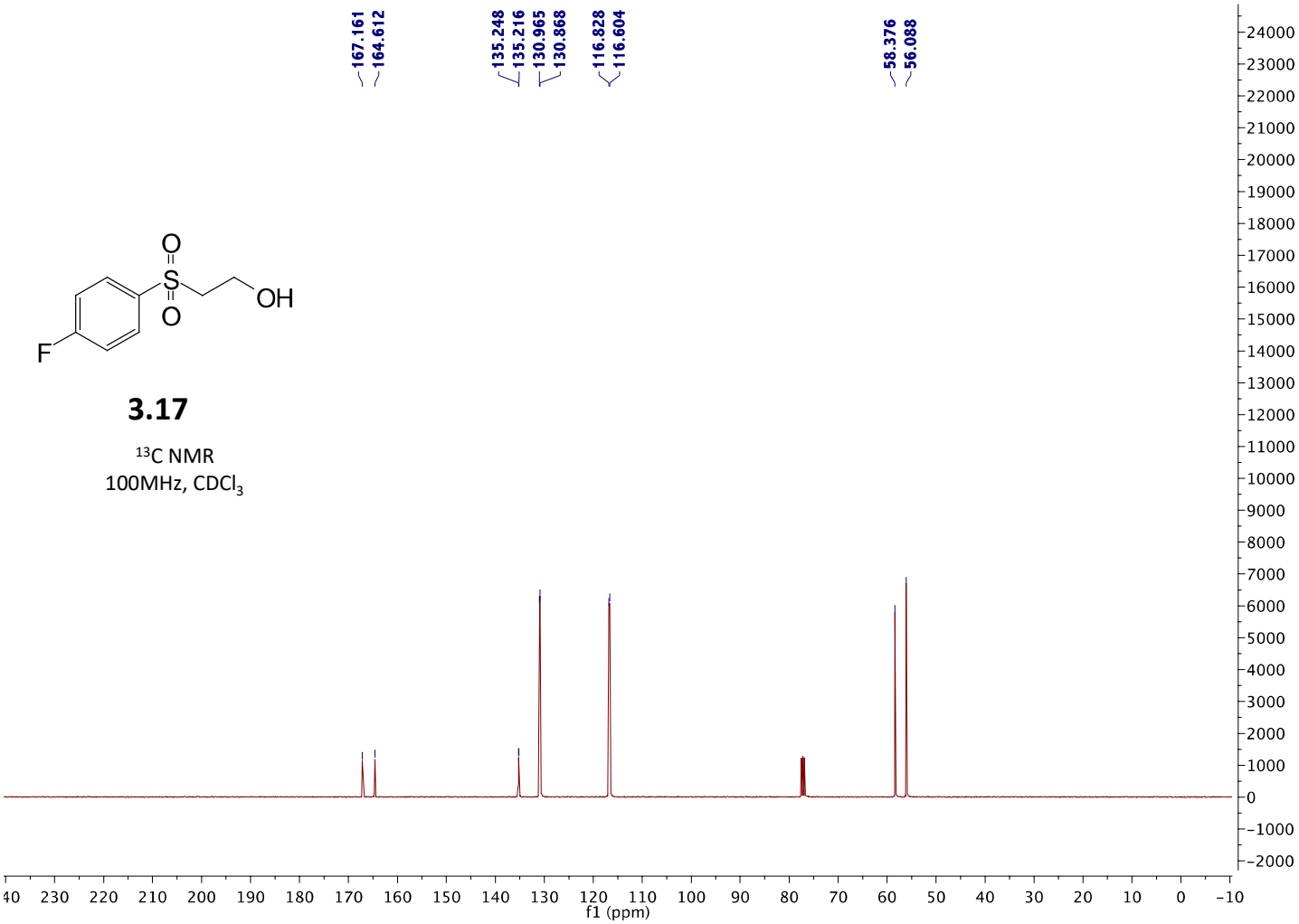
167.161
164.612
135.248
135.216
130.965
130.868
116.828
116.604
58.376
56.088
O
S
O
OH
F
3.17
13C NMR
100MHz, CDCl3
f1 (ppm)

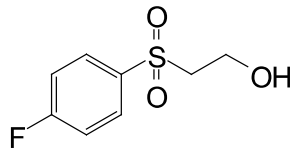

3.17

^{19}F NMR

376MHz, $CDCl_3$

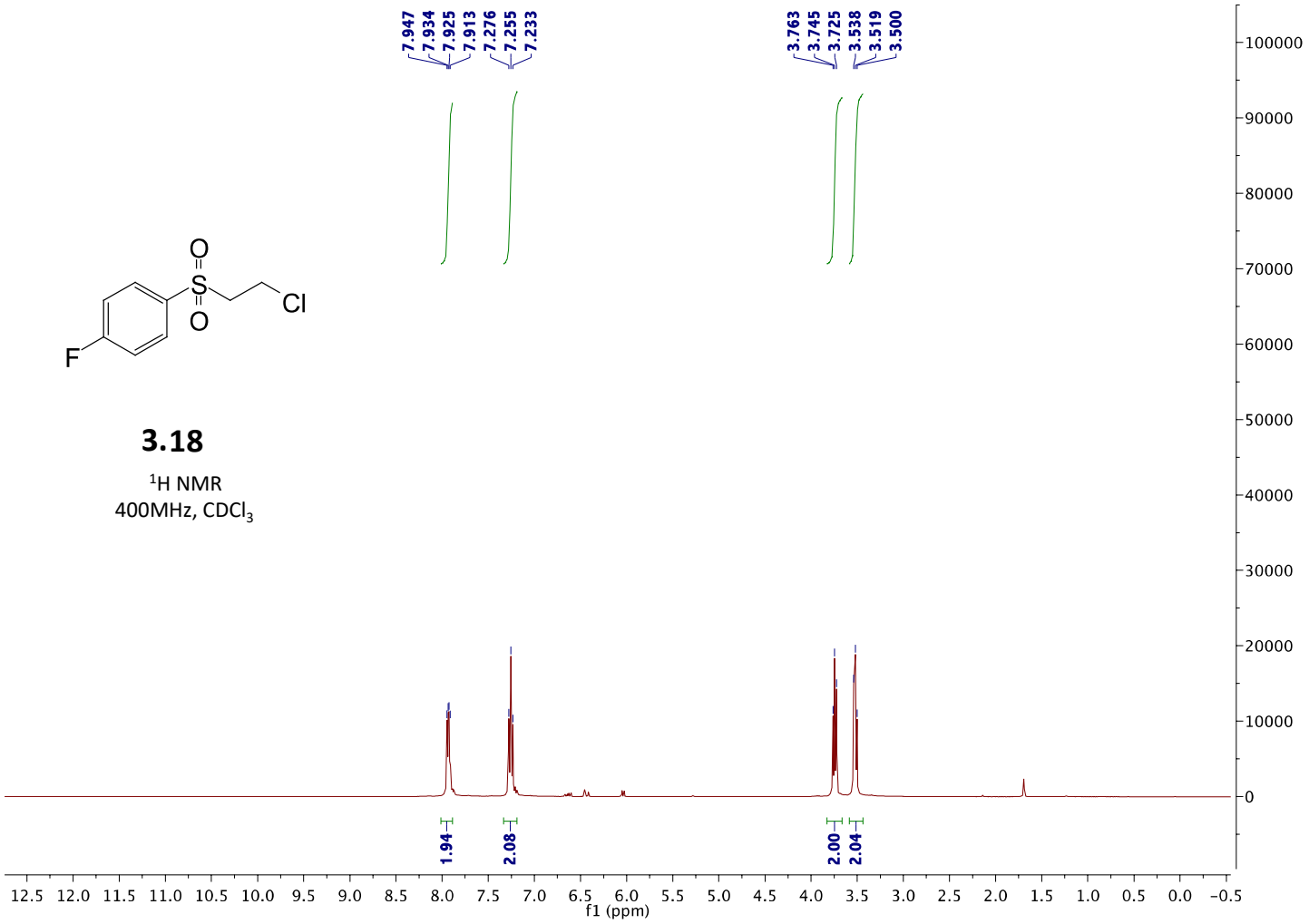
7.947
7.934
7.925
7.913
7.276
7.255
7.233
3.763
3.745
3.725
3.538
3.519
3.500
O
S
O
Cl
F
3.18
1H NMR
400MHz, CDCl3
1.94
2.08
2.00
2.04
f1 (ppm)

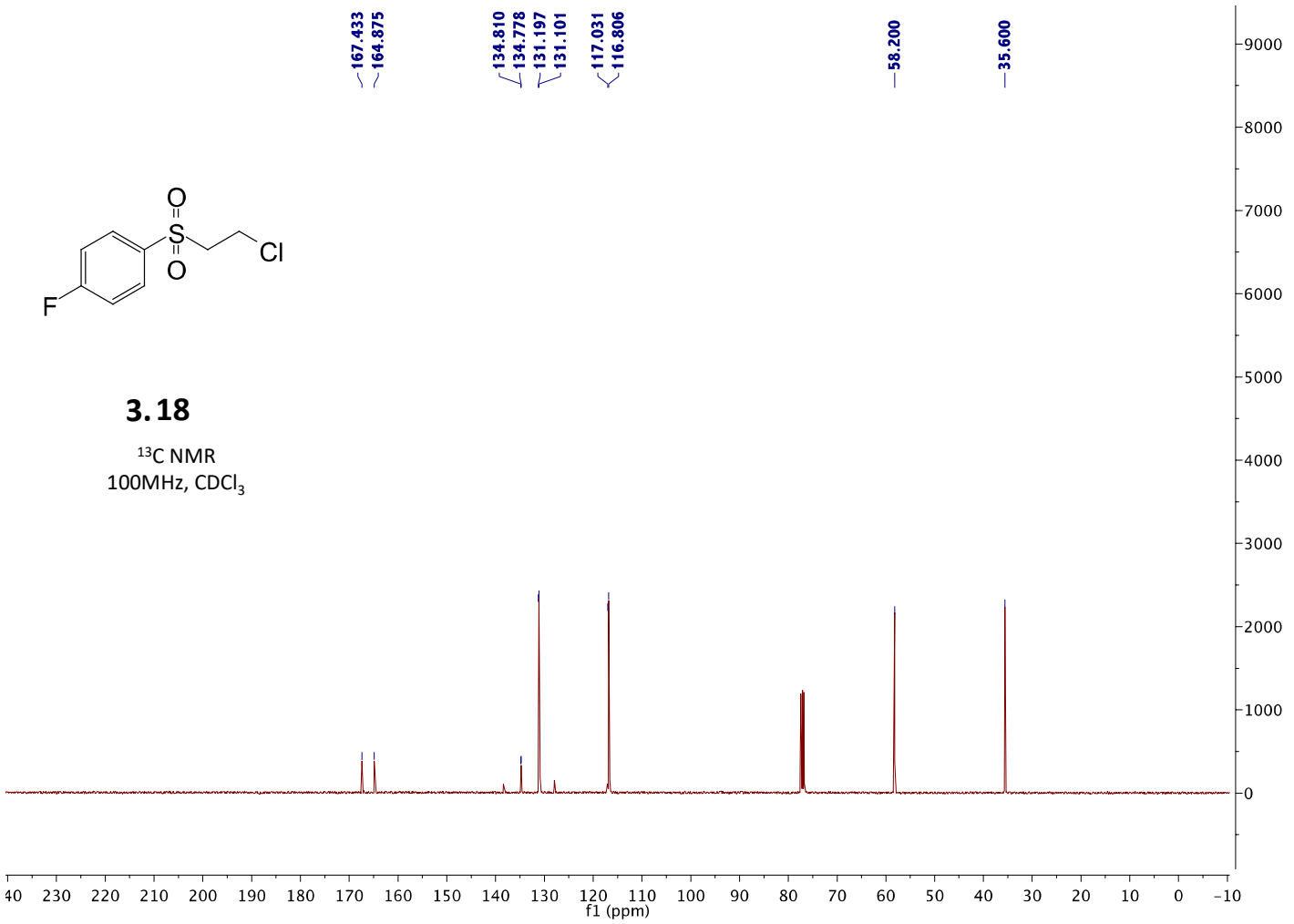

3.18

^{13}C NMR
100MHz, $CDCl_3$

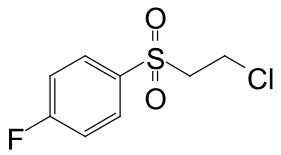

3.18

^{19}F NMR
376MHz, $CDCl_3$

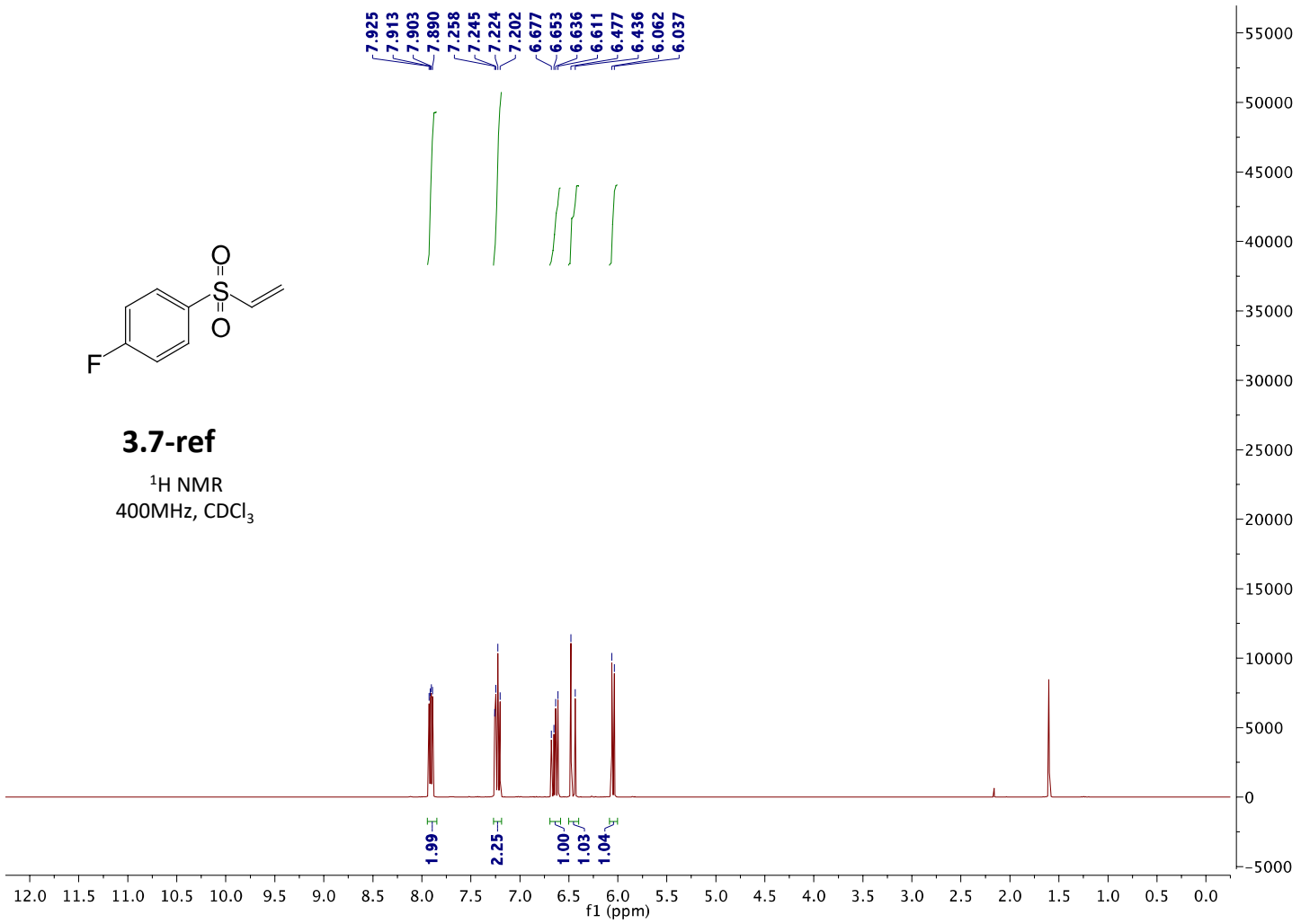
7.925
7.913
7.903
7.890
7.258
7.245
7.224
7.202
6.677
6.653
6.636
6.611
6.477
6.436
6.062
6.037
O
S
O
F
3.7-ref
1H NMR
400MHz, CDCl3
1.99
2.25
1.00
1.03
1.04
f1 (ppm)

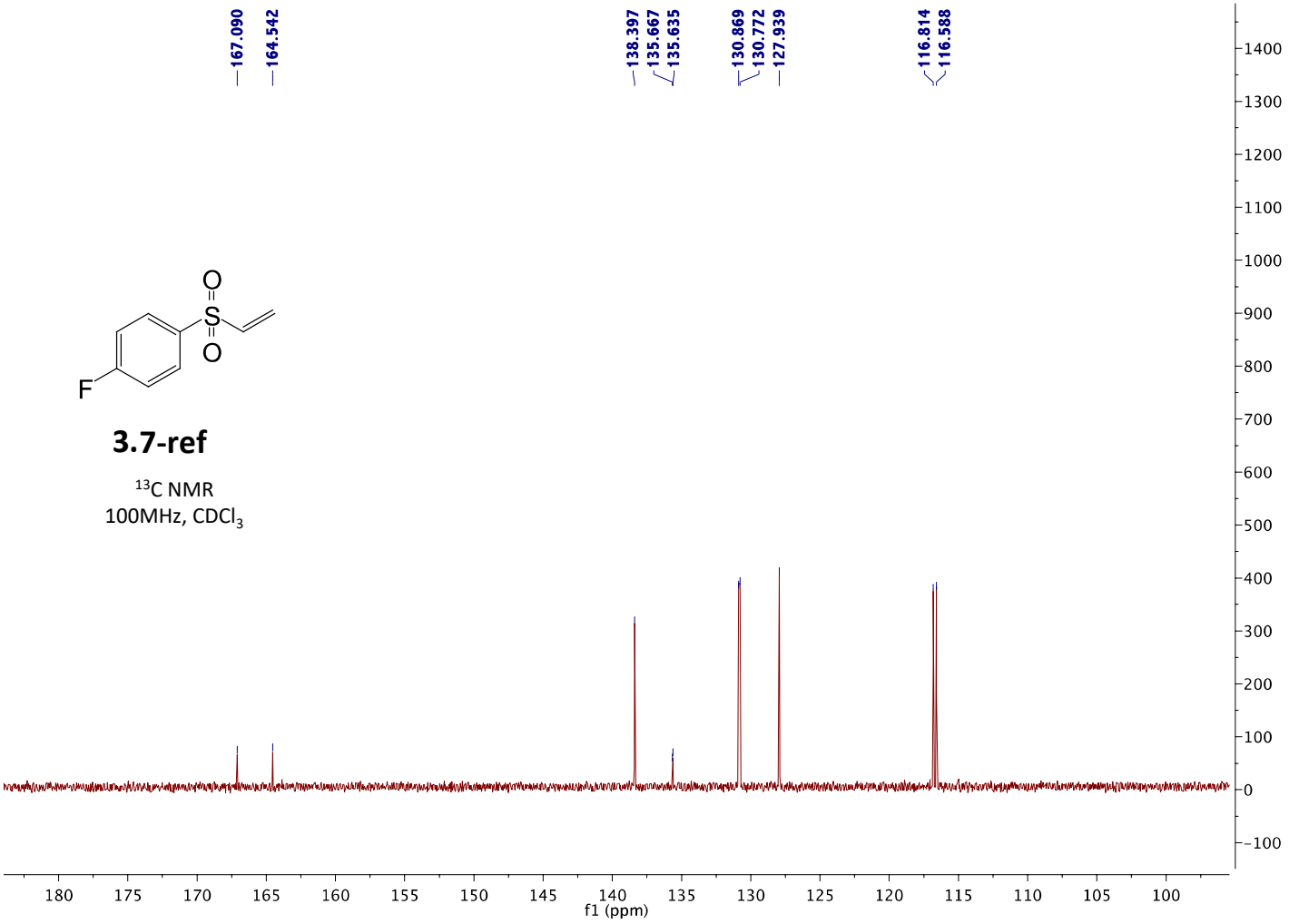
167.090
164.542
138.397
135.667
135.635
130.869
130.772
127.939
116.814
116.588
O
S
O
F
3.7-ref
13C NMR
100MHz, CDCl3
f1 (ppm)

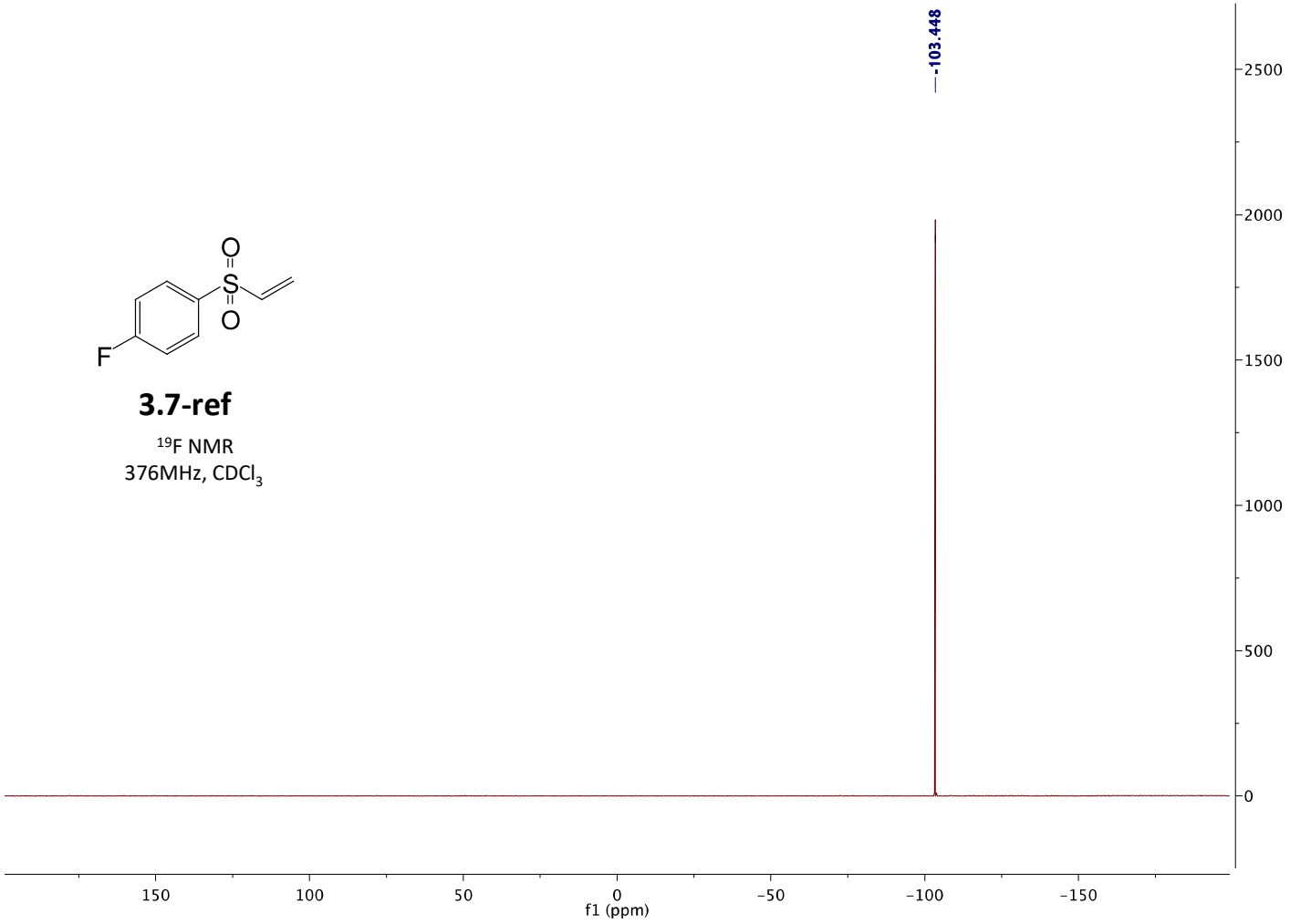

3.7-ref

^{19}F NMR

376MHz, $CDCl_3$

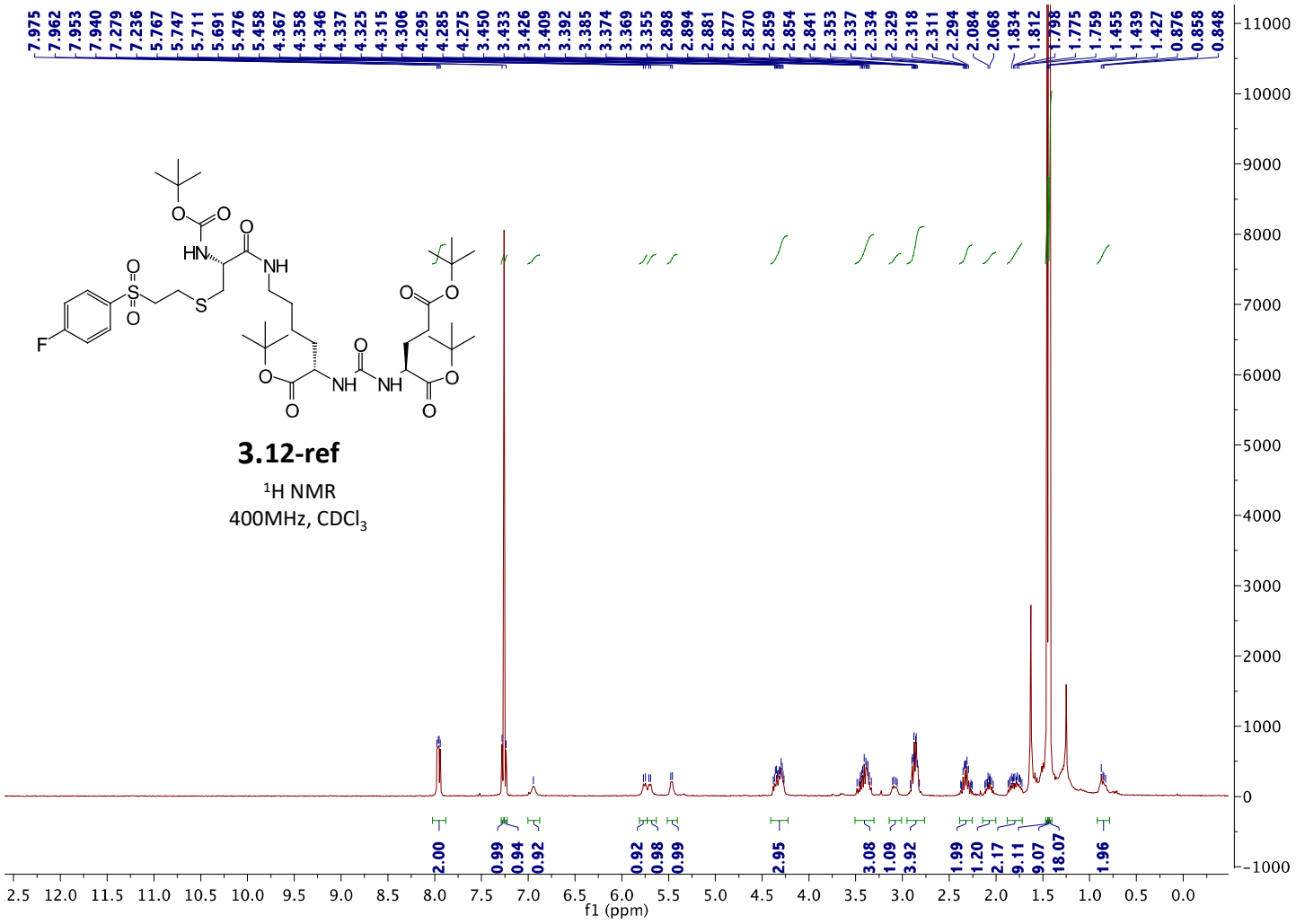
7.975
7.962
7.953
7.940
7.279
7.236
5.767
5.747
5.711
5.691
5.476
5.458
4.367
4.358
4.346
4.337
4.325
4.315
4.306
4.295
4.285
4.275
3.450
3.433
3.426
3.409
3.392
3.385
3.374
3.369
3.355
2.898
2.894
2.881
2.877
2.870
2.859
2.854
2.841
2.353
2.337
2.334
2.329
2.318
2.311
2.294
2.084
2.068
1.834
1.812
1.798
1.775
1.759
1.455
1.439
1.427
0.876
0.858
0.848
3.12-ref
1H NMR
400MHz, CDCl3
2.00
0.99
0.94
0.92
0.92
0.98
0.99
2.95
3.08
1.09
3.92
1.99
1.20
2.17
9.11
9.07
18.07
1.96
f1 (ppm)

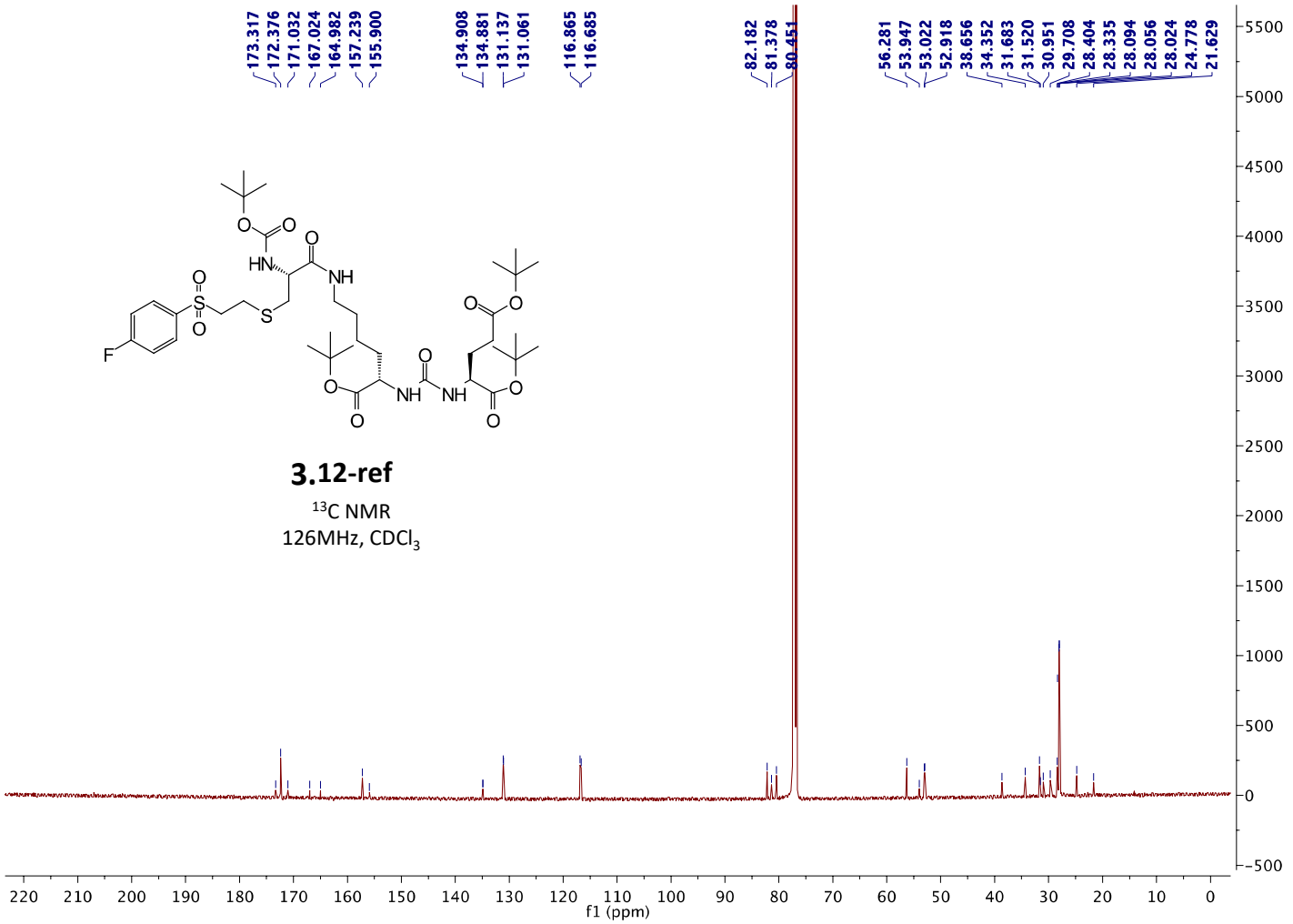
173.317
172.376
171.032
167.024
164.982
157.239
155.900
134.908
134.881
131.137
131.061
116.865
116.685
82.182
81.378
80.451
56.281
53.947
53.022
52.918
38.656
34.352
31.683
31.520
30.951
29.708
28.404
28.335
28.094
28.056
28.024
24.778
21.629
3.12-ref
13C NMR
126MHz, CDCl3
f1 (ppm)

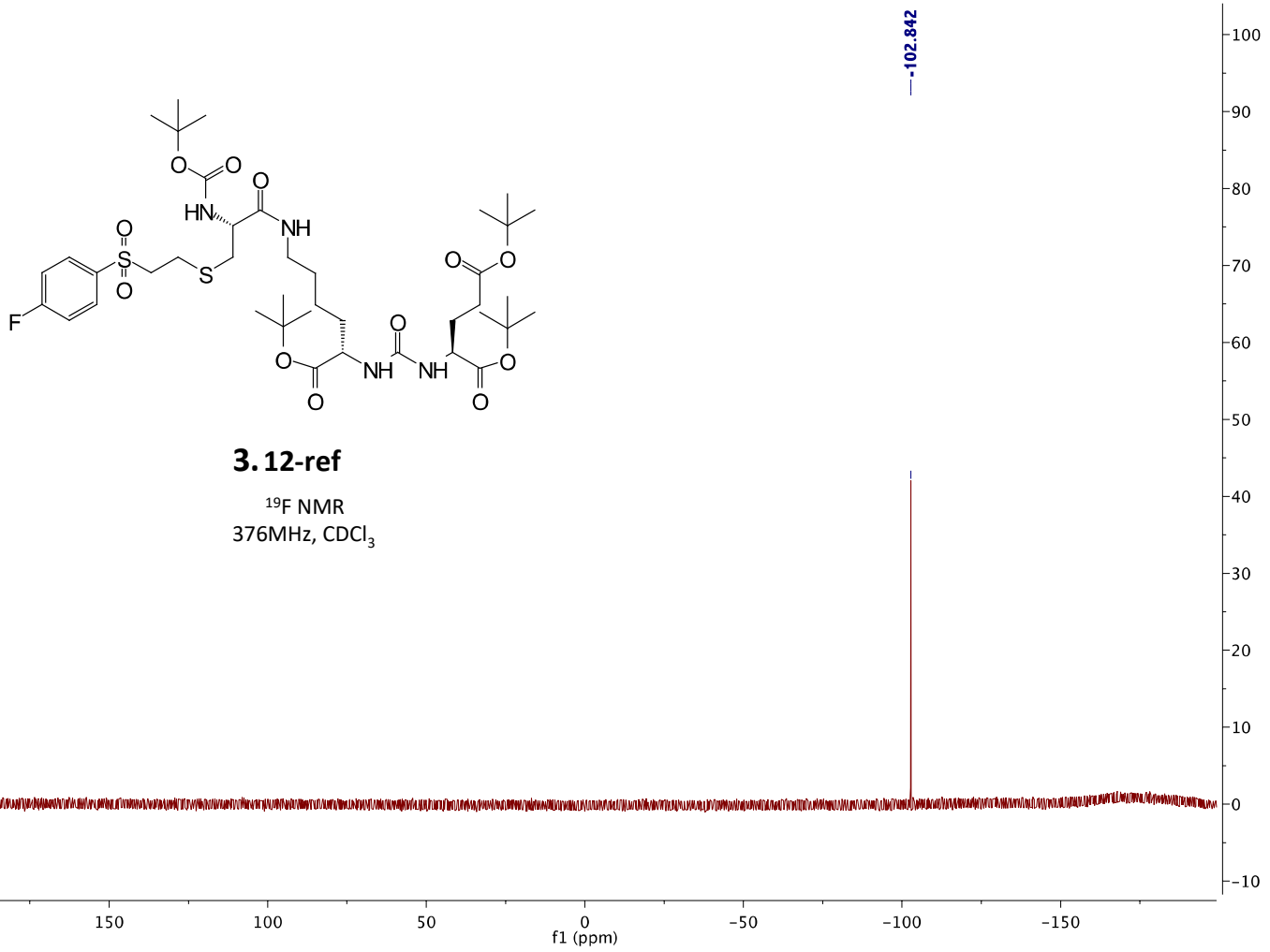

3. 12-ref

^{19}F NMR

376MHz, $CDCl_3$

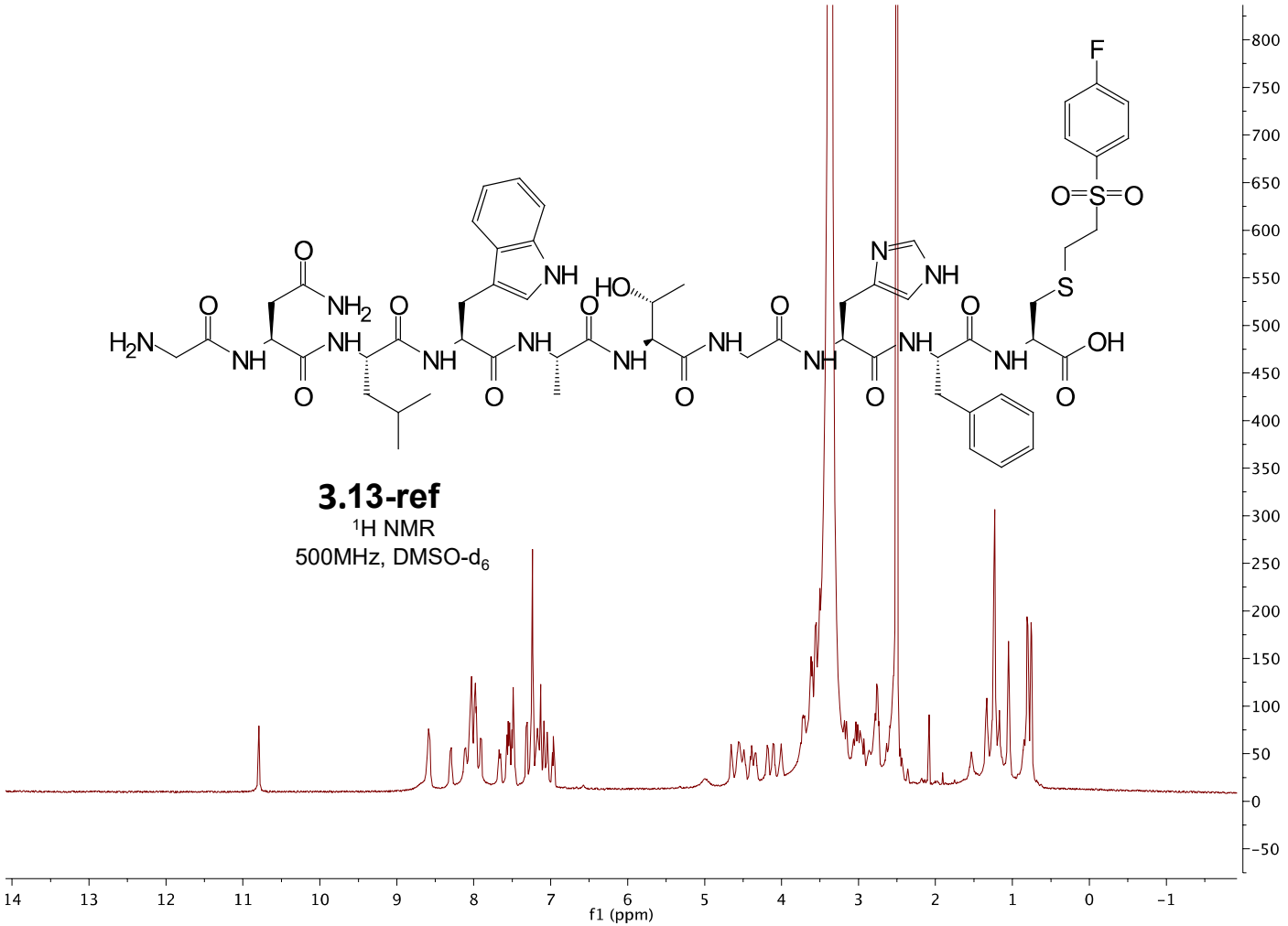
3.13-ref
1H NMR
500MHz, DMSO-d6
f1 (ppm)

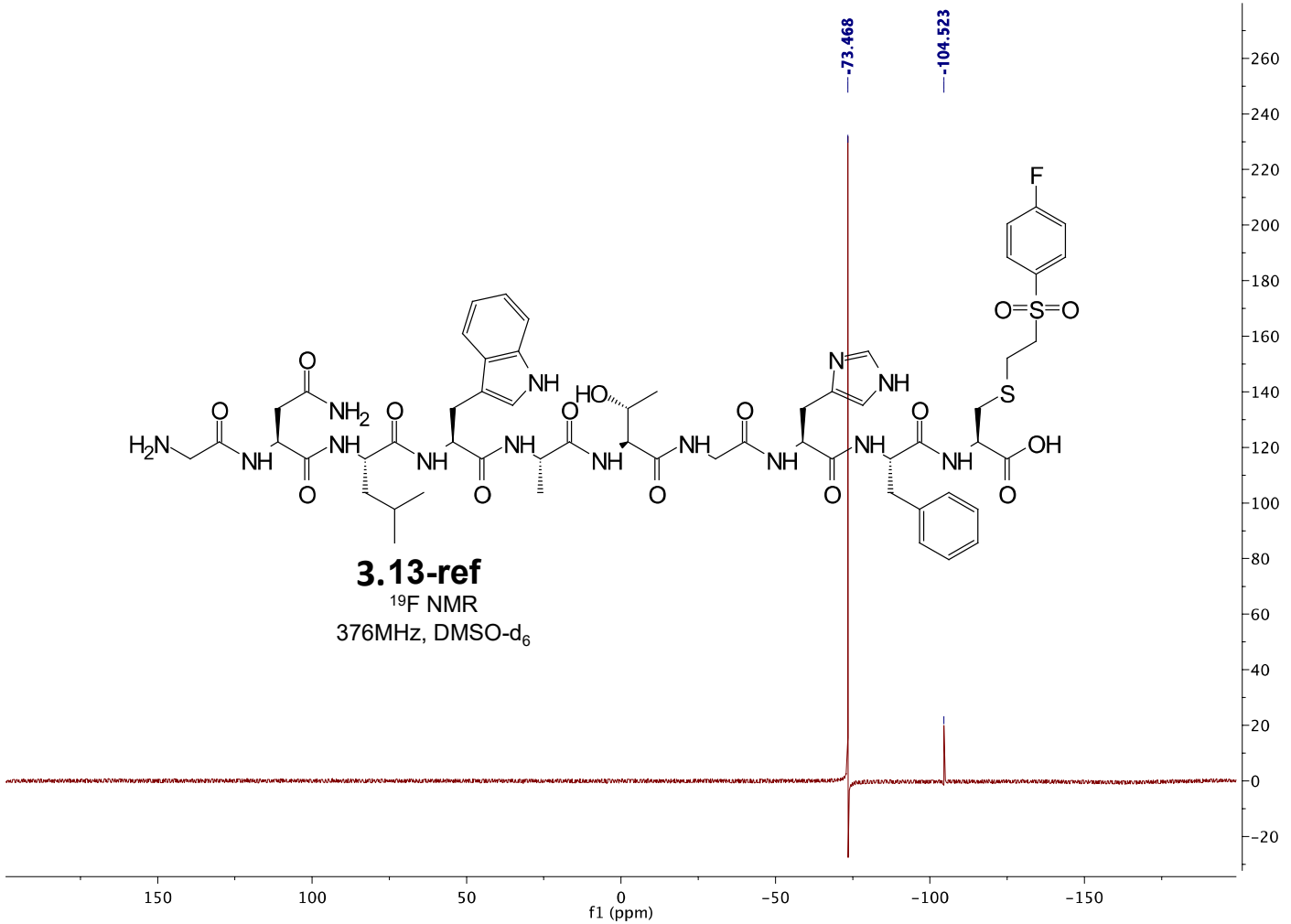
-73.468
-104.523
F
O=S=O
S
OH
HO
NH
NH2
H2N
3.13-ref
19F NMR
376MHz, DMSO-d6
260
240
220
200
180
160
140
120
100
80
60
40
20
0
-20
150
100
50
0
-50
-100
-150
f1 (ppm)

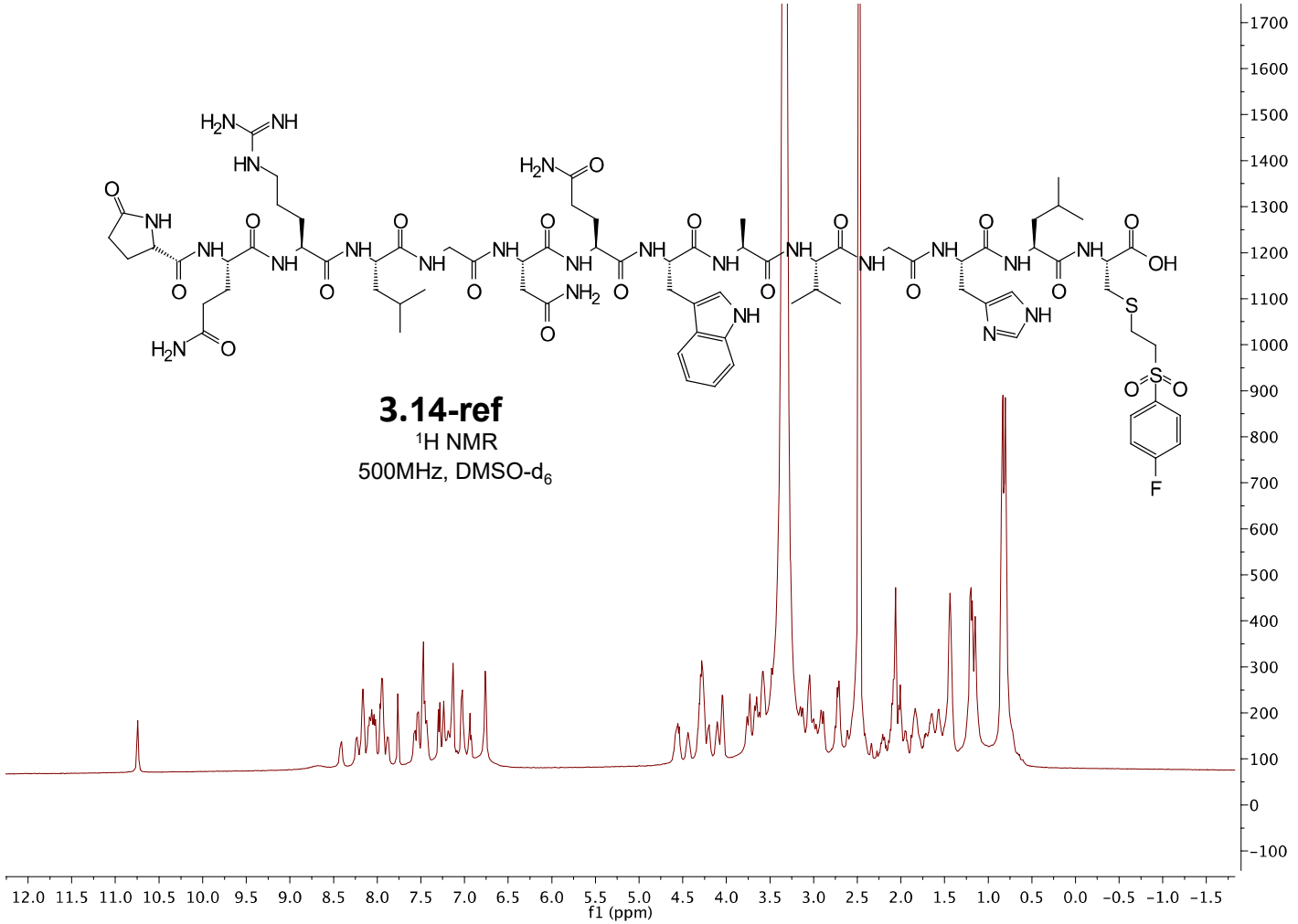
3.14-ref
1H NMR
500MHz, DMSO-d6
f1 (ppm)

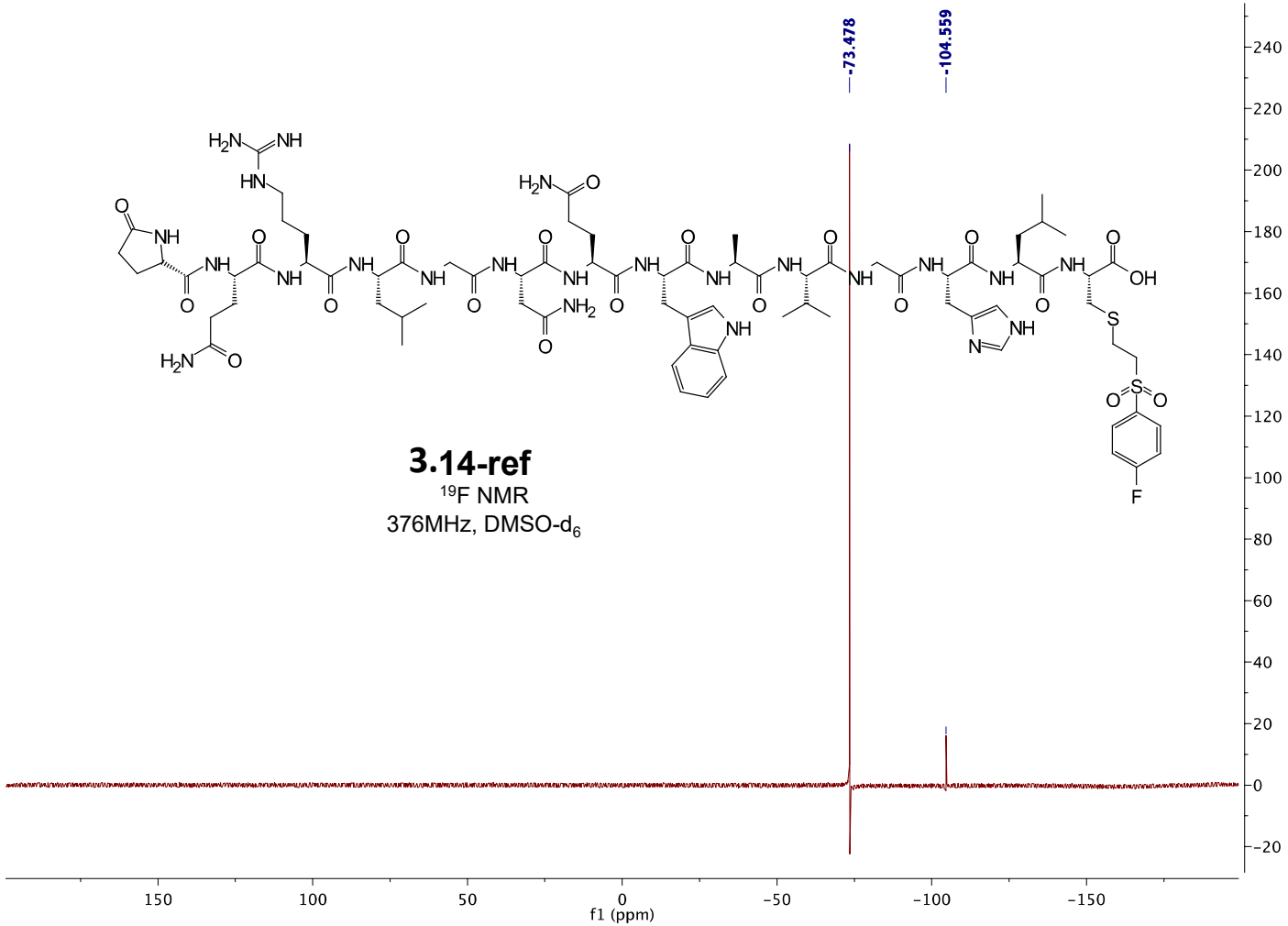
-73.478
-104.559
3.14-ref
19F NMR
376MHz, DMSO-d6
240
220
200
180
160
140
120
100
80
60
40
20
0
-20
150
100
50
0
-50
-100
-150
f1 (ppm)

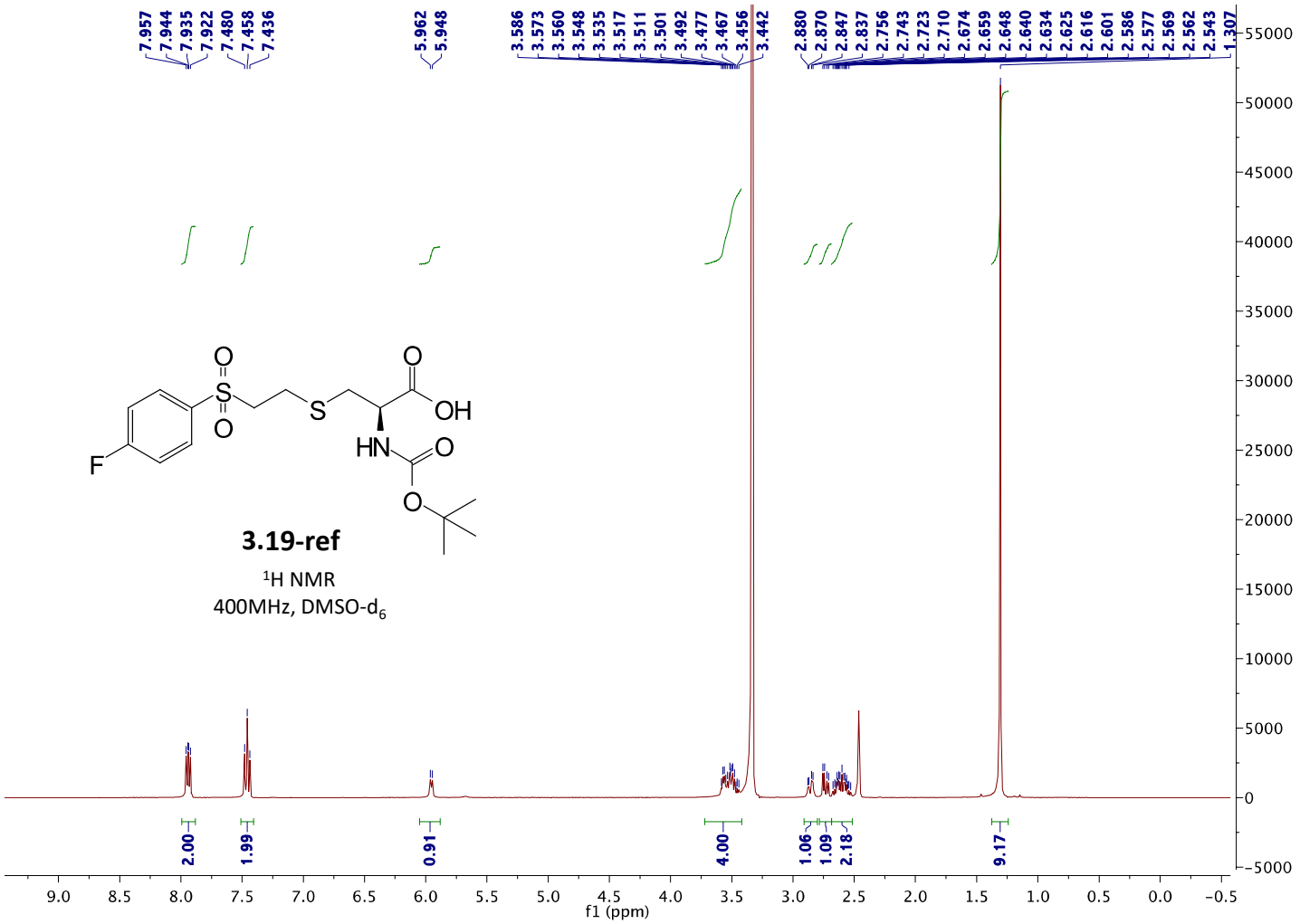
7.957
7.944
7.935
7.922
7.480
7.458
7.436
5.962
5.948
3.586
3.573
3.560
3.548
3.535
3.517
3.511
3.501
3.492
3.477
3.467
3.456
3.442
2.880
2.870
2.847
2.837
2.756
2.743
2.723
2.710
2.674
2.659
2.648
2.640
2.634
2.625
2.616
2.601
2.586
2.577
2.569
2.562
2.543
1.307
F
S
O
O
S
O
O
OH
HN
O
O
3.19-ref
1H NMR
400MHz, DMSO-d6
2.00
1.99
0.91
4.00
1.06
1.09
2.18
9.17
f1 (ppm)

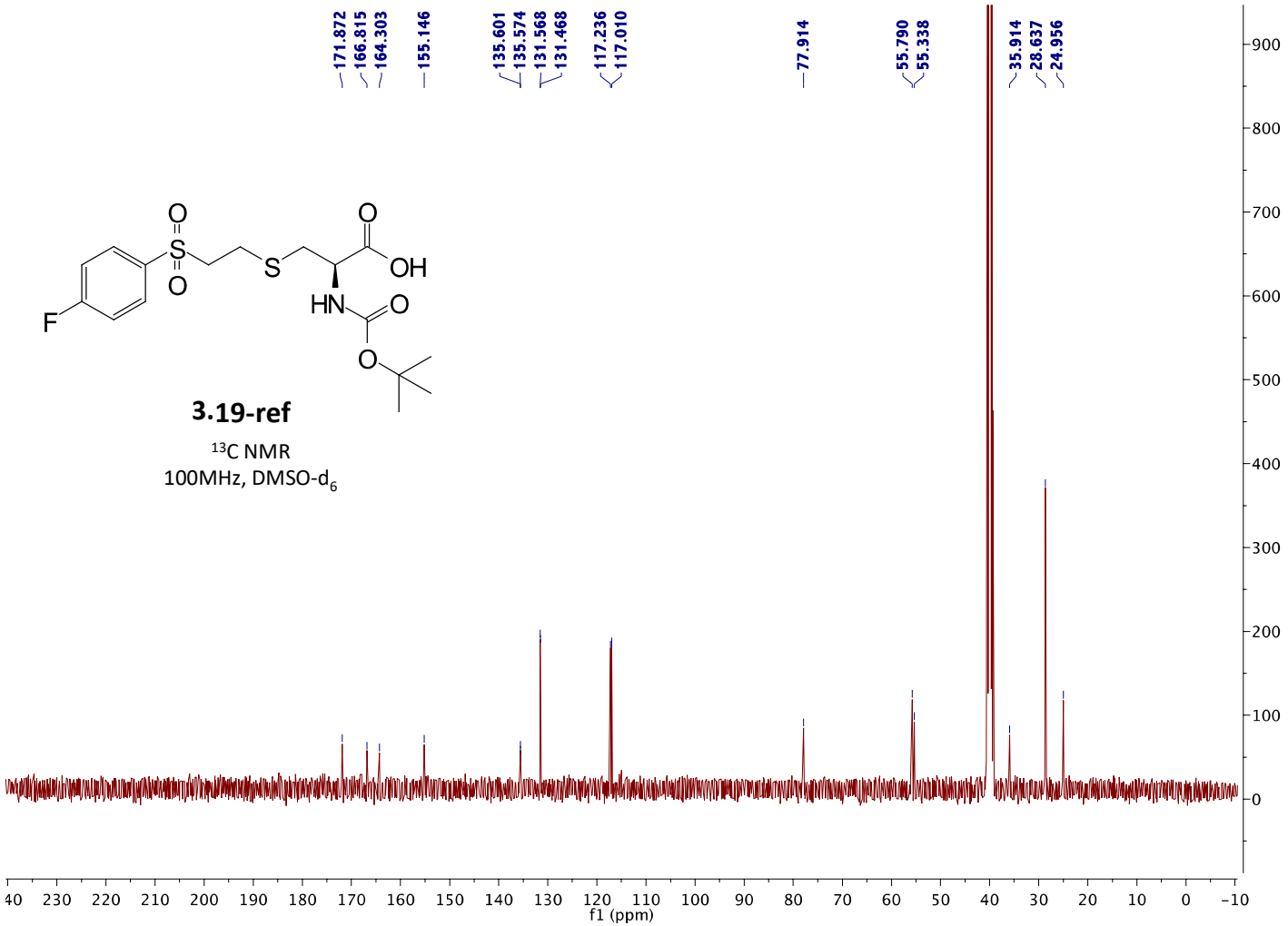
171.872
166.815
164.303
155.146
135.601
135.574
131.568
131.468
117.236
117.010
77.914
55.790
55.338
35.914
28.637
24.956
O
S
O
S
O
OH
HN
O
O
F
3.19-ref
13C NMR
100MHz, DMSO-d6
f1 (ppm)

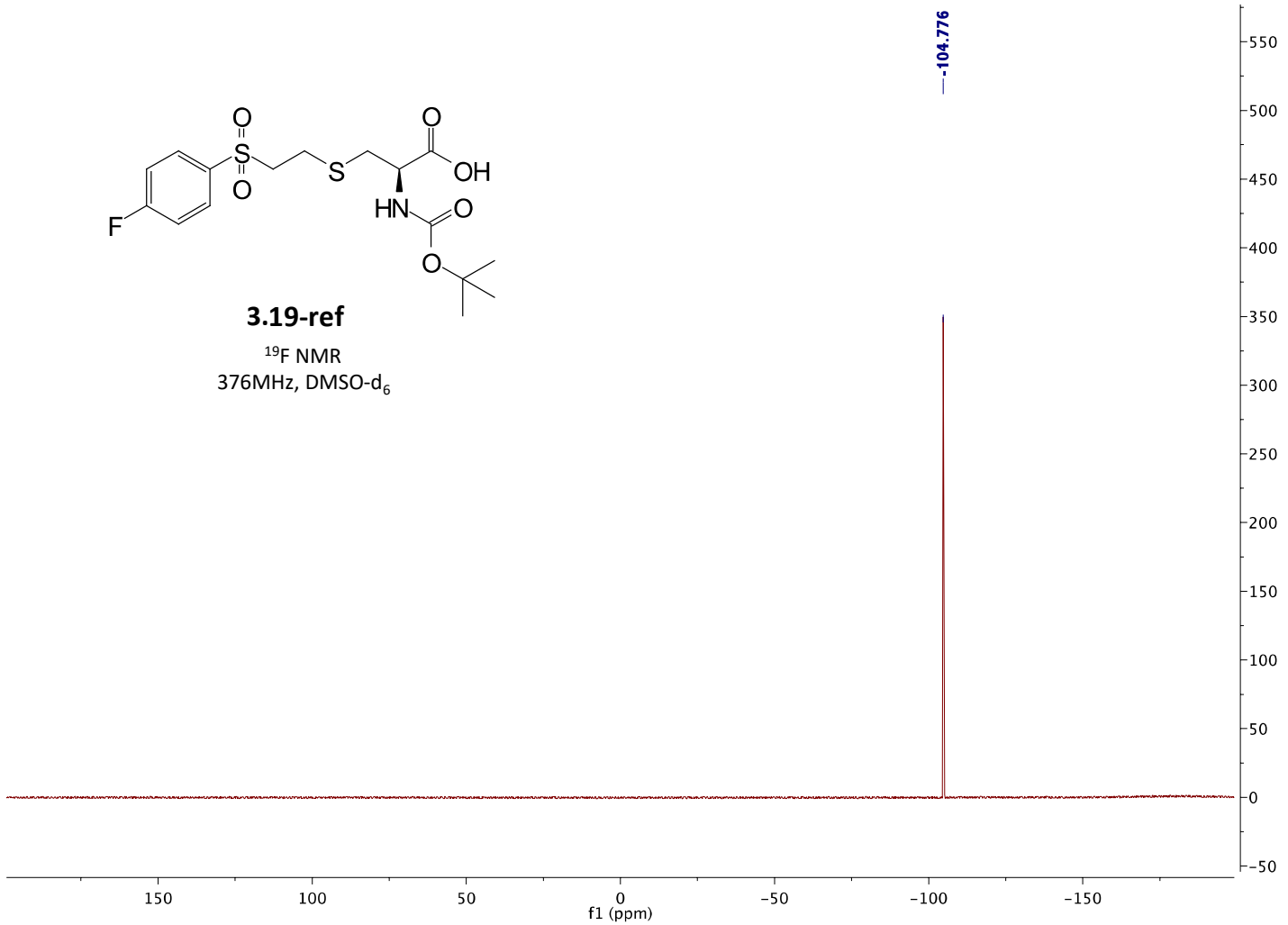

3.19-ref

^{19}F NMR

376MHz, DMSO-d_6

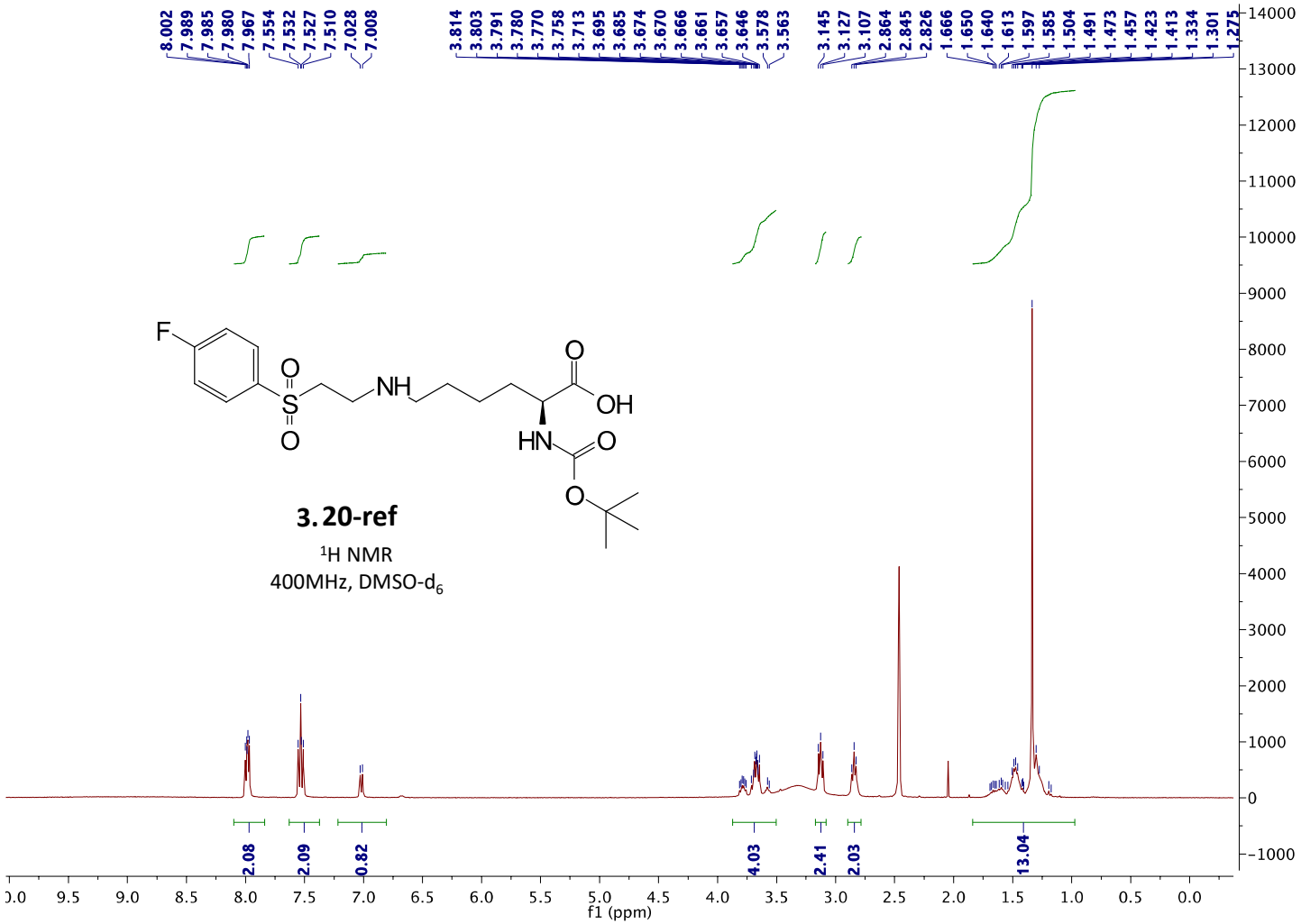
8.002
7.989
7.985
7.980
7.967
7.554
7.532
7.527
7.510
7.028
7.008
3.814
3.803
3.791
3.780
3.770
3.758
3.713
3.695
3.685
3.674
3.670
3.666
3.661
3.657
3.646
3.578
3.563
3.145
3.127
3.107
2.864
2.845
2.826
1.666
1.650
1.640
1.613
1.597
1.585
1.504
1.491
1.473
1.457
1.423
1.413
1.334
1.301
1.275
F
O
S
O
NH
O
OH
HN
O
O
3.20-ref
1H NMR
400MHz, DMSO-d6
2.08
2.09
0.82
4.03
2.41
2.03
13.04
f1 (ppm)

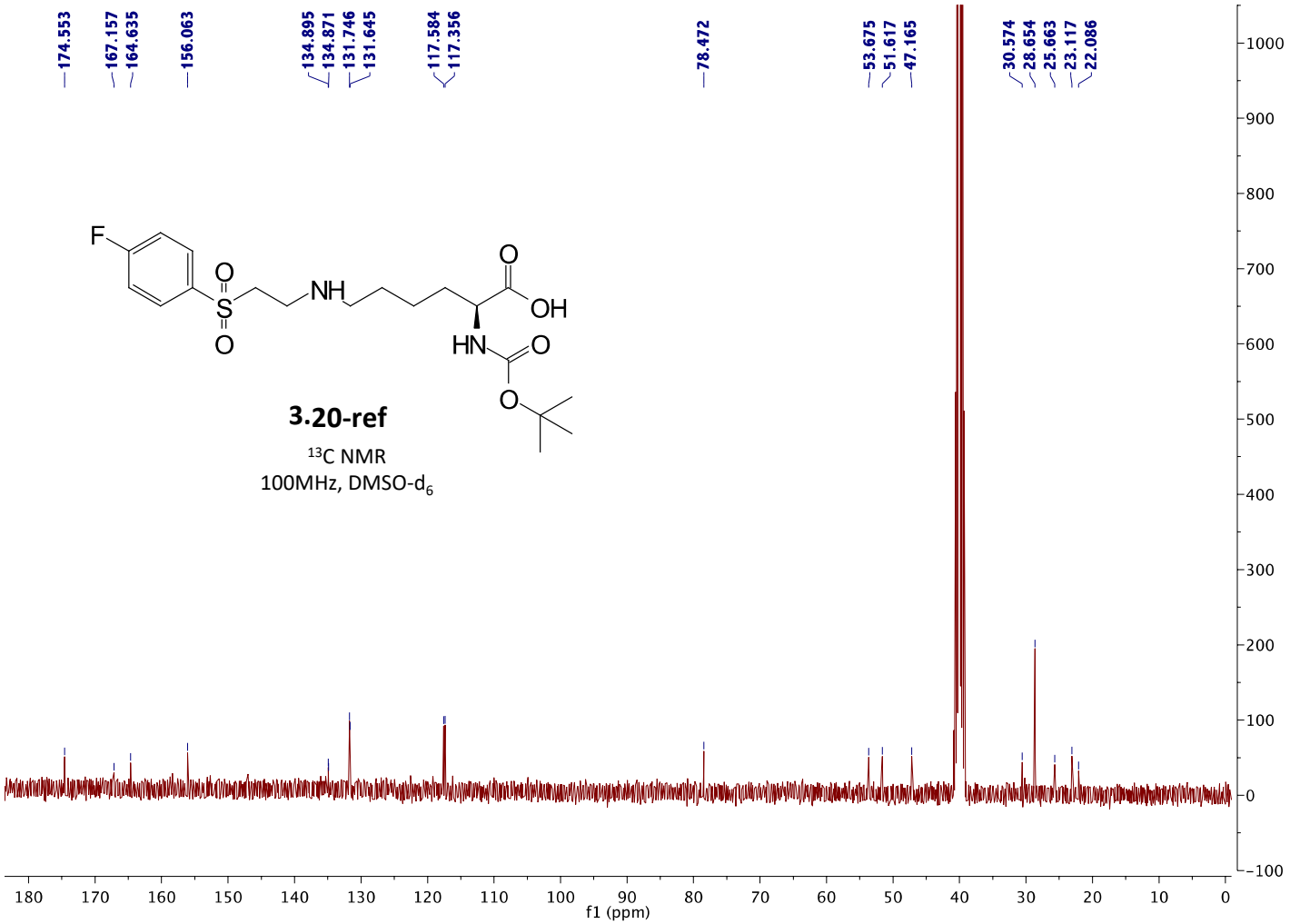
174.553
167.157
164.635
156.063
134.895
134.871
131.746
131.645
117.584
117.356
78.472
53.675
51.617
47.165
30.574
28.654
25.663
23.117
22.086
F
O
S
O
NH
O
OH
HN
O
O
3.20-ref
13C NMR
100MHz, DMSO-d6
1000
900
800
700
600
500
400
300
200
100
0
-100
180
170
160
150
140
130
120
110
100
90
80
70
60
50
40
30
20
10
0
f1 (ppm)

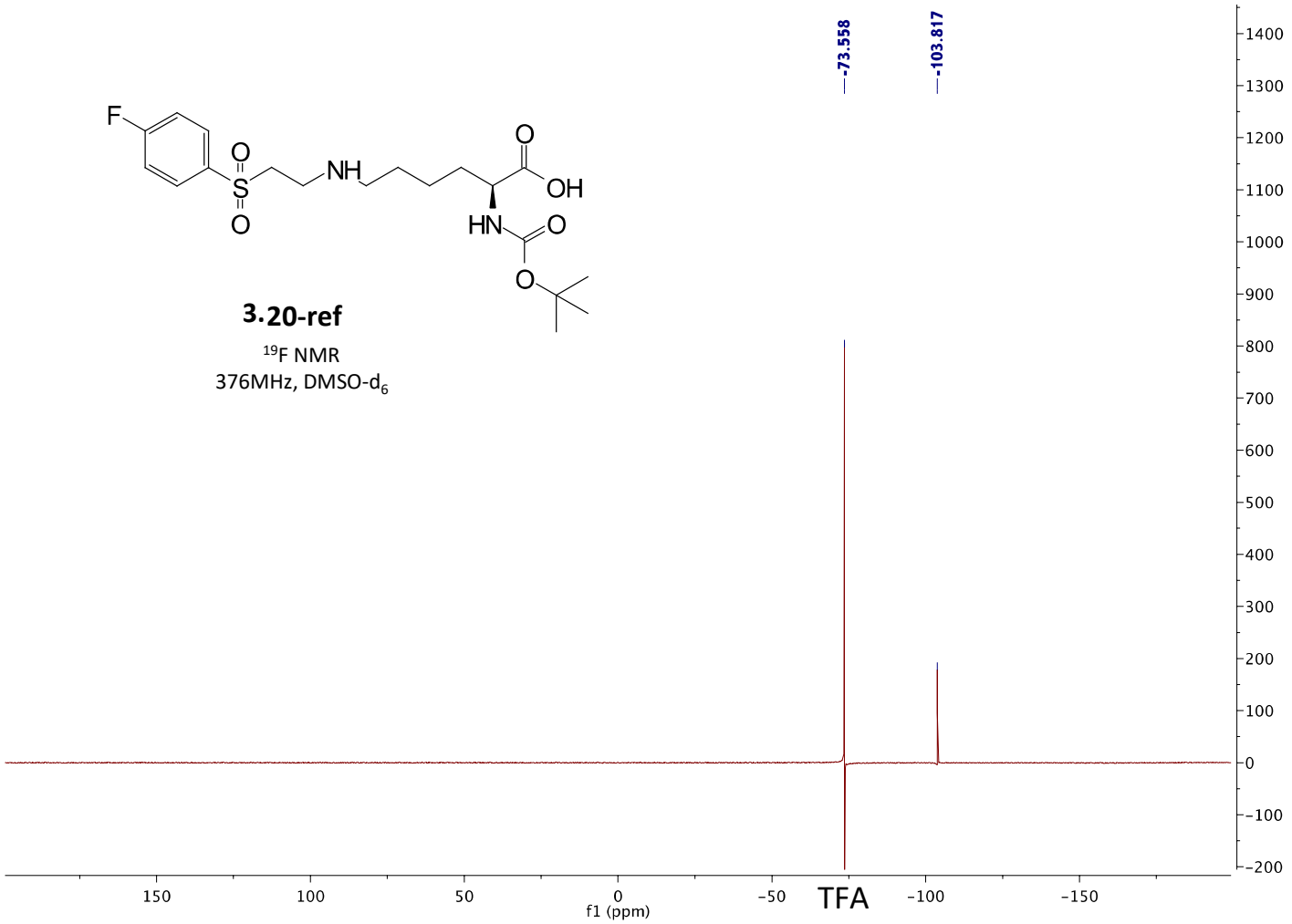
F
O
S
O
NH
O
OH
HN
O
O
-73.558
-103.817
3.20-ref
19F NMR
376MHz, DMSO-d6
1400
1300
1200
1100
1000
900
800
700
600
500
400
300
200
100
0
-100
-200
150
100
50
0
f1 (ppm)
-50
TFA
-100
-150

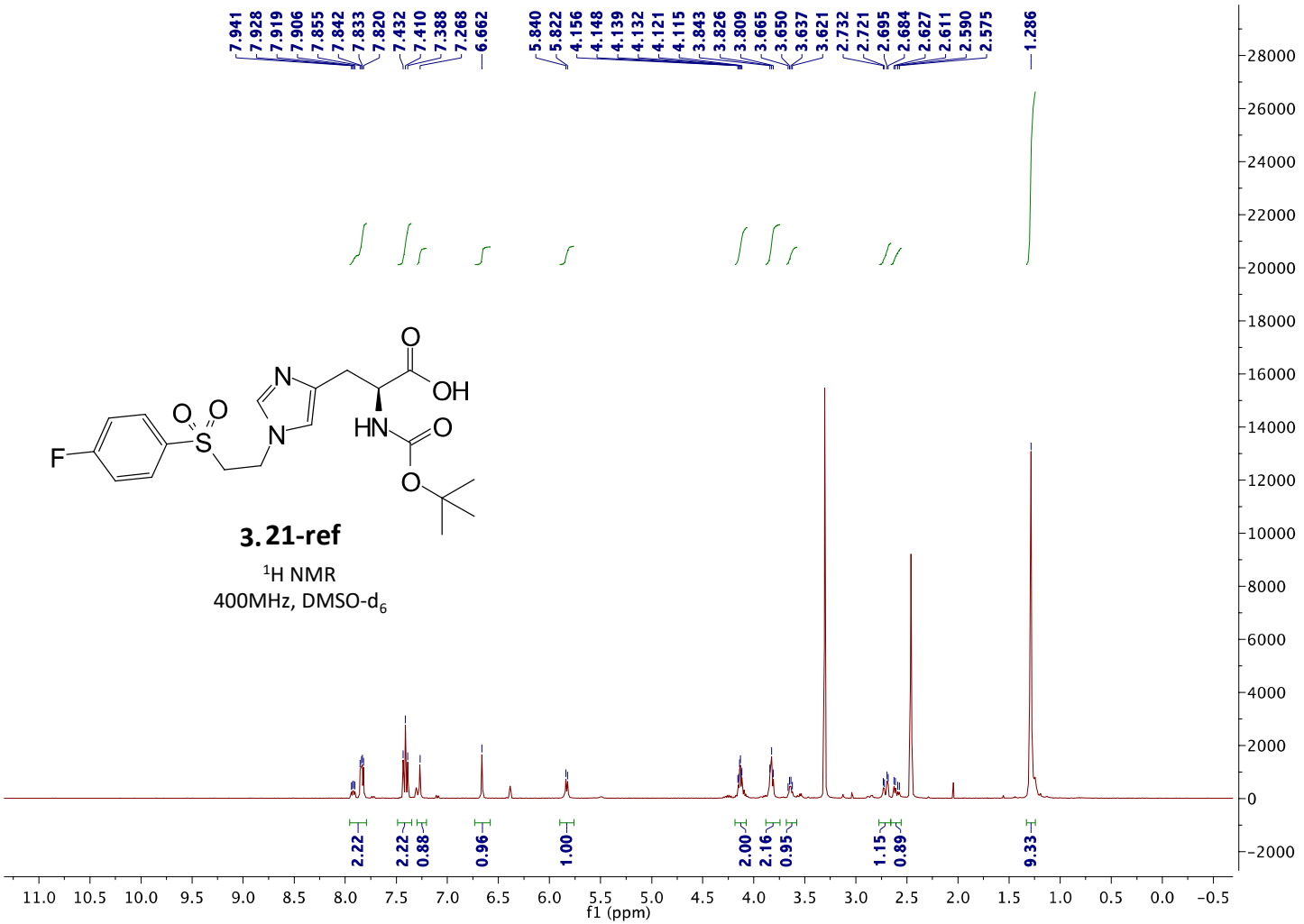
7.941
7.928
7.919
7.906
7.855
7.842
7.833
7.820
7.432
7.410
7.388
7.268
6.662
5.840
5.822
4.156
4.148
4.139
4.132
4.121
4.115
3.843
3.826
3.809
3.665
3.650
3.637
3.621
2.732
2.721
2.695
2.684
2.627
2.611
2.590
2.575
1.286
F
S
O
O
N
N
HN
O
OH
O
O
3.21-ref
1H NMR
400MHz, DMSO-d6
2.22
2.22
0.88
0.96
1.00
2.00
2.16
0.95
1.15
0.89
9.33
f1 (ppm)

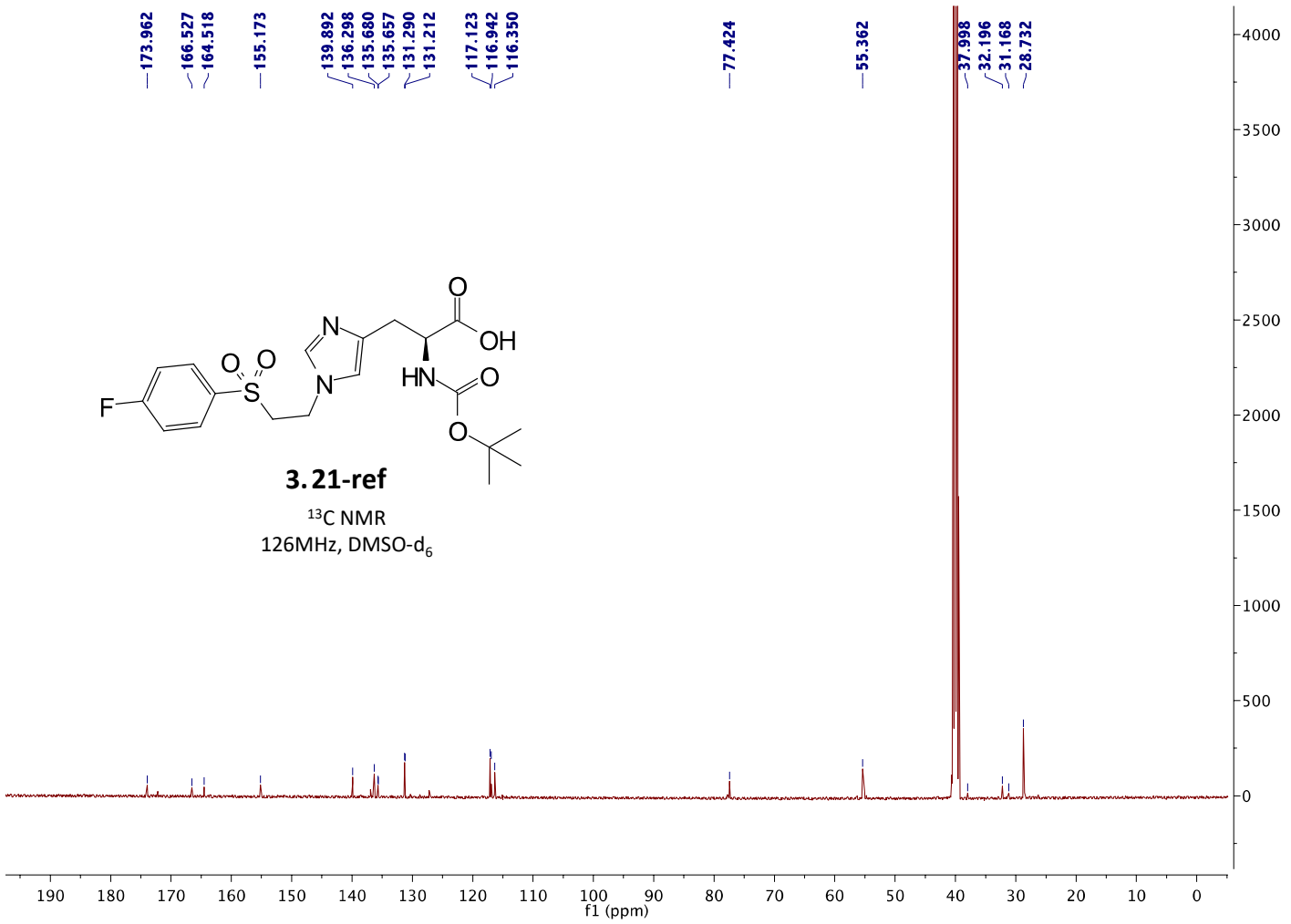
173.962
166.527
164.518
155.173
139.892
136.298
135.680
135.657
131.290
131.212
117.123
116.942
116.350
77.424
55.362
37.998
32.196
31.168
28.732
F
S
O
O
N
N
HN
O
OH
O
O
3.21-ref
13C NMR
126MHz, DMSO-d6
f1 (ppm)

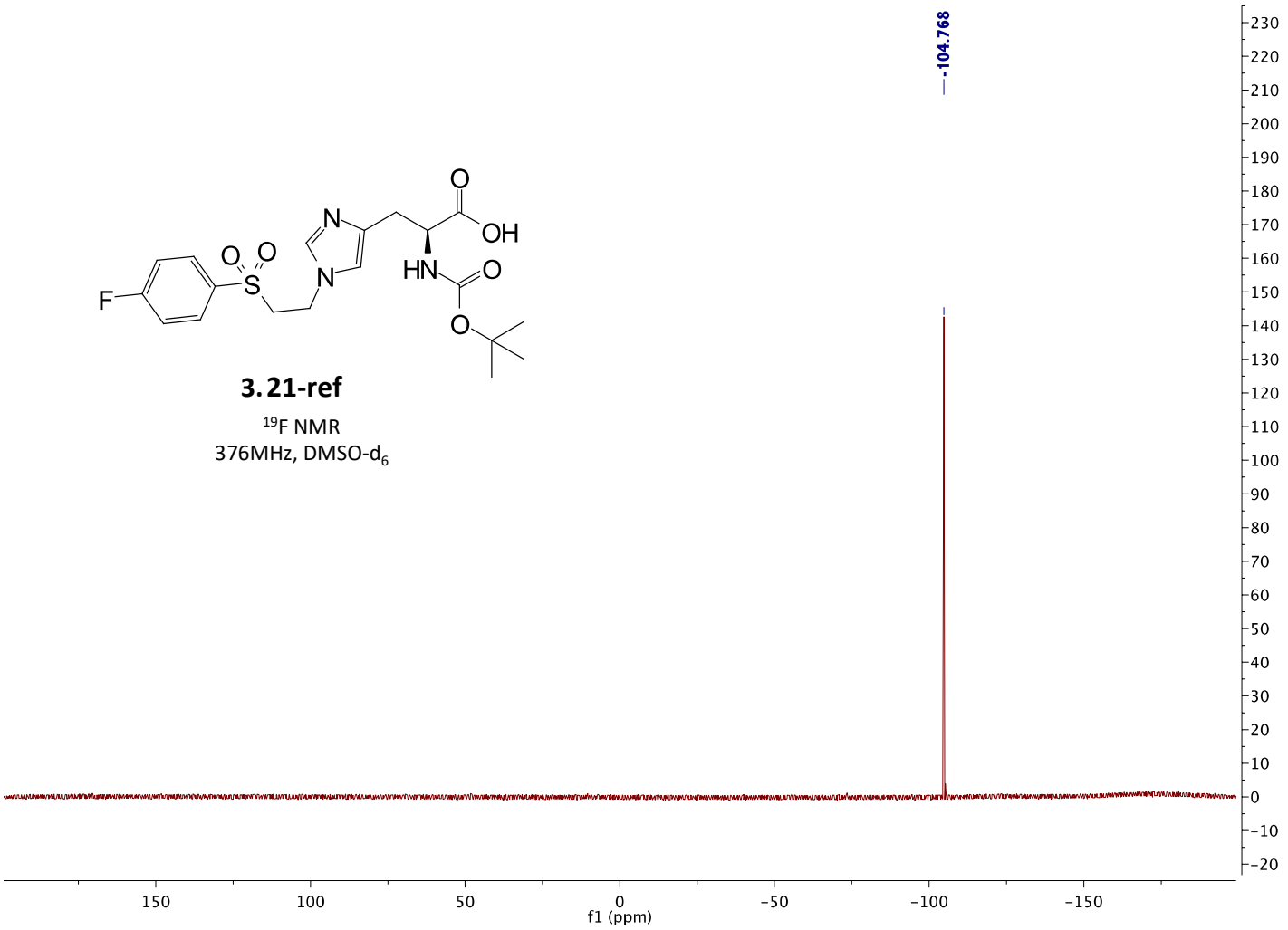
-104.768
F
O
O
S
N
N
O
OH
HN
O
O
3.21-ref
19F NMR
376MHz, DMSO-d6
150
100
50
0
f1 (ppm)
-50
-100
-150
230
220
210
200
190
180
170
160
150
140
130
120
110
100
90
80
70
60
50
40
30
20
10
0
-10
-20

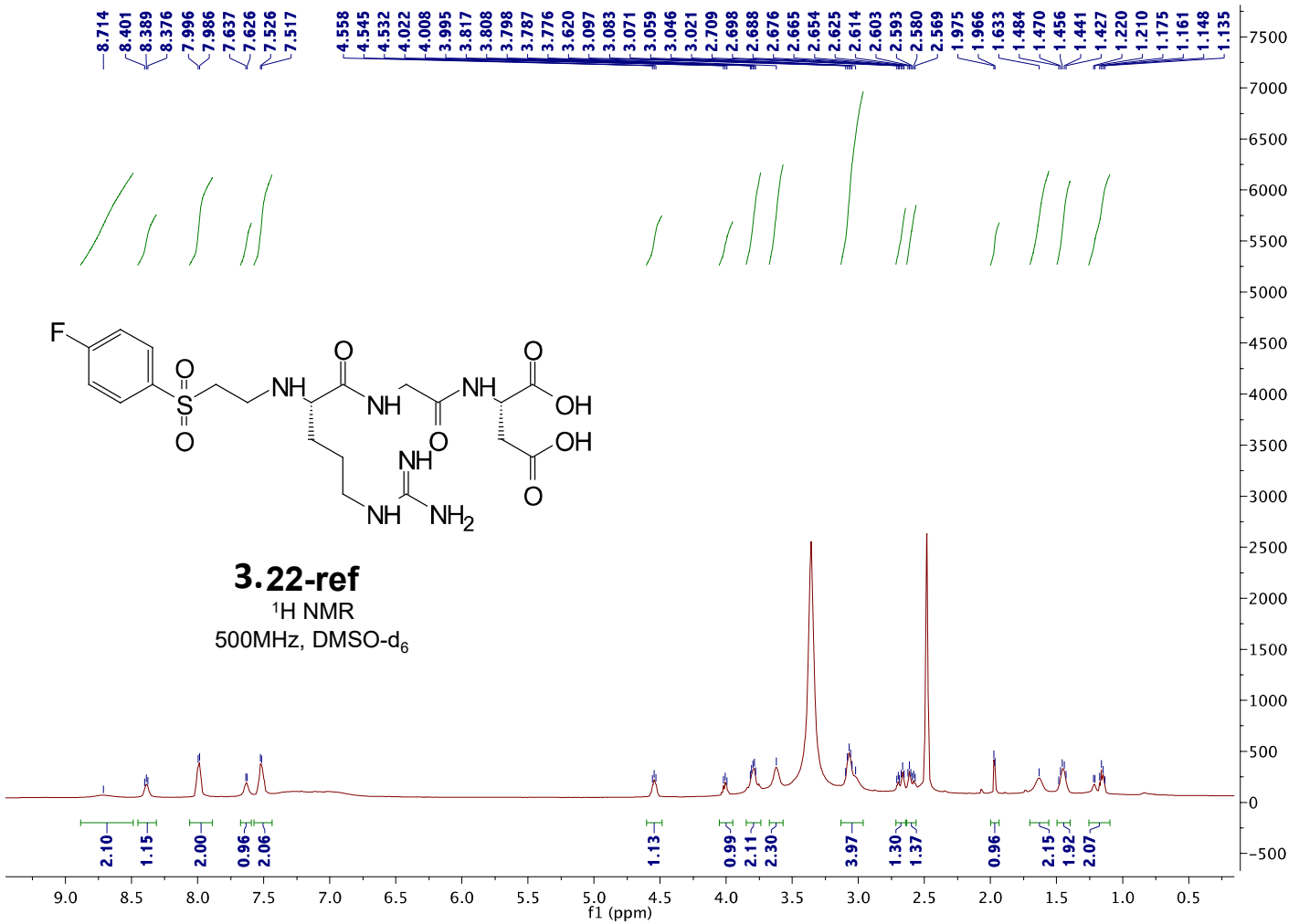
8.714
8.401
8.389
8.376
7.996
7.986
7.637
7.626
7.526
7.517
4.558
4.545
4.532
4.022
4.008
3.995
3.817
3.808
3.798
3.787
3.776
3.620
3.097
3.083
3.071
3.059
3.046
3.021
2.709
2.698
2.688
2.676
2.665
2.654
2.625
2.614
2.603
2.593
2.580
2.569
1.975
1.966
1.633
1.484
1.470
1.456
1.441
1.427
1.220
1.210
1.175
1.161
1.148
1.135
F
O
S
O
NH
O
NH
NH
O
O
OH
OH
O
NH
NH
NH2
3.22-ref
1H NMR
500MHz, DMSO-d6
2.10
1.15
2.00
0.96
2.06
1.13
0.99
2.11
2.30
3.97
1.30
1.37
0.96
2.15
1.92
2.07
9.0
8.5
8.0
7.5
7.0
6.5
6.0
5.5
5.0
4.5
4.0
3.5
3.0
2.5
2.0
1.5
1.0
0.5
f1 (ppm)
7500
7000
6500
6000
5500
5000
4500
4000
3500
3000
2500
2000
1500
1000
500
0
-500

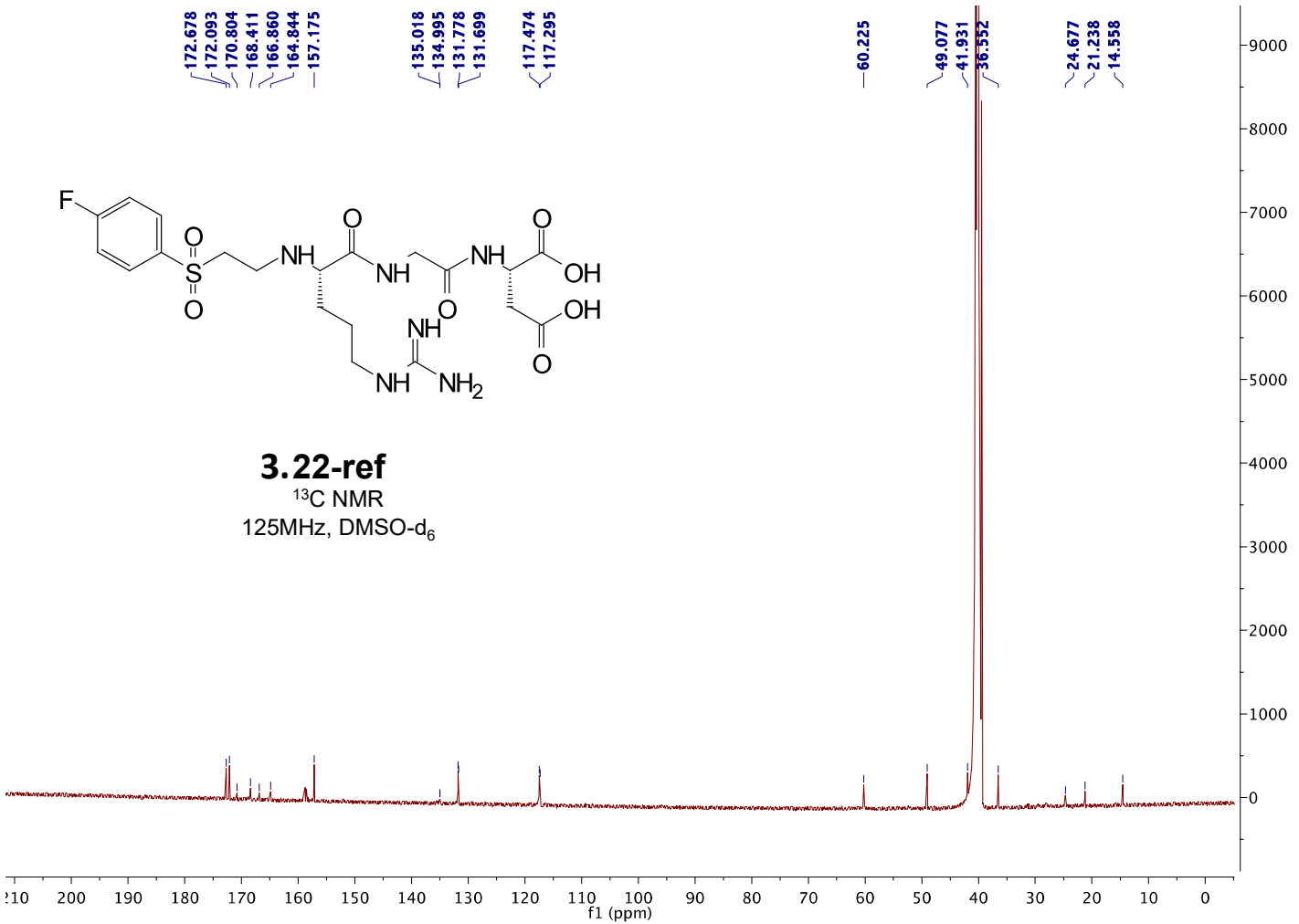
172.678
172.093
170.804
168.411
166.860
164.844
157.175
135.018
134.995
131.778
131.699
117.474
117.295
60.225
49.077
41.931
36.552
24.677
21.238
14.558
F
O
S
O
NH
O
NH
NH
O
O
OH
OH
O
NH
NH
NH2
3.22-ref
13C NMR
125MHz, DMSO-d6
9000
8000
7000
6000
5000
4000
3000
2000
1000
0
210 200 190 180 170 160 150 140 130 120 110 100 90 80 70 60 50 40 30 20 10 0
f1 (ppm)

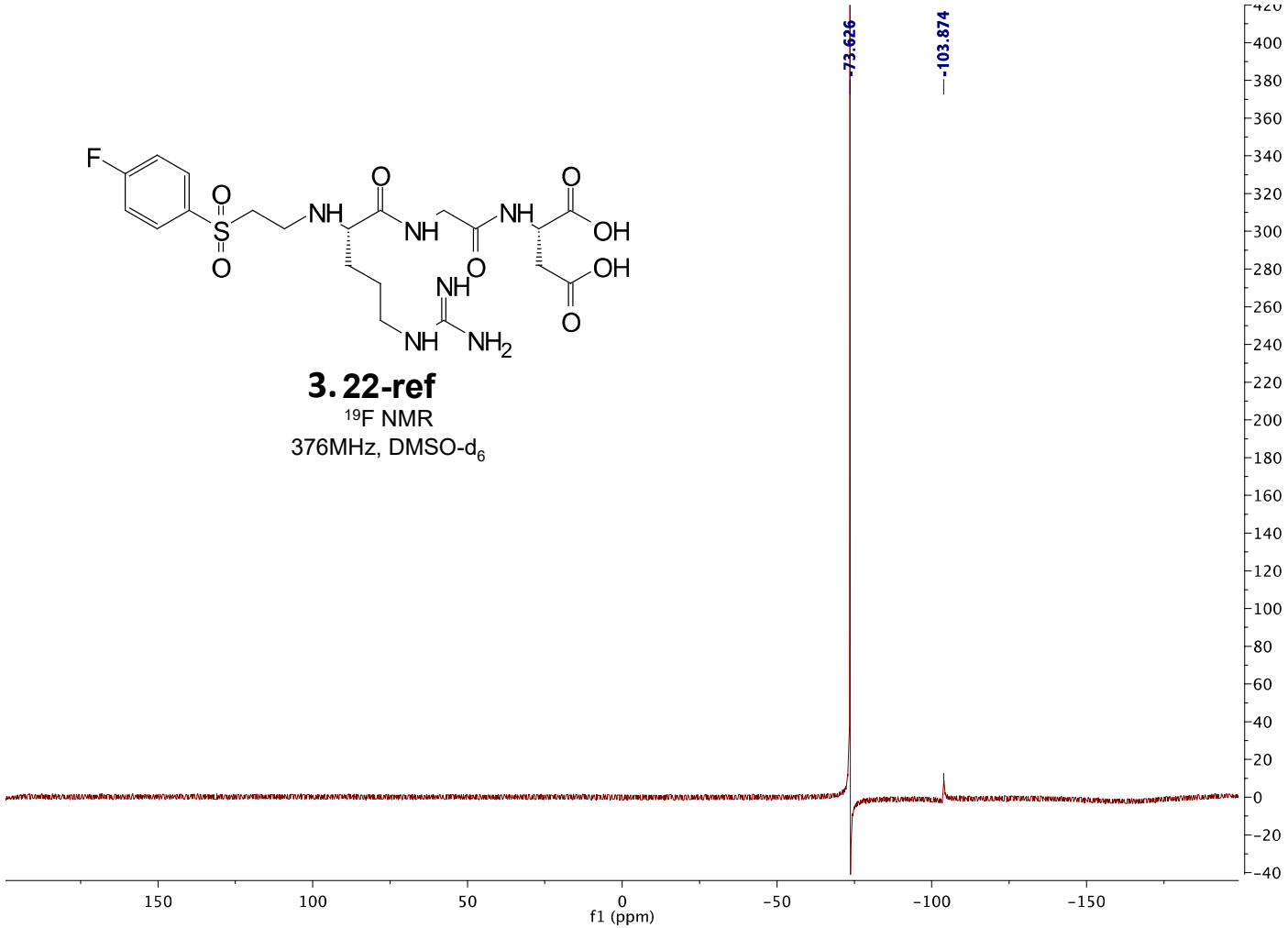

3. 22-ref

^{19}F NMR

376MHz, DMSO-d_6

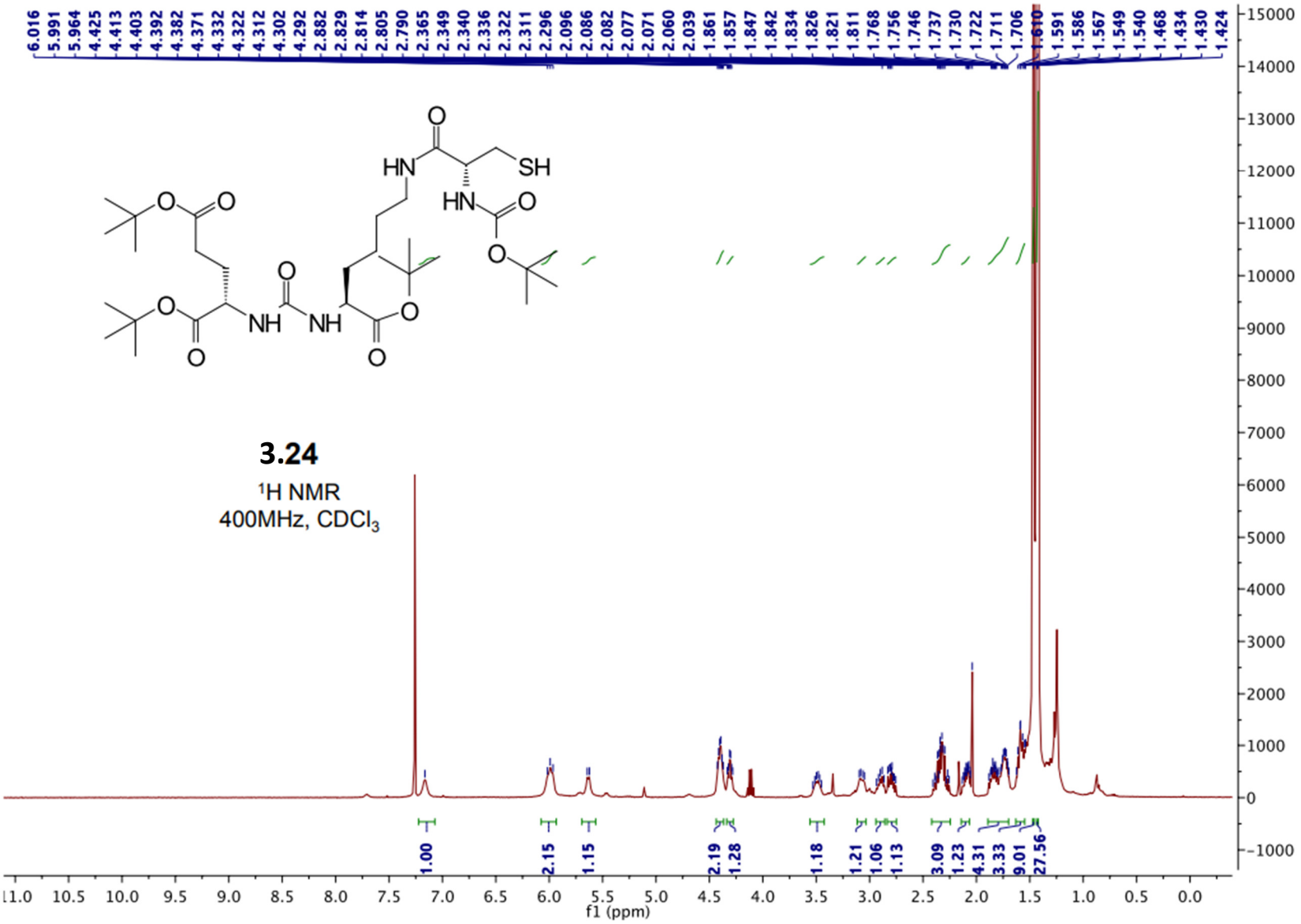
3.24
1H NMR
400MHz, CDCl3
f1 (ppm)

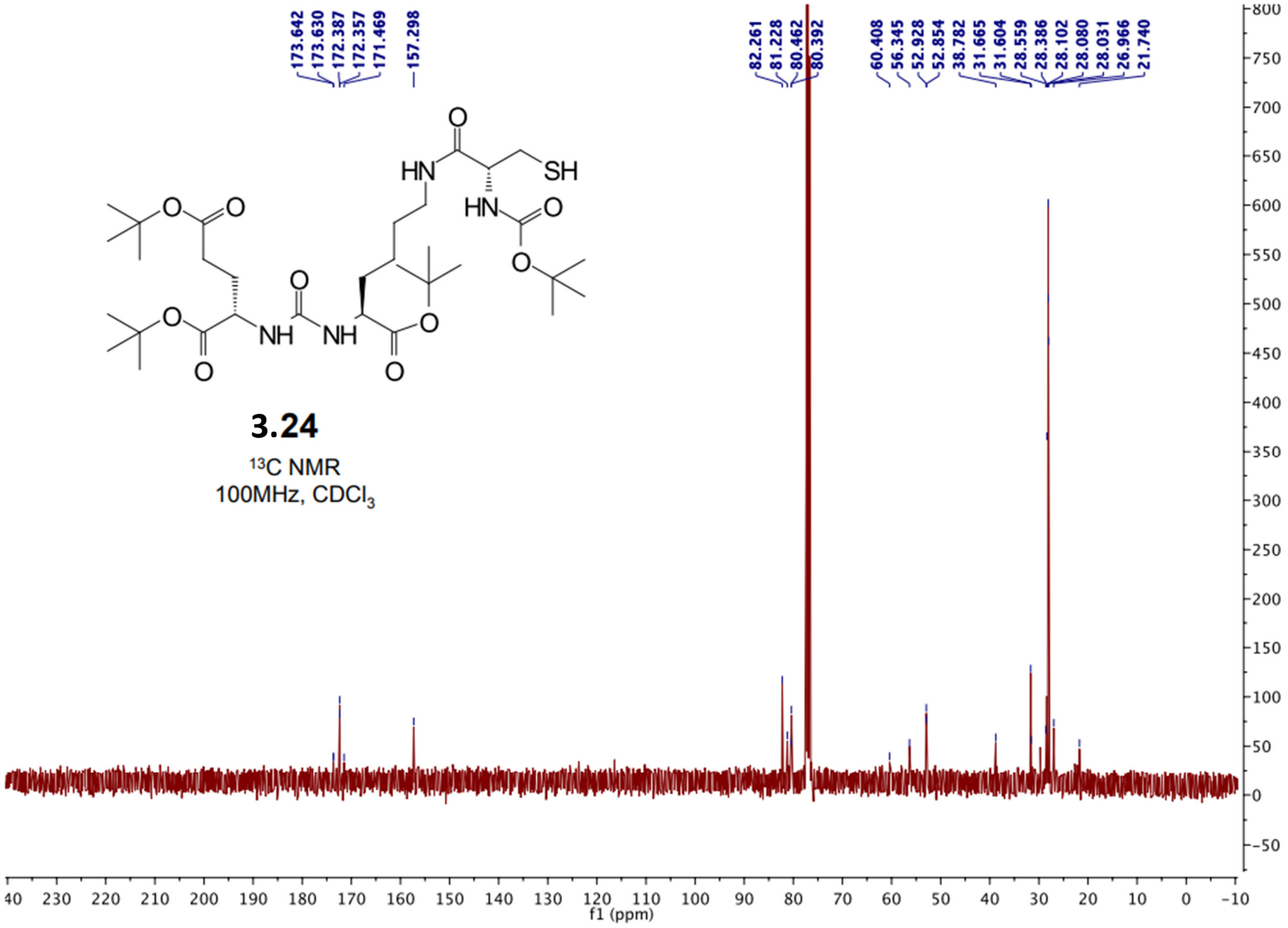

3.24

^{13}C NMR
100MHz, $CDCl_3$

3.7. Notes and References

1. Charron, C. L.; Hickey, J. L.; Nsiama, T. K.; Cruickshank, D. R.; Turnbull, W. L.; Luyt, L. G., Molecular imaging probes derived from natural peptides. *Natural Product Reports.* **2016,** *33* (6), 761-800.

2. Fani, M.; Maecke, H. R.; Okarvi, S. M., Radiolabeled Peptides: Valuable Tools for the Detection and Treatment of Cancer. *Theranostics.* **2012,** *2* (5), 481-501.

3. Jackson, I. M.; Scott, P. J. H.; Thompson, S., Clinical Applications of Radiolabeled Peptides for PET. *Seminars in Nuclear Medicine.* **2017,** *47* (5), 493-523.

4. Okarvi, S. M., Peptide-based radiopharmaceuticals: Future tools for diagnostic imaging of cancers and other diseases. *Medicinal Research Reviews.* **2004,** *24* (3), 357-397.

5. Sun, X.; Li, Y.; Liu, T.; Li, Z.; Zhang, X.; Chen, X., Peptide-based imaging agents for cancer detection. *Advanced Drug Delivery Reviews.* **2017,** *110-111*, 38-51.

6. Neumann, C. N.; Hooker, J. M.; Ritter, T., Concerted nucleophilic aromatic substitution with $^{19}F^-$ and $^{18}F^-$. *Nature.* **2016,** *534* (7607), 369-373.

7. Preshlock, S.; Tredwell, M.; Gouverneur, V., 18 F-Labeling of Arenes and Heteroarenes for Applications in Positron Emission Tomography. *Chemical Reviews.* **2016,** *116* (2), 719-766.

8. Rickmeier, J.; Ritter, T., Site-Specific Deoxyfluorination of Small Peptides with [^{18}F]Fluoride. *Angewandte Chemie.* **2018,** *57* (43), 14207-14211.

9. Verhoog, S.; Kee, C. W.; Wang, L.; Khotavivattana, T.; Wilson, T. C.; Kersemans, V.; Smart, S.; Tredwell, M.; Davis, B. G.; Gouverneur, V., 18 F-Trifluoromethylation of Unmodified Peptides with 5-[^{18}]F-(Trifluoromethyl)dibenzothiophenium Trifluoromethanesulfonate. *Journal of the American Chemical Society.* **2018,** *140* (5), 1572-1575.

10. Yuan, Z.; Nodwell, M. B.; Yang, H.; Malik, N.; Merkens, H.; Bénard, F.; Martin, R. E.; Schaffer, P.; Britton, R., Site-Selective, Late-Stage C−H ^{18}F-Fluorination on Unprotected Peptides for Positron Emission Tomography Imaging. *Angewandte Chemie.* **2018,** *57* (39), 12733-12736.

11. Glaser, M.; Årstad, E., "Click Labeling" with 2-[^{18}F]Fluoroethylazide for Positron Emission Tomography. *Bioconjugate Chemistry.* **2007,** *18* (3), 989-993.

12. Jacobson, O.; Kiesewetter, D. O.; Chen, X., Fluorine-18 Radiochemistry, Labeling Strategies and Synthetic Routes. *Bioconjugate Chemistry.* **2015,** *26* (1), 1-18.

13. Krishnan, H. S.; Ma, L.; Vasdev, N.; Liang, S. H., ^{18}F-Labeling of Sensitive Biomolecules for Positron Emission Tomography. *Chemistry: a European journal.* **2017,** *23* (62), 15553-15577.

14. Marik, J.; Sutcliffe, J. L., Click for PET: rapid preparation of [^{18}F]fluoropeptides using CuI catalyzed 1,3-dipolar cycloaddition. *Tetrahedron Letters.* **2006,** *47* (37), 6681-6684.

15. Richter, S.; Wuest, F., ^{18}F-Labeled Peptides: The Future Is Bright. *Molecule.* **2014,** *19* (12), 20536-20556.

16. van der Born, D.; Pees, A.; Poot, A. J.; Orru, R. V. A.; Windhorst, A. D.; Vugts, D. J., Fluorine-18 labelled building blocks for PET tracer synthesis. *Chemical Society Reviews.* **2017,** *46* (15), 4709-4773.

17. Chalker, J. M.; Bernardes, G. J. L.; Lin, Y. A.; Davis, B. G., Chemical Modification of Proteins at Cysteine: Opportunities in Chemistry and Biology. *Chemistry, an Asian Journal.* **2009,** *4* (5), 630-640.

18. Koniev, O. W., A., Developments and recent advancements in the field of endogenous amino acid selective bond forming reactions for bioconjugation. *Chemical Society Reviews.* **2015,** *44* (15), 5495-5551.

19. McKay, C. S.; Finn, M. G., Click Chemistry in Complex Mixtures: Bioorthogonal Bioconjugation. *Cell Metabolism.* **2014,** *21* (9), 1075-1101.

20. Spicer, C. D.; Davis, B. G., Selective chemical protein modification. *Nature Communications.* **2014,** *5* (1), 4740.

21. Cai, W.; Zhang, X.; Wu, Y.; Chen, X., *The Journal of Nuclear Medicine.* **2006,** *47*, 1172-1180.

22. de Bruin, B.; Kuhnast, B.; Hinnen, F.; Yaouancq, L.; Amessou, M.; Johannes, L.; Samson, A.; Boisgard, R.; Tavitian, B.; Dollé, F., 1-[3-(2-[^{18}F]Fluoropyridin-3-yloxy)propyl]pyrrole-2,5-dione: Design, Synthesis, and Radiosynthesis of a New [^{18}F]Fluoropyridine-Based Maleimide Reagent for the Labeling of Peptides and Proteins. *Bioconjugate Chemistry.* **2005,** *16* (2), 406-420.

23. Kiesewetter, D. O.; Jacobson, O.; Lang, L.; Chen, X., Automated radiochemical synthesis of [^{18}F]FBEM: A thiol reactive synthon for radiofluorination of peptides and proteins. *Applied Radiation and Isotopes.* **2011,** *69* (2), 410-414.

24. Kniess, T.; Kuchar, M.; Pietzsch, J., Automated radiosynthesis of the thiol-reactive labeling agent N-[6-(4-[^{18}F]fluorobenzylidene)aminooxyhexyl]maleimide ([^{18}F]FBAM). *Applied Radiation and Isotopes.* **2011,** *69* (9), 1226-1230.

25. Toyokuni, T.; Walsh, J. C.; Dominguez, A.; Phelps, M. E.; Barrio, J. R.; Gambhir, S. S.; Satyamurthy, N., Synthesis of a New Heterobifunctional Linker, N-[4-(Aminooxy)butyl]maleimide, for Facile Access to a Thiol-Reactive ^{18}F-Labeling Agent. *Bioconjugate Chemistry.* **2003,** *14* (6), 1253-1259.

26. Adumeau, P.; Davydova, M.; Zeglis, B. M., Thiol-Reactive Bifunctional Chelators for the Creation of Site-Selectively Modified Radioimmunoconjugates with Improved Stability. *Bioconjugate Chemistry.* **2018,** *29* (4), 1364-1372.

27. Baldwin, A. D.; Kiick, K. L., Tunable Degradation of Maleimide–Thiol Adducts in Reducing Environments. *Bioconjugate Chemistry.* **2011,** *22* (10), 1946-1953.

28. Shen, B.-Q.; Xu, K.; Liu, L.; Raab, H.; Bhakta, S.; Kenrick, M.; Parsons-Reponte, K. L.; Tien, J.; Yu, S.-F.; Mai, E.; Li, D.; Tibbitts, J.; Baudys, J.; Saad, O. M.; Scales, S. J.; McDonald, P. J.; Hass, P. E.; Eigenbrot, C.; Nguyen, T.; Solis, W. A., Conjugation site modulates the in vivo stability and therapeutic activity of antibody-drug conjugates. *Nature Biotechnology.* **2012,** *30* (2), 184-189.

29. Alley, S. C.; Benjamin, D. R.; Jeffrey, S. C.; Okeley, N. M.; Meyer, D. L.; Sanderson, R. J.; Senter, P. D., Contribution of Linker Stability to the Activities of Anticancer Immunoconjugates. *Bioconjugate Chemistry.* **2008,** *19* (3), 759-765.

30. Dolle, F.; Hinnen, F.; Vaufrey, F.; Tavitian, B.; Crouzel, C., A general method for labeling oligodeoxynucleotides with ^{18}F for in vivo PET imaging. *Journal of Labelled Compounds & Radiopharmaceuticals.* **1997,** *39* (4), 319-330.

31. Kuhnast, B.; de Bruin, B.; Hinnen, F.; Tavitian, B.; Dollé, F., Design and Synthesis of a New [^{18}F]Fluoropyridine-Based Haloacetamide Reagent for the Labeling of Oligonucleotides: 2-Bromo- N -[3-(2-[^{18}F]fluoropyridin-3-yloxy)propyl]acetamide. *Bioconjugate Chemistry.* **2004,** *15* (3), 617-627.

32. von Guggenberg, E.; Sader, J. A.; Wilson, J. S.; Shahhosseini, S.; Koslowsky, I.; Wuest, F.; Mercer, J. R., Automated synthesis of an ^{18}F-labelled pyridine-based alkylating agent for high yield oligonucleotide conjugation. *Applied Radiation and Isotopes.* **2009,** *67* (9), 1670-1675.

33. Wu, Z.; Li, L.; Liu, S.; Yakushijin, F.; Yakushijin, K.; Horne, D.; Conti, P. S.; Li, Z.; Kandeel, F.; Shively, J. E., Facile Preparation of a Thiol-Reactive ^{18}F-Labeling Agent and Synthesis of ^{18}F-DEG-VS-NT for PET Imaging of a Neurotensin Receptor–Positive Tumor. *The Journal of Nuclear Medicine.* **2014,** *55* (7), 1178-1184.

34. Chiotellis, A.; Sladojevich, F.; Mu, L.; Müller Herde, A.; Valverde, I. E.; Tolmachev, V.; Schibli, R.; Ametamey, S. M.; Mindt, T. L., Novel chemoselective ^{18}F-radiolabeling of thiol-containing biomolecules under mild aqueous conditions. *Chemical Communications.* **2016,** *52* (36), 6083-6086.

35. Inkster, J. A. H.; Colin, D. J.; Seimbille, Y., A novel 2-cyanobenzothiazole-based ^{18}F prosthetic group for conjugation to 1,2-aminothiol-bearing targeting vectors. *Organic & Biomolecular Chemistry.* **2015,** *13* (12), 3667-3676.

36. Jeon, J.; Shen, B.; Xiong, L.; Miao, Z.; Lee, K. H.; Rao, J.; Chin, F. T., Efficient Method for Site-Specific ^{18}F-Labeling of Biomolecules Using the Rapid Condensation Reaction between 2-Cyanobenzothiazole and Cysteine. *Bioconjugate Chemistry.* **2012,** *23* (9), 1902-1908.

37. Toda, N.; Asano, S.; Barbas, C. F., Rapid, Stable, Chemoselective Labeling of Thiols with Julia-Kocieński-like Reagents: A Serum-Stable Alternative to Maleimide-Based Protein Conjugation. *Angewandte Chemie* **2013,** *52* (48), 12592-12596.

38. Li, L.; Crow, D.; Turatti, F.; Bading, J. R.; Anderson, A.-L.; Poku, E.; Yazaki, P. J.; Carmichael, J.; Leong, D.; Wheatcroft, M. P.; Raubitschek, A. A.; Hudson, P. J.; Colcher, D.; Shively, J. E., Site-Specific Conjugation of Monodispersed DOTA-PEGn to a Thiolated Diabody Reveals the Effect of Increasing PEG Size on Kidney Clearance and Tumor Uptake with Improved 64-Copper PET Imaging. *Bioconjugate Chemistry.* **2011,** *22* (4), 709-716.

39. Li, L.; Olafsen, T.; Anderson, A.-L.; Wu, A.; Raubitschek, A. A.; Shively, J. E., Reduction of Kidney Uptake in Radiometal Labeled Peptide Linkers Conjugated to Recombinant Antibody Fragments. Site-Specific Conjugation of DOTA-Peptides to a Cys-Diabody. *Bioconjugate Chemistry.* **2002,** *13* (5), 985-995.

40. Meadows, D. C.; Gervay-Hague, J., Vinyl sulfones: Synthetic preparations and medicinal chemistry applications. *Medicinal Research Reviews.* **2006,** *26* (6), 793-814.

41. Morales-Sanfrutos, J.; Lopez-Jaramillo, J.; Ortega-Muñoz, M.; Megia-Fernandez, A.; Perez-Balderas, F.; Hernandez-Mateo, F.; Santoyo-Gonzalez, F., Vinyl sulfone: a versatile function for simple bioconjugation and immobilization. *Organic & Biomolecular Chemistry.* **2010,** *8* (3), 667-675.

42. Morpurgo, M.; Veronese, F. M.; Kachensky, D.; Harris, J. M., Preparation and Characterization of Poly(ethylene glycol) Vinyl Sulfone. *Bioconjugate Chemistry.* **1996,** *7* (3), 363-368.

43. Chen, H.; Niu, G.; Wu, H.; Chen, X., Clinical Application of Radiolabeled RGD Peptides for PET Imaging of Integrin α v β 3. *Theranostics.* **2016,** *6* (1), 78-92.

44. Good, S.; Walter, M. A.; Waser, B.; Wang, X.; Müller-Brand, J.; Béhé, M. P.; Reubi, J.-C.; Maecke, H. R., Macrocyclic chelator-coupled gastrin-based radiopharmaceuticals for targeting of gastrin receptor-expressing tumours. *European Journal of Nuclear Medicine and Molecular Imaging.* **2008,** *35* (10), 1868-1877.

45. Liu, S., Radiolabeled Cyclic RGD Peptide Bioconjugates as Radiotracers Targeting Multiple Integrins. *Bioconjugate Chemistry.* **2015,** *26* (8), 1413-1438.

46. Foss, C. A.; Mease, R. C.; Fan, H.; Wang, Y.; Ravert, H. T.; Dannals, R. F.; Olszewski, R. T.; Heston, W. D.; Kozikowski, A. P.; Pomper, M. G., Radiolabeled Small-Molecule Ligands for

Prostate-Specific Membrane Antigen: In vivo Imaging in Experimental Models of Prostate Cancer. *Clinical Cancer Research.* **2005,** *11* (11), 4022-4028.

47. Jamous, M.; Haberkorn, U.; Mier, W., Synthesis of Peptide Radiopharmaceuticals for the Therapy and Diagnosis of Tumor Diseases. *Molecules.* **2013,** *18* (3), 3379-3409.

48. Brace, N. O., An economical and convenient synthesis of phenyl vinyl sulfone from benzenethiol and 1,2-dichloroethane. *Journal of Organic Chemistry.* **1993,** *58* (16), 4506-4508.

49. Scalone, M.; Waldmeier, P., Efficient Enantioselective Synthesis of the NMDA 2B Receptor Antagonist Ro 67-8867. *Organic Process Research & Development.* **2003,** *7* (3), 418-425.

50. Neumann, C. N.; Hooker, J. M.; Ritter, T., Concerted nucleophilic aromatic substitution with $^{19}F^-$ and $^{18}F^-$. *Nature.* **2016,** *534* (7607), 369-373.

51. Maresca, K. P.; Hillier, S. M.; Femia, F. J.; Keith, D.; Barone, C.; Joyal, J. L.; Zimmerman, C. N.; Kozikowski, A. P.; Barrett, J. A.; Eckelman, W. C.; Babich, J. W., A series of halogenated heterodimeric inhibitors of prostate specific membrane antigen (PSMA) as radiolabeled probes for targeting prostate cancer. *Journal of Medicinal Chemistry.* **2009,** *52* (2), 347-57.

52. An, H.; Statsyuk, A. V., Facile synthesis of covalent probes to capture enzymatic intermediates during E1 enzyme catalysis. *Chemical Communications.* **2016,** *52* (12), 2477-2480.

CHAPTER 4: Manual and Fully Automated Protocol for ^{18}F-Labeling at Cysteine Residues via Conjugation with [^{18}F]Fluoro-4-(vinylsulfonyl)benzene ([^{18}F]FVSB)

This chapter is comprised, in part, of collaborative work from: Halder, R.; Ma, G.; McDaniel, J.; Murphy, J.; Neumann, C.; Ritter, T. Deoxyfluorination of phenols for chemoselective ^{18}F-labeling of peptides. *Nat. Protoc*., *manuscript in preparation*.

4.1. Abstract

The challenge of forming C–^{18}F bonds is often a bottleneck in the development of new ^{18}F-labeled tracer molecules for non-invasive functional imaging studies using positron emission tomography (PET). Peptide substrates, which are highly desirable targets for PET molecular imaging, are particularly challenging to label with fluorine-18 due to their dense functionality and sensitivity to harsh radiofluorination conditions. We describe a detailed, manual protocol for radiodeoxyfluorination to afford [^{18}F]fluoro-4-(vinylsulfonyl)benzene ([^{18}F]FVSB) and its subsequent ligation to the cysteine residue of Arg-Gly-Asp-Cys. Additionally, we report the details of the fully automated protocol using the ELIXYS radiochemical synthesis module.

4.2. Introduction

Positron emission tomography (PET) is a non-invasive *in vivo* imaging technique utilized in drug development and diagnostics. [1] Owing to their high binding affinities and rapid blood clearance, radiolabeled receptor-binding peptides are attractive for PET tracer development to study biochemical processes.[24] Despite their utility in nuclear medicine, the production of peptides

labeled with fluorine-18 has been impeded by challenges in chemistry. Due to the 109 min half-lifetime of the ^{18}F isotope, the introduction of ^{18}F has to occur at a late (preferably the ultimate) step of a synthetic sequence. [2] Therefore, functional group tolerance and a wide substrate scope are critically important features of general ^{18}F-labeling methods. The high basicity of [^{18}F]fluoride can lead to deprotonation and side reactions with densely functionalized peptides, which may explain the lack of a conceptional breakthrough in direct ^{18}F-labeling of peptides and rationalize the use of prosthetic groups.

One of the most universal prosthetic groups is the reactive activated ester ([^{18}F]SFB, [^{18}F]F-Py-TFP, [^{18}F]NFP, etc.) which has been widely applied to a variety of peptides via acylation of the primary amino group in lysine (***Figure 4.1***).[3-5] Similarly, prosthetic groups for alkylation[6, 7] and cross-coupling[8, 9] have been reported, albeit with few examples. In the last decade, significant interest in click-chemistry methodologies have been translated to ^{18}F-labeling approaches to take advantage of the mild conditions, rapid reaction kinetics and high chemoselectivity. [10-12] The bioorthogonal 1,3-dipolar Huisgen cycloaddition and the inverse electron demand Diels-Alder reactions have afforded radiolabeled peptides using ^{18}F-containing alkynes, azides, sydnone or transcyclooctene analogues. [13-17] Likewise, Michael addition with ^{18}F-containing maleimides and vinyl sulfones have expanded the radiochemistry toolbox for ^{18}F-labeling of peptides and proteins. [13, 18-22] Alternatively, the Gouverneur group showed the direct introduction of fluorine-18 at cysteine or homocysteine residues with [^{18}F]CF_3 to afford radiolabeled thioethers using an [^{18}F]Umemoto reagent.[29]

Due to its efficiency, convenience, and reliability, S_NAr with [^{18}F]fluoride is widely employed for the introduction of ^{18}F into aromatic small molecules. [23] The presence of a basic fluoride anion and the intermediacy of the negatively charged Meisenheimer complex, limits S_NAr

in functional group tolerance and substrate scope, although direct labeling of peptides bearing suitable pre-installed leaving groups amenable to S_NAr have been reported. [24-26] The demand for mild approaches for late-stage introduction of ^{18}F has led to the investigation of isotope exchange protocols that employ highly fluorophilic elements to form Si-F, B-F or Al-F bonds. [25, 27-31] These protocols display a wide substrate scope, employ mild reaction conditions and, in many cases, tolerate protic functional groups.

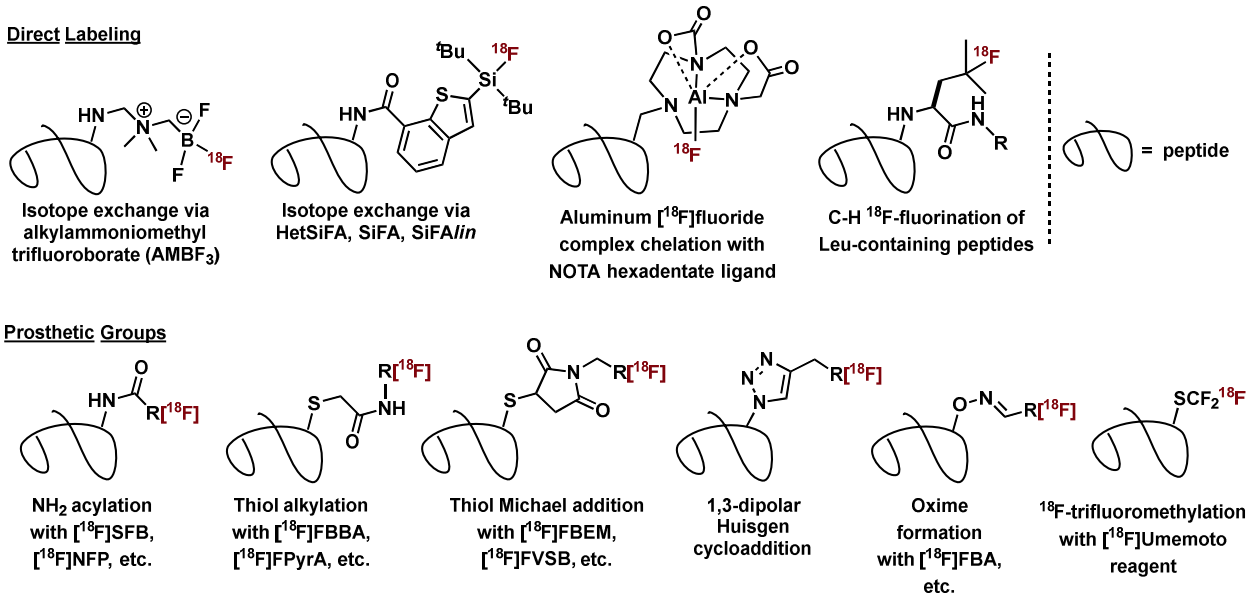

Figure 4.1. Other strategies for radiolabeling peptides.

Methods to radiolabel a native polypeptide and to introduce the smallest structural perturbation, i.e. displacement of a single hydrogen atom with [^{18}F]fluoride, are scarce. A method to label small organic molecules including one example of a dipeptide with [^{18}F]fluoride through direct C–H bond fluorination was disclosed by the Groves group, but the scheme was not extended to larger peptides.[30] Likewise, the Doyle lab described the copper catalyzed H-F insertion of α-diazocarbonyl compounds and applied it to the direct ^{18}F-labeling of a tripeptide. [32] The Britton

group reported direct C–H fluorination of Leu-containing peptides using difficult to make and handle [^{18}F]fluorine gas.[31] The Gouverneur group reported the indirect C-H ^{18}F-trifluoromethylation of tyrosine and tryptophan residues in native peptides via a radical 2-step approach. [32]

4.3. Metal-free ^{18}F-Deoxyfluorination for Labeling at Cysteine Residues

Due to the inherent dangers of working with radioactive materials, appropriate safety instruction is required for all personnel performing synthetic work with ^{18}F. Following radiation safety training, uronium radiodeoxyfluorination is highly accessible to newcomers to radiosynthesis, if detailed operating procedures are available. In our own experience, chemistry PhD students with no previous radiochemistry experience were rapidly able to acquire sufficient skills to independently perform uronium radiodeoxyfluorination after instruction by a more experienced radiochemist.

This chapter details the synthesis of the ^{18}F-synthon **4.1** and its ligation to a cysteine residue in the polypeptide Arg-Gly-Asp-Cys, including automation of the synthetic protocol on the ELIXYS FLEX/CHEM radiochemical synthesis module (***Figure 4.2*** and ***Figure 4.3***). The electronically activated radiosynthon precursor enables deoxyfluorination to proceed in one-step, in high efficiency and RCY and facilitates the rapid conjugation with free thiols to form stable thioether linkages. We envision this protocol to be utilized for the production of ^{18}F-labeled peptides to develop molecular imaging tools for the noninvasive study of important biochemical processes.

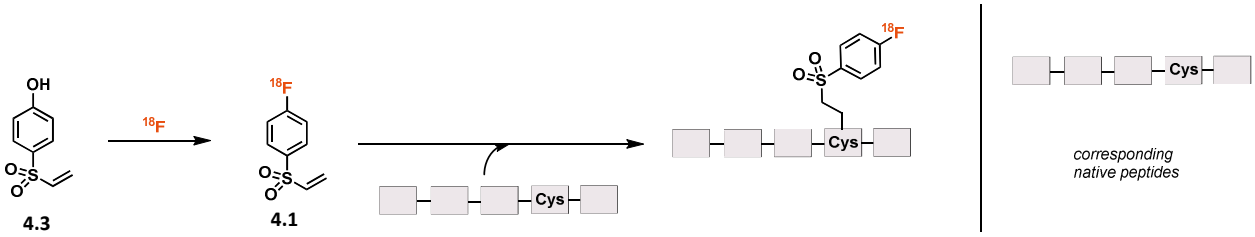

Figure 4.2. General scheme for metal-free ^{18}F-deoxyfluorination and ^{18}F-labeling of cysteine containing peptides with [^{18}F]FVSB (**4.1**); (Ar = 2,6-diisopropylphenyl).

The deoxyfluorination of phenols is an attractive reaction as it allows the replacement of a hydroxyl substituent with its bioisostere fluorine. The displacement of hydroxyl substituents via S_NAr is unfavorable because hydroxide is a poor leaving group, which, in the presence of basic fluoride nucleophiles may be deprotonated to yield phenoxide anions, thus further deactivating the arene toward S_NAr. Deoxyfluorination of phenols therefore typically consists of a two-step process, consisting of conversion of the hydroxyl group into a good leaving group, followed by S_NAr. In 2002, the Hayashi group reported on the 2,2-difluoro-1,3-dimethylimidazolidine (DFI)-mediated deoxyfluorination of phenols.[34] In the first step, the hydroxyl substituent is converted into uronium bifluoride, which is a good leaving group. In a subsequent step, the arene is attacked by fluoride and a highly exergonic removal of corresponding urea follows. Despite the good leaving group properties of urea, only electron-poor arenes could be deoxyfluorinated. More electron-rich arenes such as phenol formed the key uronium bifluoride intermediate, but subsequent aryl fluoride formation does not take place.

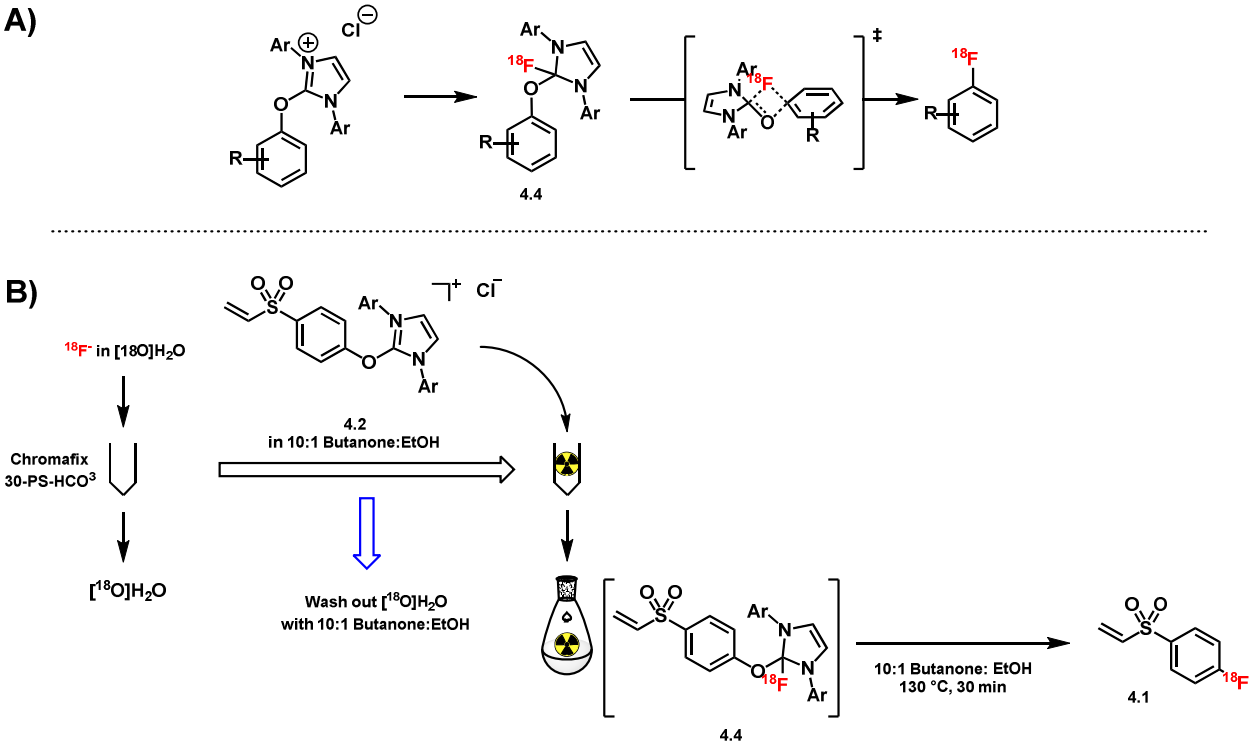

Figure 4.3. A) Overall reaction scheme of ^{18}F-deoxyfluorination. B) Cartoon work flow of the ^{18}F-deoxyfluorination of imidazolium precursor (**4.2**) to make [`^{18}F]FVSB (**4.1**).

In 2011, the Ritter lab developed the PhenoFluor reagent, which has a similar scaffold to DFI and also takes advantage of the strongly exothermic formation of the corresponding urea as a driving force.[35] Later, the Ritter group translated the PhenoFluor-mediated deoxyfluorination of phenols to a radiodeoxyfluorination method that yields ^{18}F-aryl fluorides with high specific activity.[36] Because PhenoFluor contains two fluorine-19 atoms that would lower the molar activity during radiolabeling, chloroimidazolium chloride **4.5** (^{iPr}ImCl) was used to gain access to the uronium chloride intermediate **4.2**. The chloride counterion is exchanged with [^{18}F]fluoride using an anion exchange cartridge to form key intermediate **4.4** that thermally decomposes to ^{18}F-aryl fluoride (***Figure 4.3***).

Alcohols, unlike phenols, do not form stable uronium salts with **4.5** and no additional reagent has to be used if aliphatic hydroxyl groups are present in the substrate. Ethanol is used as a co-solvent in the reaction, which indicates that the presence of aliphatic hydroxyl groups does not interfere with the ^{18}F-deoxyfluorination reaction. Even chemoselective deoxyfluorination in the presence of additional aromatic hydroxyl substituents is possible if the hydroxyl moieties are sufficiently electronically differentiated.

4.4. Advantages and Limitations

Metal-free uronium ^{18}F-deoxyfluorination has several advantages over existing methods: First, preparation of the labeling precursor is facile, and a simple filtration yields crude material suitable for ^{18}F labeling. Second, azeotropic drying of [^{18}F]fluoride, required in many radiolabeling procedures to enhance the reactivity of [^{18}F]fluoride, is not needed, saving valuable synthesis time[2]. Third, the clean reaction profile of the deoxyfluorination in combination with the large polarity difference between the labeling precursor and the aryl fluoride product gives rise to a straight-forward (and consequently reliable) purification. Fourth, no special precautions to exclude air or moisture are needed, and the labeling precursors are bench-stable for at least six months. Lastly, heterocycles which are often problematic substrates for metal-mediated radiofluorination methods are broadly compatible to ^{18}F-deoxyfluorination.

Specifically in the context of ^{18}F-labeling of peptides, methods that exploit lysines or cysteines and employ amine-reactive or thiol-reactive radiosynthons have demonstrated broad utility, yet most reported protocols require multistep syntheses, azeotropic drying of [^{18}F]fluoride and HPLC purification prior to peptide conjugation. These constraints result in a lengthy production process and low radiochemical yield of the ^{18}F-labeled peptide. The Murphy group

recently developed the first aryl vinyl sulfone radiosynthon capable of chemoselective peptide ligation via cysteine residues described in **CHAPTER 3**:. The simplicity of this method is emphasized by the preparation of a stable uronium radiofluorination precursor that does not require rigorous exclusion of air or moisture nor stringent purification procedures. The radiosynthon is synthesized via ^{18}F-deoxyfluorination in one step with high RCY and can be used directly for peptide conjugation without HPLC purification. Most notably, this approach forms a stable thioether linkage, overcoming the major limitation to current thiol-based radiosynthons.

4.5. Experimental Design

This chapter describes the preparation of a bench-stable uronium precursor **4.2** and the one-step, ^{18}F-deoxyfluorination using aqueous [^{18}F]fluoride to afford [^{18}F]fluoro-4-(vinylsulfonyl)benzene **[^{18}F]4.1** ([^{18}F]FVSB), including automation of the protocol using a radiochemical synthesis module (***Figure 4.3***). Details of the chemical synthesis and characterization of the uronium precursor **4.2** are provided in **section 4.5.1** (***Figure 4.4***). Details for the subsequent chemoselective radiolabeling of a commercial peptide with the thiol reactive synthon **[^{18}F]4.1** are described in s**ection 4.5.3**. Variations in the peptide bioconjugation efficiency with **[^{18}F]4.1** can be observed due to peptide solubility factors. To obtain the highest RCYs and most efficient bioconjugation, reaction optimization for each specific peptide is suggested. All reagents and solvents used are commercially available and are used without further purification. Chloroimidazolium chloride **4.5** can either be purchased (*e.g.*, Strem Chemicals 07-0620) or obtained through the chlorination of *i*Pr carbene. [33, 34]

In order to verify that the correct ^{18}F radiosynthon is obtained during a radiolabeling experiment, the ^{19}F isotopologue must be available to match the HPLC retention time of the ^{18}F

product to a fully characterized ^{19}F isotopologue of the desired product. Described in s**ection 4.5.2**, we chose to prepare the reference standard required for this protocol. Commercially available fluoro-4-(vinylsulfonyl)benzene (**^{19}F-4.1)** was incubated with the commercial peptide **4.7** at room temperature in a buffer:methanol (1:1) mixture for 1 h to obtain the ^{19}F-peptide reference standard (***Figure 4.5***). Alternatively, the reference standards could be prepared from the phenols available for the preparation of the labeling precursor using PhenoFluor-mediated deoxyfluorination. Deoxyfluorination with the PhenoFluor and PhenoFluorMix reagents shows almost identical functional group tolerance to the radiodeoxyfluorination described in this protocol and successful preparation of the reference standard indicates that all functional groups present in the target molecule will likely be well tolerated in the radiofluorination. Fluoro-4-(vinylsulfonyl)benzene reference standard **^{19}F-4.1** can also be prepared from 4-fluorobenzenethiol **4.9** and is described in **section 4.6.2**.

4.5.1. Step 1. Synthesis and Characterization of Uronium Labeling Precursor 4.2

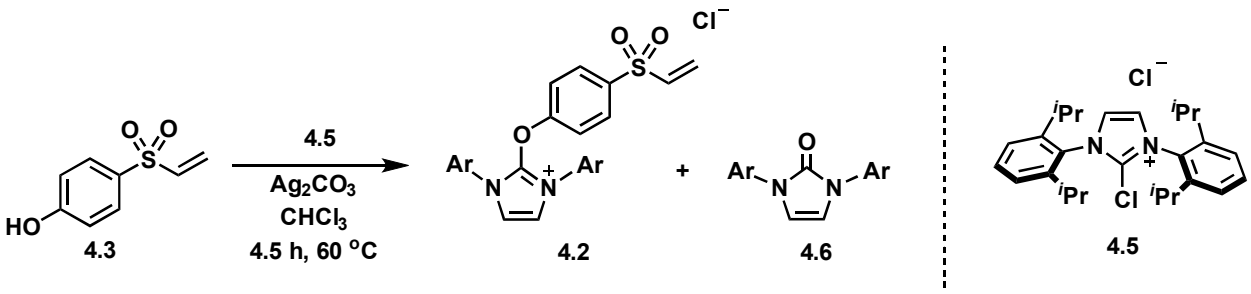

Figure 4.4. Synthesis of the uronium precursor **4.2**

Reagents

- Silver carbonate (Ag_2CO_3, CAS no. 534-16-7, 99%, Sigma-Aldrich, cat. No. 179647)

- Chloroform ($CHCl_3$, CAS no. 67-66-3, ACS solvent grade, Fisher Scientific, cat. No. C298)
- 4-(vinylsulfonyl)phenol **4.3** (Chemieliva Pharmaceutical, 95%, cat. No. CB0046526; alternatively, **4.3** can be prepared from 4-mercaptophenol as described in the **section 4.6.1**)
- Chloroimidazolium chloride **4.5** (CAS no. 1228185-09-8, 98+%, Strem Chemicals, supplier number: 07-0620; alternatively, **4.5** can be prepared from *i*Pr carbene[33, 34])

Equipment

- 4-dram borosilicate reaction vials, with PTFE lined solid PTFE black caps (Chemglass Life Sciences, cat. No. CG-4900-B-03)
- Teflon-coated magnetic stir bar (VWR, 10 x 3 mm, cat. No. 58948-375)
- Magnetic stirrer hot plate (Chemglass Life Sciences)
- Analytical balance (Mettler Toledo™ Excellence XSR Analytical Balance)
- Buchner filter funnel with frit, capacity 15 mL, disc diam. 20 mm, porosity 10-20 μm, Joint: 14/20 (Sigma-Aldrich)
- Whatman qualitative filter paper (Sigma-Aldrich, diam. 150 mm, Grade 1 circles, cat. No. WHA1001150)
- Rotary evaporator (Büchi)
- Polypropylene syringe (Fisher Scientific, 3 mL, cat. No., 03-377-21)
- Disposable syringe needle (Fisher Scientific, cat. No. 14-840-93)

Procedure

1. Weigh phenol **4.3** (36.0 mg, 195 μmol), chloroimidazolium chloride **4.5** (90.0 mg, 196 μmol) and Ag_2CO_3 (26.0 mg, 94.3 μmol) into a 4-dram vial containing a 10 x 3 mm magnetic stir bar.
2. Add 1.5 mL of chloroform to the vial at 23 °C.
3. Purge the headspace by flushing the vial with argon gas for about 10 seconds (Using an argon line fitted with a syringe, place the syringe in the open vial for 10 seconds while the argon is flowing, then immediately cap the vial with a PTFE solid black cap).
4. Place the vial in an oil bath heated to 60 °C and stir the reaction mixture (600 rpm) for 4.5 h at 60 °C.

5. Remove the vial from the oil bath and let the reaction vial cool to 23 °C.
6. Cut one piece of Whatman filter paper to fit flush within the 20 mm diameter of a Buchner filter funnel containing a 10-20 μm porosity frit. Place the filter paper in the funnel which is fitted to a round bottom flask. Pull a vacuum and filter the reaction suspension in the vial through the funnel into the flask. Wash the vial with 1 mL $CHCl_3$ and pour the chloroform rinse through the funnel to filter any remaining salts.
7. Concentrate the filtrate under reduced pressure using a rotary evaporator at 23 °C to obtain the uronium labeling precursor **4.2** (95.0 mg, 156 μmol, 80% yield) as a colorless solid, which was used without further purification in **section 4.5.3**.

If the filter from Step 6 is too coarse, silver impurities will remain in the labeling precursor. In order to remove silver salts efficiently at the end of the reaction, a solvent exchange to chloroform or dichloromethane prior to filtration may be necessary. Small amounts of silver salt impurities are tolerated in the radiolabeling reaction, but the presence of larger amounts of silver salts can interfere with the labeling reaction or lead to clogging of the anion exchange cartridge. It is important to note that cationic **4.5** can compete with the labeling precursor for ^{18}F-fluoride during fluoride elution off the anion exchange cartridge; hydrolysis of excess **4.5** by trace water contained in ACS grade chloroform affords hydrolysis product **4.6** which is innocuous for the labeling reaction. Unpurified labeling precursor **4.2**, which contains around 12% urea **4.6**, can be used for ^{18}F deoxyfluorination without additional purification. Chromatography on silica gel is not recommended as a means of purification because decomposition of the labeling precursor can occur.

The labeling precursor can be stored on the benchtop for at least 6 months or at –4 °C for up to 12 months without noticeable decrease in activity. No color change was observed and no decomposition of the uronium salt was found by ^{1}H-NMR spectroscopy upon storage.

Table 4.1. Troubleshooting table

Problem	Possible reasons	Solution
Silver impurities contained in the labeling intermediate lead to low RCY in the ^{18}F labeling reaction	The porosity of the pore filter used is too high	Filter through a fine pore filter

Characterization Data for Uronium Precursor 4.2:

^{1}H NMR (500 MHz, $CDCl_3$, δ): 8.43 (s, 2H), 7.70 (d, *J* = 9 Hz, 2H), 7.56 (t, *J* = 7.5 Hz, 2H), 7.30 (d, *J* = 7.5 Hz, 4H), 6.67 (d, *J* = 9 Hz, 2H), 6.51-6.40 (m, 2H), 6.08 (d, *J* = 9 Hz, 1H), 2.49 (hept, *J* = 6.5 Hz, 4H), 1.30 (d, *J* = 6.5 Hz, 12H), 1.18 (d, *J* = 6.5 Hz, 12H).

^{13}C NMR (100 MHz, $CDCl_3$, δ): 156.4, 145.3, 143.0, 139.0, 137.4, 132.8, 130.9, 129.6, 127.0, 125.3, 124.1, 118.4, 29.6, 25.8, 22.9.

HRMS-ESI (m/z) calc'd for $C_{35}H_{43}N_2O_3S$ $[M\text{-}Cl]^+$, 571.2994; Found 571.2986, deviation: 1 ppm.

4.5.2. Step 2. Synthesis and Characterization of the Reference Material ^{19}F-4.8

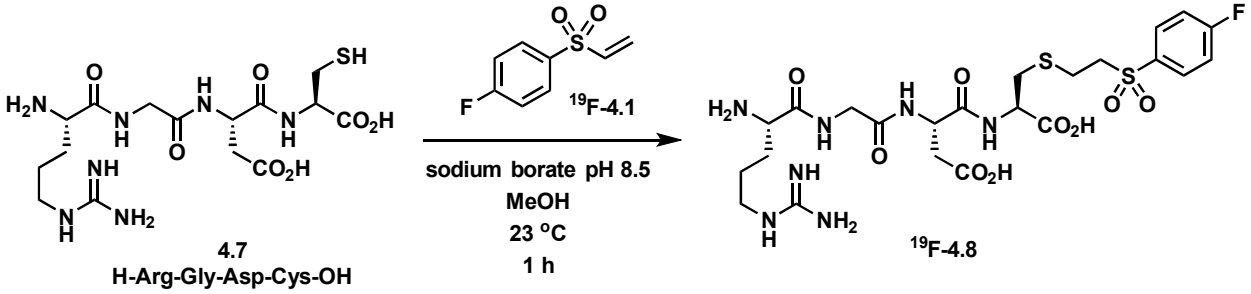

Figure 4.5. Synthesis of reference standard **^{19}F-4.8**.

Reagents

- Fluoro-4-(vinylsulfonyl)benzene **^{19}F-4.1** (CAS no. 28122-14-7, Enamine Building Blocks, >95.0%, cat. No. EN300-115569; alternatively, **^{19}F-4.1** can be prepared from 4-fluorobenzenethiol as described in the **section 4.6.2**
- H-Arg-Gly-Asp-Cys-OH trifluoroacetate salt **4.7** (CAS no. 109292-46-8, Bachem, cat. No. H-3156)
- Borate Buffer (0.5 M Borate buffer, pH 8.5, VWR, cat. No. AAJ60803-AK)

Equipment

- 4-dram borosilicate reaction vials, with PTFE lined solid PTFE black caps (Chemglass Life Sciences, cat. No. CG-4900-B-03)
- Teflon-coated magnetic stir bar
- Magnetic stirrer hot plate (Chemglass Life Sciences)
- Analytical balance (Mettler Toledo^{TM} Excellence XSR Analytical Balance)
- HPLC System equipped with a UV detector (Knauer Smartline HPLC system)
- HPLC column (Phenomenex reverse-phase Luna, 10 x 250 mm, 5 μm for semi-preparative purification)
- Polypropylene syringe (Fisher Scientific, 1 mL, cat. No. 03-377-20)
- Disposable syringe needle (Fisher Scientific, cat. No. 14-840-93)
- Hamilton syringe (VWR, Model 725 N syringe, 250 μL, cat. No. 60373-061)

Procedure

1. Weigh fluoro-4-(vinylsulfonyl)benzene **^{19}F-4.1** (2.4 mg, 13 μmol) and H-Arg-Gly-Asp-Cys-OH peptide **4.7** (6.0 mg, 13 μmol) into a 4-dram vial equipped with a 10 x 3 mm magnetic stir bar.
2. Add 500 μL methanol and 500 μL sodium borate buffer pH 8.5 and stir the reaction mixture at 23 °C for 1 h. The reaction mixture can be stirred for 20 h at 23 °C.
3. Purify the reaction mixture by semi-preparative HPLC. Load 250 μL of the vial contents onto the HPLC loop and inject the reaction mixture onto the semi-preparative HPLC column for purification (the reaction mixture was sequentially purified in 250 μL aliquot injections by semi-preparative HPLC). The reaction mixture was purified using a flow rate set to 3 mL/min, with an isocratic mixture of 5:95 (MeCN:water, 0.1% TFA, v:v) for 3 minutes, followed by a linear gradient to 80:20 (MeCN:water, 0.1% TFA, v:v) over 30 minutes and a linear gradient to 95:5 (MeCN:water, 0.1% TFA, v:v) over 10 minutes. The collected fractions containing the product were combined and concentrated *in vacuo* to dryness to afford the desired product **^{19}F-4.8** (5.8 mg, 69% yield) as a white solid.

Characterization Data for peptide conjugate reference standard ^{19}F- 4.8:

^{1}H NMR (400 MHz, DMSO-d_6, δ): 8.67 (t, *J* = 5.6 Hz, 1H), 8.42 (d, *J* = 8.0 Hz, 1H), 8.01 (d, *J* = 7.2 Hz, 1H), 7.95 (dd, *J* = 8.8, 5.2 Hz, 2H), 7.47 (dd, *J* = 8.8, 8.8 Hz, 2H), 7.28 (m, 3H), 4.54-4.49 (m, 1H), 4.11 (dd, *J* = 12.8, 6.4 Hz, 1H), 3.91-3.71 (m, 3H), 3.57-3.53 (m, 2H), 3.13 (s, 2H), 3.09-3.02 (m, 2H), 2.88 (dd, *J* = 13.6, 5.2 Hz, 1H), 2.73-2.60 (m, 4H), 1.73 (m, 2H), 1.58-1.45 (m, 2H).

^{13}C NMR (125 MHz, DMSO-d_6, δ): 172.45, 172.36, 170.9, 169.2, 168.6, 165.6 (C-F, 1JC-F = 251.4 Hz), 157.3, 135.5 (C-F, 4JC-F = 2.8 Hz), 131.6 (C-F, 3JC-F = 9.8 Hz), 117.2 (C-F, 2JC-F = 22.4 Hz), 55.4, 53.0, 52.3, 50.1, 42.2, 36.6, 33.5, 29.5, 29.0, 24.7, 24.3.

^{19}F NMR (376 MHz, DMSO-d_6, δ): -104.6.

HRMS-ESI (m/z) calc'd for $C_{23}H_{35}FN_7O_9S_2$ $[M+H]^+$, 636.1922; Found 636.1902, deviation: 3 ppm.

4.5.3. Step 3. ^{18}F-Labeling of Peptide 4.7

[^{18}F]Fluoride decays by positron emission and represents a radiological hazard. Solutions that contain [^{18}F]fluoride must be handled in an approved radiochemistry facility by trained personnel following appropriate institutional radiation safety guidelines including ALARA principles. Depending on the amount of radioactivity used, working with [^{18}F]fluoride has to be conducted with proper shielding, such as in a hot cell or behind a lead-reinforced shield to minimize radiation exposure to the researcher. A Geiger counter should be turned on for live monitoring of radioactivity within the laboratory as well as to monitor all personnel coming/going from the facility. Appropriate PPE, including dosimeters, must be worn at all times and the radiation exposure to all personnel must be closely monitored. Working with fluorine-18 is time sensitive as it is a radioisotope with a half-life of 109.8 min. Before starting the protocol, all materials and equipment (HPLC, heating block, etc) should be prepared in advance as described and ready for use.

MATERIALS

Reagents

- Uronium precursor **4.2**
- Fluoro-4-(vinylsulfonyl)benzene **^{19}F-4.1** (CAS no. 28122-14-7, Enamine Building Blocks, >95.0%, cat. No. EN300-115569; alternatively, **^{19}F-4.1** can be prepared from 4-fluorobenzenethiol as described in **section 4.6.2**
- Peptide conjugate reference standard **^{19}F-4.8**
- H-Arg-Gly-Asp-Cys-OH trifluoroacetate salt **4.7** (CAS no. 109292-46-8, Bachem, cat. No. H-3156)
- Borate Buffer (0.5 M Borate buffer, pH 8.5, VWR, cat. No. AAJ60803-AK)
- Methanol (CAS no. 67-56-1, Sigma-Aldrich, cat. No. 322415-100ML, anhydrous 99.8%)
- [^{18}F]Fluoride in water (from an in-house cyclotron or purchased and delivered from a supplier)
- 2-Butanone (CAS no. 78-93-3, Fisher Scientific, cat. No. M209-500, Certified ACS)
- Ethanol (CAS no. 64-17-5, Sigma-Aldrich, cat. No. 459836-100ML, 200 proof, anhydrous, ≥99.5%)
- Diethyl ether (CAS no. 60-29-7, Fisher Scientific, cat. No. E134-4)
- Acetonitrile (CAS no. 75-05-8, Fisher Scientific, cat. No. A998-4, HPLC grade)
- Ultrapure water system (18 Megaohm, Milli-Q system containing a Biopak Polisher cat. No. CDUFBI001, MilliporeSigma)
- Trifluoroacetic acid (CAS no. 76-05-1, Sigma-Aldrich, cat. No. 302031-100ML, HPLC grade)
- Potassium oxalate monohydrate (CAS no. 6487-48-5, Alfa Aesar, cat. No. 13452-22, ACS, 98.5-101%)

Equipment

- Green solid top polypropylene screw caps, TFE Septa, 15x45mm, 13-425 Thread (Chemglass Life Sciences, cat. No. CG-895-02)
- 1-dram borosilicate reaction vials (Chemglass Life Sciences, cat. No. CG-4900-01)
- 20 mL scintillation vial (Chemglass Life Sciences, cat. No. CG-4900-04)
- 50 mL centrifuge tube (Fisher Scientific, cat. No. 14-432-22)
- 2 mL microcentrifuge tube (Fisher Scientific, cat. No. 05-407-34)
- TLC silica gel plates (Fisher Scientific, cat. No. 02-003-912)
- Oasis® HLB plus short (Waters Corporation, cat. No. 186000132),
- Chromafix 30-PS-HCO_3 cartridges (ABX, cat. No. 00260110)
- HPLC System with a UV and gamma detector (Knauer Smartline HPLC system)
- HPLC column (Phenomenex C18 Luna 5µ 100Å, 4.6 x 250 mm, for analytical analysis and Phenomenex C18(2) Luna 10µ 100Å 10 x 250 mm for semi-preparative purification)
- Hamilton microliter syringes (Fisher Scientific, 250 µL, 100 µL, 50 µL, 10 µL, cat. No. 14-685-204, 14-685-184)
- Heating block for 1-dram vials

- Magnetic stirrer hot plate (Chemglass Life Sciences)
- Analytical balance (Mettler Toledo^{TM} Excellence XSR Analytical Balance)
- Magnetic stir bar (Fisher Scientific, cat. No. 22-067645)
- Polypropylene syringe (Fisher Scientific, 10 mL, 5 mL, 3 mL, 1 mL, cat. No. 03-377-23, 03-377-22, 03-377-21, 03-377-20)
- Disposable syringe needles (Fisher Scientific, cat. No. 14-840-93 and 14-840-97)
- Rotary evaporator (Büchi)
- Fume hood with lead shielding or hot cell
- Shielded area to perform elution step
- Ion chamber (Capintec dose calibrator, Capintec, Inc.)
- Radio-TLC scanner (Raytest Beta Detector GMC)
- Sonicator (Branson 3510 Ultrasonic Cleaner)
- ELIXYS radiochemical synthesizer (Sophie biosciences)

Equipment setup

Instruments used for measuring radioactivity should be properly maintained and calibrated via routine quality control procedures.

HPLC for analytical analysis

Turn on the instrument and allow the detectors to warm up for 45 min. Degas eluent A and eluent B. Purge the lines for eluent A and B to remove any air bubbles or residual solvent. Equilibrate the reverse-phase HPLC column by flowing A:B = 95:5 eluent through the column at a flow rate of 1.0 mL/min for 30 min. before use. Confirm the flow is steady and the back pressure is consistent.

HPLC for semi-preparative purification

Turn on the instrument and allow the detectors to warm up for 45 min. Degas eluent A and eluent B. Purge the lines for eluent A and B to remove any air bubbles or residual solvent. Equilibrate the reverse-phase HPLC column by flowing A:B = 95:5 eluent through the column at a flow rate of 4.0 mL/min for 30 min. before use. Confirm the flow is steady and the back pressure is consistent.

Radio-TLC scanner

Turn on the instrument and allow the detector to warm up for 60 min. Before use, run a background scan to confirm the scanner is clean with no radioactivity contamination.

Cartridge preconditioning

Oasis® HLB plus short LP cartridges were preconditioned by sequentially pushing absolute ethanol (5 mL) and water (10 mL) through the cartridge. For this, load a 10-mL polypropylene syringe with 5 mL of ethanol, attach the cartridge to the barrel of the syringe and push the solution through the cartridge with the plunger. Remove the cartridge from the syringe and repeat this process with 10 mL of water. Chromafix 30-PS-HCO_3 cartridges were preconditioned by sequentially pushing a potassium oxalate monohydrate solution (3 mL) and water (2 mL) through the cartridge, using a 5 mL and 3 mL polypropylene syringe respectively, following the same process described above.

Heating block

Place the heating block on the magnetic stir/hot plate inside a well-ventilated, lead-shielded chemical fume hood. Turn on the heating unit to maintain a temperature of 130 °C.

Reagent setup

HPLC Eluent

Solvent A = 0.1% CF_3CO_2H in water, Solvent B = 0.1% CF_3CO_2H in acetonitrile.

Add 1 mL trifluoroacetic acid to 999 mL water (for solvent A) or 999 mL acetonitrile (for solvent B) and store in an HPLC borosilicate glass bottle fitted with a two-port screw cap, sonicating for 30 min to degas before using.

TLC Eluent

Prepare a 95:5 acetonitrile:water stock solution by adding 150 μL water to 2.85 mL acetonitrile.

Potassium oxalate monohydrate solution

Prepare a stock solution by weighing 40 mg of potassium oxalate monohydrate in a 50 mL centrifuge tube and adding 40 mL of water to the vial. Gently mix to ensure the salt completely dissolves in solution.

Deoxyfluorination reaction solvent

Prepare a stock solution by adding 18 mL of 2-butanone and 1.8 mL of ethanol to a 20-mL scintillation vial. Gently mix vial contents, agitating by hand, to ensure homogeneity.

[^{18}F]Fluoride

No-carrier-added ^{18}F-fluoride was produced from water 97% enriched in ^{18}O (Sigma-Aldrich) by the nuclear reaction ^{18}O(p,n)^{18}F using a Siemens RDS-112 cyclotron at 11 MeV using a 1 mL tantalum target with havar foil at the UCLA Ahmanson Biomedical Cyclotron Facility (BMC) of the Ahmanson Translational Imaging Division. The produced ^{18}F-fluoride in water was transferred from the cyclotron target by helium push into a septum-capped glass vial. The vial was kept behind a lead shield in a lead-lined container.

4.5.4. Manual ^{18}F-Labeling Protocol

Small quantities of radioactivity are initially used for experimental studies and are conducted via a manual process to verify that the radiochemical method is successful. In this case, “small scale”

refers to the use of smaller quantities (<15 mCi) of radioactivity rather than a reflection of the amount of labeling precursor. For the purpose of *in vivo* PET imaging studies, larger doses of radioactivity are needed, and the protocol must be performed via an automated procedure (**section 4.6.5**).

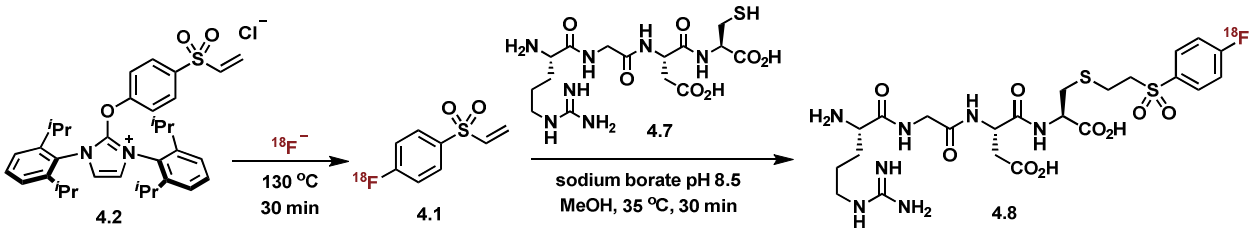

Scheme 4.1. ^{18}F-Deoxyfluorination of the labeling precursor and subsequent chemoselective conjugation to H-Arg-Gly-Asp-Cys-OH peptide **4.7**.

Procedure

1. Weigh 5.0 mg (8.2 µmol) labeling precursor **4.2** into a 2 mL microcentrifuge tube.
2. Add 1.0 mL of the butanone:ethanol (10:1) solvent mixture and shake to ensure precursor **4.2** dissolves completely
3. Using a 5 mL polypropylene syringe fitted with a disposable needle, insert the needle into a 5 mL borosilicate V-vial located in the lead-lined container (pig) and draw up 2.5 mL of aqueous [^{18}F]fluoride containing 15 mCi of radioactivity.
4. Remove the needle and connect the polypropylene syringe containing aqueous [^{18}F]fluoride to the preconditioned Chromafix 30-PS-HCO_3 anion exchange cartridge. Slowly, over 20–30 seconds, push the [^{18}F]fluoride solution through the anion exchange cartridge collecting the [^{18}O]water in a 50 mL centrifuge tube (***Figure 4.6a***). The [^{18}F]fluoride is trapped on the cartridge with >95% efficiency. Using a 5 mL polypropylene

syringe, fill the syringe with 2 mL ultrapure water at ambient temperature, connect the barrel of the syringe to the anion exchange cartridge and push the water through the cartridge, in a period of ~20 seconds. Ensure that the anion exchange cartridge is fitted securely to the luer slip nozzle of the syringe before pushing the [^{18}F]fluoride solution through the cartridge to avoid over pressuring the system and ejecting the cartridge.

5. Using a 10 mL polypropylene syringe, fill the syringe with air by pulling back the plunger to its maximum capacity. Connect the barrel of the syringe to the anion exchange cartridge and push air through the cartridge by pressing on the plunger, for ~3 seconds. Remove the syringe from the cartridge. Repeat this process two more times to remove excess water from the cartridge (***Figure 4.6b***). ^{18}F-Deoxyfluorination proceeds less efficiently in the presence of water. For the deoxyfluorination to proceed efficiently, it is important to remove excess water from the cartridge.

6. Using a 5 mL polypropylene syringe fitted with a disposable needle, draw up 2 mL of the butanone:ethanol (10:1) solvent mixture and push the solution through the anion exchange cartridge collecting the waste in a 50 mL centrifuge tube, in a period of ~20 seconds. Remove excess solvent from the cartridge by repeating step 5 (***Figure 4.6b***).

7. Using a 1 mL polypropylene syringe, draw up the solution of labeling precursor prepared in step 2 and attach the barrel of the syringe to the anion exchange cartridge. Slowly, over 20–30 seconds, push the solution through the anion exchange cartridge to elute [^{18}F]fluoride from the cartridge into a 4 mL borosilicate reaction vial containing a magnetic stir bar (***Figure 4.6c*****).** About 84% of the radioactivity initially placed on the anion exchange column should be found in the borosilicate reaction vial.

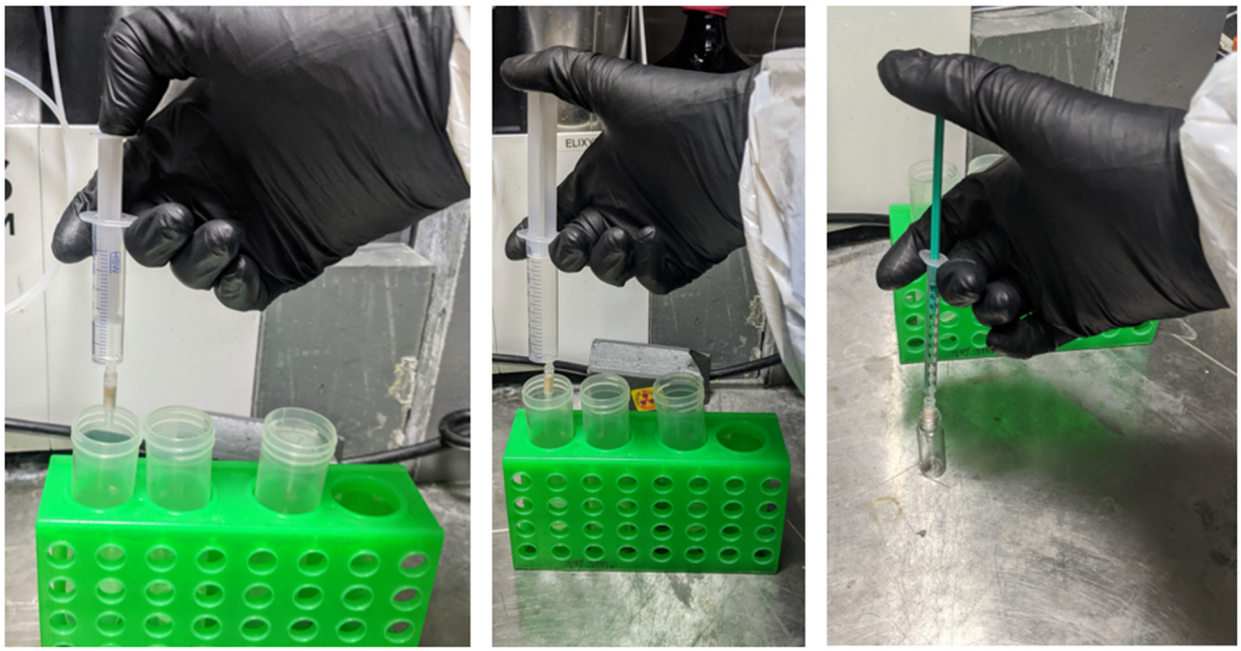

Figure 4.6. Photographs of the ^{18}F-deoxyfluorination protocol. a) Aqueous [^{18}F]fluoride is pushed through the Chromafix 30-PS-HCO_3 anion exchange cartridge (step 4); b) Excess water is removed from the cartridge (step 5); c) The labeling precursor is passed through the cartridge to elute [^{18}F]fluoride (step 7). Photographs were taken in a hot cell but without the presence of radioactivity.

8. Seal the borosilicate reaction vial with a Teflon lined cap and place the vial in a heating block heated to 130 °C for 30 min with stirring (***Figure 4.7a***).
9. Remove the reaction vial from the heating block and let the reaction mixture cool to room temperature. Set the heating unit to maintain a temperature of 55 °C.
10. Using a 5 mL polypropylene syringe fitted with a disposable needle, draw up the reaction mixture and transfer it to a 50 mL centrifuge tube containing 20 mL water.

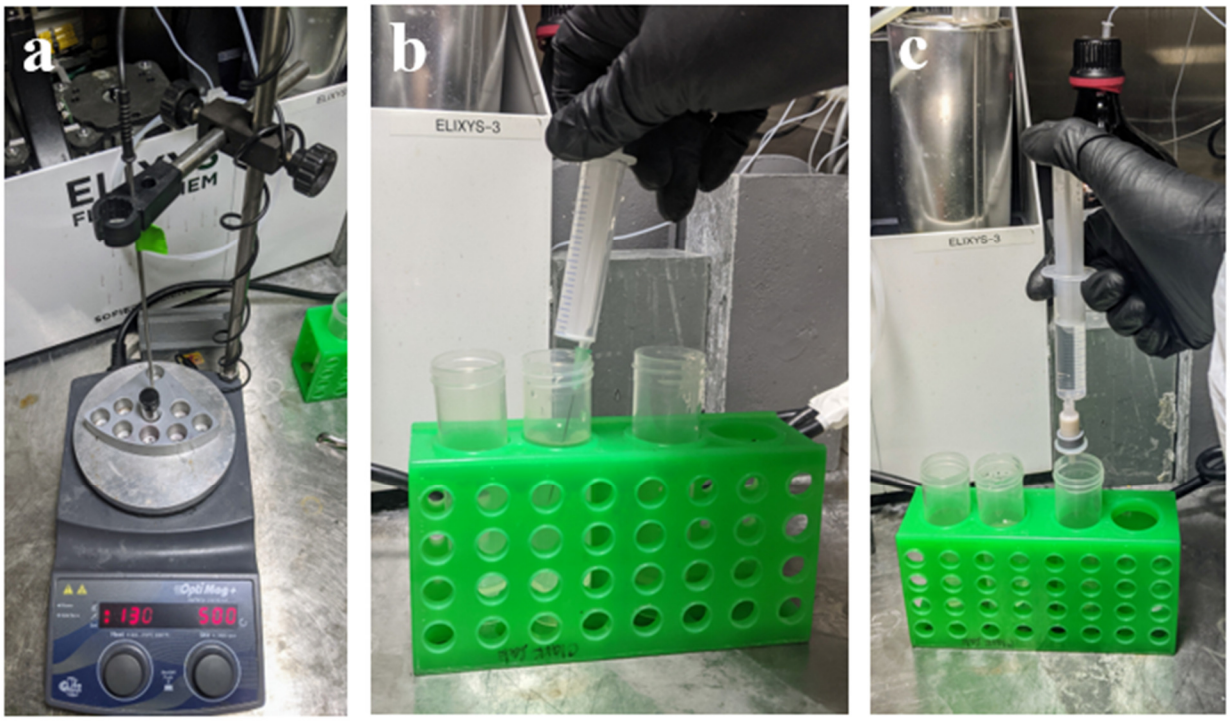

Figure 4.7 Photographs of the ^{18}F-deoxyfluorination protocol. a) The reaction vial is sealed and heated to 130 °C (step 8); b) The reaction mixture/water is drawn up in a syringe (step 11); c) The reaction mixture/water is passed through the Oasis HLB plus short cartridge to elute unreacted [^{18}F]fluoride (step 11). Photographs were taken in a hot cell but without the presence of radioactivity.

11. Using a 10 mL polypropylene syringe fitted with a disposable needle, draw up 10 mL of the contents of the centrifuge tube in step 10 (***Figure 4.7b***). Remove the needle from the syringe and attach the barrel of the syringe to the Oasis HLB plus short cartridge. Push the solution through the HLB cartridge in a dropwise fashion, collecting the waste in a 50 mL centrifuge tube (***Figure 4.7c***). Reaffix the needle to the syringe and repeat drawing up the reaction contents and passing them through the Oasis HLB plus short cartridge in a dropwise fashion to trap **[^{18}F]4.1** on the cartridge with >90% efficiency.

12. Wash the Oasis HLB plus short cartridge with 5 mL of water and remove excess solvent from the cartridge by repeating step 5.
13. Using a 5 mL polypropylene syringe fitted with a disposable needle, draw up 2 mL of the diethyl ether and attach the barrel of the syringe to the HLB cartridge. Push the ether through the cartridge in a dropwise fashion to elute **[^{18}F]4.1** from the cartridge into a clean 4 mL borosilicate scintillation vial containing a magnetic stir bar.
14. Remove 50 µL for evaluation of product identity and purity using an analytical HPLC column attached to a radioactivity and a UV-detector.

The retention time of the **^{18}F-4.1** peak is determined prior to the radiolabeling experiment by injection of an authentic reference standard, **^{19}F-4.1**, onto the HPLC using the same mobile phase. The HPLC method should be as short as possible while ensuring a clean separation of the [^{18}F]aryl fluoride from any other impurities observed in the UV trace of the crude reaction mixture. Product identity is determined by comparing the γ-trace of **^{18}F-4.1** with the UV-trace of **^{19}F-4.1** via coinjection (***Figure 4.15***).

15. Evaporate the diethyl ether by placing the vial in a heating block heated to 55 °C for 3 min with stirring (***Figure 4.8a***).
16. Remove the vial from the heating block and set the heating unit to maintain a temperature of 35 °C.
17. Weigh 3.0 mg (6.5 µmol) H-Arg-Gly-Asp-Cys-OH peptide **4.7** into a 2 mL microcentrifuge tube. If working with peptides in limited supply, 2.0 µmol peptide loading is sufficient to afford the radiolabeled conjugate in high RCY.

Figure 4.8. Photographs of the ^{18}F-deoxyfluorination protocol. A) Diethyl ether is evaporated at 55 °C (step 15); b) Peptide solution is added to the dried, ^{18}F radiosynthon (step 19); c) The reaction vial is sealed and heated to 35 °C (step 20). Photographs were taken in a hot cell but without the presence of radioactivity.

18. Using a 1 mL polypropylene syringe fitted with a disposable needle, add 250 µL of methanol followed by 250 µL sodium borate buffer pH 8.5 to the microcentrifuge tube. Place the tube in a sonicator, with the water bath at ambient temperature, and sonicate for 5 mins. The solubility of individual peptides used in this protocol can vary significantly. For the peptide conjugation to proceed efficiently and provide high RCY, it is important to sonicate the vial containing the peptide solution for 5–10 min at 24 °C.

19. Using a 1 mL polypropylene syringe fitted with a disposable needle, draw up the peptide solution prepared in step 18 and add it to the **^{18}F-4.1** prepared in step 17 (***Figure 4.8b***).
20. Seal the borosilicate reaction vial with a Teflon lined cap and place the vial in a heating block heated at 35 °C for 30 min with stirring (***Figure 4.8c***).
21. Dilute the reaction mixture with 500 μL sodium borate buffer and withdraw the entire solution into a Hamilton microliter syringe. Inject the syringe contents onto a semi-preparative reverse-phase HPLC column and initiate the HPLC program using the following program: A:B = 95:5 for 5 minutes then a gradient A:B = 95:5 to A:B = 45:55 over 15 minutes followed by 30 minutes of A:B = 45:55. Flow rate = 4 mL/min. Monitor the radioactivity detector for the appearance of the purified **4.8** product. If solids are detected in the reaction mixture, it must be filtered prior to injection onto the HPLC to avoid clogging. Over-pressurization of the HPLC column can occur due to injection of the solvent mixture onto the HPLC, and care must be taken to monitor the column pressure during the injection phase.
22. Collect the purified product in a 50 mL centrifuge tube and remove 50 μL for analysis of the purity of the product using an analytical HPLC column attached to a radioactivity and a UV-detector (***Figure 4.17***).
23. If desired, determine the molar activity of the isolated **4.8** by determining the intensity of the UV signal at the retention time at which to ^{18}F-labeled peptide is observed. Compare the intensity of the UV signal to the standard curve of UV intensity versus amount of injected material (***Figure 4.16***).

The location of the isolated **4.8** peak is determined prior to the radiolabeling experiment by injection of an authentic reference standard, **^{19}F-4.8**, of the peptide conjugate onto the HPLC using the same mobile phase. Product identity is determined by comparing the γ-trace of **4.8** to the UV-trace of **^{19}F-4.8** via coinjection (***Figure 4.15***). Note: a fixed delay by 0.10 min is present due to the spatial separation between the UV and radioactivity detectors, causing the γ-trace to be slightly offset.

Table 4.2. Troubleshooting table.

Problem	Possible reasons	Solution
Low levels of radioactivity trapped on the HLB cartridge after ^{18}F-fluorination	Inefficient trapping of the ^{18}F radiosynthon during cartridge purification	Increase the volume of water added to the reaction mixture prior to passing the contents through the HLB cartridge
Incomplete conjugation of **[^{18}F]4.1** to peptide	Poor solubility of the peptide substrate in the solvent system	Change the organic solvent to DMF or DMSO; Change the buffer to HEPES buffer pH 7.3; Perform sonication of peptide solution at slightly elevated temperature (30 – 40 °C)
Incomplete conjugation of **[^{18}F]4.1** to peptide	Oxidation of peptide substrate due to improper or lengthy storage	Use a peptide with >95% purity
Impure ^{18}F-labeled peptide obtained	The HPLC method or column is not suitable for the separation of the labeled peptide product	Change the mobile phase or gradient or switch to a different HPLC column
Low levels of radioactivity present in the reaction vial compared to amount loaded on anion exchange cartridge	Inefficient elution of ^{18}F from the anion exchange cartridge	Increase the amount of labeling precursor and solvent used in the elution step, decrease the rate at which the solution is passed through the anion exchange cartridge, flip the cartridge for "reverse elution"
Poor peak resolution on radio-HPLC trace	Insufficient amount of radioactivity loaded on HPLC	Ensure that a sufficient amount of radioactivity is eluted off the anion exchange column per experiment so that a trace of acceptable resolution can be obtained

4.5.5. Automated ^{18}F-Labeling of 4.7 Including Purification and Reformulation

After successful testing of the radiolabeling procedure using small quantities of radioactivity, the preparation of larger amounts of ^{18}F-labeled peptide for the purposes of PET imaging is commonly desired. The amounts of labeling precursor are the same for small- and large-scale synthesis, but the quantity of radioactivity is significantly increased. For large-scale synthesis minimization of radiation exposure to the researcher requires a different work-flow and the employment of an automated synthesis module located in a well-shielded hot cell.

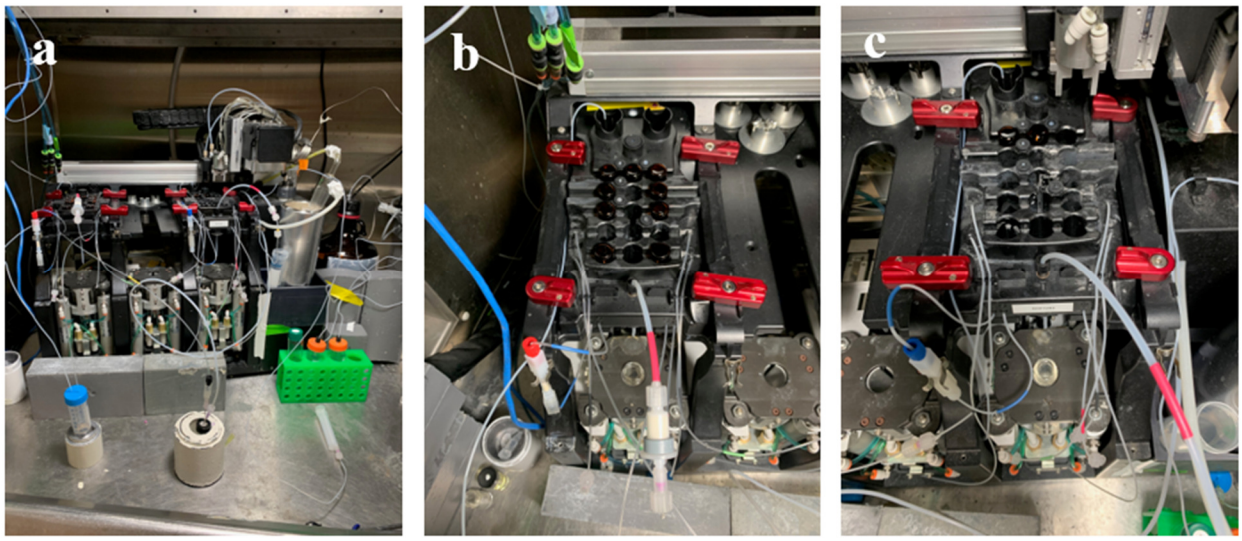

Figure 4.9. Photographs of the ELIXYS radiochemical synthesis module setup. a) General automation setup in the hot cell; b) First cassette setup; c) Second cassette setup.

Procedure for automated radiosynthesis

Preparation of the ELIXYS radiochemical synthesis module

- Clean two ELIXYS automated radiosynthesizer cassettes by flushing each flow pathway with 10 mL ultrapure water (18 Megaohm, Milli-Q system containing a Biopak Polisher

cat. No. CDUFBI001, MilliporeSigma) followed by 10 mL acetonitrile (CAS no. 75-05-8, Fisher Scientific, cat. No. A998-4, HPLC grade), using 12 mL syringes for each solvent respectively. Dry all flow pathways by flowing a nitrogen stream through the pathways for ~30 seconds, at three distinct intervals, for a total of ~1.5 min. The inlet and outlet tubing should be connected directly together during the cleaning. During the cleaning protocol for ELIXYS cassettes, ensure there are no leaks in the joints, fittings, and tubing of the cassette.

- Clean 11 brown vials, 2 Glass V-vials and 2 stir bars by thoroughly rinsing with a soap solution (10 – 12 grams of powder detergent in 16 oz water, Alconox, cat. No. 1104-1), followed by rinsing with clean water. All items should undergo a final rinse with acetone and be dried in a heated oven overnight. The commercial brown vials that store reagents in the cassettes must be manually cleaned following the protocol. Direct use, without cleaning, will cause [^{18}F]fluoride elution from the Chromafix cartridge during the water washing (step 3, below) due to trace contaminants resulting from the manufacturing of the brown vials.
- Clean HPLC loop and collection lines: Fill a 12 mL syringe with water and pass the water through the injection loop to a waste container. Use the empty 12 mL syringe to push air through the loop (2x) to remove remaining water in the loop. To clean the collection line, run the HPLC and let the HPLC solvents flow through each collection line for 2 min.
- Connect two cassettes by transfer line (***Figure 4.10***).
- Connect the second cassette and HPLC injection loop by transfer line (***Figure 4.10***).

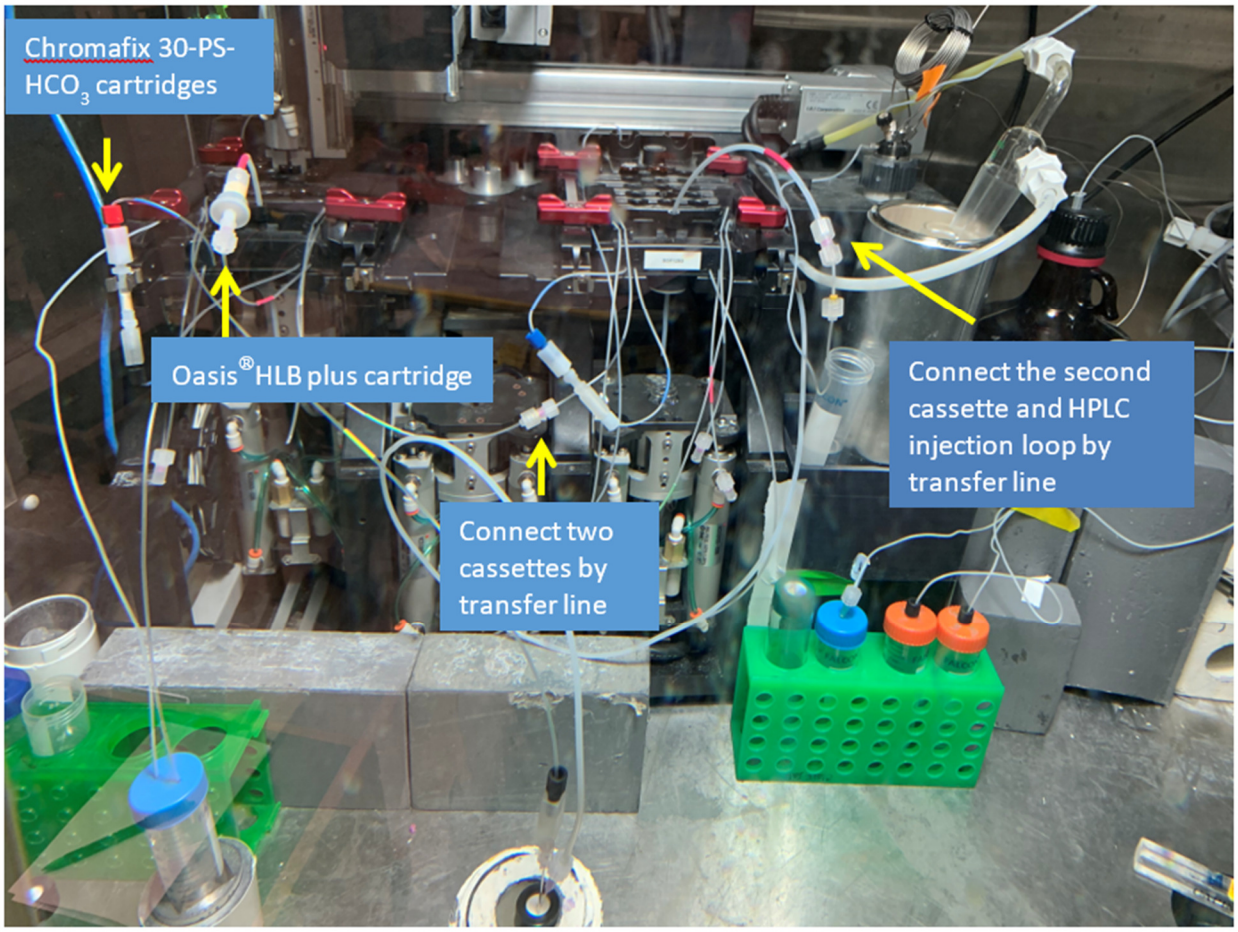

Figure 4.10. Photographs of the ELIXYS radiochemical synthesis module setup.

Modified code to be inputted into the ELIXYS software:

For the “ELUTE ISOTOPE” operation, solvent flow is directed into the reaction vial. In our protocol, several washing steps are included prior to [^{18}F]fluoride elution. For these steps, solvent flow needs to be redirected into the waste container. A piece of code was modified and inputted into the software to alter the solvent flow to the waste line. This modified “ELUTE ISOTOPE" operation is used in steps 3–5.

Website to input code:

http://192.168.100.101:5000/command_line.html

Code to submit:

{"request":"calibrate","request_data":{"calibrate":{"name": "reactors", "type": "control", "parameters":{"control_type": "stopcock", "reactor": 0, "stopcock": 2, "position": "counterclockwise"}}}}

MATERIALS

Equipment

- 11 Brown vials (Voigt Global Distribution, cat. No. 62413P-2)
- Rubber septa for brown vials (Wheaton, cat. No. 224100-072)
- Crimp cap for brown vials (Wheaton, cat. No. 224177-01)
- 3 Glass V-vials (Wheaton, cat. No.W986259NG)
- 2 Stir bars (10x3mm, VWR, cat. No. 58948-375)
- ELIXYS cassette-based radiochemical synthesis module (Sofie Biosciences)

Reagents

All reagents listed under Cassettes 1 and 2 are stored in pre-washed brown vials and sealed with a septum and crimp cap. All solvents and cartridges used in the automated protocol are from the same sources as those used in the manual protocol (listed above), unless stated otherwise.

Glass V-vial (source vial):

- 1 mL H_2O (CAS no. 7732-18-5, Sigma-Aldrich, cat. No. 00612-2.5L)

Cassette 1: (reagents used in sequence in the automation process)

- 2 mL H_2O (CAS no. 7732-18-5, Sigma-Aldrich, cat. No. 00612-2.5L)
- 2 mL acetonitrile (CAS no. 75-05-8, Sigma-Aldrich, cat. No. 271004-100mL, anhydrous 99.8%)
- 2 mL freshly prepared 2-butanone/ethanol (10:1)
- 5 mg uronium precursor **4.2** in 2-butanone/ethanol (1 mL, 10:1)
- 3 mL H_2O (CAS no. 7732-18-5, Sigma-Aldrich, cat. No. 00612-2.5L)
- 2 mL H_2O (CAS no. 7732-18-5, Sigma-Aldrich, cat. No. 00612-2.5L)
- 3mL H_2O (CAS no. 7732-18-5, Sigma-Aldrich, cat. No. 00612-2.5L)
- 2 mL H_2O (CAS no. 7732-18-5, Sigma-Aldrich, cat. No. 00612-2.5L)
- 2mL diethyl ether (CAS no. 60-29-7, Thermo Scientific™, cat. No. AC615080040)

Cassette 2:

- Glutathione (1.5 mg) in 1:1 methanol/sodium borate buffer, pH 8.5 (0.65 mL)
- 2 mL H_2O (same as Cassette 1)

1. [^{18}F]fluoride in [^{18}O]H_2O was collected into the source vial from a cyclotron dispenser.
2. Aqueous [^{18}F]Fluoride (1 mL) was transferred from the source vial to the ELIXYS via nitrogen gas push, at between 3 – 5 psi, and was trapped onto a Chromafix 30-PS-HCO_3 using the “TRAP ISOTOPE” operation. Excess water was removed by nitrogen gas push, at 25 psi, for 3 minutes.
3. The cartridge trapped [^{18}F]fluoride was washed with water (2 mL) by nitrogen push at between 3 – 5 psi, using the modified “ELUTE ISOTOPE” operation. Excess water was removed by nitrogen gas push, at 25 psi, for 3 minutes.
4. Anhydrous acetonitrile (2 mL) was delivered through the same fluid pathway of the cassette by nitrogen push, at between 3 – 5 psi, using another modified “ELUTE ISOTOPE” operation. Excess solvent was removed by nitrogen gas push, at 25 psi, for 3 minutes.

5. 2-Butanone/ethanol (2 mL, 10:1) was delivered through the same fluid pathway by nitrogen push, at between 3 – 5 psi, using another modified "ELUTE ISOTOPE" operation. Excess solvent was removed by nitrogen gas push, at 25 psi, for 7–8 minutes.
6. The trapped [^{18}F]fluoride was eluted into a V-vial reactor 1, under the normal "ELUTE ISOTOPE" operation, with a solution of uronium precursor **4.2** (5 mg) in 2-butanone/ethanol (1 mL, 10:1) and a pressure of 1.5 psi.
7. Reactor 1 vial was sealed against the ELIXYS gasket and heated at 130 °C for 30 min with stirring.
8. Reactor 1 vial was cooled to 35 °C. Two aliquots of H_2O (3 mL and 2 mL) were added sequentially to the reaction mixture via nitrogen push at 5 psi and the solution was stirred for 15-20 seconds.
9. The contents in reactor 1 vial were passed through the HLB cartridge via nitrogen push at 5 psi (stir is "on") to trap the **^{18}F-4.1** product while unreacted [^{18}F]fluoride passed through to a waste container.
10. The HLB cartridge was rinsed by adding another two aliquots of H_2O (3 mL and 2 mL) to the reactor 1 vial and passing it through the HLB cartridge via nitrogen push by following the same processes of steps 8 and 9.
11. The HLB cartridge was flushed with nitrogen at 25 psi for 5 min.
12. To the reactor 1 vial was added Et_2O (2 mL, 3 psi driving pressure) and the ether was stirred for 20 sec. The ether was transferred through the HLB cartridge via nitrogen push at 1.5 psi into a clean V-vial in reactor 2 below the second cassette.
13. Reactor 2 vial was heated at 45 °C under 0 psi with stirring for 8 min to remove half of the volume, leaving ~1 mL in the vial.

14. Reactor 2 vial was cooled to 35 °C. A solution of L-glutathione (1.5 mg) in methanol and pH 8.5 sodium borate buffer (1:1, 0.65 mL) was added to the reactor 2 vial. The vial was sealed against the ELIXYS gasket and heated at 35 °C for 30 min.
15. H_2O (2 mL) was added to the reactor 2 vial and the reaction mixture was transferred to a semi-preparative HPLC by remote loading into the HPLC loop provided on the ELIXYS and injecting the contents into the HPLC column. HPLC purification was initiated using the following program: A:B = 95:5 for 5 minutes then a gradient A:B = 95:5 to A:B = 70:30 over 50 minutes. Flow rate = 3 mL/min.
16. Appearance of the purified conjugated product on the radio-HPLC trace was monitored. The purified product was collected in a 50 mL centrifuge tube. An aliquot (50 µL) of isolated product was removed for HPLC analysis of the purity of the product using an analytical HPLC column attached to a radioactivity and a UV-detector.

Conclusion: For the fully automated process, the ^{18}F-labeled peptide conjugate **^{18}F-4.8** FVSB-GSH was isolated in 20% ± 5% decay-corrected radiochemical yield (n = 3) with a molar activity of 1.2 Ci · µmol^{-1} (44 GBq · µmol^{-1}).

Table 4.3. Troubleshooting table

Problem	Possible reasons	Solution
Poor elution efficiency from Chromafix 30-PS-HCO_3 cartridges	The uronium precursor solution is passed too quickly through the cartridge	Adjust N_2 flow pressure to a lower psi. For our Elixys instrument, 1.5 psi is the lowest psi we can use.
Radioactivity trapped on the Chromafix 30-PS-HCO_3 cartridge was eluted during the water wash step	Impurity inside water source	Use HPLC grade water and pre-clean the commercial brown vials with a soap solution (as described above) prior to use
Low levels of radioactivity measured on the HLB cartridge after solvent exchange	Inefficient trapping of the ^{18}F-labeled vinyl sulfone during cartridge purification	Increase the volume of water (5mL) added to the reaction mixture prior to passing the contents through the HLB cartridge And apply "stir" command during water addition step to obtain uniform solution
Radioactivity was lost during evaporation of diethyl ether	^{18}F-FVSB is volatile and can also evaporate during this step if the parameters are too harsh	Perform mild evaporation. Decrease the temperature to 40 °C and carefully watch that the reactor vial does not go completely dry
Leaking during solvent elution through the cartridges	Loose fitting and connections	Check fittings and joints before experiment starts
Undesirable byproduct was obtained instead of the desired ^{18}F-FVSB	Residual water is present during the uronium precursor elution	The Chromafix 30-PS-HCO_3 cartridge must be thoroughly dried prior to ^{18}F-fluoride elution. Remove excess water by nitrogen gas push, at 25 psi, for extended time. Or increase the nitrogen pressure. Use anhydrous acetonitrile for the cartridge washing step.
Impure ^{18}F-labeled peptide obtained	The HPLC method or column is not suitable for the separation of the labeled peptide product	Adjust the mobile phase or elution gradient or switch to a different HPLC column

4.6. Experimental Section

4.6.1. Synthesis and Characterization of Phenol 4.3

The synthesis of intermediate compounds **4.10** and **4.11** are adapted from **reference 22**. Spectra for the intermediates were previously reported.[22]

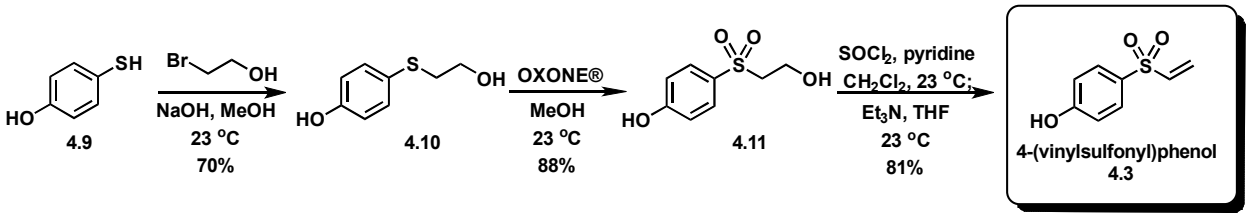

Figure 4.11. Synthesis of 4-(vinylsulfonyl)phenol (**4.3**).

Reagents

- 4-Mercaptophenol **4.9** (CAS no. 637-89-8, Alfa Aesar, 97%, cat. No. AAL0442906)
- Methanol (CAS no. 67-56-1, ACS reagent, ≥ 99.8%, Fisher Scientific, cat. No. A412-4)
- 2-Bromoethanol (CAS no. 540-51-2, >95.0%, TCI America, cat. No. B0590)
- NaOH (CAS no. 1310-73-2, ACS reagent, Fisher Scientific, cat. No. S318-500)
- Diethyl ether (CAS no. 60-29-7, ≥99%, Fisher Scientific, cat. No. E138-20)
- Sodium bicarbonate (CAS no. 144-55-8, $NaHCO_3$, Fisher Scientific, cat. No. S233-10)
- Sodium sulfate (CAS no. 7757-82-6, Na_2SO_4, Sigma-Aldrich, cat. No. SX0760-10)
- Ethyl acetate (EtOAc, CAS no. 141-78-6, ≥99.5%, Fisher Scientific, cat. No. E145-20)
- Hexane (CAS no. 110-54-3, ≥98.5%, Fisher Scientific, cat. No. H292-20)
- OXONE® (CAS no. 70693-62-8, Alfa Aesar, cat. No. 89892-22)
- Sodium hydrogen sulfite (CAS no. 7631-90-5, Certified ACS, Fisher Scientific, cat. No. S654-500)
- Pyridine (CAS no. 110-86-1, 99%, Oakwood, cat. No. 005154)
- Dichloromethane (CAS no. 75-09-2, Fisher Scientific, cat. No. D151-4)
- Thionyl chloride (CAS no. 7719-09-7, ≥99%, Sigma-Aldrich, cat. No. 230464)
- Tetrahydrofuran (THF, CAS no. 109-99-9, ≥99%, Fisher Scientific, cat. No. 397-4)
- Triethylamine (Et_3N, CAS no. 121-44-8, Fisher Scientific, cat. No. O4885)
- Silica-gel (230-400 Mesh, Fisher, cat. No. S825-25)
- TLC plates (TLC Silica gel 60 F_{254} Aluminium sheets 20x20 cm, Supelco. Cat. No. HX91185454)
- $CDCl_3$ (99.8%, Cambridge Isotope Laboratories, cat. No. DLM-7-100)
- DMSO-d_6 (99.9%, Cambridge Isotope Laboratories, cat. No. DLM-10-10)

Procedure

1. Weigh 2.0 g (15.8 mmol) 4-mercaptophenol **4.9** into a 100-mL round-bottom flask containing a Teflon-coated magnetic stir bar. With a polypropylene syringe fitted with a 20-guage disposable needle, add 10 mL of methanol and cool the reaction mixture to -5 °C. With a polypropylene syringe fitted with a 20-guage disposable needle, add an aqueous solution of NaOH (1.0 N, 17.3 mL) dropwise over 30 mins at -5 °C. Prepare a solution of 2-bromoethanol (2.3 mL) in methanol (7 mL) and add the resulting solution dropwise, over 15 min at -5 °C, to the round-bottom flask. Stir the reaction mixture at 23 °C for 21 h. Concentrate the reaction mixture in a rotary evaporator and treat the crude residue with 5 mL of water and 20 mL of diethyl ether. After extraction and phase separation, wash the organic phase with 10 mL of saturated aqueous $NaHCO_3$ and then 10 mL of brine. Dry the organic phase over Na_2SO_4 and remove the solvent under reduced pressure to yield crude product. Purify the crude residue by flash column chromatography on silica-gel (10-30% ethyl acetate in *n*-hexane) to afford **4.10** (1.87 g, 11 mmol, 70% yield) as a white solid.

2. Weigh 1.0 g (5.87 mmol) 4-((2-hydroxyethyl)thio)phenol **4.10** into a 15-mL round bottom flask containing a Teflon-coated magnetic stir bar. With a polypropylene syringe fitted with a disposable needle, slowly add 5 mL of methanol and cool the reaction mixture to 10 °C. Add 5.43 g (8.82 mmol) of OXONE® at 10 °C, over 20 min. Stir the suspension at 23°C (exothermic reaction) for 2 h. Using a Buchner filter funnel equipped with a medium porosity frit, filter the precipitate. Wash the filtrate with a 38- 40% (v/v) aqueous sodium hydrogen sulfite solution (0.5 mL) and adjust the pH of the reaction mixture to ~7.0 by adding 1.0 M aqueous NaOH. Filter the suspension and concentrate the filtrate to dryness

under reduced pressure using a rotary evaporator at approximately 23 °C. Purify the crude residue by flash column chromatography on silica-gel (20-60% ethyl acetate in *n*-hexane) to afford 4-((2-hydroxyethyl)sulfonyl)phenol **4.11** (1.0 g, 5.20 mmol, 88% yield) as a white solid.

3. Weigh 1.0 g (5.19 mmol) 4-((2-hydroxyethyl)sulfonyl)phenol **4.11** into a 25-mL round bottom flask containing a magnetic stir bar. With a polypropylene syringe fitted with a disposable needle, add 6 mL of dichloromethane followed by 0.8 mL (10 mmol) of pyridine at 23 °C. Cool the reaction mixture to 0 °C. With a polypropylene syringe fitted with a disposable needle, draw up 0.64 mL (8.8 mmol) thionyl chloride and add it to a vial containing 5 mL of dichloromethane. With a polypropylene syringe fitted with a disposable needle, draw up the thionyl chloride/dichloromethane solution and add it dropwise, over 15 min, to the reaction mixture in the 25-mL round bottom flask. Stir the reaction at 23 °C for 20 h. Dilute the reaction mixture with 1 mL brine and extract the suspension/contents of the flask. Combine the organic layers and wash them with 2 mL of brine and extract. Repeat and wash the organic layers with brine a second time. Combine the organic layers, add dry Na_2SO_4, and filter using a filter funnel. Concentrate the filtrate to dryness under reduced pressure using a rotary evaporator to afford 4-((2-chloroethyl)sulfonyl)phenol which was used directly without further purification.

4. Weigh 0.8 g (3.6 mmol) 4-((2-chloroethyl)sulfonyl)phenol into a 25-mL round bottom flask containing a Teflon-coated magnetic stir bar. With a polypropylene syringe fitted with a disposable needle, add 8 mL of THF. With a polypropylene syringe fitted with a

disposable needle, draw up 0.76 mL (5.4 mmol) triethylamine and add it to a vial containing 5 mL of THF. With a polypropylene syringe fitted with a disposable needle, draw up the triethylamine/THF solution and add it to the reaction mixture in the 25-mL round bottom flask at 23 °C. Allow the reaction mixture to stir at 23 °C for 24 h. Using a filter funnel, filter the triethylamine hydrochloride salt that precipitates from of the reaction mixture. Concentrate the colorless filtrate to dryness under reduced pressure using a rotary evaporator at approximately 23 °C. Purify the crude solid by flash column chromatography on silica-gel (5-30% ethyl acetate in *n*-hexane) to give 4-(vinylsulfonyl)phenol **4.3** (0.53 g, 2.90 mmol, 81% yield) as a white solid.

Characterization data for 4-(vinylsulfonyl)phenol 4.3:

^{1}H NMR (400 MHz, DMSO-d_6, δ): 10.62 (s, 1H), 7.63 (d, *J* = 8.8 Hz, 2H), 6.97 (dd, *J* = 16.4, 9.6 Hz, 2H), 6.92 (d, *J* = 8.8 Hz, 1H), 6.17 (d, *J* = 16.8 Hz, 1H), 6.04 (d, *J* = 9.6 Hz, 1H).

^{13}C NMR (100 MHz, DMSO-d_6, δ): 162.7, 139.9, 130.4, 129.5, 127.2, 116.5.

HRMS (ESI-TOF) m/z: [M+Na] + Calc'd for $C_8H_8O_3SNa$ 207.0092; Found 207.0084.

Melting point: 64 – 66 °C

4.6.2. Synthesis and Characterization of ^{19}F-Reference Standard ^{19}F-4.1. [35, 36]

The synthesis of intermediate compounds **4.13** and **4.14** are adapted from **reference 22**. Spectra for the intermediates were previously reported. [22]

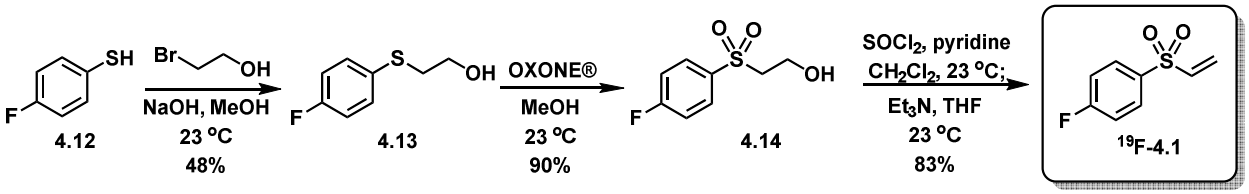

Figure 4.12. Synthesis of ^{19}F reference standard

Reagents

- Chemical reagents used in these steps are identical to those used for the preparation of 4-(vinylsulfonyl)phenol **4.3** (***Figure 4.11***) and reagent details are listed above, in **section 4.6.1**
- 4-fluorobenzenethiol **4.12** (CAS no. 371-42-6, TCI America, >98.0%, cat. No. 50-014-34924)

Procedure

1. Weigh 280 mg (2.19 mmol) 4-fluorobenzenethiol **4.12** (280 mg, 2.19 mmol) into a 4-dram borosilicate vial. With a polypropylene syringe fitted with a 20-guage disposable needle, add 3 mL of methanol and cool the vial to -5 °C. With a polypropylene syringe fitted with a 20-guage disposable needle, add aqueous NaOH (1N, 2.4 mL) in a dropwise fashion, over a period of 15 min and stir the reaction at -5 °C for 1 h. Prepare a solution of 2-bromoethanol (0.3 mL, 2.4 mmol) in methanol (1 mL) and add the resulting solution dropwise, over 10 min at -5 °C, to the 4-dram vial. Allow the vial to warm to room temperature and stir for 21 h at 23 °C. Remove the methanol under reduced pressure using a rotary evaporator at approximately 23 °C. Add 20 mL of diethyl ether and 5 mL of water to the crude residue and extract the organic layer from the aqueous layer. Separate the phases and extract the aqueous layer with diethyl ether again. Combine the organic layers and wash them with saturated aqueous $NaHCO_3$ and brine. Combine the organic layers,

add dry Na_2SO_4, and filter using a filter funnel. Concentrate the filtrate to dryness under reduced pressure using a rotary evaporator and purify the crude residue by flash column chromatography on silica-gel (5-20% EtOAc in *n*-hexane) to obtain 2-((4-fluorophenyl)thio)ethanol **4.13** (0.18 g, 1.05 mmol, 48% yield) as a light yellow oil.

2. Weigh 181 mg (1.05 mmol) 2-((4-fluorophenyl)thio)ethanol **4.13** into a 15-mL round bottom flask containing a Teflon-coated magnetic stir bar. With a polypropylene syringe fitted with a disposable needle, slowly add 4 mL of methanol and cool the reaction mixture to 10 °C. Add 972 mg (1.58 mmol) of OXONE® at 10 °C, over 20 min. Stir the suspension at 23 °C (exothermic reaction) for 2 h. Using a Buchner filter funnel equipped with a medium porosity frit, filter the precipitate. Wash the filtrate with a 38- 40% (v/v) aqueous sodium hydrogen sulfite solution (0.5 mL), dry the filtrate over Na_2SO_4 and concentrate to dryness under reduced pressure using a rotary evaporator to afford crude 2-((4-fluorophenyl)sulfonyl)ethanol **4.14** (0.19 g, 0.95 mmol, 90% yield) as a light yellow oil which was used without further purification.

3. Weigh 190 mg (0.95 mmol) 2-((4-fluorophenyl)sulfonyl)ethanol **4.14** into a 15-mL round bottom flask containing a Teflon-coated magnetic stir bar. With a polypropylene syringe fitted with a disposable needle, add 3 mL of dichloromethane followed by 0.15 mL (1.86 mmol) of pyridine at 23 °C. Cool the reaction mixture to 0 °C. With a microsyringe, draw up 119 µL (1.61 mmol) thionyl chloride and add it to a vial containing 1 mL of dichloromethane. With a polypropylene syringe fitted with a disposable needle, draw up the thionyl chloride/dichloromethane solution and add it dropwise, over 15 min, to the

reaction mixture in the 15-mL round bottom flask. Stir the reaction at 23 °C for 20 h. Dilute the reaction mixture with 1 mL brine and extract the suspension/contents of the flask. Combine the organic layers and wash them with 2 mL of brine and extract. Repeat and wash the organic layers with brine a second time. Combine the organic layers, add dry Na_2SO_4, and filter using a filter funnel. Concentrate the filtrate to dryness under reduced pressure using a rotary evaporator to afford 1-((2-chloroethyl)sulfonyl)-4-fluorobenzene (0.20 g, 0.90 mmol, 94% yield) as a yellow solid. *Note:* 1-((2-chloroethyl)sulfonyl)-4-fluorobenzene is slightly unstable and undergoes spontaneous elimination to afford vinyl sulfone **^{19}F-4.1**, which can be seen in the NMR of this intermediate. For this reason, 1-((2-chloroethyl)sulfonyl)-4-fluorobenzene was taken on to the next step without further purification.

4. Weigh 202 mg (0.9 mmol) 1-((2-chloroethyl)sulfonyl)-4-fluorobenzene into a 15-mL round bottom flask containing a Teflon-coated magnetic stir bar. With a polypropylene syringe fitted with a disposable needle, add 3 mL of THF. With a microsyringe, draw up 187 µL (1.35 mmol) triethylamine and add it to a vial containing 1 mL of THF at 23 °C. With a polypropylene syringe fitted with a disposable needle, draw up the triethylamine/THF solution and add it to the reaction mixture in the 15-mL round bottom flask at 23 °C. Allow the reaction mixture to stir at 23 °C for 1 h. With a polypropylene syringe fitted with a disposable needle, add 1.0 mL of aqueous HCl (1.0 M) to quench the reaction. Add 4 mL of ethyl acetate to the flask and extract the aqueous phase twice using 3 mL of ethyl acetate. Combine the organic layers and wash them with 2 mL of brine and extract. Repeat and wash the organic layers with brine a second time. Combine the organic

layers, add dry Na_2SO_4, and filter using a filter funnel. Concentrate the filtrate to dryness under reduced pressure using a rotary evaporator and purify by flash column chromatography on silica-gel (10-30% EtOAc in *n*-hexane) to afford fluoro-4-(vinylsulfonyl)benzene **^{19}F-4.1** (0.15 g, 0.79 mmol, 88% yield) as a light yellow oil.

Characterization data for fluoro-4-(vinylsulfonyl)benzene ^{19}F-4.1:

^{1}H NMR (400 MHz, $CDCl_3$, δ): 7.91 (dd, *J* = 8.8, 4.8 Hz, 2H), 7.26-7.2 (m, 2H), 6.6 (dd, *J* = 16.4, 10 Hz, 2H), 6.46 (d, *J* = 16.4 Hz, 1H), 6.05 (d, *J* = 10 Hz, 1H).

^{13}C NMR (100 MHz, $CDCl_3$, δ): 165.8 (C-F, 1JC-F = 254.8 Hz), 138.4, 135.6 (C-F, 4JC-F = 3.2 Hz), 130.8 (C-F, 3JC-F = 9.7 Hz), 127.9, 116.8 (C-F, 2JC-F = 22.6 Hz).

^{19}F NMR (376 MHz, $CDCl_3$, δ): -103.4.

HRMS (ESI-TOF) m/z: [M+Na] + Calc'd for $C_8H_7FO_2SNa$ 209.0049; Found 209.0041.

Analytical data

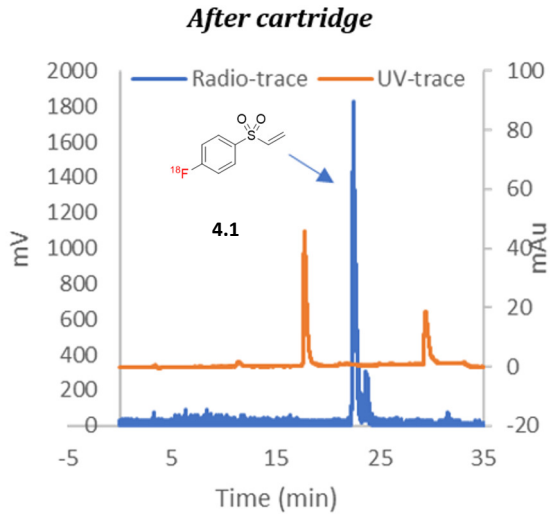

Figure 4.13. Analytical radio-HPLC with 254 nm UV trace (orange) and radioactive trace (blue) of cartridge purified ^{18}F-FVSB **^{18}F-4.1**, obtained in 85% radiochemical purity (RCP).

The cartridge-purified **^{18}F-4.1** is obtained in ~85% radiochemical purity (RCP), determined by radio-HPLC analysis, and can be directly used in the next step without further purification. Alternatively, if the cartridge-purified **^{18}F-4.1** is obtained in less than 80% RCP, the crude material from step 9 can be subjected to semi-preparative HPLC purification. Use the following program for semi-preparative HPLC purification: A:B = 85:15 for 10 minutes then a gradient A:B = 85:15 to A:B = 65:35 over 15 minutes followed by 30 minutes of A:B = 65:35. Flow rate = 4 mL/min. Monitor the radioactivity detector for the appearance of the purified **^{18}F-4.1**product (***Figure 4.14***).

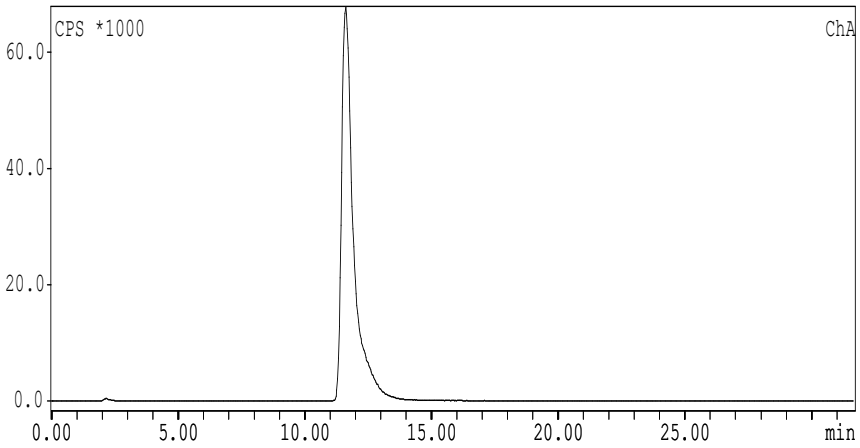

Figure 4.14. Analytical HPLC γ-chromatogram for HPLC purified ^{18}F-FVSB, **^{18}F-4.1**.

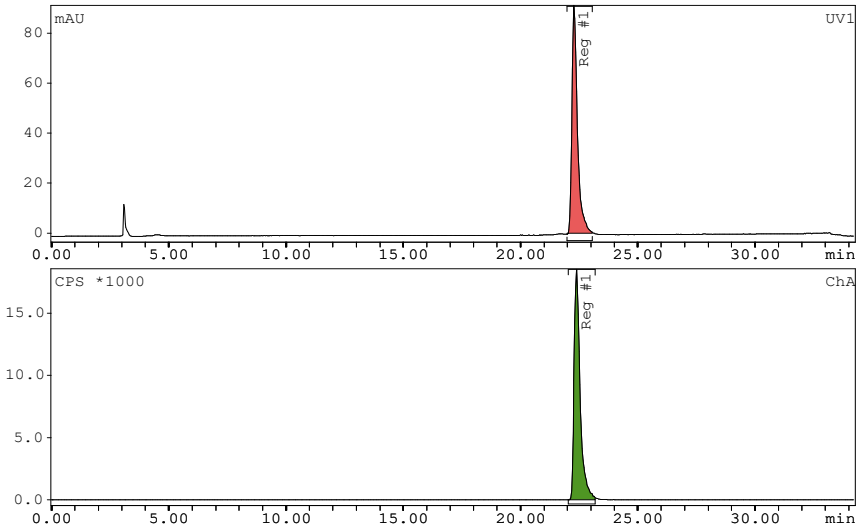

Figure 4.15. Coinjection of HPLC purified ^{18}F-FVSB **^{18}F-4.1** spiked with an aliquot of ^{19}F-FVSB **^{19}F-4.1** reference standard using an analytical HPLC column. γ-trace (lower) and 254 nm UV trace (upper).

4.6.3. Molar Activity Determination

Using the authentic reference material ^{19}F-peptide **^{19}F-4.8,** a standard curve was generated by integration of the UV absorbance signal (at 254 nm) of **^{19}F-4.8** different known amounts (performed in triplicate):

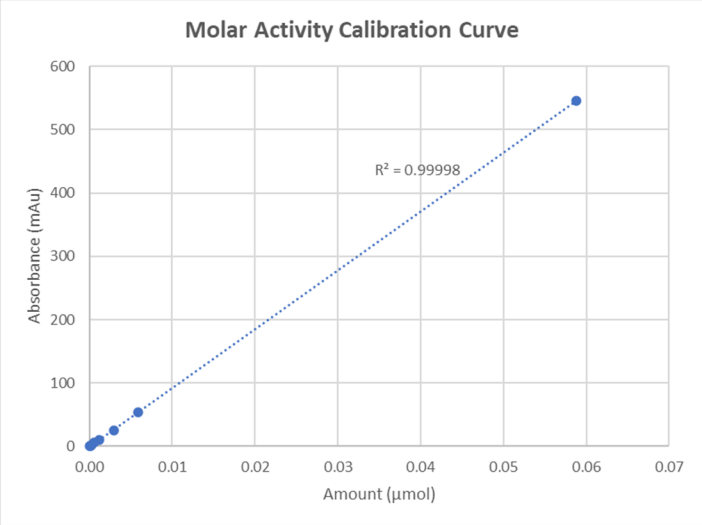

Figure 4.16. Standard curve of the UV absorbance vs amount of the authentic reference standard ^{19}F-peptide **^{19}F-4.8**.

^{18}F-Deoxyfluorination of uronium precursor **4.2** was performed and subsequent peptide labeling was conducted to furnish ^{18}F-peptide **4.8** which was purified by semi-preparative HPLC. The reaction mixture was concentrated and dissolved in 100 µL methanol. An aliquot of purified ^{18}F-peptide **4.8** was injected into an analytical HPLC for analysis. From comparison with the standard curve, it was determined that the molar activity of the sample was 1.2 Ci · µmol^{-1} (44 GBq · µmol^{-1}).

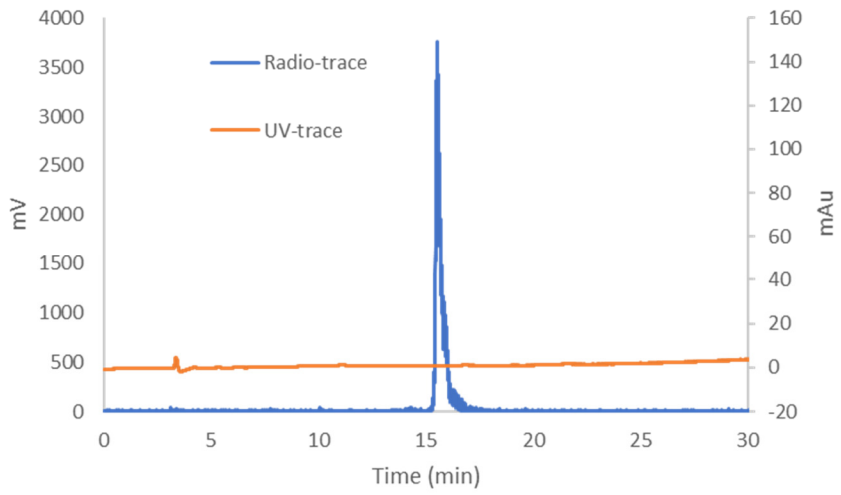

Figure 4.17. Analytical HPLC chromatogram obtained for HPLC purified ^{18}F-labeled peptide conjugate **^{18}F-4.8**. (γ-trace = blue, 254 nm UV trace = orange).

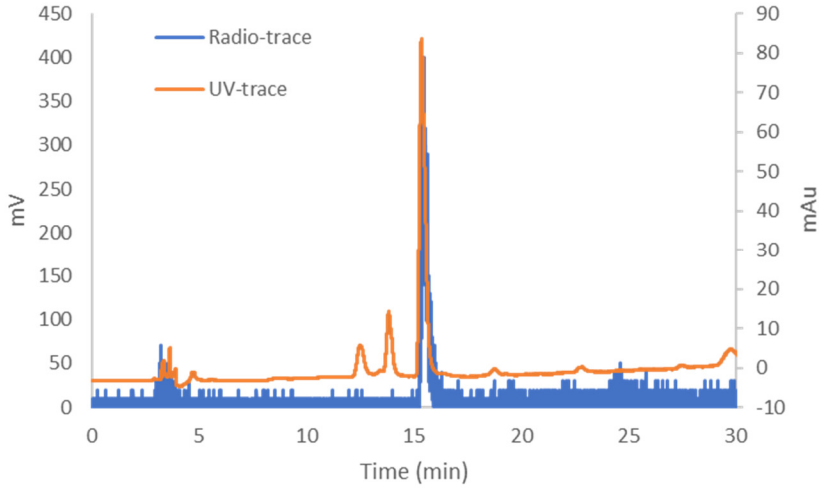

Figure 4.18. Coinjection of crude ^{18}F-labeled peptide conjugate **^{18}F-4.8** spiked with an aliquot of **^{19}F-4.8** reference standard using an analytical HPLC column. (γ-trace = blue, 254 nm UV trace = orange).

4.7. Notes and References

1. Phelps, M. E., PET: The Merging of Biology and Imaging into Molecular Imaging. *Journal of Nuclear Medicine* **2000,** *41* (4), 661-681.

2. Lasne, M.-C.; Perrio, C.; Rouden, J.; Barré, L.; Roeda, D.; Dolle, F.; Crouzel, C., Chemistry of β^+-Emitting Compounds Based on Fluorine-18. In *Contrast Agents II*, Krause, W., Ed. Springer Berlin Heidelberg: 2002; Vol. 222, pp 201-258.

3. Chin, F. T.; Shen, B.; Liu, S.; Berganos, R. A.; Chang, E.; Mittra, E.; Chen, X.; Gambhir, S. S., First experience with clinical-grade ([^{18}F]FPP(RGD$_2$): an automated multi-step radiosynthesis for clinical PET studies. *Molecular imaging and biology* **2012,** *14* (1), 88-95.

4. Van Der Born, D.; Pees, A.; Poot, A. J.; Orru, R. V. A.; Windhorst, A. D.; Vugts, D. J., Fluorine-18 labelled building blocks for PET tracer synthesis. *Chem. Soc. Rev.* **2017,** *46* (15), 4709-4773.

5. Tang, G.; Tang, X.; Wang, X., A facile automated synthesis of N-succinimidyl 4-[^{18}F]fluorobenzoate ([^{18}F]SFB) for 18F-labeled cell-penetrating peptide as PET tracer. *Journal of Labelled Compounds and Radiopharmaceuticals* **2010,** *53* (8), 543-547.

6. Kuhnast, B.; de Bruin, B.; Hinnen, F.; Tavitian, B.; Dollé, F., Design and Synthesis of a New [^{18}F]Fluoropyridine-Based Haloacetamide Reagent for the Labeling of Oligonucleotides: 2-Bromo-N-[3-(2-[^{18}F]fluoropyridin-3-yloxy)propyl]acetamide. *Bioconjugate Chemistry* **2004,** *15* (3), 617-627.

7. von Guggenberg, E.; Sader, J. A.; Wilson, J. S.; Shahhosseini, S.; Koslowsky, I.; Wuest, F.; Mercer, J. R., Automated synthesis of an 18F-labelled pyridine-based alkylating agent for high yield oligonucleotide conjugation. *Applied Radiation and Isotopes* **2009,** *67* (9), 1670-1675.

8. Gao, Z.; Gouverneur, V. r.; Davis, B. G., Enhanced aqueous Suzuki–Miyaura coupling allows site-specific polypeptide ^{18}F-labeling. *Journal of the American Chemical Society* **2013,** *135* (37), 13612-13615.

9. Way, J. D.; Bergman, C.; Wuest, F., Sonogashira cross-coupling reaction with 4-[^{18}F] fluoroiodobenzene for rapid ^{18}F-labelling of peptides. *Chemical Communications* **2015,** *51* (18), 3838-3841.

10. Pretze, M.; Pietzsch, D.; Mamat, C., Recent trends in bioorthogonal click-radiolabeling reactions using fluorine-18. *Molecules* **2013,** *18* (7), 8618-8665.

11. Meyer, J.-P.; Adumeau, P.; Lewis, J. S.; Zeglis, B. M., Click chemistry and radiochemistry: the first 10 years. *Bioconjugate chemistry* **2016,** *27* (12), 2791-2807.

12. Schirrmacher, R.; Wängler, B.; Bailey, J.; Bernard-Gauthier, V.; Schirrmacher, E.; Wängler, C. In *Small prosthetic groups in ^{18}F-radiochemistry: useful auxiliaries for the design of ^{18}F-PET tracers*, Seminars in nuclear medicine, Elsevier: 2017; pp 474-492.

13. Marik, J.; Sutcliffe, J. L., Click for PET: rapid preparation of [^{18}F]fluoropeptides using CuI catalyzed 1,3-dipolar cycloaddition. *Tetrahedron Letters* **2006,** *47* (37), 6681-6684.

14. Glaser, M.; Årstad, E., "Click labeling" with 2-[^{18}F] fluoroethylazide for positron emission tomography. *Bioconjugate chemistry* **2007,** *18* (3), 989-993.

15. Li, Z.; Cai, H.; Hassink, M.; Blackman, M. L.; Brown, R. C.; Conti, P. S.; Fox, J. M., Tetrazine–trans-cyclooctene ligation for the rapid construction of ^{18}F labeled probes. *Chemical Communications* **2010,** *46* (42), 8043-8045.

16. Liu, H.; Audisio, D.; Plougastel, L.; Decuypere, E.; Buisson, D. A.; Koniev, O.; Kolodych, S.; Wagner, A.; Elhabiri, M.; Krzyczmonik, A., Ultrafast click chemistry with fluorosydnones. *Angewandte Chemie* **2016,** *128* (39), 12252-12256.

17. Narayanam, M. K.; Ma, G.; Champagne, P. A.; Houk, K. N.; Murphy, J. M., Synthesis of [^{18}F]fluoroarenes by nucleophilic radiofluorination of N-arylsydnones. *Angewandte Chemie* **2017,** *129* (42), 13186-13190.

18. Kiesewetter, D. O.; Jacobson, O.; Lang, L.; Chen, X., Automated radiochemical synthesis of [^{18}F]FBEM: a thiol reactive synthon for radiofluorination of peptides and proteins. *Applied Radiation and Isotopes* **2011,** *69* (2), 410-414.

19. Kniess, T.; Kuchar, M.; Pietzsch, J., Automated radiosynthesis of the thiol-reactive labeling agent N-[6-(4-[^{18}F]fluorobenzylidene) aminooxyhexyl] maleimide ([^{18}F]FBAM). *Applied Radiation and Isotopes* **2011,** *69* (9), 1226-1230.

20. Morgat, C.; Mishra, A. K.; Varshney, R.; Allard, M.; Fernandez, P.; Hindié, E., Targeting neuropeptide receptors for cancer imaging and therapy: perspectives with bombesin, neurotensin, and neuropeptide-Y receptors. *Journal of Nuclear Medicine* **2014,** *55* (10), 1650-1657.

21. Adumeau, P.; Davydova, M.; Zeglis, B. M., Thiol-reactive bifunctional chelators for the creation of site-selectively modified radioimmunoconjugates with improved stability. *Bioconjugate chemistry* **2018,** *29* (4), 1364-1372.

22. Ma, G.; McDaniel, J. W.; Murphy, J. M., One-step synthesis of [^{18}F]Fluoro-4-(vinylsulfonyl) benzene: a thiol reactive synthon for selective radiofluorination of peptides. *Organic Letters* **2020,** *23* (2), 530-534.

23. Fernández, I.; Frenking, G.; Uggerud, E., Rate-Determining Factors in Nucleophilic Aromatic Substitution Reactions. *J. Org. Chem.* **2010,** *75* (9), 2971-2980.

24. Cheron, N.; El Kaim, L.; Grimaud, L.; Fleurat-Lessard, P., Evidences for the key role of hydrogen bonds in nucleophilic aromatic substitution reactions. *Chem. Eur. J.* **2011,** *17* (52), 14929-34.

25. Jacobson, O.; Zhu, L.; Ma, Y.; Weiss, I. D.; Sun, X.; Niu, G.; Kiesewetter, D. O.; Chen, X., Rapid and simple one-step F-18 labeling of peptides. *Bioconjugate chemistry* **2011,** *22* (3), 422-428.

26. Becaud, J.; Mu, L.; Karramkam, M.; Schubiger, P. A.; Ametamey, S. M.; Graham, K.; Stellfeld, T.; Lehmann, L.; Borkowski, S.; Berndorff, D., Direct one-step18F-labeling of peptides via nucleophilic aromatic substitution. *Bioconjugate chemistry* **2009,** *20* (12), 2254-2261.

27. McBride, W. J.; Sharkey, R. M.; Karacay, H.; D'Souza, C. A.; Rossi, E. A.; Laverman, P.; Chang, C.-H.; Boerman, O. C.; Goldenberg, D. M., A novel method of ^{18}F-radiolabeling for PET. *Journal of nuclear medicine* **2009,** *50* (6), 991-998.

28. Lang, L.; Li, W.; Guo, N.; Ma, Y.; Zhu, L.; Kiesewetter, D. O.; Shen, B.; Niu, G.; Chen, X., Comparison study of [^{18}F]FAl-NOTA-PRGD2, [^{18}F]FPPRGD2, and [^{68}Ga]Ga-NOTA-PRGD2 for PET imaging of U87MG tumors in mice. *Bioconjugate chemistry* **2011,** *22* (12), 2415-2422.

29. Perrin, D. M., [^{18}F]-Organotrifluoroborates as radioprosthetic groups for PET imaging: from design principles to preclinical applications. *Accounts of Chemical Research* **2016,** *49* (7), 1333-1343.

30. Bernard-Gauthier, V.; Bailey, J. J.; Liu, Z.; Wängler, B. r.; Wängler, C.; Jurkschat, K.; Perrin, D. M.; Schirrmacher, R., From unorthodox to established: The current status of ^{18}F-trifluoroborate-and ^{18}F-SiFA-based radiopharmaceuticals in PET nuclear imaging. *Bioconjugate chemistry* **2016,** *27* (2), 267-279.

31. Bernard-Gauthier, V.; Lepage, M. L.; Waengler, B.; Bailey, J. J.; Liang, S. H.; Perrin, D. M.; Vasdev, N.; Schirrmacher, R., Recent advances in ^{18}F radiochemistry: a focus on B-^{18}F,

Si-^{18}F, Al-^{18}F, and C-^{18}F radiofluorination via spirocyclic iodonium ylides. *Journal of Nuclear Medicine* **2018,** *59* (4), 568-572.

32. Gray, E. E.; Nielsen, M. K.; Choquette, K. A.; Kalow, J. A.; Graham, T. J.; Doyle, A. G., Nucleophilic (radio) fluorination of α-diazocarbonyl compounds enabled by copper-catalyzed H–F insertion. *Journal of the American Chemical Society* **2016,** *138* (34), 10802-10805.

33. Fujimoto, T.; Becker, F.; Ritter, T., PhenoFluor: Practical Synthesis, New Formulation, and Deoxyfluorination of Heteroaromatics. *Org. Process Res. Dev.* **2014,** *18* (8), 1041-1044.

34. Tang, P.; Wang, W.; Ritter, T., Deoxyfluorination of Phenols. *J. Am. Chem. Soc.* **2011,** *133* (30), 11482-11484.

35. Scalone, M.; Waldmeier, P., Efficient enantioselective synthesis of the NMDA 2B receptor antagonist Ro 67-8867. *Organic process research & development* **2003,** *7* (3), 418-425.

36. Brace, N. O., An economical and convenient synthesis of phenyl vinyl sulfone from benzenethiol and 1, 2-dichloroethane. *The Journal of Organic Chemistry* **1993,** *58* (16), 4506-4508.

CHAPTER 5: An Organometallic Gold(III) Reagent for ^{18}F-Labeling of Unprotected Peptides and Sugars in Aqueous Media

James W. McDaniel, Julia M. Stauber, Evan A. Doud, Alexander M. Spokoyny,* and Jennifer M. Murphy*

(Org. Lett. **2022**, *in review)*

5.1. Abstract

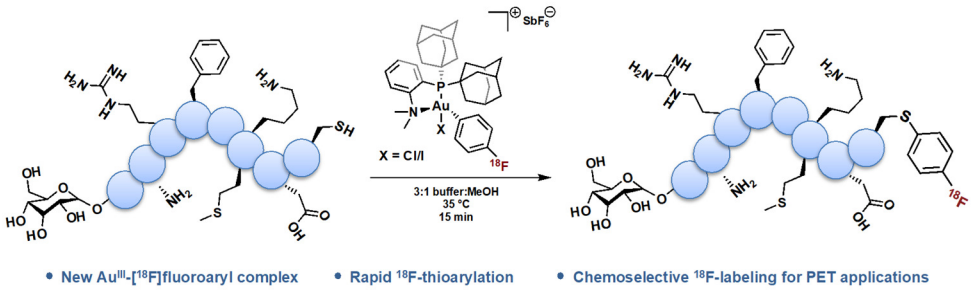

The ^{18}F-labeling of unprotected peptides and sugars via thioarylation using a Au(III)-[^{18}F]fluoroaryl complex is reported. The chemoselective method generates ^{18}F-labeled *S*-aryl bioconjugates in an aqueous environment in 15 min with high radiochemical yields and displays excellent functional group tolerance. This approach utilizes an air and moisture stable, robust organometallic Au(III) complex and highlights the versatility of designer organometallic reagents as efficient agents for rapid radiolabeling of biomolecules.

5.2. Introduction

The rapid kinetics and high chemoselectivity of transition-metal-based transformations have resulted in major advances in organic synthesis, in particular for the modification of complex small molecules.[1, 2] In the context of ^{18}F-labeling, significant effort has been devoted to the

development of transition-metal mediated radiofluorination methods, often translated from modern fluorine-19 related approaches.[3-5] Importantly, the translation of fluorine-19 to fluorine-18 chemistry presents distinct challenges that are non-trivial and rigorous optimization is generally required for smooth translation to radiochemistry.[6] Perhaps the most notable obstacle is that ^{18}F is always the limiting reagent and is in nanomole or lower quantities amongst a large excess of other reagents. Additionally, chemical modifications must be conducted quickly, ideally within minutes, due to the radioactive decay and half-life of ^{18}F.

Over the last decade, reports exploiting the redox activity of transition-metals such as Pd, Ni and Cu to lower the barrier for C–^{18}F bond formation have surged.[3, 6-18] In particular, Cu-mediated methods have found wide use in the construction of ^{18}F-labeled small molecules for positron emission tomography (PET) imaging applications.[11, 19, 20] Modern Cu-mediated methods have become a truly powerful advancement in radiochemical synthesis, unlocking access to radiolabeled constructs that were previously inaccessible. However, metal-based modifications employing unprotected peptides for direct radiofluorination processes are scarce.[21-28]

The unique properties of cysteine, largely its thiol reactivity and low natural abundance, have stimulated efforts toward the chemoselective bioconjugation of this key residue.[29, 30] Pioneering work by the Buchwald and Pentelute groups demonstrating palladium-mediated cysteine arylation to afford *S*-aryl bioconjugates has encouraged the development of Pd-based strategies for labeling peptides with positron-emitting radioisotopes, such as ^{11}C or ^{18}F.[31-33] In the context of ^{11}C-labeling, Hooker and Buchwald utilized a biarylphosphine supported Pd(II)-complex to prepare ^{11}CN-labeled unprotected peptides (***Figure 5.1a***).[34] The Pd-mediated sequential cross-coupling proceeds with initial *S*-arylation of the cysteine-containing peptides followed by direct ^{11}C-cyanation. In addition, Neumaier recently reported a Pd-mediated cysteine

S-arylation using the XantPhos Pd-based cyclometallated precatalyst system previously developed by Buchwald with 2-[^{18}F]fluoro-5-iodopyridine (***Figure 5.1a***).[28] The radiolabeled aryl iodide was synthesized from a 1,4-diazabicyclo[2.2.2]octane (DABCO) precursor and obtained after solid-phase extraction (SPE) with a modest molar activity of 29 GBq·μmol^{-1} and could be directly used for bioconjugation, delivering a remarkably quick overall procedure. However, nonradioactive impurities formed in the initial radiofluorination step were shown to impede the consecutive *S*-arylation step. To sequentially perform the protocol and maintain high conversion during *S*-arylation, minimal DABCO precursor was used, triggering a modest RCY of 2-[^{18}F]fluoro-5-iodopyridine.

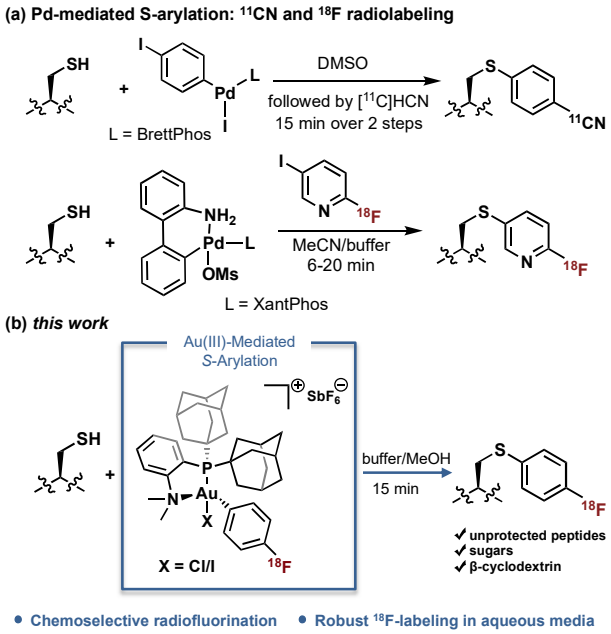

Figure 5.1. (a) ^{11}C- and ^{18}F-labeling of unprotected peptides via Pd-mediated S-arylation. (b) This work, ^{18}F-labeling of unprotected peptides, sugars and β-cyclodextrin via Au-mediated S-arylation.

Recently, Au(III)-aryl oxidative addition complexes supported by the aminophosphine Me-DalPhos ligand (Me-DalPhos = ($Ad_2P(o\text{-}C_6H_4)NMe_2$)) provided rapid access to *S*-aryl bioconjugates under mild conditions at ambient temperature.[35-37] The air-stable organometallic Au(III) complexes were prepared in a straightforward one-step synthesis from commercial (Me-DalPhos)AuCl with a 3-fold excess of aryl iodides.[38] The extremely rapid reaction rate of *S*-arylation for this system (approaching 10^4 $M^{-1}s^{-1}$) suggests this chemistry can be potentially amenable to transformations where rapid kinetics is critical. Importantly, competition experiments revealed superior kinetics for the Au-mediated system over the Pd-mediated system, with a ratio of 9:1.[35] We therefore hypothesized that an ^{18}F-labeled Au(III)-aryl oxidative addition complex could be prepared by using a radiolabeled aryl iodide such as 4-[^{18}F]fluoroiodobenzene and subsequently used for rapid radiolabeling of biomolecules.[39]

Despite differences in the stoichiometry by several orders of magnitude when transitioning to fluorine-18, we reasoned that the high efficiency of the oxidative addition and the rapid reaction kinetics of the Au(III) arylation could provide a powerful platform for the chemoselective radiofluorination of thiols. Here, we report the synthesis of a Au(III)-[^{18}F]fluoroaryl complex and its application toward Au-mediated radiofluorination of thiol-containing substrates to afford stable *S*-[^{18}F]fluoroaryl bioconjugates (***Figure 5.1b***). This approach is, to our knowledge, the first gold-mediated methodology for chemoselective ^{18}F-labeling of thiol-containing substrates.[40]

5.3. Results and Discussion

Table 5.1. Preparation of Au(III)-[^{18}F]Fluoroaryl Complex **[^{18}F]1**

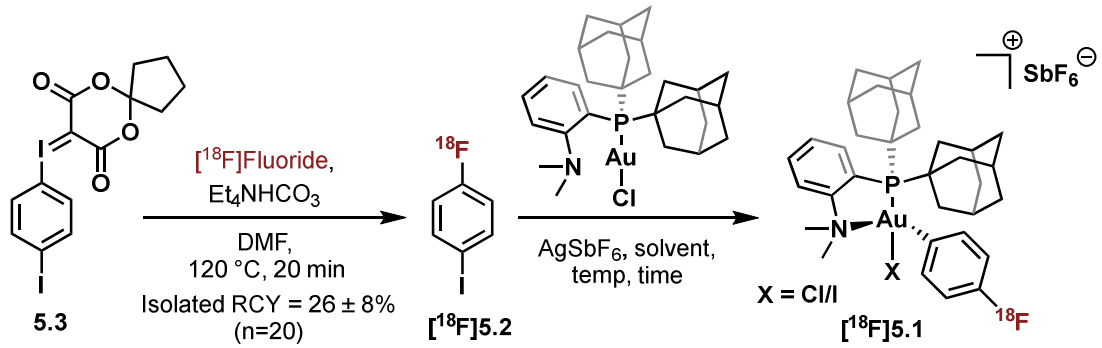

entry[a]	Au(I)/$AgSbF_6$ (mg)[b]	solvent	time (min)	temp. (°C)	RCY (%)[c]
1	10/5 (1.5 equiv)	DCM	10	55	38 ± 27
2	8/4 (1.2 equiv)	DCM	10	55	49 ± 15
3	**6/3 (0.9 equiv)**	**DCM**	**10**	**55**	**95 ± 7**
4	6/3 (0.9 equiv)	DCM	20	55	87 ± 16
5	6/3 (0.9 equiv)	DCE	10	60	87 ± 8
6	6/3 (0.9 equiv)	DCE	10	80	83 ± 15
7	6/3 (0.9 equiv)	DCE	20	80	94 ± 6

[a]Conditions: **[^{18}F]5.2** (~500 μCi) per reaction, solvent (1.5 mL). [b]equiv are relative to ylide precursor **5.3**. [c]RCY was determined by radio-TLC analysis of complex **[^{18}F]1**, n > 3 for all entries.

We first sought to prepare a radiolabeled aryl iodide that could undergo oxidative addition with the (Me-DalPhos)AuCl complex in the presence of $AgSbF_6$ to generate the radiolabeled Au(III)-aryl complex, [(Me-DalPhos)Au(4-[^{18}F]fluorobenzene)Cl][SbF_6] (**[^{18}F]5.1**).[35, 38] Synthesis of 4-[^{18}F]fluoroiodobenzene (**[^{18}F]5.2**) was achieved using a one-step radiofluorination protocol via a spirocyclic hypervalent iodonium ylide (***Table 5.1***).[41, 42] Following a slightly modified literature protocol, iodonium yilde **5.3** was prepared and subsequently subjected to radiofluorination.[43, 44] Preparation of **[^{18}F]5.2** was fully automated on the ELIXYS FLEX/CHEM radiochemical synthesis module (Sofie Biosciences) and conducted using [^{18}F]Et_4NF in DMF at

120 °C for 20 min which, after HPLC purification, furnished aryl iodide **[^{18}F]5.2** in 26 ± 8% isolated radiochemical yield (RCY), decay-corrected (***Table 5.1***).

We next focused on the oxidative addition reaction to yield **[^{18}F]5.1** (***Table 5.1***). In contrast to 4-fluoroiodobenzene, which can be employed at 3-fold excess, 4-[^{18}F]fluoroiodobenzene is the limiting reagent that is present in nanomolar or picomolar concentration, severely altering the stoichiometry of the oxidative addition step. Formation of **[^{18}F]5.1** proceeded in 38% ± 27% RCY upon the treatment of 4-[^{18}F]fluoroiodobenzene in CH_2Cl_2 with (Me-DalPhos)AuCl (1.5 equiv) in the presence of $AgSbF_6$ (1.5 equiv) heated at 55 °C in a sealed vial for 10 min (***Table 5.1***, entry 1). We initially screened the stoichiometry of (Me-DalPhos)AuCl and $AgSbF_6$, keeping the relative 1:1 ratio of gold to silver reagents consistent with the previous report,[35] and observed that lowering the stoichiometry of Au(I) to 0.9 equiv afforded **[^{18}F]5.1** in 95% ± 7% RCY at 55 °C in 10 min (Table 1, entry 3). Further lowering the Au(I) equivalents resulted in no observable product. The reaction was also evaluated in DCE at elevated temperatures and **[^{18}F]5.1** was obtained in comparable yields albeit at slightly extended reaction times (***Table 5.1***, entries 5-7). Of note, these reactions were performed in a sealed reaction vial with no rigorous exclusion of oxygen or water and conducted using commercial, unpurified solvents. Precursor **5.3** showed excellent stability when stored in the dark at -20 °C for up to 18 months with no detectable degradation or loss in RCY. The Au(I) complex could be stored on the benchtop and the $AgSbF_6$ in the glovebox with exclusion from light for up to 3 months and used with no detectable degradation.

Table 5.2. Thio Arylation of L-Glutathione with Au(III)-[^{18}F]Fluoroaryl Complex **[^{18}F]5.1**

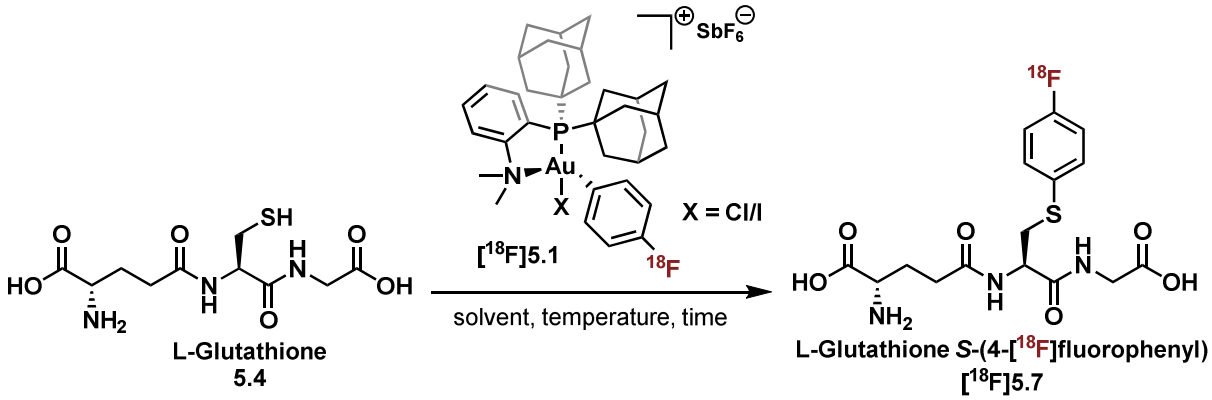

entry[a]	solvent	Time (min)	temp. (°C)	RCY (%)[b]
1	PBS pH 7.4	30	23	16 ± 13
2	HEPES pH 7.3	30	23	43 ± 18
3	Tris pH 8.0	30	23	54 ± 16
4	Tris pH 8.0	30	35	93 ± 1
5	Tris pH 8.0	30	45	95 ± 1
6	Tris pH 8.0	20	35	72 ± 14
7	Tris pH 8.0	15	35	78 ± 12
8	Tris pH 8.0	10	35	44 ± 1
9	**Tris pH 8.0/MeOH, 3/1**	**15**	**35**	**97 ± 3**
10[c]	**Tris pH 8.0/MeOH, 3/1**	**15**	**35**	**97 ± 4**
11[d]	**Tris pH 8.0/MeOH, 3/1**	**15**	**35**	**91 ± 5**
12[e]	Tris pH 8.0/MeOH, 3/1	15	35	70
13[f]	Tris pH 8.0/MeOH, 3/1	15	35	52

[a]Conditions: Au(III) complex **[^{18}F]5.1** (~1 mCi) per reaction, L-glutathione **5.4** (16 μmol), solvent (1 mL). [b]Non-isolated RCY is estimated by radio-HPLC analysis of crude peptide **[^{18}F]5.7**, n = 2-6. [c]Peptide = H-Asp-Arg-Lys-Cys-Ala-Thr-NH_2 **5.5** (7 μmol). [d]Peptide = H-Cys-Arg-Gly-Asp-NH_2 **5.6** (11 μmol). [e]L-glutathione **5.4** (0.71 μmol), n = 1. [f]L-glutathione **5.4** (0.39 μmol), n=1.

Product identity and purity of **[^{18}F]5.1** were determined by analytical HPLC analysis, comparing the radio-trace of **[^{18}F]5.1** with the UV-trace of the ^{19}F-reference standard, via coinjection. Rapid and clean conversion of 4-[^{18}F]fluoroiodobenzene to **[^{18}F]5.1** enabled its direct

use without the need for HPLC purification. The crude reaction mixture containing **[^{18}F]5.1** was simply filtered and concentrated under mild heating to afford **[^{18}F]5.1**, which was directly used in subsequent thioarylation reactions (see ***Figure 5.11***).

The reactivity of the novel Au(III)-complex, **[^{18}F]5.1**, was examined and optimized with L-glutathione as a model peptide substrate (***Table 5.2***). Initial thioarylation was observed in 16% ± 13% RCY upon treatment of L-glutathione 4 (16 μmol) with **[^{18}F]5.1** in PBS buffer (pH 7.4) at 23 °C in 30 min (***Table 5.2***, entry 1). A buffer screen revealed that Tris buffer (pH 8.0) increased the yield to 54 ± 16% but the reaction remained sluggish at ambient temperature (***Table 5.2***, entry 3). Upon slight heating to 35–45 °C, the [^{18}F]fluoroaryl product **[^{18}F]5.7** was generated in 93–95% RCY (***Table 5.2***, entries 4-5). Attempts to shorten the reaction time led to a reduction in yield with a significant drop for reactions under 15 min (***Table 5.2***, entries 6-8).

From our previous results with peptide conjugation chemistry,[45] co-solvents have proven valuable in improving reagent solubility; we predicted that a co-solvent could further boost the Au(III)-[^{18}F]fluoroaryl solubility and facilitate complete reaction conversion. Employing a Tris buffer/methanol (3/1) solvent system improved the reaction conversion and provided the [^{18}F]fluoroaryl conjugate **[^{18}F]5.7** in 97% ± 3% RCY in 15 min (***Table 5.2***, entry 9). Similarly, peptide substrates **5.5** and **5.6** also revealed a significant improvement in RCY with addition of methanol to the reaction mixture (***Table 5.2***, entries 10-11). High radiolabeling efficiency while using low micromolar amounts of peptide precursor is advantageous in the context of radiolabeling expensive peptides with limited availability, and allows for a simplified purification process of the ^{18}F-labeled product. With sub-micromolar peptide loading, ^{18}F-thioarylation was achieved in 70% RCY using 0.71 μmol **4** and in 52% RCY using 0.39 μmol **4** (***Table 5.2***, entries 12-13)

The optimized *S*-arylation conditions were applied to a series of thiol-containing substrates to establish the versatility and scope of our methodology (***Figure* 5.2**). High chemoselectivity for *S*-arylation of thiol-containing substrates in the presence of a variety of additional functional groups was observed in Tris buffer (pH 8.0)/methanol (3/1) within 15 min in 72–97% RCY. Substrates containing a free carboxylic acid, primary or secondary amine, guanidine residue, and thioether functional groups were well tolerated as well as sugar-based substrates containing free alcohols. Additionally, *S*-arylation of peptides in which the cysteine residue is positioned at the N-terminus (**[^{18}F]5.9**) or within an intrachain position (**[^{18}F]5.10**) still maintained high efficiency. Performing the ^{18}F-thioarylation with 3 μmol L-glutathione **5.4**, afforded ^{18}F-labeled conjugate **[^{18}F]5.7** in 97% ± 1% RCY (***Figure 5.2***). A hexapeptide containing a nucleophilic lysine residue cleanly delivered the *S*-aryl conjugate **[^{18}F]8** in 97% ± 4% RCY with 7.0 μmol precursor loading. Notably, **[^{18}F]8** was furnished in 49% ± 6% RCY when using only 0.62 μmol precursor.

A critical motif utilized for noninvasive PET imaging of angiogenesis is the RGD sequence and numerous peptide-based analogues have demonstrated value, including clinical benefit.[46, 47] The Au(III)-mediated ^{18}F-thioarylation of peptides containing the RGD sequence was successfully executed to provide peptide conjugates **[^{18}F]5.9** and **[^{18}F]5.10** in 72% ± 11% and 94% ± 5% RCY, respectively. In addition, synthesis of an ^{18}F-labeled β-amyloid peptide fragment[48] was successfully accomplished, using 4 μmol peptide precursor, to afford [^{18}F]fluoroaryl conjugate **[^{18}F]5.11** in 77% ± 10% RCY. Finally, the protocol was applied to sugar-based substrates to assess compatibility with alternative thiol-containing constructs containing free alcohols. Thio-β-D-glucose and thio-β-D-galactose underwent efficient [^{18}F]fluoroarylation in MeCN/H_2O (1/1) in 93% ± 8% and 88% ± 11% RCY, respectively.

Cyclodextrin-based polymers have been used as carrier systems for chemotherapeutics or small molecule drugs and their unique properties, such as enhanced solubility, improved pharmacokinetics and increased efficacy compared to the small molecules, have garnered interest towards utility in biomedical imaging applications.[49-51] For example, a cyclodextrin polymer-based nanoparticle containing the chemotherapeutic camptothecin was labeled with ^{64}Cu and imaged in tumor-bearing mice to noninvasively determine multi-organ pharmacokinetics, whole-body biodistribution and tumor localization.[52] Limited examples of ^{18}F-labeled β-cyclodextrins in the literature prompted us to investigate our protocol for radiofluorination of the cyclic oligosaccharides. The Au(III)-mediated ^{18}F-thioarylation was performed with 4 μmol of a monothiolated β-cyclodextrin precursor to furnish construct **[^{18}F]5.14** in 90% ± 5% RCY.

To evaluate the practicality of our approach, *S*-aryl glutathione conjugate **[^{18}F]5.7** was synthesized from using 6-8 mCi of **[^{18}F]5.1** and subjected to HPLC purification which afforded isolated **[^{18}F]5.7** in 23% ± 5% activity yield (non-decay-corrected, n=3) with a molar activity of 2.9 ± 1.8 Ci·μmol^{-1} (108 ± 68 GBq·μmol^{-1}). ICP-OES analysis revealed that the purified product contained 44 ± 7 ppb of Au (n=3), which is well below the acceptable limit for human injection.[53] The focus of this work is the design, optimization and efficient construction of a novel Au^{III}-[^{18}F]fluoroaryl complex for the ^{18}F-labeling of unprotected peptides and sugars. Future work is directly aimed at automating the full protocol and conducting PET imaging studies with a labeled peptide in preclinical mouse models.

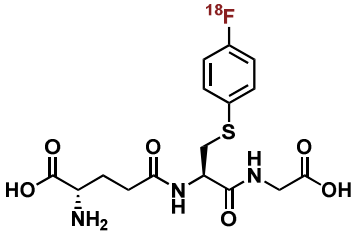

L-Glutathione *S*-(4-[^{18}F]fluorophenyl)
[^{18}F]5.7
RCY = 97 ± 1% (n=2)[a]
Activity Yield = 23 ± 5% (n=3)
molar activity = 2.9 ± 1.8 Ci μmol^{-1}

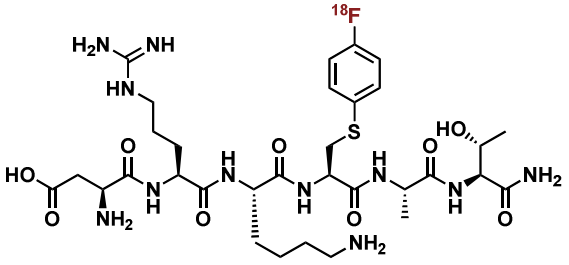

H-Asp-Arg-Lys-Cys(4-[^{18}F]fluorophenyl)-Ala-Thr-NH$_2$
[^{18}F]5.8
RCY = 97 ± 4% (n=2)
RCY = 49 ± 6% (n = 2)[b]

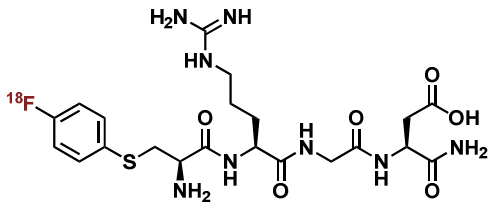

H-Cys(4-[^{18}F]fluorophenyl)-Arg-Gly-Asp-NH$_2$
[^{18}F]5.9
RCY = 72 ± 11% (n=2)

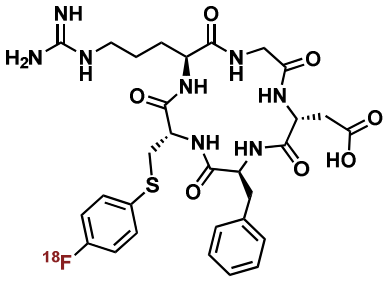

***c*(Arg-Gly-Asp-Phe-Cys(4-[^{18}F]fluorophenyl))**
[^{18}F]5.10
RCY = 94 ± 5% (n=2)

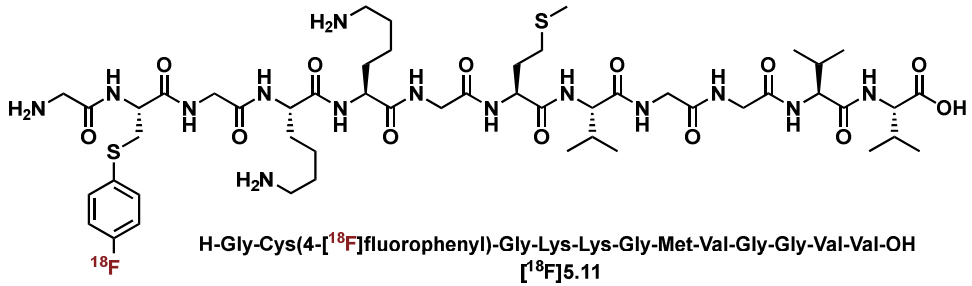

H-Gly-Cys(4-[^{18}F]fluorophenyl)-Gly-Lys-Lys-Gly-Met-Val-Gly-Gly-Val-Val-OH
[^{18}F]5.11
RCY = 77 ± 10% (n=2)

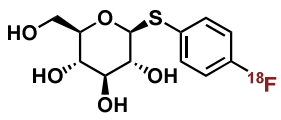

D-Glucose *S*-(4-[^{18}F]fluorophenyl)
[^{18}F]5.12[c]
RCY = 93 ± 8% (n=2)

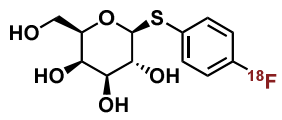

D-Galactose *S*-(4-[^{18}F]fluorophenyl)
[^{18}F]5.13[c]
RCY = 88 ± 11% (n=2)

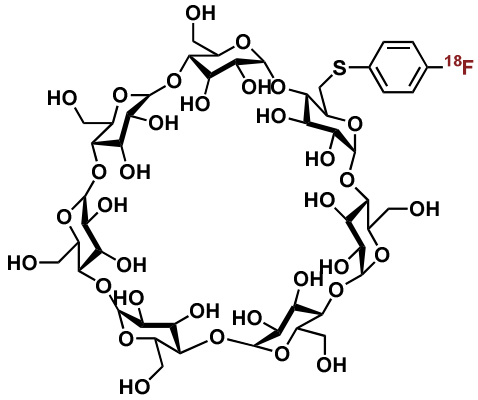

Mono-(6-*S*-(4-[^{18}F]fluorophenyl)-6-deoxy)-β-cyclodextrin
[^{18}F]5.14[c]
RCY = 90 ± 5% (n=2)

Figure 5.2. ^{18}F-Labeling of peptides via Au^{III}-mediated *S*-arylation. Reaction conditions: substrate (5 mg), **[^{18}F]5.1** (0.5 – 2.0 mCi), Tris buffer pH 8.0 (750 μL), MeOH (250 μL), 35 °C, 15 min. Radiochemical purity (RCP) was calculated by dividing the integrated area of the ^{18}F-labeled product peak by the total integrated area of all ^{18}F-labeled peaks, as determined by radio-HPLC. The decay-corrected radiochemical yield (RCY) was calculated by dividing final activity of the labeled product by starting **[^{18}F]5.1** activity, multiplied by the RCP. Identity of each labeled product was confirmed by co-injection with the ^{19}F-reference standard. [a]Substrate (3 μmol). [b]Substrate (0.62 μmol), Tris buffer pH 8.0 (562 μL), MeOH (188 μL). [c]MeCN (500 μL), H_2O (500 μL).

5.4. Conclusions

In summary, we report a robust Au(III)-[^{18}F]fluoroaryl reagent **[^{18}F]5.1** for the ^{18}F-labeling of thiol-containing substrates via *S*-arylation in aqueous media. To our knowledge, this is the first Au-mediated ^{18}F-labeling methodology of unprotected peptides and thiol-containing constructs. The practical advantages of our method are highlighted by the mild reaction conditions, broad substrate scope and rapid reaction kinetics. The oxidative addition complex **[^{18}F]5.1** was rapidly generated in 10 min and directly used to furnish ^{18}F-labeled conjugates in excellent chemoselectivity and high molar activity in 15 min. The protocol was applied to a diverse range of thiol-containing substrates, including unprotected peptides, and could achieve RCYs up to 97% using sub micromolar peptide loading. This work expands on the growing space of organometallic reagents that are applied towards radiochemical modifications which demand rapid reaction rates. We anticipate the availability of **[^{18}F]5.1** will further advance the accessible radiolabeling space for biomedical imaging applications.

5.5. Experimental Section

5.5.1. Materials and Methods

All chemicals and reagents were purchased from commercial sources and used without further purification. (Me-DalPhos)AuCl was purchased from Sigma Aldrich and 4-fluoroiodobenzene was purchased from Strem Chemicals and both were used as received. $AgSbF_6$ (Sigma Aldrich) was stored under an inert atmosphere of purified N_2 in a Vacuum Atmospheres NexGen glovebox prior to use. [(Me-DalPhos)Au(4-fluorobenzene)Cl][SbF_6] was prepared according to a previously reported procedure.[35] The *c*(Arg-Gly-Asp-Phe-Cys) peptide was purchased from Bachem Americas Inc. and the amyloid-β fragment H-Gly-Cys-Gly-Lys-Lys-Gly-Met-Val-Gly-Gly-Val-Val-OH was purchased from Biopeptek Pharmaceutricals LLC. and both were used as received. All other peptides were synthesized via solid-phase peptide synthesis as described in **Section 5.5.2**. All deuterated solvents were obtained from Cambridge Isotope Laboratories and used as received. Unless otherwise noted, reactions were carried out in oven-dried glassware using commercially available anhydrous solvents. Solvents used for extractions and chromatography were not anhydrous. Reactions and chromatography fractions were analyzed by thin-layer chromatography (TLC) using Merck precoated silica gel 60 F_{254} glass plates (250 μm) and visualized by ultraviolet irradiation or by staining with permanganate solution. Flash column chromatography was performed using E. Merck silica gel 60 (230−400 mesh) with compressed air.

For the preparation of ^{19}F reference standards (peptides, sugars, cyclodextrin): All manipulations were performed under open atmosphere conditions in a fume hood unless otherwise indicated. Solvents (dichloromethane (DCM), acetonitrile (MeCN), dimethylformamide (DMF), diethyl ether (Et_2O), trifluoroacetic acid (TFA), 4-methylpiperidine, Milli-Q H_2O) were used as received

without further purification unless otherwise specified. L-glutathione (reduced) was purchased from Sigma Aldrich and stored at -20 °C prior to use. Na[1-thio-β-D-glucose] (Sigma Aldrich), Na[1-thio-β-D-galactose] (ChemImpex International), mono-(6-mercapto-6-deoxy)-β-cyclodextrin (Zhiyuan Biotechnology), and triisopropylsilane (TIPS, Strem Chemicals) were used as received and stored at -20 °C prior to use. 1-Hydroxy-7-azabenzotriazole solution (HOAt, 0.6 M in DMF), 1-[Bis(dimethylamino)methylene]-1H-1,2,3-triazolo[4,5-b]pyridinium 3-oxid hexafluorophosphate (HATU), *N*,*N*,*N*′,*N*′-Tetramethyl-O-(1H-benzotriazol-1-yl)uronium hexafluorophosphate (HBTU), Fmoc-rink amide resin (0.7-0.9 mmol/g, 70-90 mesh), Fmoc-L-Arg(Pbf)-OH, Fmoc-L-Ala-OH, Fmoc-L-Cys(Trt)-OH, Fmoc-L-Gly-OH, Fmoc-L-Asp(OtBu)-OH, Fmoc-L-Lys(Boc)-OH, and Fmoc-L-Thr were purchased from ChemImpex International and stored at 4 °C prior to use. Aqueous solutions of Tris (tris(hydroxymethyl)aminomethane) buffer were prepared by dissolution of Tris•HCl (Sigma Aldrich) in Milli-Q water and adjusted to the indicated pH with an aqueous solution of NaOH (1 M).

NMR spectra were recorded on a Bruker ARX 400 (400 MHz for ^{1}H; 100 MHz for ^{13}C, 376 MHz for ^{19}F) or a Bruker ARX 500 (500 MHz for ^{1}H; 126 MHz for ^{13}C, 471 MHz for ^{19}F) spectrometer. Chemical shifts are reported in parts per million (ppm, δ) using the residual solvent peak as the reference. The coupling constants, *J*, are reported in Hertz (Hz), and the multiplicity identified as the following: br (broad), s (singlet), d (doublet), t (triplet), q (quartet) and m (multiplet). High-resolution electrospray mass spectrometry (ESI-HRMS) data were acquired with a Thermo Scientific™ Q-Exactive Plus Spectrometer with a quadrupole mass filter and Orbitrap mass analyzer. For some samples, high-resolution mass spectra were obtained on a Thermo Scientific™ Exactive Mass Spectrometer with DART ID-CUBE, an Agilent 1260 Infinity 6530 Q-TOF ESI

instrument using an Agilent ZORBAX 300SB-C18 column (2.1 × 150 mm, 5 μm), or on a Waters LCT-Premier XE Time of Flight Instrument controlled by MassLynx 4.1 software (Waters Corporation, Milford MA). The instrument was equipped with the Multi Mode Ionization source operated in the electrospray mode. A solution of Leucine Enkephalin (Sigma Chemical, L9133) was used in the Lock-Spray to obtain accurate mass measurements. Samples were infused using direct loop injection on a Waters Acquity UPLC system. Fluorine-19 reference standards were synthesized from the peptide precursors and high-performance liquid chromatography (HPLC) purification of the arylated bioconjugates were performed on an Agilent Technologies 1260 Infinity II HPLC instrument equipped with a Variable Wavelength Detector (VWD, 254, 214 nm) and using an Agilent ZORBAX SB-C18 (9.4 × 250 mm, 5 μm) reversed-phase column.

Gold ICP-OES analysis was conducted using an Agilent 5110 ICP-OES (inductively coupled plasma-optical emission spectrometer). Volumetric glassware (pipets and flasks) was used to create a dilution series of aqueous Au standards. A Sigma-Aldrich 1000 ppm (Lot value: 999 ppm ± 2 ppm, 5% w/w HCl) Gold Standard for ICP was used as a stock solution to create standards of concentrations 100 ppm, 10 ppm, 1 ppm, and 100 ppb. The subsequent calibration curve was generated for each standard by integrating the signal corresponding to the characteristic Au emission (242.79 nm).

5.5.2. Experimental Procedure and Characterization Data

5.5.2.1. Preparations of iodonium ylide precursor

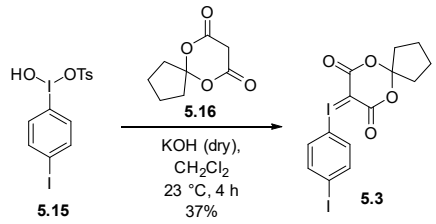

[Hydroxy(tosyloxy)iodo]-4-iodobenzene **5.15** and 6,10-Dioxaspiro[4.5]decane-7,9-dione **5.16** were synthesized according to literature procedure.[43, 44] The ^{1}H and ^{13}C NMR spectroscopic data were consistent with previously reported values. To a slurry of [hydroxy(tosyloxy)iodo]-4-iodobenzene **5.15** (486 mg, 0.94 mmol) and dione **5.16** (173 mg, 1.02 mmol) in dichloromethane (10 mL) was added dry KOH (400 mg, 7.13 mmol). The slurry was stirred at 23 °C for 4 h and the mixture was filtered over celite and concentrated. The crude solid was triturated in hexanes and sonicated in a 0 °C water bath. The mixture was allowed to stand at 4 °C for 20 h and the solids filtered to yield iodonium ylide **5.3** (170.7 mg, 0.35 mmol, 37% yield) as a light-yellow powder, which was used without further purification.

^{1}H NMR (500 MHz, DMSO-d_6, δ): 7.82 (d, J = 8.5 Hz, 2H), 7.53 (d, J = 8.5 Hz, 2H), 2.00-1.97 (m, 4H), 1.70-1.67 (m, 4H) ppm.

^{13}C NMR (125 MHz, DMSO-d_6, δ): 164.0, 140.1, 134.7, 116.2, 112.7, 98.5, 59.3, 37.3, 23.2 ppm.

Mass Spec *m/z*: calc'd for $[M+H]^+$ for $C_{14}H_{13}I_2O_4$ 498.89034; found 498.88911

5.5.2.2. Preparations of peptides 5.17 and 5.18

General Procedure for Solid-Phase Peptide Synthesis

Resin preparation:

Rink amide resin (1 g, 0.7-0.9 mmol/g) was suspended in a 50/50 (v/v) mixture of DCM/DMF (10 mL) and the suspension was allowed to stir for 1 h to allow the resin to adequately swell. The suspension was subsequently transferred to a coarse-porosity fritted-25 mL peptide synthesis vessel and the resin was washed with DMF (3 × 10 mL), DCM (3 × 10 mL), and DMF (3 × 10 mL).

Resin deprotection:

A 4-methylpiperidine/DMF (20:80, v/v, 10-15 mL) solution was transferred to the vessel, and the suspension was shaken for 20 min. The solution was removed from the vessel, and the resin was washed with DMF (10 mL). To the vessel was added a fresh solution of 4-methylpiperidine/DMF (20:80, v/v, 10-15 mL), and the vessel was shaken for an additional 5 min. The solution was removed, and the resin was washed with DMF (3 × 10 mL).

Amino acid coupling:

To a DMF (10 mL) solution of each amino acid (3 equiv with respect to resin) and HBTU (2.9 equiv with respect to resin) was added *N*,*N*-diisopropylethylamine (6 equiv with respect to resin), and the mixture was allowed to stir for 1 min and then transferred to the vessel containing the resin. The vessel was shaken for 45 min, after which the solution was removed, and the resin was thoroughly washed with DMF (3 × 10 mL). The deprotection procedure (*vide infra*) was performed following each amino acid coupling step.

Cysteine coupling only:

Coupling was performed following a method adapted from the literature to minimize the occurrence of cysteine racemization.[54] To a DCM/DMF (50:50, v/v, 12 mL) solution of cysteine (3 equiv with respect to resin), HATU (4 equiv with respect to resin), and HOAt (0.6 M in DMF, 4 equiv with respect to resin) was added 2,4,6-trimethylpyridine (4 equiv with respect to resin), and the mixture was quickly transferred to the vessel. The mixture was shaken for 1 h, after which the resin was thoroughly washed with DMF (5 × 10 mL).

Amino acid deprotection:

After each coupling procedure, a solution of 4-methylpiperidine/DMF (20:80, v/v, 10-15 mL) was transferred to the vessel and the vessel was shaken for 10 min, at which point the solution was removed, and the resin was washed with DMF (10 mL). To the vessel was transferred a solution of 4-methylpiperidine/DMF (20:80, v/v, 10-15 mL), and the vessel was shaken for an additional 5 min. The solution was removed, and the resin was then thoroughly washed with DMF (3 × 10 mL).

Peptide cleavage from resin:

After deprotection of the final amino acid residue, the resin was washed with DCM (3 × 10 mL), and then transferred to a 50 mL round bottom flask. A light stream of N_2 was flowed over the resin for 5 min to evaporate residual DCM. To the dry resin was added a cleavage cocktail consisting of a 95:2.5:2.5 (v/v/v) mixture of TFA:H_2O:TIPS. The slurry was stirred under an atmosphere of N_2 for 3-4 h (cleavage time is dependent on the amino acid composition). The suspension was then transferred back to the peptide vessel, and the solution was filtered away from the resin. The resulting filtrate was transferred to a 50 mL conical tube and concentrated under a stream of N_2 to

a final volume of ca. 5 mL. To this solution was added cold (-20 °C) Et_2O (40 mL), resulting in the precipitation of the crude peptide. The suspension was centrifuged (2,500 × g, 5 min), and the supernatant was removed and discarded. To the tube containing the solids was added Et_2O (40 mL), and the tube was sonicated (5 min) to suspend the crude peptide. The suspension was centrifuged (2,500 × g, 5 min), the supernatant was decanted, and the crude peptide was dried under reduced pressure and stored at -20 °C prior to purification.

Purification:

The crude product was purified by reversed-phase HPLC using an Agilent Technologies 1260 Infinity II HPLC instrument equipped with a Variable Wavelength Detector (VWD, 254, 214 nm) and using an Agilent ZORBAX SB-C18 reversed-phase column (9.4 × 250 mm, 5 μm). The HPLC method was run with gradient elution consisting of a mobile phase composed of H_2O (spiked with 0.1% (v/v) TFA, solvent A) and MeCN (spiked with 0.1% (v/v) TFA, solvent B) solutions and with a flow rate of 3 mL/min using the specific solvent gradient as indicated. The fractions containing the pure product were combined and the solvent was lyophilized to afford the purified peptide, which was stored at -20 °C prior to use.

H-Cys-Arg-Gly-Asp-NH_2 (5.17)

The general method for solid-phase peptide synthesis was performed, and the following solvent gradient was used for HPLC purification: 0–15 min, A (100%); 15–35 min, A (100–60%) : B (0–40%); 35–40 min, A (60–0%) : B (40–100%); 40–44 min, B (100%). The fractions containing the pure product were combined and the solvent was lyophilized to afford the purified peptide, which was stored at -20 °C prior to use.

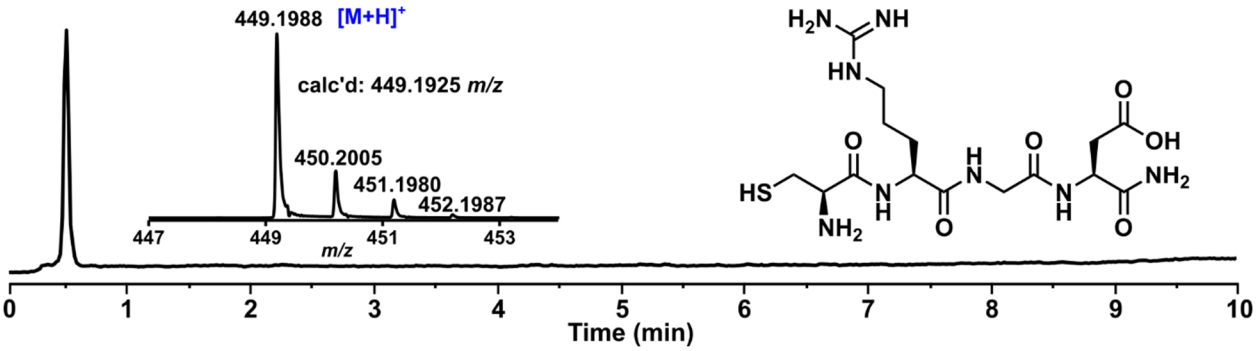

Figure 5.3. LC-MS data of H-Cys-Arg-Gly-Asp-NH_2 (**5.17**).

H-Asp-Arg-Lys-Cys-Ala-Thr-NH_2 (5.18)

The general method for solid-phase peptide synthesis was performed, and the following solvent gradient was used for HPLC purification: 0–10 min, A (100%); 10–55 min, A (100–60%) : B (0–40%); 55–65 min, A (60–0%) : B (40–100%); 65–70 min, B (100%). The fractions containing the pure product were combined and the solvent was lyophilized to afford the purified peptide, which was stored at -20 °C prior to use.

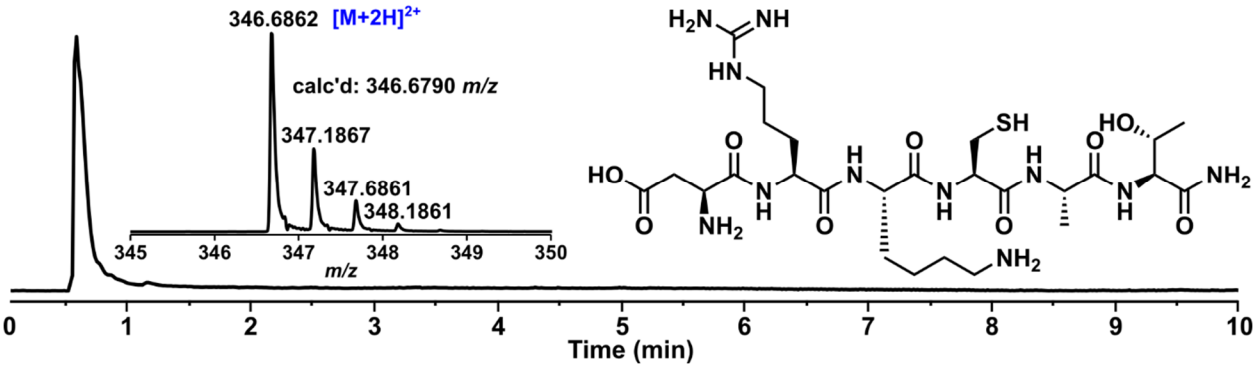

Figure 5.4. LC-MS data of H-Asp-Arg-Lys-Cys-Ala-Thr-NH_2 (**5.18**).

5.5.3. Preparation of ^{19}F-Fluorinated Reference Standards

General Procedure for Peptide Thiol Arylation

To a cooled (-20 °C) DCM solution (0.75 mL) containing (Me-DalPhos)AuCl (3 equiv with respect to peptide) and 4-fluoroiodobenzene (15 equiv with respect to peptide), was added a cooled (-20 °C) DCM solution (0.75 mL) of $AgSbF_6$ (3 equiv with respect to peptide) under protection from light. The reaction mixture immediately changed color from colorless to bright yellow concomitant with the precipitation of yellow precipitate. The reaction mixture was filtered through a pad of Celite to remove liberated AgI, and the resulting bright yellow filtrate was dried under reduced pressure to yield the crude [(Me-DalPhos)Au(4-fluorobenzene)Cl][SbF_6] salt as a yellow residue. The crude product was dissolved in MeCN (1 mL) and added to an aqueous Tris-buffered solution (1 mL, 200 mM, pH 7) of the peptide at ambient temperature. Pale yellow solids immediately precipitated from the reaction mixture upon addition, and the resulting pale-yellow suspension was vortexed to ensure efficient mixing, and then allowed to stand for a total of 5 min. All volatiles were removed from the reaction mixture, and then the crude product was purified by reversed-phase HPLC using an Agilent Technologies 1260 Infinity II HPLC instrument equipped with a Variable Wavelength Detector (VWD, 254, 214 nm) and using an Agilent ZORBAX SB-C18 reversed-phase column (9.4 × 250 mm, 5 μm). Gradient elution consisted of a mobile phase composed of H_2O (with 0.1% (v/v) TFA, solvent A) and MeCN (with 0.1% (v/v) TFA, solvent B) solutions and with a flow rate of 3 mL/min using the specific solvent gradient as indicated. The fractions containing the pure product were combined and the solvent was lyophilized to afford the arylated bioconjugates as powders.

L-Glutathione *S*-(4-fluorophenyl) (5.7)

The general procedure for peptide thiol arylation was followed using (Me-DalPhos)AuCl (26 mg, 0.039 mmol, 2.0 equiv), $AgSbF_6$ (13 mg, 0.039 mmol, 2.0 equiv), *p*-fluoroiodobenzene (22 µL, 0.19 mmol, 10 equiv), and L-glutathione (6 mg, 0.02 mmol, 1 equiv). Yield: 4 mg, 0.01 mmol, 50%. The following solvent gradient was used for HPLC purification: 0–5 min, A (100%); 5–65 min, A (100–60%) : B (0–40%); 65–75 min, A (60–0%) : B (40–100%).

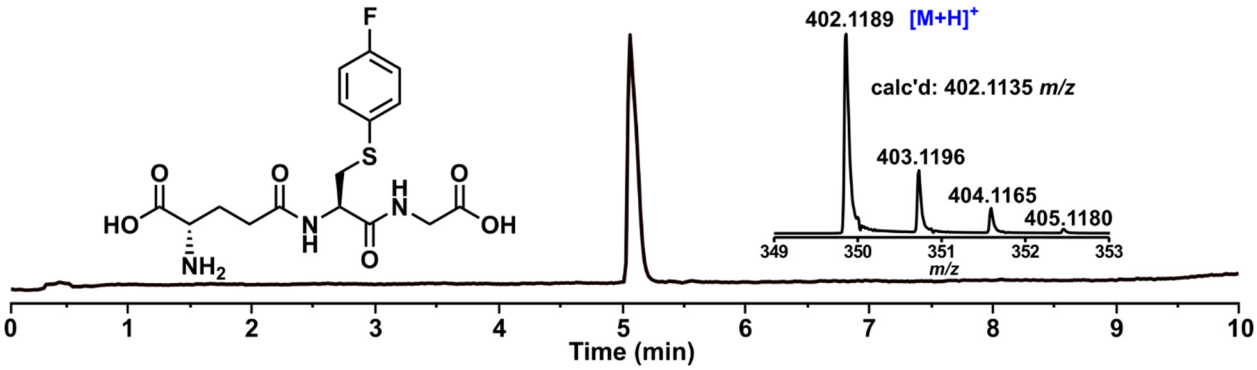

Figure 5.5. LC-MS data of L-glutathione *S*-(4-fluorophenyl) **5.7**.

H-Asp-Arg-Lys-Cys(4-fluorophenyl)-Ala-Thr-NH_2 (5.8)

The general procedure for peptide thiol arylation was followed using (Me-DalPhos)AuCl (17 mg, 0.026 mmol, 2.0 equiv), $AgSbF_6$ (9 mg, 0.03 mmol, 3 equiv), *p*-fluoroiodobenzene (15 µL, 0.13 mmol, 15 equiv), and H-Asp-Arg-Lys-Cys-Ala-Thr-NH_2 (**5.17)** (6 mg, 0.009 mmol, 1 equiv). Yield: 3 mg, 0.004 mmol, 42%. The following solvent gradient was used for HPLC purification: 0–5 min, A (100%); 5–45 min, A (100–60%) : B (0–40%); 45–60 min, A (60–0%) : B (40–100%). The fractions containing the pure product were combined and the solvent was lyophilized to afford the purified peptide, which was stored at -20 °C prior to use.

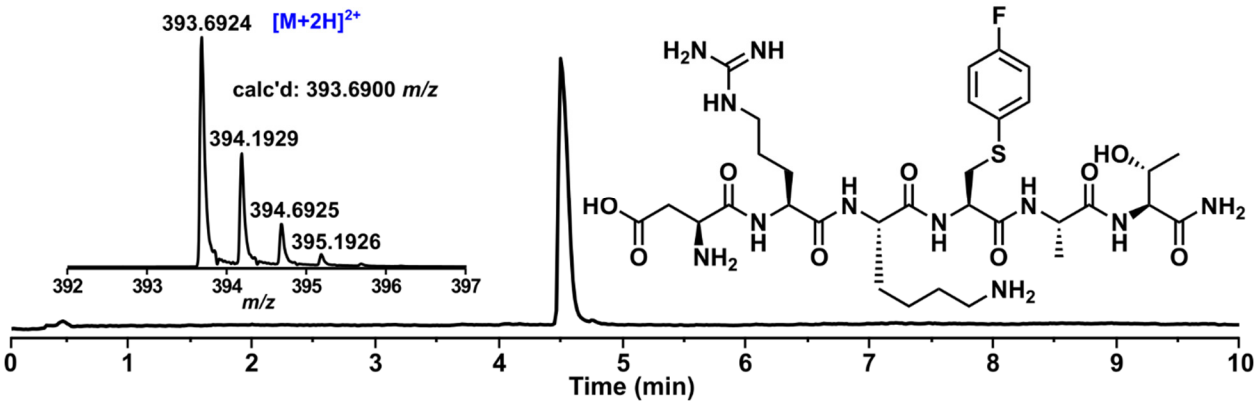

Figure 5.6. LC-MS data of H-Asp-Arg-Lys-Cys(4-fluorophenyl)-Ala-Thr-NH_2 **5.8**.

H-Cys(4-fluorophenyl)-Arg-Gly-Asp-NH_2 (5.9)

The general procedure for peptide thiol arylation was followed using (Me-DalPhos)AuCl (22 mg, 0.034 mmol, 2.0 equiv), $AgSbF_6$ (12 mg, 0.034 mmol, 2.0 equiv), *p*-fluoroiodobenzene (20 µL, 0.17 mmol, 10 equiv), and H-Cys-Arg-Gly-Asp-NH_2 (**5.18**) (8 mg, 0.02 mmol, 1 equiv). Yield: 5 mg, 0.009 mmol, 47%. The following solvent gradient was used for HPLC purification: 0–5 min, A (100%); 5–40 min, A (100–60%) : B (0–40%); 40–60 min, A (60–0%) : B (40–100%). The fractions containing the pure product were combined and the solvent was lyophilized to afford the purified peptide, which was stored at -20 °C prior to use.

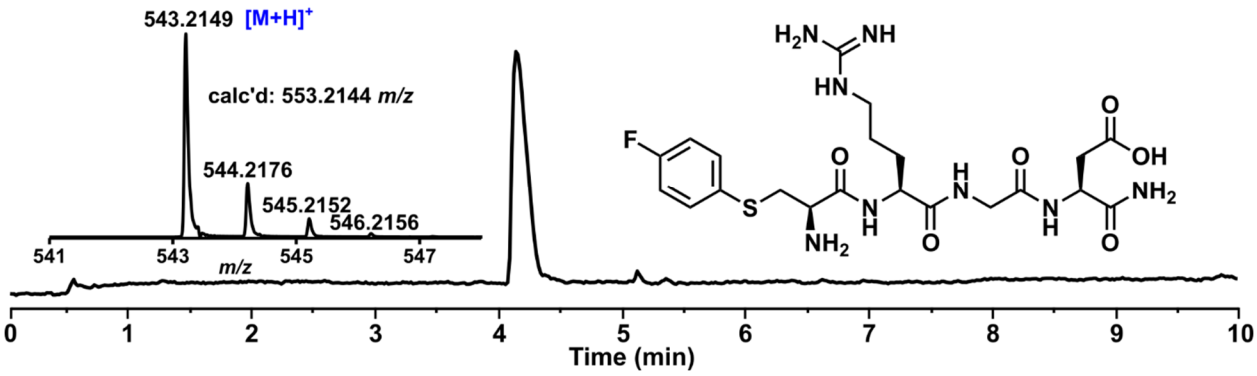

Figure 5.7. LC-MS data of H-Cys(4-fluorophenyl)-Arg-Gly-Asp-NH_2 **5.9**.

***c*(Arg-Gly-Asp-Phe-Cys(4-fluorophenyl)) (5.10)**

The general procedure for peptide thiol arylation was followed using (Me-DalPhos)AuCl (10 mg, 0.016 mmol, 3.0 equiv), $AgSbF_6$ (5 mg, 0.02 mmol, 3 equiv), *p*-fluoroiodobenzene (9 µL, 0.08 mmol, 15 equiv), and *c*(Arg-Gly-Asp-Phe-Cys) (3 mg, 0.005 mmol, 1 equiv). Yield: 2 mg, 0.003 mmol, 59%. The following solvent gradient was used for HPLC purification: 0–5 min, A (100%); 5–40 min, A (100–60%) : B (0–40%); 40–60 min, A (60–0%) : B (40–100%).

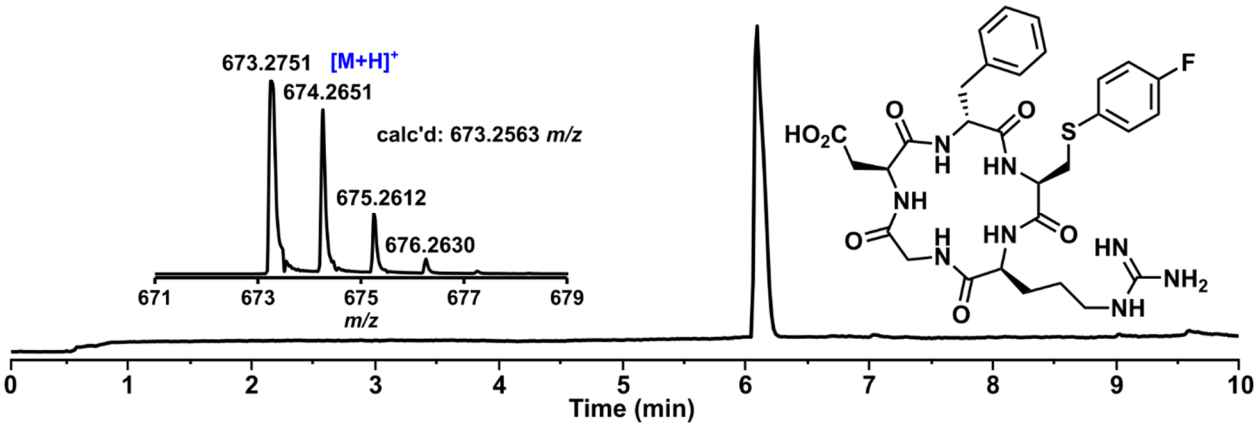

Figure 5.8. LC-MS data of c(Arg-Gly-Asp-Phe-Cys(4-fluorophenyl)) **5.10**.

Amyloid-β fragment H-Gly-Cys(4-fluorophenyl)-Gly-Lys-Lys-Gly-Met-Val-Gly-Gly-Val-Val-OH (5.11)

The general procedure for peptide thiol arylation was followed using (Me-DalPhos)AuCl (11 mg, 0.016 mmol, 3.0 equiv), $AgSbF_6$ (5 mg, 0.02 mmol, 3 equiv), *p*-fluoroiodobenzene (9 µL, 0.08 mmol, 15 equiv), and H-Gly-Cys-Gly-Lys-Lys-Gly-Met-Val-Gly-Gly-Val-Val-OH (6 mg, 0.005 mmol, 1 equiv). Yield: 4 mg, 0.003 mmol, 67%. The following solvent gradient was used for HPLC purification: 0–5 min, A (100%); 5–45 min, A (100–60%) : B (0–40%); 45–65 min, A (60–0%) : B (40–100%).

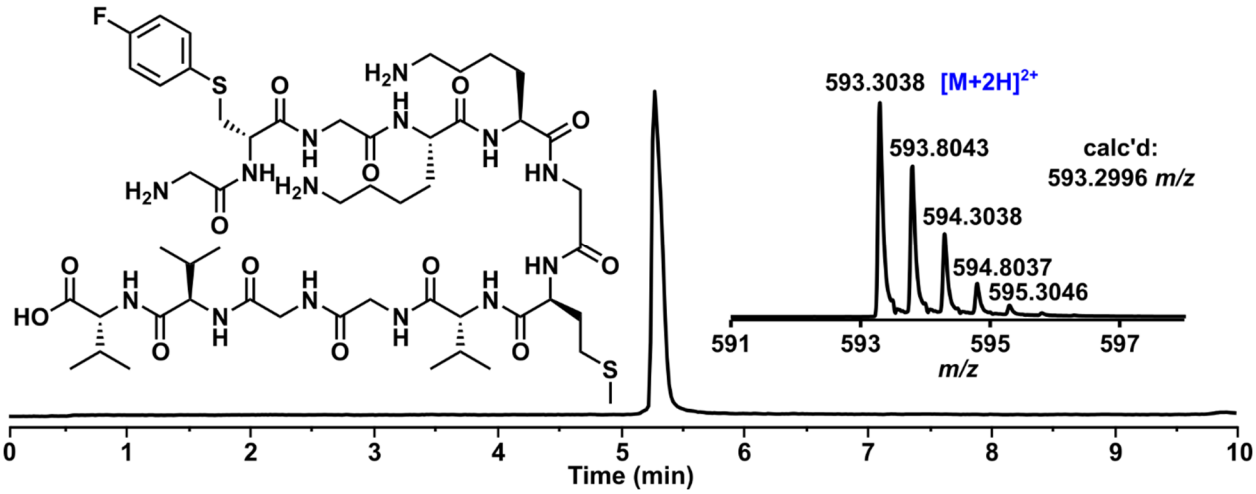

Figure 5.9. LC-MS data of H-Gly-Cys(4-fluorophenyl)-Gly-Lys-Lys-Gly-Met-Val-Gly-Gly-Val-Val-OH **5.11**.

β-D-Glucose *S*-(4-fluorophenyl) (5.12)

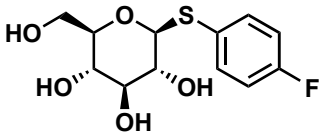

To a cooled (-20 °C) DCM solution (0.75 mL) containing (Me-DalPhos)AuCl (21 mg, 0.032 mmol, 1.0 equiv) and *p*-fluoroiodobenzene (18 μL, 0.16 mmol, 5.0 equiv) was added a cooled (-20 °C) DCM solution (0.75 mL) of $AgSbF_6$ (11 mg, 0.032 mmol, 1.0 equiv) under protection from light. The reaction mixture immediately changed color from colorless to bright yellow concomitant with the precipitation of yellow precipitate. The reaction mixture was filtered through a pad of Celite to remove liberated AgI, and the resulting bright yellow filtrate was dried under reduced pressure to yield the crude [(Me-DalPhos)Au(4-fluorobenzene)Cl][SbF_6] salt as a yellow residue. To a solution of Na[1-thio-β-D-glucose] (7 mg, 0.03 mmol, 1 equiv) in H_2O (1 mL) was added a solution of the crude [(Me-DalPhos)Au(4-fluorobenzene)Cl][SbF_6] salt in MeCN (1 mL) at 25 °C. Pale yellow solids precipitated from the reaction mixture immediately upon addition, and the

resulting suspension was sonicated for 15 min at 25 °C, and then all volatiles were removed from the resulting colorless suspension under reduced pressure. To the solid residue was added H_2O (2 mL), resulting in a colorless suspension. The suspension was centrifuged (2,200 × g, 5 min), and the supernatant was removed and filtered through a 0.45 μm PTFE filter. The H_2O was lyophilized to afford the *S*-aryl conjugate **5.12** (6 mg, 0.02 mmol, 69% yield) as a colorless powder.

^{1}H NMR (400 MHz, D_2O, 25 °C, δ): 7.59 (dd, *J* = 8.0, 8.0 Hz, 2H), 7.14 (t, *J* = 8.0 Hz, 2H), 4.68 (d, *J* = 12.0 Hz, 1H), 3.87 (d, *J* = 12.0 Hz, 1H), 3.70 (dd, *J* = 12.0, 8.0 Hz, 1H), 3.49-3.30 (m, 3H), 3.28 (t, *J* = 8.0 Hz, 1H) ppm.

^{13}C NMR (125 MHz, D_2O, 25 °C, δ): 162.6 (d, *J* = 243.8 Hz), 134.6 (d, *J* = 8.8 Hz), 126.5 (d, *J* = 2.5 Hz), 116.0 (d, *J* = 21.3 Hz), 87.4, 79.7, 77.0, 71.4, 69.2, 60.6 ppm.

^{19}F NMR (376 MHz, D_2O, 25 °C, δ): -113.88 ppm.

HRMS: m/z $[M+Na]^+$ Calc'd for $C_{12}H_{15}FO_5SNa$ 313.0522; Found 313.0522.

β-D-Galactose *S*-(4-fluorophenyl) (5.13)

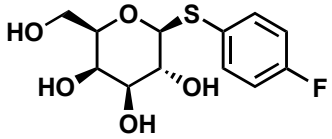

To a cooled (-20 °C) DCM solution (0.75 mL) containing (Me-DalPhos)AuCl (21 mg, 0.032 mmol, 1.0 equiv) and *p*-fluoroiodobenzene (18 μL, 0.16 mmol, 5.0 equiv) was added a cooled (-20 °C) DCM solution (0.75 mL) of $AgSbF_6$ (11 mg, 0.032 mmol, 1.0 equiv) under protection from light. The reaction mixture immediately changed color from colorless to bright yellow concomitant with the precipitation of yellow precipitate. The reaction mixture was filtered through a pad of Celite to remove liberated AgI, and the resulting bright yellow filtrate was dried under reduced pressure to yield the crude [(Me-DalPhos)Au(4-fluorobenzene)Cl][SbF_6] salt as a yellow residue.

To a solution of Na[1-thio-β-D-galactose] (7 mg, 0.03 mmol, 1 equiv) in H_2O (1 mL) was added a solution of the crude [(Me-DalPhos)Au(4-fluorobenzene)Cl][SbF_6] salt in MeCN (1 mL) at 25 °C. Pale yellow solids precipitated from the reaction mixture immediately upon addition, and the resulting suspension was sonicated for 15 min at 25 °C, and then all volatiles were removed from the resulting colorless suspension under reduced pressure. To the solid residue was added H_2O (2 mL), resulting in a colorless suspension. The suspension was centrifuged (2,200 × g, 5 min), and the supernatant was removed and filtered through a 0.45 μm PTFE filter. The H_2O was lyophilized to afford the *S*-aryl conjugate **13** (4 mg, 0.01 mmol, 46% yield) as a colorless powder.

^{1}H NMR (400 MHz, D_2O, 25 °C, δ): 7.59 (dd, *J* = 8.0, 4.0 Hz, 2H), 7.13 (t, *J* = 8.0 Hz, 2H), 4.66 (d, *J* = 12.0 Hz, 1H), 3.96 (d, *J* = 4.0 Hz, 1H), 3.76-3.64 (m, 4H), 3.57 (dd, *J* = 8.0, 8.0 Hz, 1H) ppm.

^{13}C NMR (125 MHz, D_2O, 25 °C, δ): 162.4 (d, *J* = 243.8 Hz), 134.1 (d, *J* = 7.5 Hz), 127.2 (d, *J* = 2.5 Hz), 116.0 (d, *J* = 22.5 Hz), 88.3, 78.8, 73.8, 69.0, 68.5, 60.8 ppm.

^{19}F NMR (376 MHz, D_2O, 25 °C, δ): -114.26 ppm.

HRMS m/z $[M+Na]^+$ Calc'd for $C_{12}H_{15}FO_5SNa$ 313.0522; Found 313.0522.

Mono-(6-*S*-(4-fluorophenyl)-6-deoxy)-β-cyclodextrin (5.14)

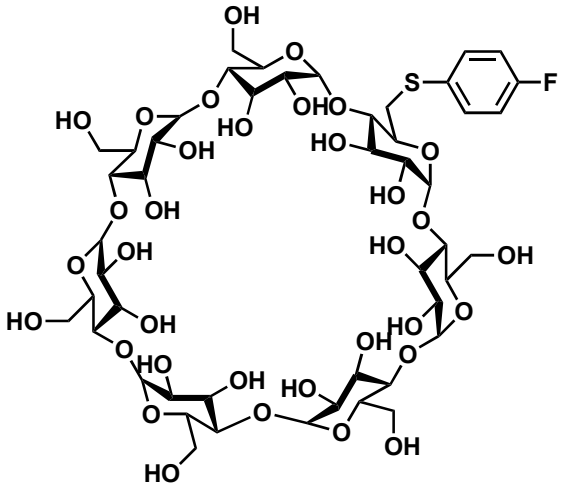

To a cooled (-20 °C) DCM solution (0.75 mL) containing (Me-DalPhos)AuCl (9 mg, 0.01 mmol, 1 equiv) and 4-fluoroiodobenzene (8 μL, 0.07 mmol, 5 equiv) was added a cooled (-20 °C) DCM solution (0.75 mL) of $AgSbF_6$ (5 mg, 0.01 mmol, 1 equiv) under protection from light. The reaction mixture immediately changed from colorless to bright yellow concomitant with the precipitation of yellow precipitate. The reaction mixture was filtered through a pad of Celite to remove liberated AgI, and the resulting bright yellow filtrate was dried under reduced pressure to yield the crude [(Me-DalPhos)Au(4-fluorobenzene)Cl][SbF_6] salt as a yellow residue. To a solution of mono-(6-mercapto-6-deoxy)-β-cyclodextrin (15 mg, 0.013 mmol, 1.0 equiv) and K_3PO_4 (8 mg, 0.04 mmol, 3 equiv) in H_2O (1 mL) was added a solution of the crude [(Me-DalPhos)Au(4-fluorobenzene)Cl][SbF_6] salt in MeCN (1 mL) at 25 °C. Pale yellow solids precipitated from the reaction mixture immediately upon addition, and the resulting suspension was sonicated for 15 min at 25 °C, and then all volatiles were removed from the resulting colorless suspension under reduced pressure. To the solid residue was added H_2O (4.5 mL), resulting in a colorless suspension. The suspension was sonicated (5 min), and then centrifuged (2,200 × g, 5 min), and the supernatant was removed and filtered through a 0.45 μm PTFE filter into a Pall Microsep™ Advance 1K

Omega Centrifugal Filter sample reservoir. The device was capped and centrifuged for 75 min at 7,500 × g. The device was then removed from the centrifuge, the solution in the filtrate receiver tube removed, and H_2O (5 mL) was added to the reservoir containing the aqueous solution of the product. This process was repeated twice more for a total of three centrifuge cycles. After the third cycle, the solution in the sample reservoir (ca. 0.5 mL) was removed, transferred to a 15 mL conical tube, and the H_2O was lyophilized overnight to afford the *S*-aryl conjugate **5.14** (8 mg, 0.006 mmol, 49% yield) as a colorless powder.

^{1}H NMR (400 MHz, D_2O, 25 °C, δ): 7.53 (dd, *J* = 8.5, 5.5 Hz, 2H), 7.13 (t, *J* = 8.8 Hz, 2H), 5.14-4.99 (m, 7H), 3.93-3.40 (m, 37H) ppm.

^{13}C NMR (125 MHz, D_2O, 25 °C, δ): 164.7 (d, *J* = 371.3 Hz), 129.3, 125.3, 115.9 (d, *J* = 21.3 Hz), 101.8, 81.1, 73.7, 73.3, 73.3, 73.1, 72.8, 72.2, 72.1, 72.0, 71.9, 71.8, 71.8, 71.4, 60.1, 59.8 ppm.

^{19}F NMR (376 MHz, D_2O, 25 °C, δ): -113.41 ppm.

HRMS m/z $[M+H]^+$ Calc'd for $C_{48}H_{73}FO_{34}S$ 1245.3688; Found 1245.3766.

5.5.4. Radiochemistry

5.5.4.1. General materials and methods

No-carrier-added [^{18}F]fluoride was produced by the $^{18}O(p,n)^{18}F$ nuclear reaction in a Siemens RDS-112 cyclotron at 11 MeV using a 1 mL tantalum target with havar foil. Unless otherwise stated, reagents and solvents were commercially available and used without further purification. (Me-DalPhos)AuCl was purchased from Sigma Aldrich and 4-fluoroiodobenzene was purchased from Frontier Scientific and both were used as received. HPLC grade acetonitrile and

trifluoroacetic acid were purchased from Fisher Scientific. DI water was obtained from a Water Purification System. Anhydrous dimethylformamide was purchased from Acros Organics and used as received. Reaction glass vials were purchased from Chemglass. Sep-Pak tC18 plus short cartridges (Part No. WAT036810) were purchased from Waters Corporation. Pre-conditioned Sep-Pak® Light QMA cartridges (Part No. K-920) were purchased from ABX advanced biochemical compounds GmbH. Radio-TLCs were analyzed using a miniGITA* TLC scanner. HPLC purifications were performed on a Knauer Smartline HPLC system with inline Knauer UV (254 nm) detector and gamma-radiation coincidence detector and counter (Bioscan Inc.). Semi-preparative HPLC was performed using Phenomenex reverse-phase Luna column (10 × 250 mm, 5 μm). Final purity and identity of compounds were determined by analytical HPLC analysis performed with a Phenomenex reverse-phase Luna column (4.6 × 250 mm, 5 μm). All chromatograms were collected by a GinaStar (Raytest) analog to digital converter and GinaStar software.

HPLC Eluents

Eluent A

Solvent A = H_2O + 0.1% TFA, Solvent B = MeCN + 0.1% TFA, Flow rate = 1.5 mL/min

0 – 2 min = 95% A

2 – 5 min = 95% A to 60% A

5 – 20 min = 60% A to 5% A

20+ min = 5% A

Eluent B

Solvent A = H_2O + 0.1% TFA, Solvent B = MeCN + 0.1% TFA, Flow rate = 4 mL/min

0 – 15 min = 95% to 30% A

15 – 30 min = 30 to 5% A

30+ min = 5% A

Eluent C

Solvent A = H_2O + 0.1% TFA, Solvent B = MeCN + 0.1% TFA, Flow rate = 1 mL/min

0 – 30 = 80% A

Eluent D

Solvent A = H_2O + 0.1% TFA, Solvent B = MeCN + 0.1% TFA

0 – 5 min = 95% A; 2 mL/min to 95% A; 3 mL/min

5 – 30 min = 95% A; 3 mL/min to 60% A; 3 mL/min

30 – 50 min = 60% A; 3 mL/min

50 – 60 min = 60% A; 3 mL/min to 5% A; 3 mL/min

Cartridge Preconditioning:

Sep-Pak tC18 plus short cartridges were preconditioned by sequentially pushing absolute ethanol (5 mL) and H_2O (10 mL) through the cartridge. QMA cartridges were used as received, without further preconditioning.

5.5.4.2. Preparation of 4-[^{18}F]fluoroiodobenzene [^{18}F]5.2

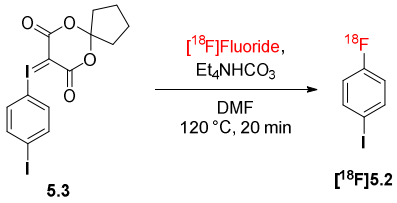

4-[^{18}F]Fluoroiodobenzene **[^{18}F]5.2** was prepared via a spirocyclic hypervalent iodine(III)-mediated radiofluorination methodology.[41] Radiofluorination of iodonium ylide **5.3** was performed on an ELIXYS automated radiosynthesizer (Sofie Biosciences). [^{18}F]Fluoride was delivered to the ELIXYS in [^{18}O]H_2O (1 mL) via nitrogen gas push and trapped onto a QMA anion-exchange cartridge to remove the [^{18}O]H_2O. Trapped [^{18}F]fluoride was subsequently eluted into the reaction vial using a solution of Et_4NHCO_3 (4.8 – 5.2 mg, 25 – 27 μmol) in acetonitrile and water (1.2 mL, 9:3 v:v). The vial contents were evaporated by heating the vial to 110 °C while applying a vacuum for 5 min, with stirring. Acetonitrile (1.2 mL) was passed through the QMA cartridge to wash remaining activity into the reaction vial. The combined contents in the reaction vial were dried by azeotropic distillation (heating to 110 °C while applying a vacuum, with stirring) for 5 min. Anhydrous acetonitrile (1.2 mL) was directly added to the reaction vial and azeotropic distillation was repeated once more until dryness, 5 min. The reaction vial was cooled to 30 °C under nitrogen pressure. To the dry [^{18}F]fluoride, freshly prepared* iodonium ylide **5.3** (5 mg, 10 μmol) in anhydrous DMF (1.2 mL) was added and the contents were stirred at 120 °C for 20 min. The reaction mixture was cooled to 23 °C and quenched with H_2O (3.8 mL).

Note: The iodonium ylide **5.3** must be freshly prepared in solution. Rapid decomposition of the ylide precursor was observed when it was allowed to sit in solution for prolonged periods of time (1-2 h) which resulted in a significant decrease in radiochemical yield of 4-[^{18}F]fluoroiodobenzene

[^{18}F]5.2. See image below of precursor ylide **5.3** in DMSO-d_6 at 23 °C, on the benchtop after 20 min, 4 h and 24 h time periods.

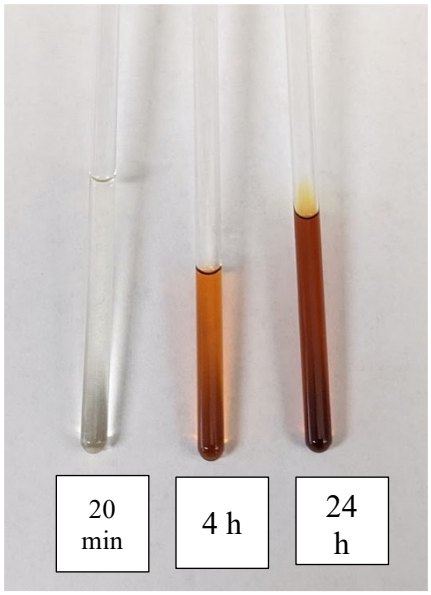

An aliquot of the crude reaction mixture was spotted on a silica gel coated TLC plate, developed in a glass chamber using EtOAc as the eluent and analyzed by radio-TLC using a miniGITA* TLC scanner. The radiochemical yield, RCY_{TLC}, was calculated by dividing the integrated area of the ^{18}F-fluorinated product peak by the total integrated area of all peaks on the TLC and multiplying by 100 to convert to percentage units. Analytical HPLC was used to confirm product identity and purity via UV absorbance at 254 nm by coinjection with the ^{19}F-reference standard. An aliquot of the crude reaction mixture was added to the ^{19}F-reference standard (1 mg/mL) in methanol and the sample was injected into the analytical HPLC.

The crude solution was injected into the semi-preparative HPLC for purification using Eluent B. The purified 4-[^{18}F]fluoroiodobenzene **[^{18}F]5.2** was collected in a glass walled centrifuge tube (50 mL) containing water (40 mL) and passed through a Sep-Pak tC18 plus short cartridge. The trapped

4-[^{18}F]fluoroiodobenzene **[^{18}F]5.2** was dried with pressurized nitrogen and subsequently eluted from the cartridge into a 20 mL borosilicate scintillation vial with DCM (2 mL). The isolated RCY was determined by measuring the final activity of the HPLC-purified 4-[^{18}F]fluoroiodobenzene **[^{18}F]5.2** versus starting [^{18}F]fluoride activity and is decay corrected.

Table 5.3. Preparation of 4-[^{18}F]fluoroiodobenzene **[^{18}F]5.2**

Entry	**Starting Activity (mCi)**	**Isolated Activity after Purification (mCi)**	**Synthesis Time (min)[a]**	**RCY$_{TLC}$ (%)[b]**	**Isolated RCY (%)[c]**
1	65.5	5.6	105	33	17
2	45.5	6.7	95	44	27
3	76.5	18.4	87	70	42
4	79.6	12.4	84	59	27
5	78.2	10.3	94	48	24
6	74.6	16.5	98	70	41
7	103.2	12.8	102	45	24
8	72.5	17.4	83	53	41
9	75.5	13.0	85	48	29
10	94.0	12.0	94	32	23
11	104.8	18.3	105	58	34
12	107.7	11.5	94	45	19
13	117.8	15.0	80	66	21
14	177.5	20.2	92	43	20
15	116.4	11.3	88	43	17
16	125.8	16.4	85	47	22
17	115.5	15.6	86	61	23
18	139.3	16.1	87	47	20
19	147.1	17.8	95	44	22
20	144.3	22.1	89	40	27
Mean ± SD			***91 ± 7***	***50 ± 11***	***26 ± 8***

[a]Calculated as the time to obtain HPLC-purified 4-[^{18}F]fluoroiodobenzene **[^{18}F]5.2** relative to aqueous [^{18}F]fluoride; [b]RCY$_{TLC}$ was determined by radio-TLC analysis of the crude product; [c]Isolated RCY is decay corrected.

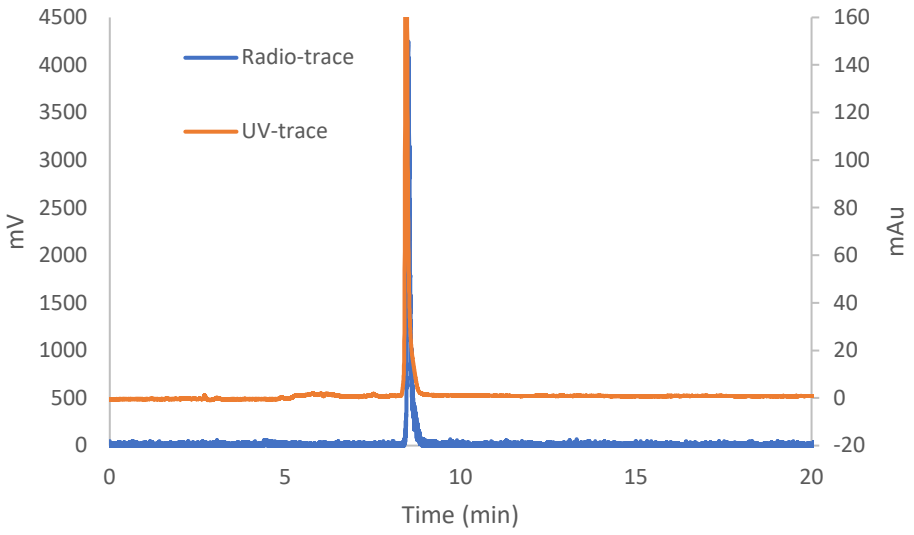

Figure 5.10. Analytical HPLC trace. Coinjection of purified 4-[^{18}F]fluoroiodobenzene **[^{18}F]5.2** (radio-HPLC trace = blue) with the authentic ^{19}F reference standard (UV trace = orange)

5.5.4.3. Preparation of [(Me-DalPhos)Au(4-[^{18}F]fluorobenzeneCl][SbF_6] [^{18}F]5.1

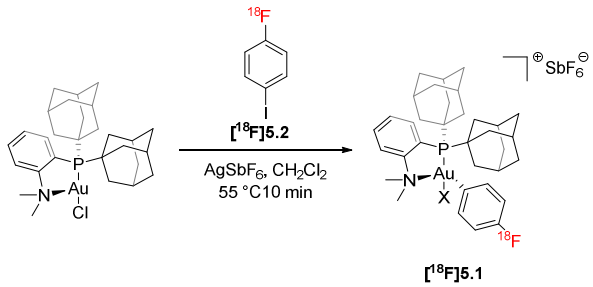

To a 1-dram scintillation vial with (Me-DalPhos)AuCl (6 mg, 9 µmol) was added 4-[^{18}F]fluoroiodobenzene **[^{18}F]5.2** (~500 µCi) in DCM (0.5 – 1.0 mL). The solution was stirred and a suspension of $AgSbF_6$ (3 mg, 9 µmol) in DCM (0.5 – 1.0 mL) was added. The vial was sealed with a Teflon lined cap and heated at 55 °C in an aluminum heating block while stirring for 10 min. The reaction mixture was allowed to cool to room temperature for 5 min. The cooled solution was filtered through Celite (***Figure 5.11***) to yield crude **[^{18}F]5.1** in DCM (1.5 mL).

Figure 5.11. Picture of the homemade cartridge for filtration of AgI. A filter frit was added to a disposable polypropylene column. To it, was added Celite and another filter frit. The disposable column was fitted with luer-slip style adapter and the bottom was loosely taped to a reaction vial with a stir bar (not shown). The crude reaction suspension was transferred to the homemade cartridge using a needle and syringe. The solution was filtered through the Celite using air, pushed from a 10-mL syringe attached to the luer-slip adapter. The cartridge and tape were then removed to yield the filtrate in the reaction vial

An aliquot of the crude reaction mixture was spotted on a silica gel coated TLC plate, developed in a glass chamber with EtOAc as the eluent and analyzed using a miniGITA* TLC scanner. The **[^{18}F]5.1** complex is highly polar and remains on the baseline of the TLC while the unreacted 4-[^{18}F]fluoroiodobenzene **[^{18}F]5.2** travels with the solvent front. Because all unreacted [^{18}F]fluoride has been removed by HPLC purification, the baseline peak is presumed to be solely **[^{18}F]5.1**. The RCY_{TLC} was calculated by dividing the integrated area of the ^{18}F-fluorinated product peak (on the baseline) by the total integrated area of all peaks on the radio-TLC and multiplying by 100 to

convert to percentage units. Analytical HPLC was used to confirm product identity and purity via UV absorbance at 254 nm by coinjection with the ^{19}F-reference standard.

Table 5.4. Preparation of Gold(III) complex **[^{18}F]5.1**

Entry	**RCY$_{TLC}$ (%)[a] (10 min)**
1	83
2	94
3	86
4	100
5	100
6	95
7	100
8	100
9	100
Mean ± SD	***95 ± 7***

[a]RCY$_{TLC}$ was determined by radio-TLC analysis of the crude product.

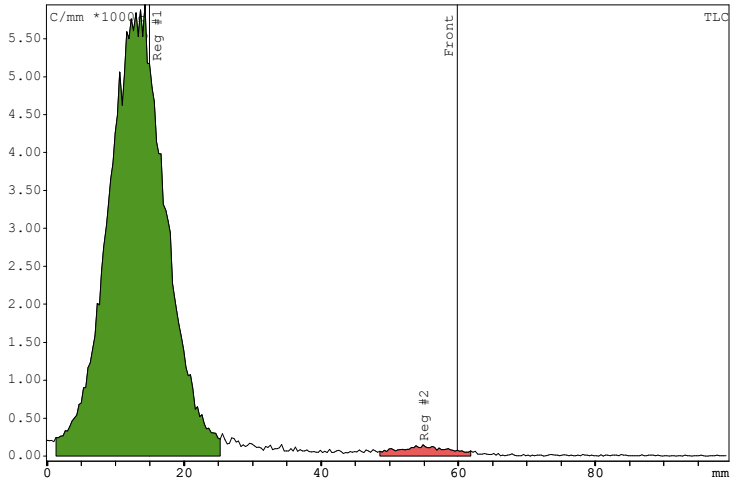

Figure 5.12. Radio-TLC scan of crude **[^{18}F]5.1** (green) and unreacted [^{18}F]-4-fluoroiodobenzene **[^{18}F]5.2** (red). TLC plate mobile phase = EtOAc.

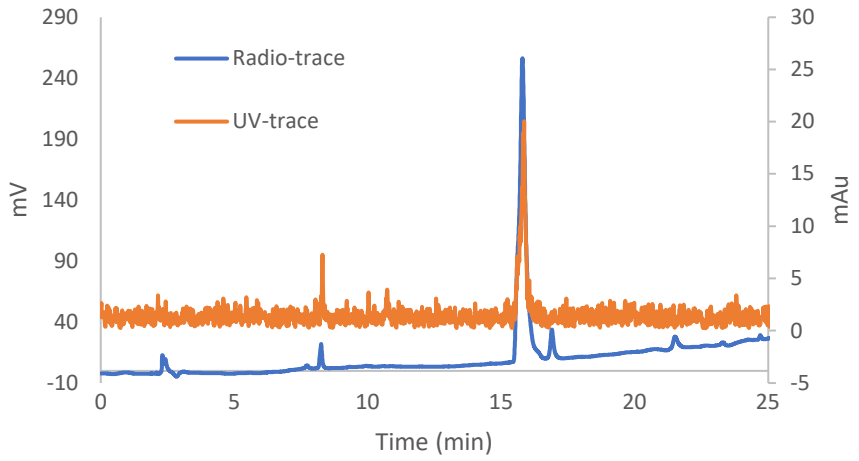

Figure 5.13. Analytical HPLC trace. Coinjection of crude **[^{18}F]5.1** (radio-HPLC trace = blue) with the authentic ^{19}F reference standard (UV trace = orange)

5.5.4.4. ^{18}F-Oxidative addition optimization

Table 5.5. Optimization of precious metal mass for oxidative addition[a]

Entry	Au(I) amount[b] mg	$AgSbF_6$ amount[b] mg	RCY_{TLC} (%)[b]	***RCY_{TLC} (%) Mean ± SD (Count)***
1	10 (1.5 equiv)	5 (1.5 equiv)	18	***38 ± 27 (n = 4)***
2	10 (1.5 equiv)	5 (1.5 equiv)	33	
3	10 (1.5 equiv)	5 (1.5 equiv)	22	
4	10 (1.5 equiv)	5 (1.5 equiv)	77	
5	8 (1.2 equiv)	4 (1.2 equiv)	55	***49 ± 15 (n = 4)***
6	8 (1.2 equiv)	4 (1.2 equiv)	66	
7	8 (1.2 equiv)	4 (1.2 equiv)	33	
8	8 (1.2 equiv)	4 (1.2 equiv)	41	
9	6 (0.9 equiv)	3 (0.9 equiv)	83	***93 ± 8 (n = 5)***
10	6 (0.9 equiv)	3 (0.9 equiv)	94	
11	6 (0.9 equiv)	3 (0.9 equiv)	86	
12	6 (0.9 equiv)	3 (0.9 equiv)	100	
13	6 (0.9 equiv)	3 (0.9 equiv)	100	

[a]Reaction conditions: 4-[^{18}F]fluoroiodobenzene (~500 μCi), dichloromethane (1.5 mL), 55 °C, 10 min. RCY_{TLC} was determined by radio-TLC analysis of the crude product. [b]equiv are relative to ylide precursor **5.3**.

Table 5.6. Optimization of reaction temperature and time for Oxidative Addition

Entry	Solvent	Time (min.)	Temperature (°C)	RCY_{TLC} (%)	***RCY_{TLC} (%) Mean ± SD (Count)***
1	DCM	10	55	83	***95 ± 7 (n = 9)***
2	DCM	10	55	94	
3	DCM	10	55	86	
4	DCM	10	55	100	
5	DCM	10	55	100	
6	DCM	10	55	95	
7	DCM	10	55	100	
8	DCM	10	55	100	
9	DCM	10	55	100	

10	DCE	10	60	79	***87 ± 8 (n = 3)***
11	DCE	10	60	87	
12	DCE	10	60	94	
13	DCE	10	80	91	***83 ± 15 (n = 7)***
14	DCE	10	80	98	
15	DCE	10	80	99	
16	DCE	10	80	77	
17	DCE	10	80	60	
18	DCE	10	80	91	
19	DCE	10	80	68	
20	DCE	20	80	88	***94 ± 6 (n = 5)***
21	DCE	20	80	100	
22	DCE	20	80	97	
23	DCE	20	80	98	
24	DCE	20	80	87	
25	DCM	20	55	45	***87 ± 16 (n = 27)***
26	DCM	20	55	87	
27	DCM	20	55	95	
28	DCM	20	55	96	
29	DCM	20	55	96	
30	DCM	20	55	95	
31	DCM	20	55	93	
32	DCM	20	55	84	
33	DCM	20	55	87	
34	DCM	20	55	100	
35	DCM	20	55	100	
36	DCM	20	55	100	
37	DCM	20	55	100	
38	DCM	20	55	98	
41	DCM	20	55	75	
42	DCM	20	55	95	
43	DCM	20	55	100	
44	DCM	20	55	100	
45	DCM	20	55	100	
46	DCM	20	55	74	
47	DCM	20	55	73	
48	DCM	20	55	86	
49	DCM	20	55	46	
50	DCM	20	55	83	

51	DCM	20	55	53	
52	DCM	20	55	100	
53	DCM	20	55	95	

[a]Reaction conditions: 4-[^{18}F]fluoroiodobenzene **[^{18}F]5.2** (~5 mCi), (Me-DalPhos)AuCl (6 mg, 0.9 equiv), $AgSbF_6$ (3 mg, 0.9 equiv), solvent (1.5 mL). RCY_{TLC} was determined by radio-TLC analysis of the crude product.

5.5.5. Thiol Arylations

5.5.5.1. Optimization of thiol arylation

Commercial L-glutathione was used for all optimization screens unless otherwise noted. The tables in each section describe the reaction conditions used, with the variable being tested denoted in the table title.

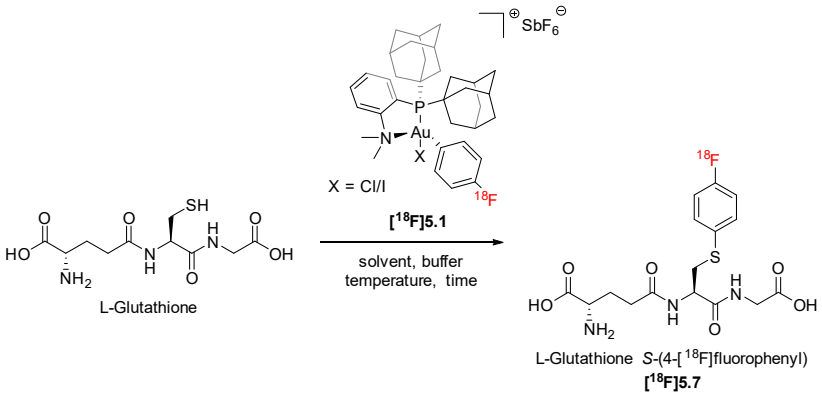

Table 5.7. Optimization of reaction solvent[a]

Entry	Solvent	RCY (%)	*RCY (%) Mean ± SD (Count)*
1	Tris Buffer pH 8.0	42	***54 ± 16***
2	Tris Buffer pH 8.0	65	***(n = 2)***
3	HEPES pH 7.3	30	***43 ± 18***
4	HEPES pH 7.3	55	***(n = 2)***
5	PBS 1X pH 7.4	25	***16 ± 13***
6	PBS 1X pH 7.4	6	***(n = 2)***

[a]Reaction conditions: **[^{18}F]5.1** (~1 mCi), L-glutathione (5 mg), solvent (1 mL), 23 °C, 30 min. RCY was determined by radio-HPLC analysis of the crude product.

Table 5.8. Optimization of reaction temperature[a]

Entry	**Temperature (°C)**	**RCY (%)**	***RCY (%) Mean ± SD (Count)***
1	23	42	***54 ± 16***
2	23	65	***(n = 2)***
3	35	93	***93 ± 1***
4	35	92	***(n = 2)***
5	45	92	***95 ± 4***
6	45	97	***(n = 2)***

[a]Reaction conditions: **[^{18}F]5.1** (~1 mCi), L-glutathione (5 mg), Tris buffer pH 8.0 (1 mL), 30 min. RCY was determined by radio-HPLC analysis of the crude product.

Table 5.9. Optimization of reaction time[a]

Entry	**Time (min)**	**RCY (%)**	***RCY (%) Mean ± SD (Count)***
1	10	43	***44 ± 1***
2	10	45	***(n = 2)***
3	15	91	***78 ± 12***
4	15	76	***(n = 4)***
5	15	63	
6	15	82	
7	20	56	***72 ± 14***
8	20	69	***(n = 6)***
9	20	77	
10	20	83	
11	20	90	
12	20	58	
13	30	92	***93 ± 1***
14	30	93	***(n = 2)***

[a]Reaction conditions: **[^{18}F]5.1** (~1 mCi), L-glutathione (5 mg), Tris buffer pH 8.0 (1 mL), 35 °C. RCY was determined by radio-HPLC analysis of the crude product.

Table 5.10. Re-Optimization of reaction solvent[a]

Entry	Solvent	RCY (%)	*RCY (%) Mean ± SD (Count)*
1[b]	Tris Buffer pH 8.0	63	***78 ± 12 (n = 4)***
2[b]	Tris Buffer pH 8.0	82	
3[b]	Tris Buffer pH 8.0	91	
4[b]	Tris Buffer pH 8.0	76	
5[b]	Tris Buffer pH 8.0 : MeOH (3:1)	95	***97 ± 3 (n = 2)***
6[b]	Tris Buffer pH 8.0 : MeOH (3:1)	99	
7[c]	Tris Buffer pH 8.0	23	***30 ± 7 (n = 3)***
8[c]	Tris Buffer pH 8.0	31	
9[c]	Tris Buffer pH 8.0	36	
10[c]	Tris Buffer pH 8.0 : MeOH (3:1)	99	***97 ± 4 (n = 2)***
11[c]	Tris Buffer pH 8.0 : MeOH (3:1)	94	
12[d]	Tris Buffer pH 8.0	23	***23 (n = 1)***
13[d]	Tris Buffer pH 8.0 : MeOH (3:1)	81	***73 ± 12 (n = 2)***
14[d]	Tris Buffer pH 8.0 : MeOH (3:1)	64	
15[e]	Tris Buffer pH 8.0 : MeOH (3:1)	70	**70 (n = 1)**
16[f]	Tris Buffer pH 8.0 : MeOH (3:1)	52	**52 (n = 1)**

[a]Reaction conditions: **[^{18}F]1** (~1 mCi), L-glutathione (5 mg, 16 µmol), solvent (1 mL), 35 °C, 15 min. RCY was determined by radio-HPLC analysis of the crude product. [b]L-Glutathione. [c]H-Asp-Arg-Lys-Cys-Ala-Thr-NH_2 (7 µmol). [d]H-Cys-Arg-Gly-Asp-NH_2 (11 µmol). [e]L-glutathione (0.71 µmol). [f]L-glutathione (0.39 µmol).

5.5.5.2. Preparation of ^{18}F-labeled conjugate

Following the filtration of the solution of **[^{18}F]5.1**, the DCM was removed via mild heating (55 °C) to afford solid **[^{18}F5.]1** for thiol arylation. To a vial containing prepared **[^{18}F]5.1** was added, a solution of peptide (5 mg) and solvent (Tris buffer pH 8.0, 750 µL : methanol, 250 µL). The combined contents were sealed with a Teflon lined cap and the vial was heated on a hot plate to 35 °C for 15 min. An aliquot of the crude reaction mixture was diluted in buffer (500 µL) and subjected to HPLC analysis. The radiochemical purity (RCP) was calculated by dividing the integrated area of the ^{18}F-labeled product peak by the total integrated area of all ^{18}F-labeled peaks,

as determined by radio-HPLC, and multiplied by 100 to convert to percentage units. The decay-corrected RCY is relative to **[^{18}F]5.1** and was determined by dividing the final activity of the crude ^{18}F-labeled molecule (decay-corrected) by the starting activity of isolated **[^{18}F]5.1**, multiplied by the RCP. Product identity and purity were determined by analytical HPLC, comparing the radio-trace of ^{18}F-labled peptide with the UV-trace of the ^{19}F-reference standard, via coinjection. HPLC mobile phase: Eluent A.

***Note*:** For thioglucose **[^{18}F]5.12**, thiogalactose **[^{18}F]5.13**, and thio-β-cyclodextrin **[^{18}F]5.14**, the solvent system used was MeCN : H_2O (500 µL : 500 µL).

L-Glutathione *S*-(4-[^{18}F]fluorophenyl) ([^{18}F]5.7)

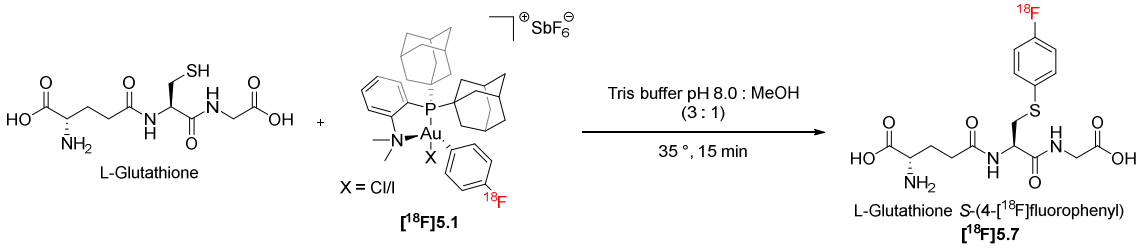

Table 5.11. Thiol arylation to generate L-glutathione S-(4-[^{18}F]fluorophenyl) (**[^{18}F]5.7**)

Entry	Starting Activity (mCi)	Crude Product Activity (mCi)	RCP (%)	RCY (%) (d.c.)
1	0.402	0.360 (0.396 d.c.)	95	93
2	0.385	0.344 (0.378 d.c.)	99	97
Mean ± SD			***97 ± 3***	***95 ± 3***
3[a]	0.129	0.116 (0.128 d.c.)	97	96
4[a]	0.320	0.286 (0.316 d.c.)	98	97
Mean ± SD			***98 ± 1***	***97 ± 1***

[a]L-glutathione (1 mg).

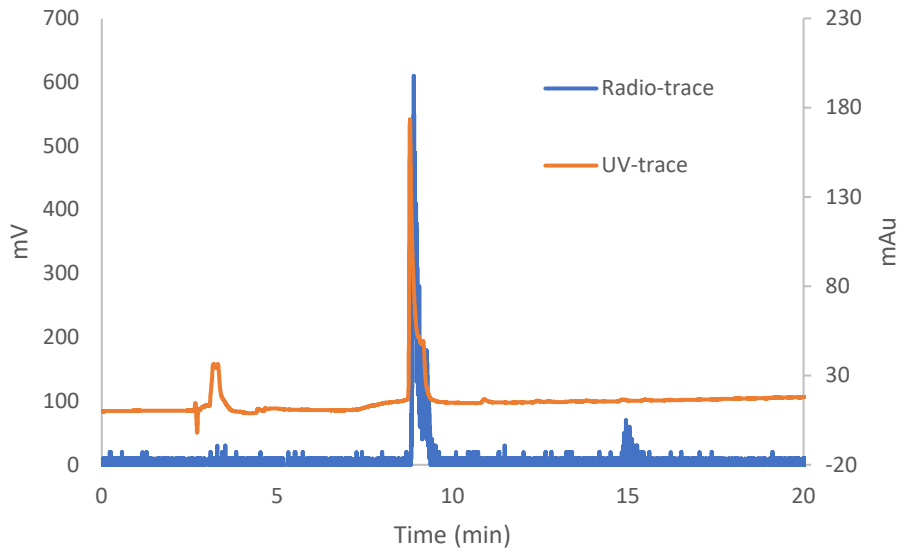

Figure 5.14. Analytical HPLC trace. Coinjection of crude L-glutathione S-(4-[^{18}F]fluorophenyl) (**[^{18}F]5.7**) (radio-HPLC trace = blue) with the purified ^{19}F reference standard (UV trace = orange).

Table 5.12. Isolated yields of HPLC-purified L-glutathione S-(4-[^{18}F]fluorophenyl) (**[^{18}F]5.7**)

	Starting Activity (mCi)	**Starting Time**	**Final Purified Activity (mCi)**	**Final Time**	**Initial Activity (d.c.) (mCi)**	**Isolated RCY (%) (non d.c.)**	**Isolated RCY (%) (d.c.)**
	10.31	12:05	1.21	13:23	6.29	12	19
	7.53	12:01	2.5	12:58	5.25	33	48
Mean ± SD						**22 ± 15**	**33 ± 20**

H-Asp-Arg-Lys-Cys(4-[^{18}F]fluorophenyl)-Ala-Thr-NH$_2$ ([^{18}F]5.8)

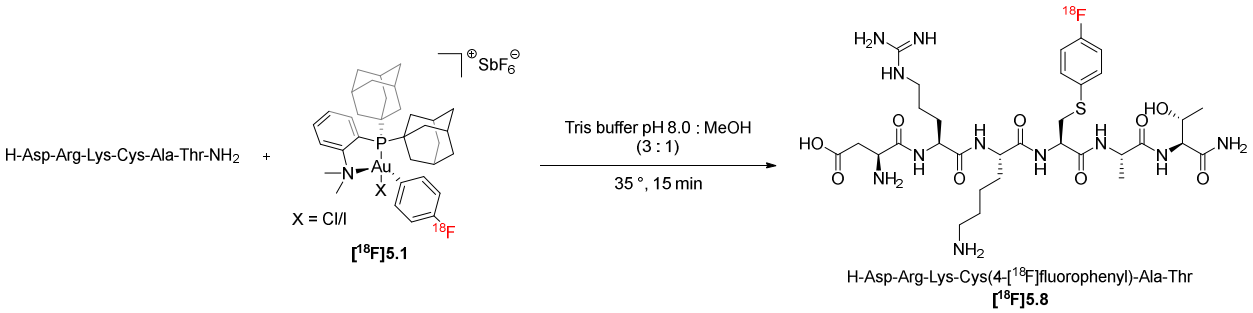

Table 5.13. Thiol arylation to generate H-Asp-Arg-Lys-Cys(4-[^{18}F]fluorophenyl)-Ala-Thr-NH$_2$ **[^{18}F]5.8**

Entry	Starting Activity (mCi)	Crude Product Activity (mCi)	RCP (%)	RCY (d.c.) (%)
1	2.12	1.93 (2.12 d.c.)	99	99
2	1.277	1.162 (1.27 d.c.)	94	94
Mean ± SD			***97 ± 4***	***97 ± 4***
3[a]	0.090	0.081 (0.090 d.c.)	53	53
4[a]	0.089	0.080 (0.089 d.c.)	45	45
Mean ± SD			***49 ± 6***	***49 ± 6***

[a]peptide (0.62 µmol), solvent (750 µL).

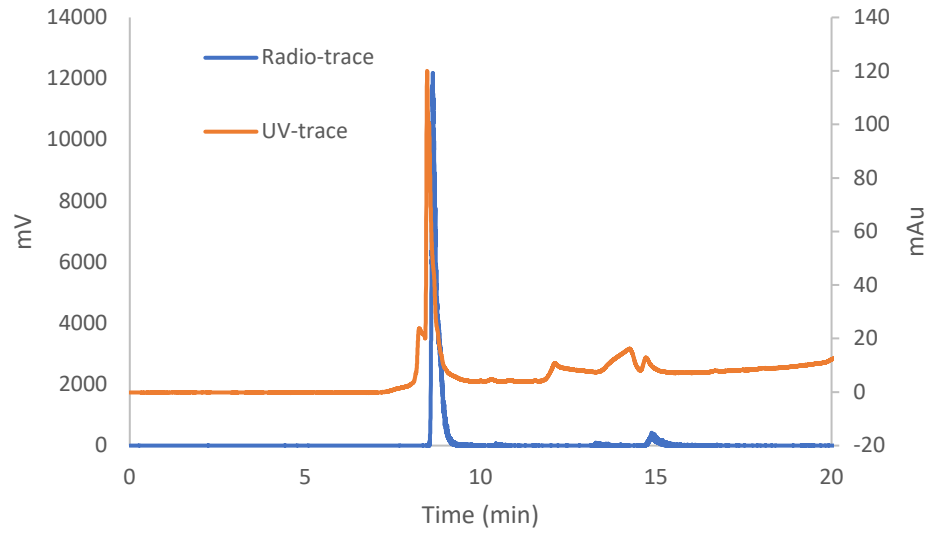

Figure 5.15. Analytical HPLC trace. Coinjection of crude **[^{18}F]5.8** (radio-HPLC trace = blue) with the purified ^{19}F reference standard (UV trace = orange).

H-Cys(4-[^{18}F]fluorophenyl)-Arg-Gly-Asp-NH$_2$ ([^{18}F]5.9)

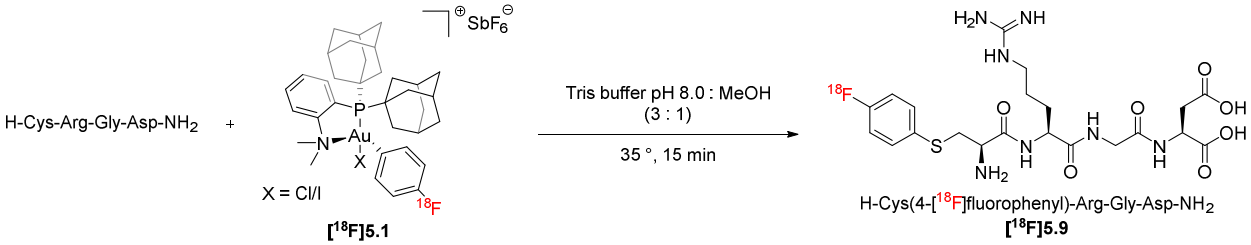

Table 5.14. Thiol arylation to generate H-Cys(4-[^{18}F]fluorophenyl)-Arg-Gly-Asp-NH$_2$ **[^{18}F]5.9**

Entry	Starting Activity (mCi)	Crude Product Activity (mCi)	RCP (%)	RCY (d.c.) (%)
1	2.09	1.818 (2.05 d.c.)	81	79
2	1.01	0.915 (1.01 d.c.)	64	64
Mean ± SD			***73 ± 12***	***72 ± 11***

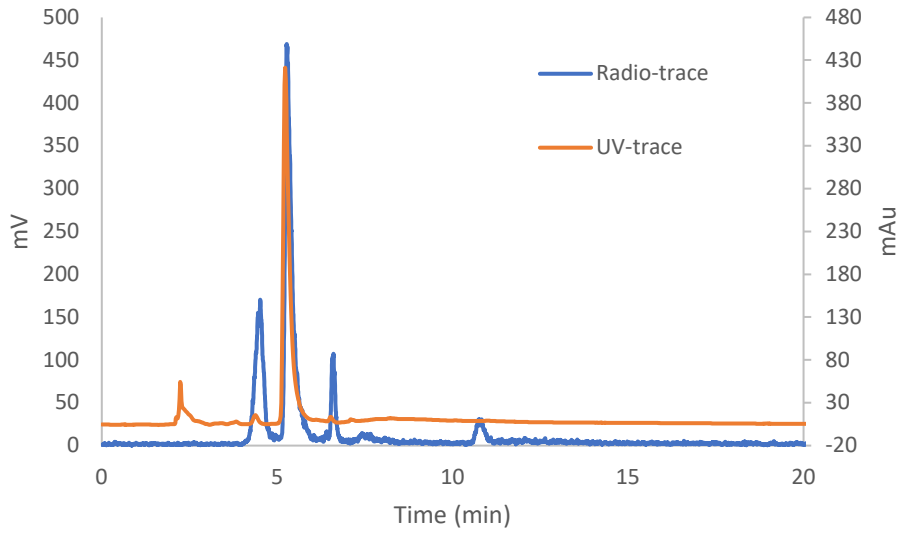

Figure 5.16. Analytical HPLC trace. Coinjection of crude **[^{18}F]5.9** (radio-HPLC trace = blue) with the purified ^{19}F reference standard (UV trace = orange).

c(Arg-Gly-Asp-Phe-Cys(4-[^{18}F]fluorophenyl)) ([^{18}F]5.10)

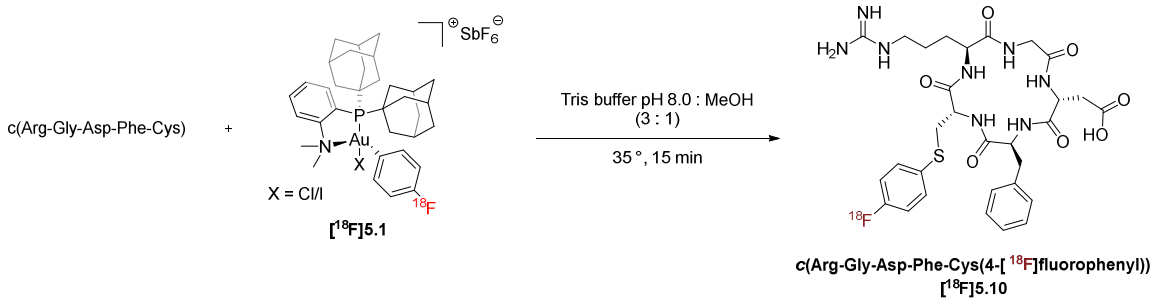

Table 5.15. Thiol arylation to generate c(Arg-Gly-Asp-Phe-Cys(4-[^{18}F]fluorophenyl)) **[^{18}F]5.10**

Entry	Starting Activity (mCi)	Crude Product Activity (mCi)	RCP (%)	RCY (d.c.) (%)
1	1.700	1.588 (1.70 d.c.)	90	90
2	1.540	1.450 (1.54 d.c.)	97	97
Mean ± SD			***94 ± 5***	***94 ± 5***

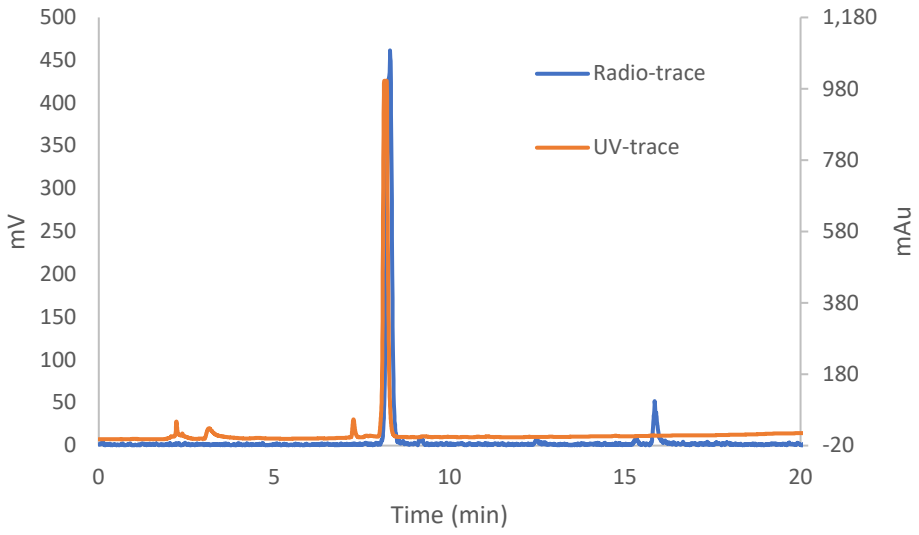

Figure 5.17. Analytical HPLC trace. Coinjection of crude **[^{18}F]5.10** (radio-HPLC trace = blue) with the purified ^{19}F reference standard (UV trace = orange)

Amyloid β fragment, H-Gly-Cys(4-[^{18}F]fluorophenyl)-Gly-Lys-Lys-Gly-Met-Val-Gly-Gly-Val-Val-OH ([^{18}F]5.11)

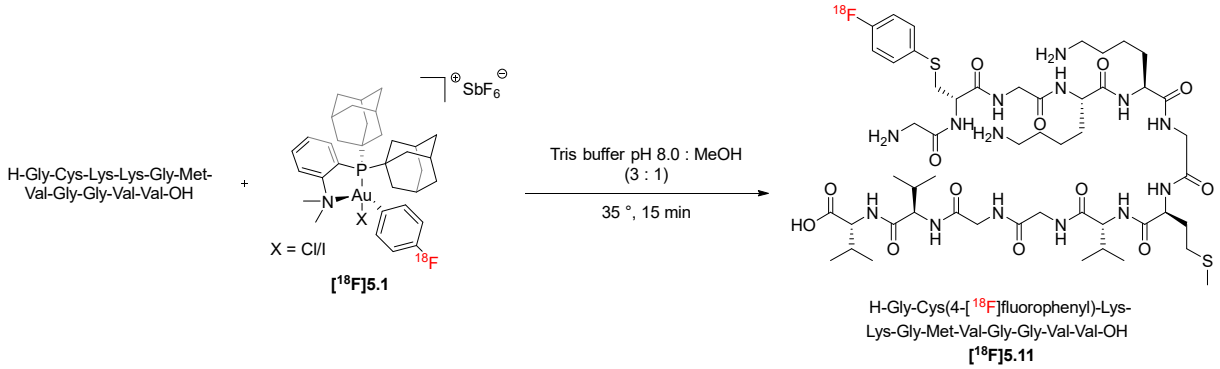

Table 5.16. Thiol arylation to generate ^{18}F-labeled amyloid β fragment **[^{18}F]5.11**

Entry	Starting Activity (mCi)	Crude Product Activity (mCi)	RCP (%)	RCY (d.c.) (%)
1	1.117	1.028 (1.02 d.c.)	85	84
2	1.687	1.517 (1.53 d.c.)	72	69
Mean ± SD			***79 ± 9***	***77 ± 10***

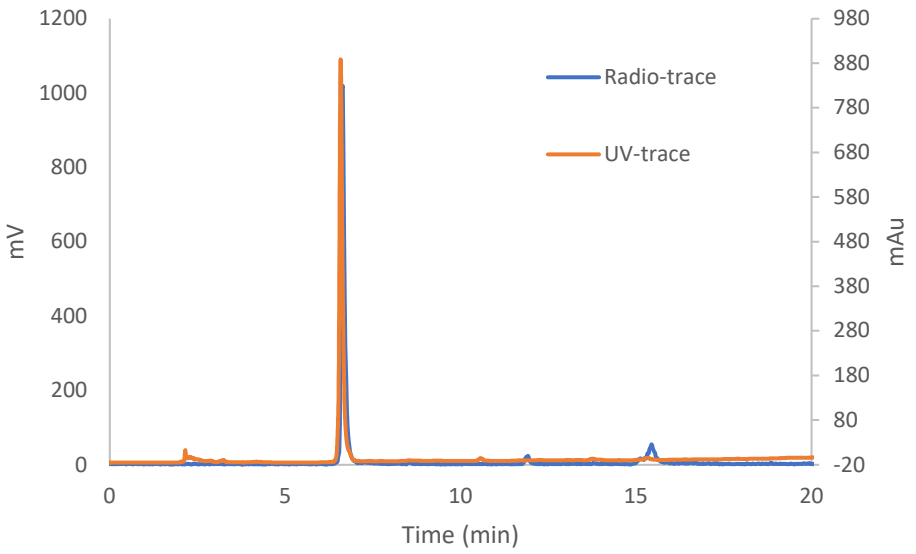

Figure 5.18. Analytical HPLC trace. Coinjection of crude **[^{18}F]5.11** (radio-HPLC trace = blue) with the purified ^{19}F reference standard (UV trace = orange).

β-D-Glucose *S*-(4-[^{18}F]fluorophenyl) ([^{18}F]5.12)

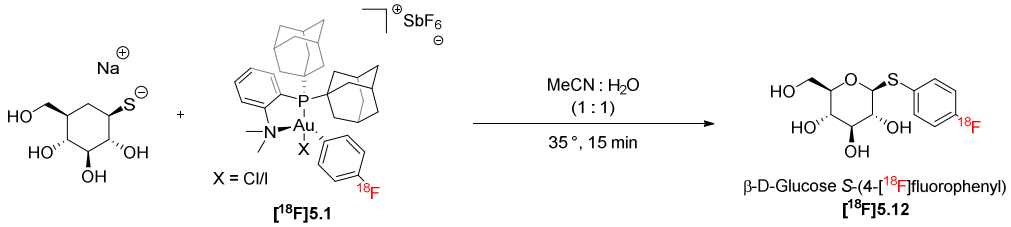

Table 5.17. Thiol arylation to generate β-D-Glucose S-(4-[^{18}F]fluorophenyl) **[^{18}F]5.12**[a]

Entry	Starting Activity (mCi)	Crude Product Activity (mCi)	RCP (%)	RCY (d.c.) (%)
1	1.616	1.409 (1.61 d.c.)	88	88
2	0.860	0.758 (0.85 d.c.)	99	98
Mean ± SD			***94 ± 8***	***93 ± 8***

[a]Reaction conditions: Na[1-thio-β-D-glucose] (5 mg), MeCN (500 µL), water (500 µL), 35 °C, 15 min

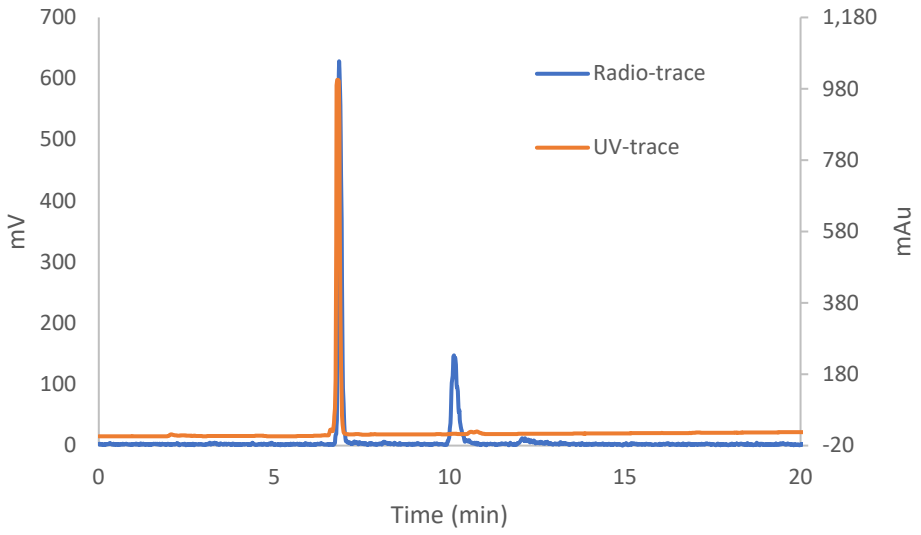

Figure 5.19. Analytical HPLC trace. Coinjection of crude **[^{18}F]5.12** (radio-HPLC trace = blue) with the purified ^{19}F reference standard (UV trace = orange)

β-D-Galactose *S*-(4-[^{18}F]fluorophenyl) ([^{18}F]5.13)

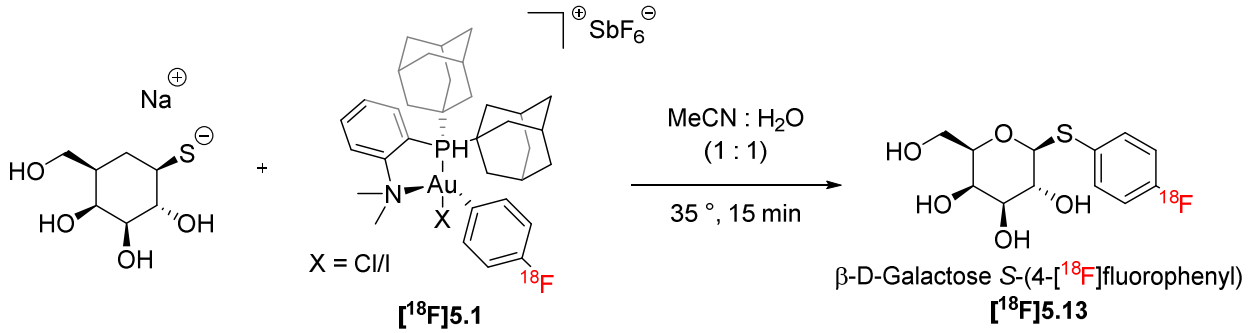

Table 5.18. Thiol arylation to generate β-D-Galactose S-(4-[^{18}F]fluorophenyl) **[^{18}F]5.13**[a]

Entry	Starting Activity (mCi)	Crude Product Activity (mCi)	RCP (%)	RCY (d.c.) (%)
1	1.052	0.936 (1.04 d.c.)	81	80
2	0.956	0.855 (0.95 d.c.)	96	96
Mean ± SD			***89 ± 11***	***88 ± 11***

[a]Reaction conditions: Na[1-thio-β-D-galactose] (5 mg), MeCN (500 µL), water (500 µL), 35 °C, 15 min

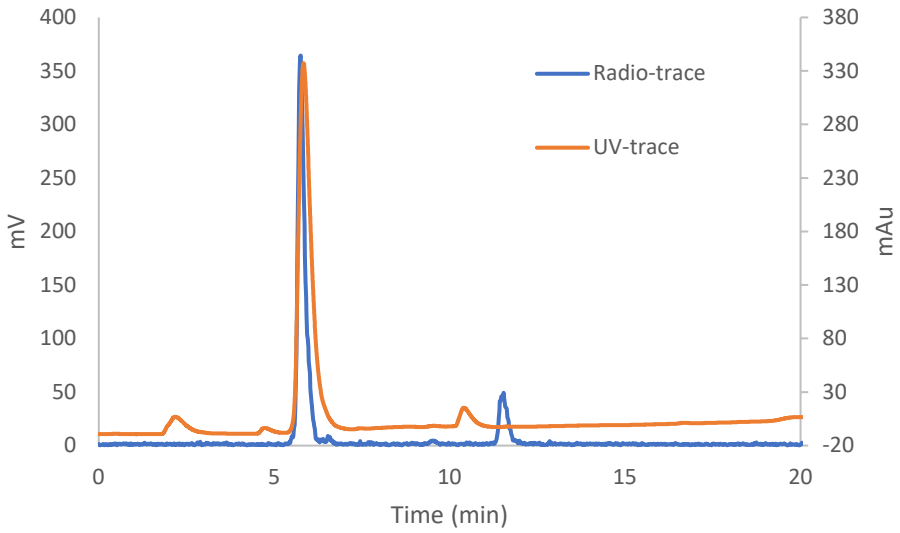

Figure 5.20. Analytical HPLC trace. Coinjection of crude **[^{18}F]5.13** (radio-HPLC trace = blue) with the purified ^{19}F reference standard (UV trace = orange).

Mono-(6-*S*-(4-[^{18}F]fluorophenyl)-6-deoxy)-β-cyclodextrin ([^{18}F]5.14)

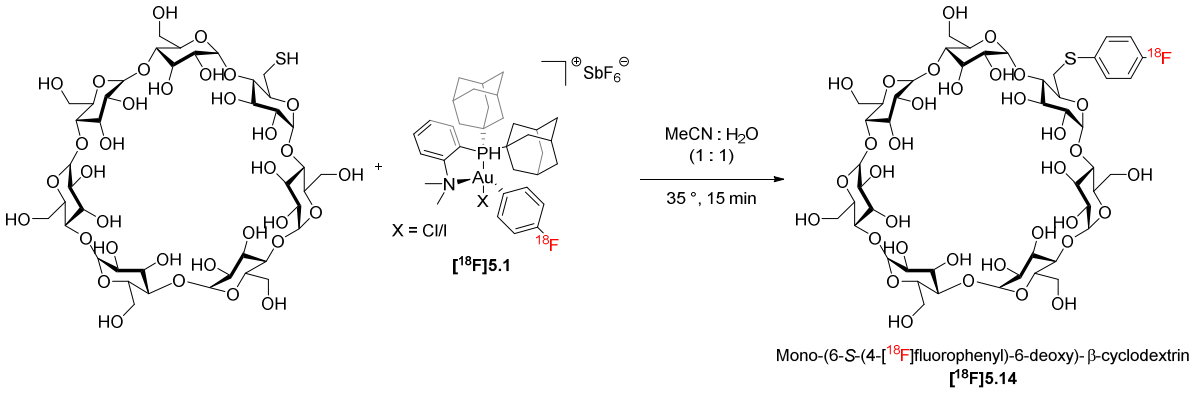

Table 5.19. Thiol arylation to generate the cyclodextrin analogue **[^{18}F]5.14**[a]

Entry	Starting Activity (mCi)	Crude Product Activity (mCi)	RCP (%)	RCY (d.c.) (%)
1	2.09	1.86 (2.04 d.c.)	95	93
2	1.522	1.333 (1.47 d.c.)	89	86
Mean ± SD			***92 ± 4***	***90 ± 5***

[a]Reaction conditions: mono-(6-mercapto-6-deoxy)-β-cyclodextrin (5 mg), MeCN (500 µL), water (500 µL), 35 °C, 15 min

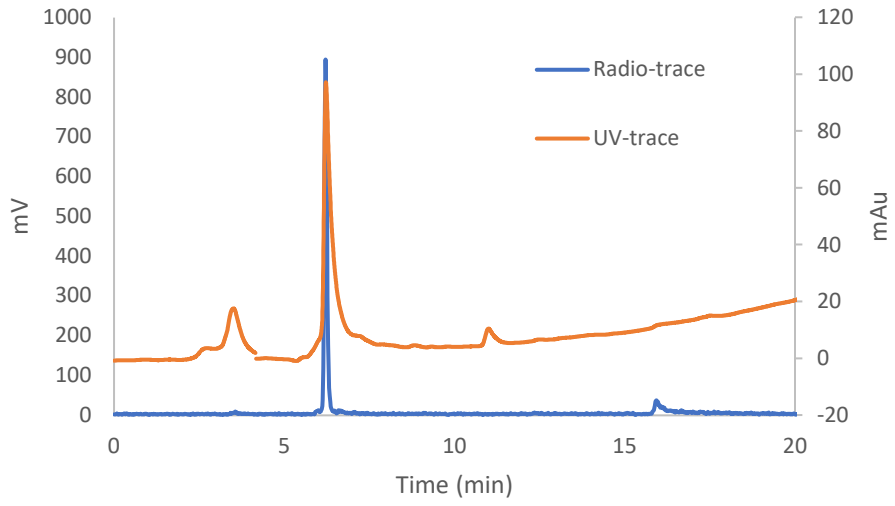

Figure 5.21. Analytical HPLC trace. Coinjection of crude ^{18}F-lableled cyclodextrin **[^{18}F]5.14** (radio-HPLC trace = blue) with the purified ^{19}F reference standard (UV trace = orange)

5.5.6. Molar Activity

A calibration curve was generated from the authentic L-glutathione S-(4-fluorophenyl) **7** reference standard, by measuring the integration of the UV absorbance signal at 254 nm for four different concentrations (***Figure 5.22***). To determine the molar activity of L-glutathione S-(4-[^{18}F]fluorophenyl) **[^{18}F]5.7**, an aliquot of HPLC-purified **[^{18}F]5.7** was injected into an analytical HPLC using Eluent D and the UV absorption corresponding to the radiolabeled product was measured (performed in duplicate). The mass amount of **[^{18}F]5.7** corresponding to the measured absorbance was calculated via linear regression analysis of the calibration curve. The molar activity of L-glutathione S-(4-[^{18}F]fluorophenyl) **[^{18}F]5.7** was determined to be 2.9 ± 1.8 Ci · μmol^{-1} (108 ± 68 GBq · μmol^{-1}).

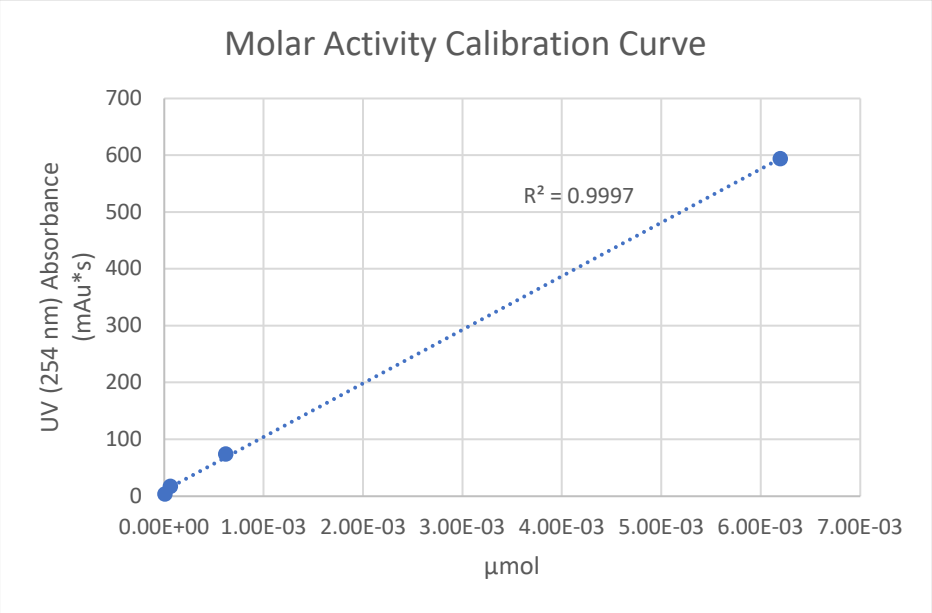

Figure 5.22. Calibration curve measuring the UV absorbance of different amounts of authentic reference standard L-glutathione S-(4-fluorophenyl) **5.7** for molar activity determination.

Table 5.20. Calibration curve data measuring the UV absorbance of different amounts of authentic reference standard L-glutathione S-(4-fluorophenyl) **5.7** for molar activity determination.

Volume Injected (µL)	**Concentration (M)**	**Moles Injected (µmol)**	**Absorbance (mAu*s)**	***Absorbance (mAu*s) Mean ±SD (Count)***
10	6.20E-04	6.20E-02	796.54	***594.29 ± 187.12 (n = 3)***
10	6.20E-04	6.20E-02	558.99	
10	6.20E-04	6.20E-02	427.33	
10	6.20E-05	6.20E-03	108.92	***74.11± 31.57 (n = 3)***
10	6.20E-05	6.20E-03	66.06	
10	6.20E-05	6.20E-03	47.34	
10	6.20E-06	6.20E-04	22.60	***17.00 ± 4.94 (n = 3)***
10	6.20E-06	6.20E-04	15.17	
10	6.20E-06	6.20E-04	13.23	
10	6.20E-07	6.20E-05	3.32	***3.46 ± 0.59 (n = 3)***
10	6.20E-07	6.20E-05	4.10	
10	6.20E-07	6.20E-05	3.00	

Table 5.21. Molar activity data of isolated L-glutathione S-(4-[^{18}F]fluorophenyl) **[^{18}F]5.7** (n=2).

Activity Injected (µCi)	**Absorbance (mAu*s)**	**Moles from Curve (µmol)**	**Molar Activity (Ci/µmol)**	**Molar Activity (GBq/µmol)**
680	105.91	1.02E-03	0.67*	24.68*
316	25.85	1.71E-04	1.84	68.22
320	15.17	5.83E-05	5.49	203.01
240	17.19	7.97E-05	3.01	111.37
72	14.97	5.62E-05	1.28	47.44
Mean ± SD			**2.9 ± 1.8**	**108 ± 68**

*This data point was collected with $AgSbF_6$ that was >6 months old; the data is left out of the mean calculation as we do not believe it accurately reflects the true molar activity due to degradation of the silver reagent. New $AgSbF_6$ was received and four additional runs were performed which are included in the table.

5.5.7. Determination of Residual Gold Content in the Purified Peptide [^{18}F]5.7

ICP-OES was used to measure the remaining gold content in the purified peptide **[^{18}F]5.7**. After isolation of **[^{18}F]5.7**, the purified peptide was allowed to fully decay in the hot cell for 24 h. A ~1 mL HPLC sample (n = 3) of purified peptide in H_2O was passed through a Millex-GV Filter, 0.22 µm in a 14 mL Falcon tube. The solution was then acidified with1 mL of HNO_3 (added via Eppendorf pipette) and then sonicated for 20 mins. The solution was diluted to a volume of 10 mL and, after mixing, was analyzed. FisherChemical Trace Metal Grade Nitric Acid was used, with a certified [Au] < 0.1 ppb. Samples were quantified using the gold emission of 242.79 nm. A 2 ppm Yttrium internal standard (371.03 nm) was run simultaneously with all samples. The residual gold content was determined to be 44 ± 7 ppb.

Gold ICP-OES analysis was conducted using an Agilent 5110 ICP-OES (inductively coupled plasma-optical emission spectrometer). Volumetric glassware (pipets and flasks) was used to create a dilution series of aqueous Au standards. A Sigma-Aldrich 1000 ppm (Lot value: 999 ppm ± 2 ppm, 5% w/w HCl) Gold Standard for ICP was used as a stock solution to create standards of concentrations 600, 300 and 50 ppb. The subsequent calibration curve was generated for each standard by integrating the signal corresponding to the characteristic Au emission (242.79 nm).

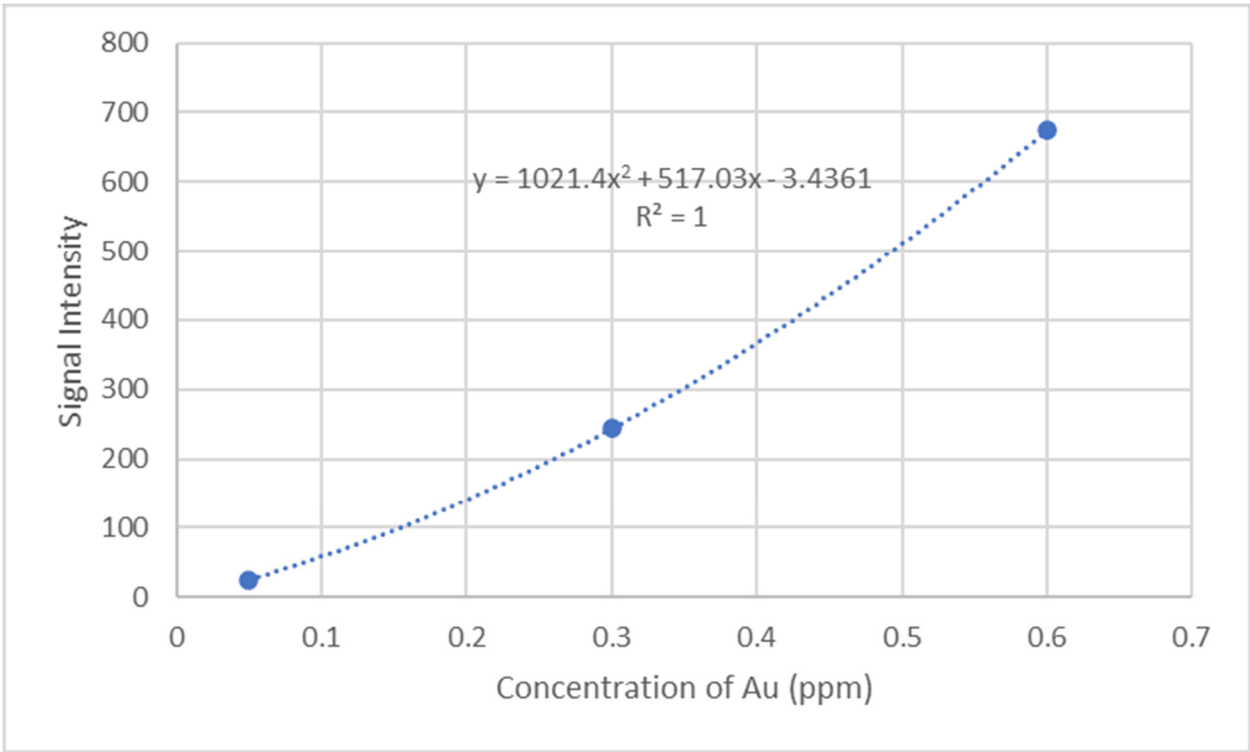

Figure 5.23. Calibration curve for residual gold determination.

5.6. Appendix

5.6.1. ^{1}H, ^{13}C, ^{19}F NMR Spectra

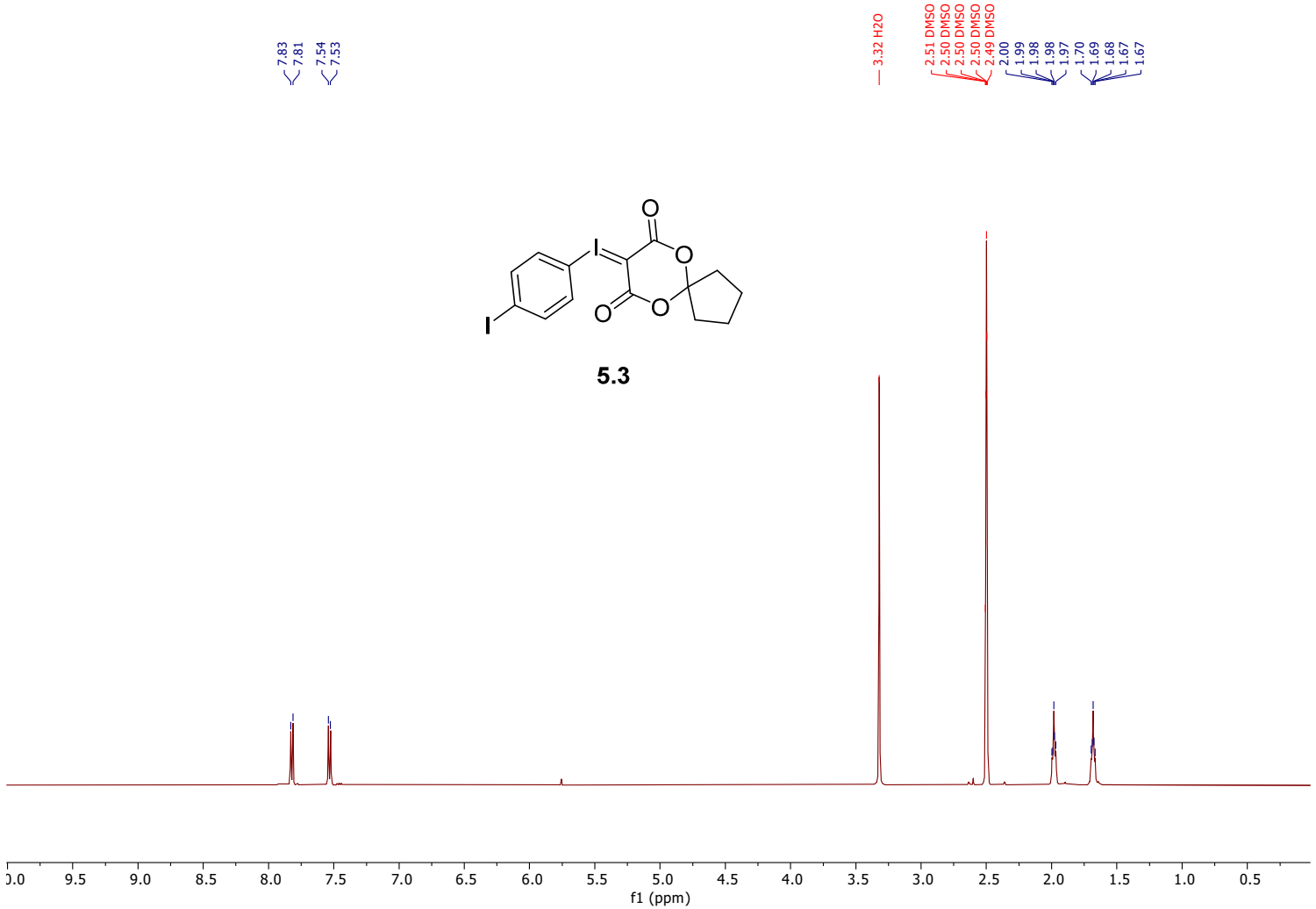

^{1}H NMR spectrum of Iodonium Ylide **5.3**. DMSO-d_6, 500 MHz, 25 °C.

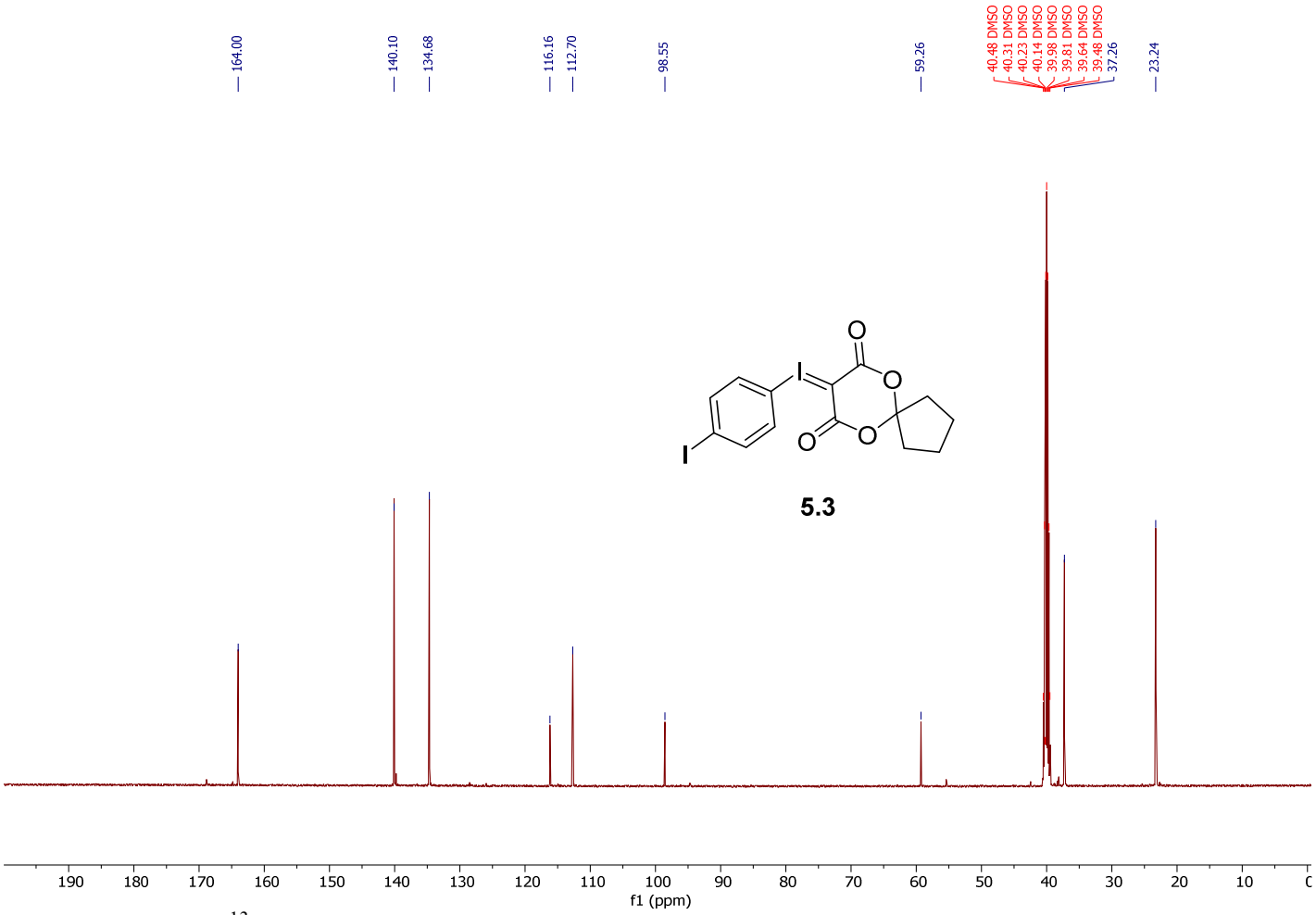

^{13}C NMR spectrum of Iodonium Ylide **5.3**. DMSO-d_6, 125 MHz, 25 °C.

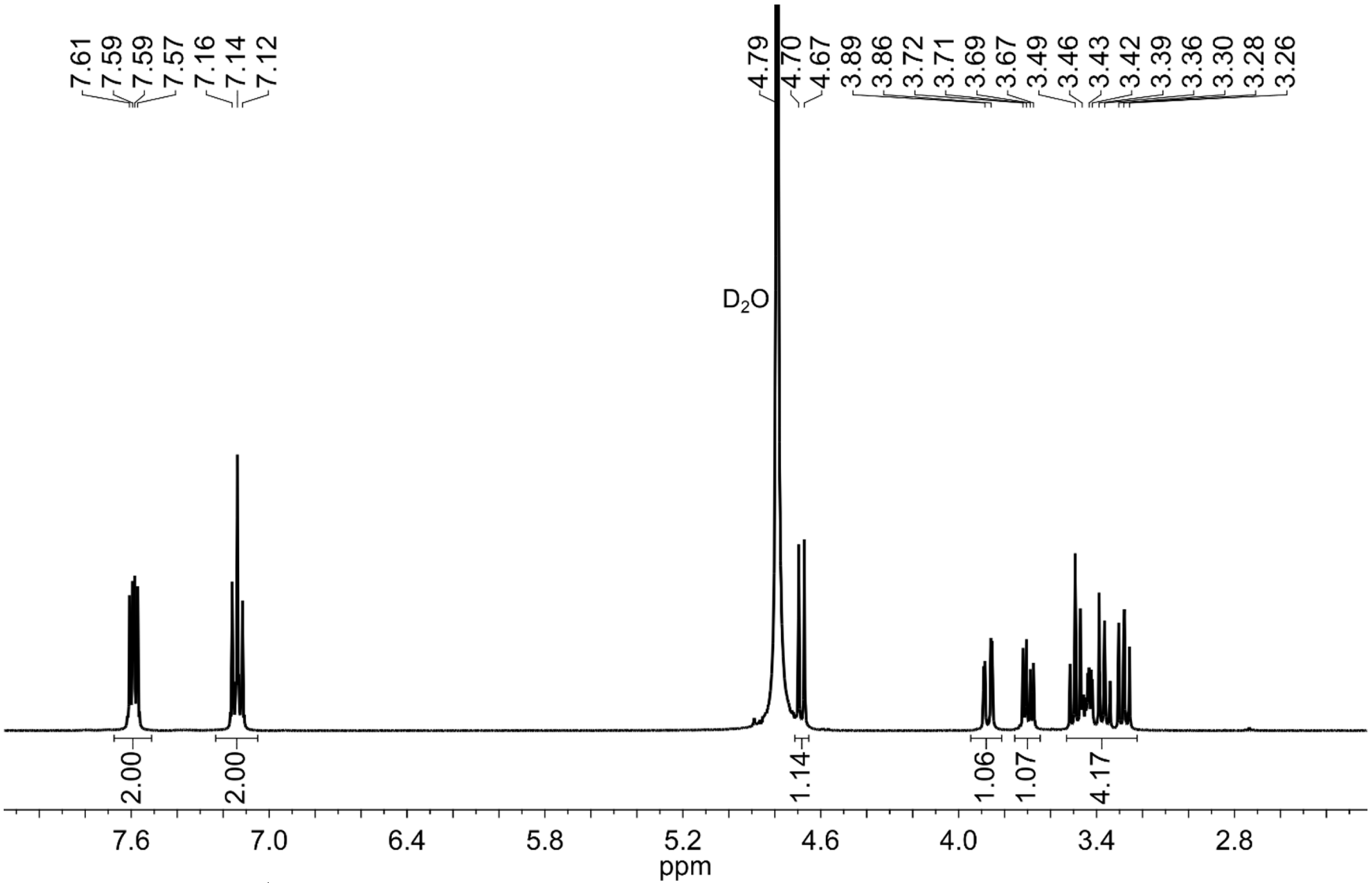

^{1}H NMR spectrum of β-D-Glucose *S*-(4-fluorophenyl) **5.12**. D_2O, 400 MHz, 25 °C.

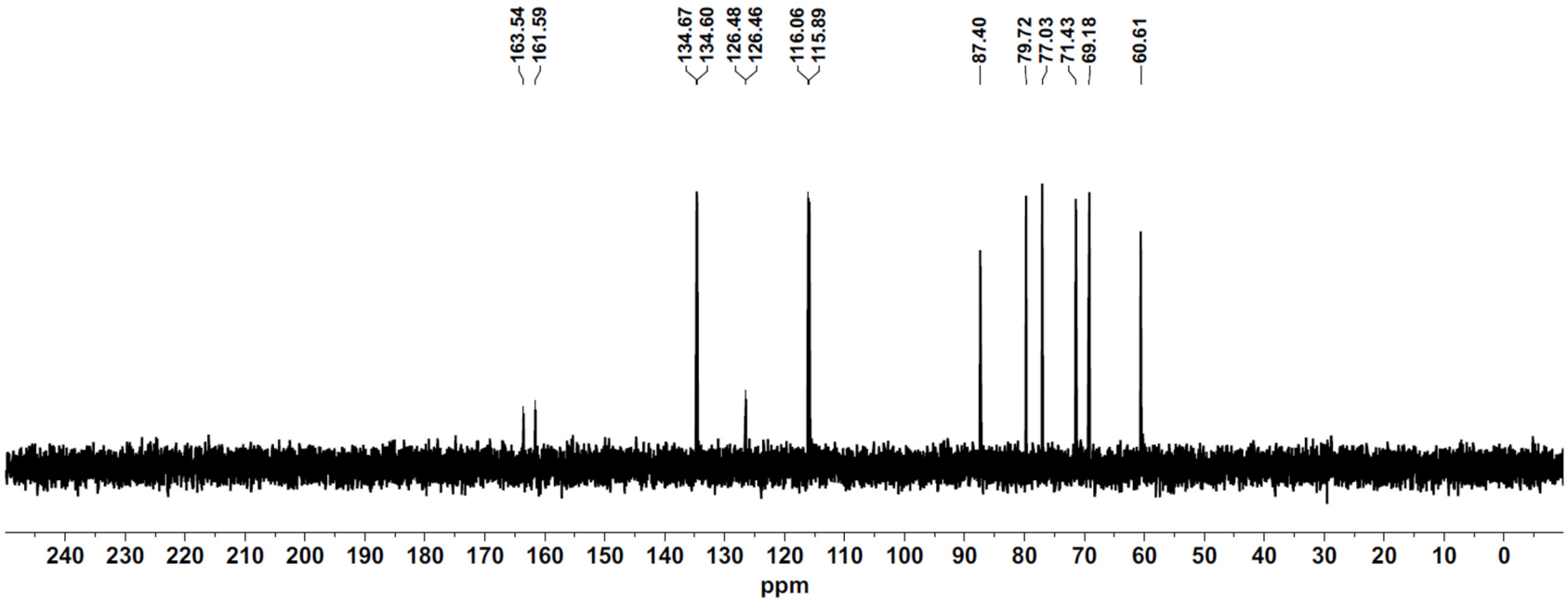

^{13}C NMR spectrum of β-D-Glucose *S*-(4-fluorophenyl) **5.12**. D_2O, 101 MHz, 25 °C.

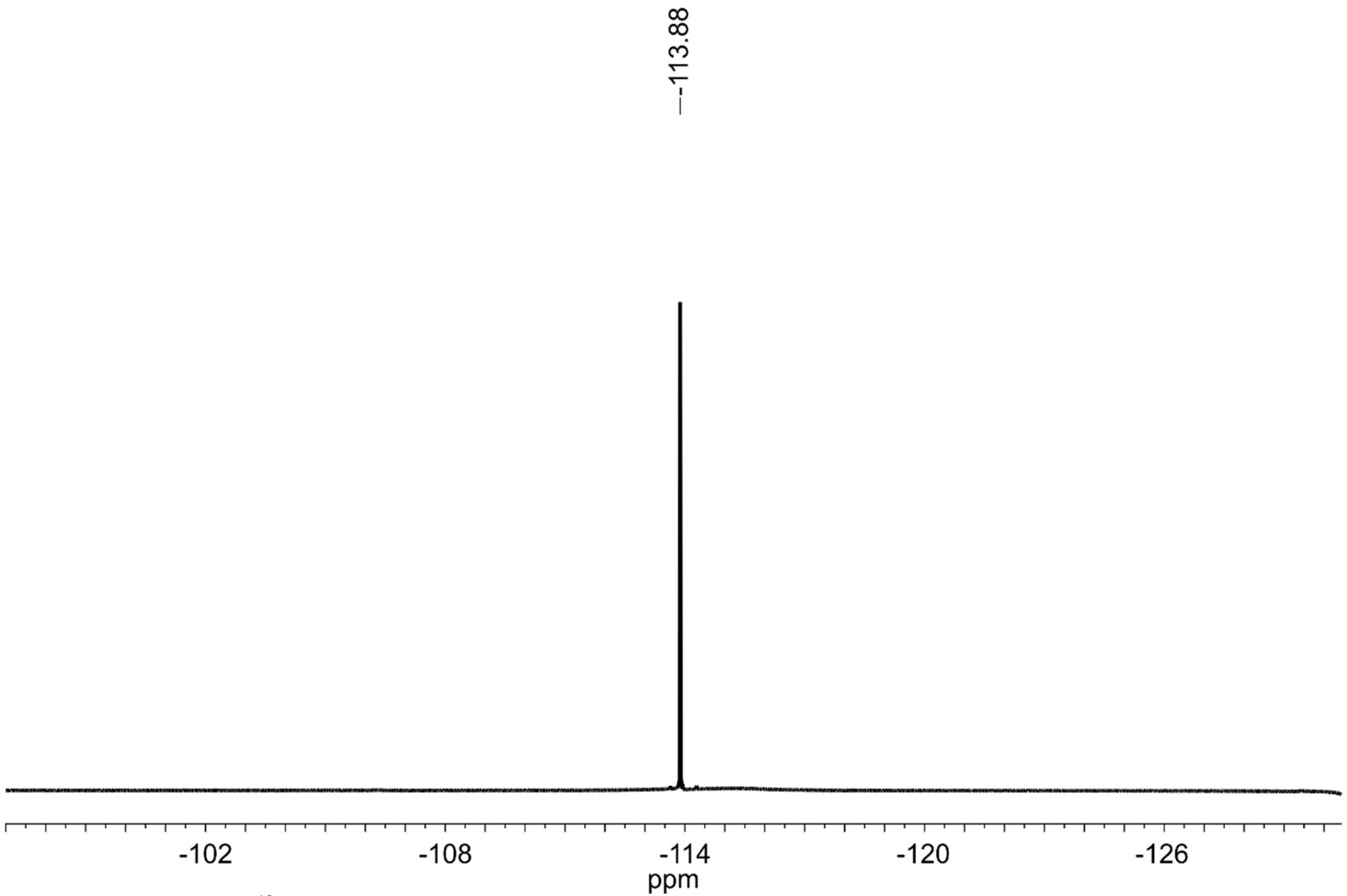

^{19}F-NMR spectrum of β-D-Glucose *S*-(4-fluorophenyl) **5.12**. D_2O, 376 MHz, 25 °C.

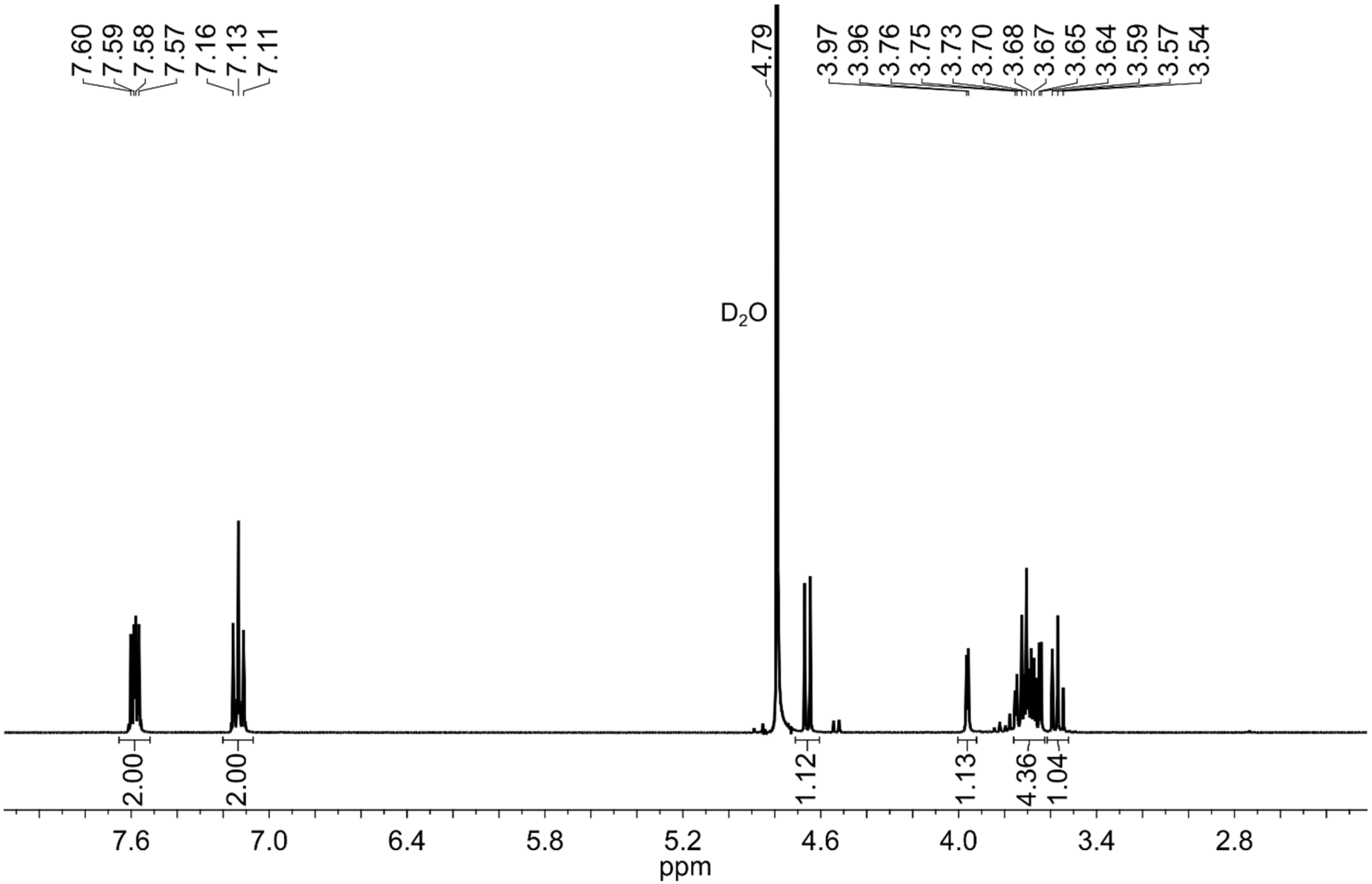

^{1}H NMR spectrum of β-D-Galactose *S*-(4-fluorophenyl) **5.13**. D_2O, 400 MHz, 25 °C.

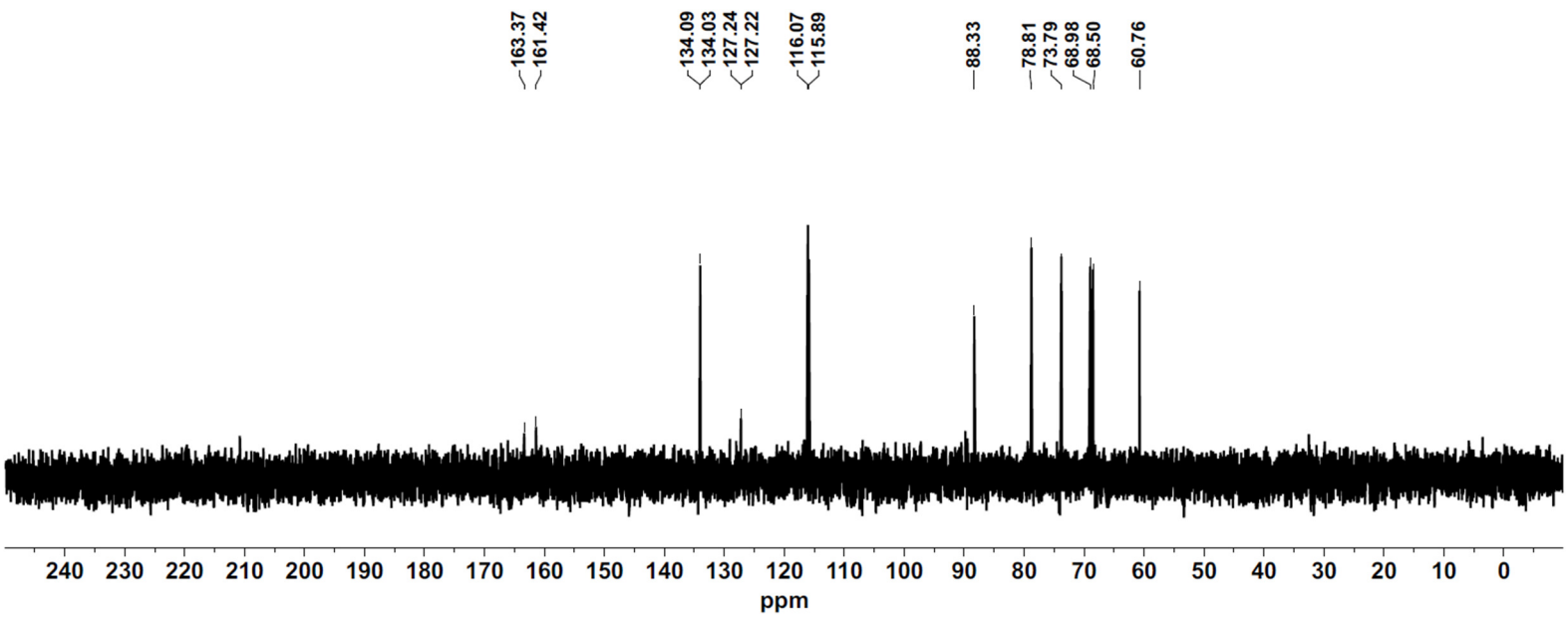

^{13}C NMR spectrum of β-D-Galactose *S*-(4-fluorophenyl) **5.13**. D_2O, 125 MHz, 25 °C.

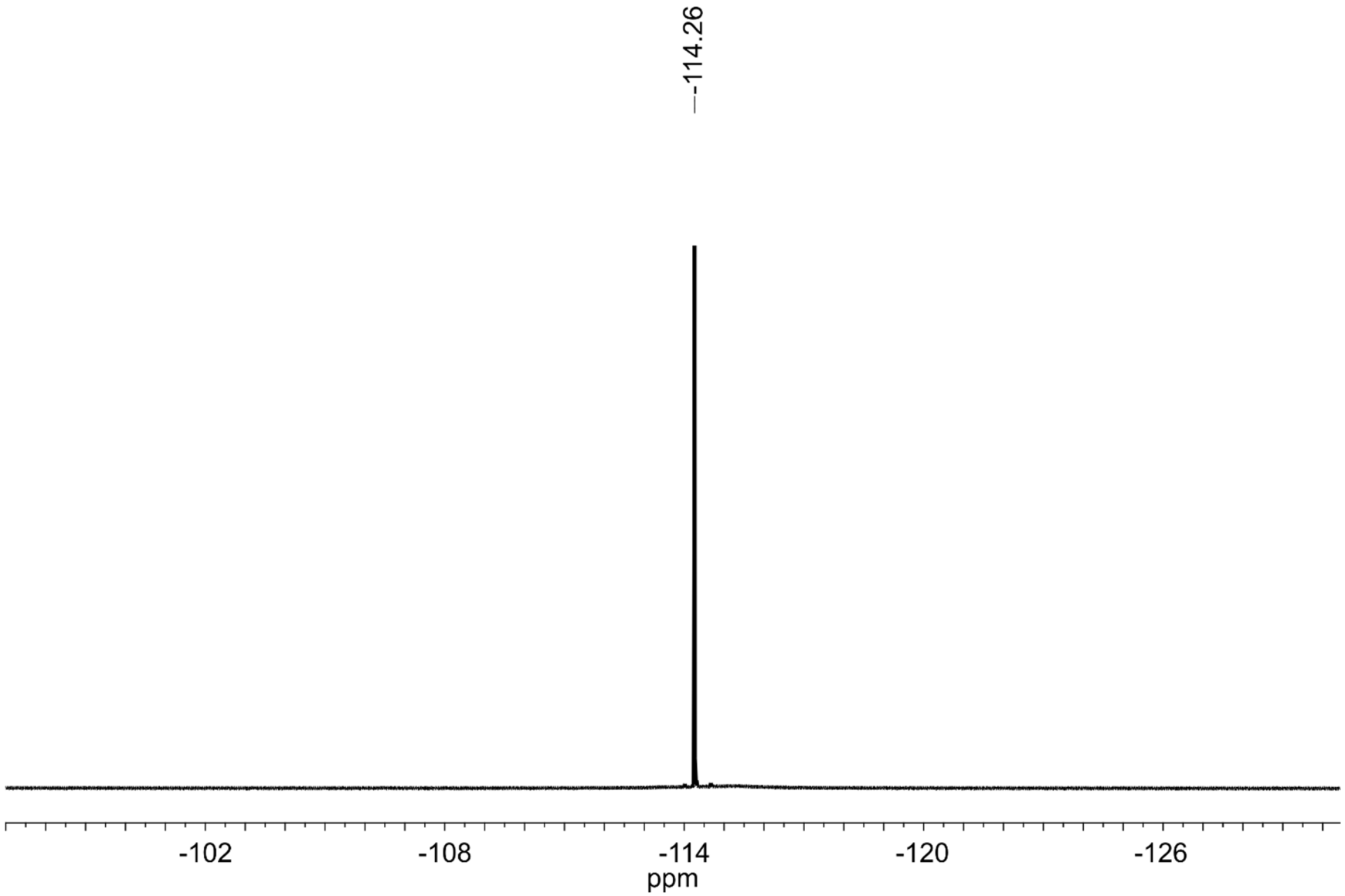

^{19}F NMR spectrum of β-D-Galactose *S*-(4-fluorophenyl) **5.13**. D_2O, 376 MHz, 25 °C.

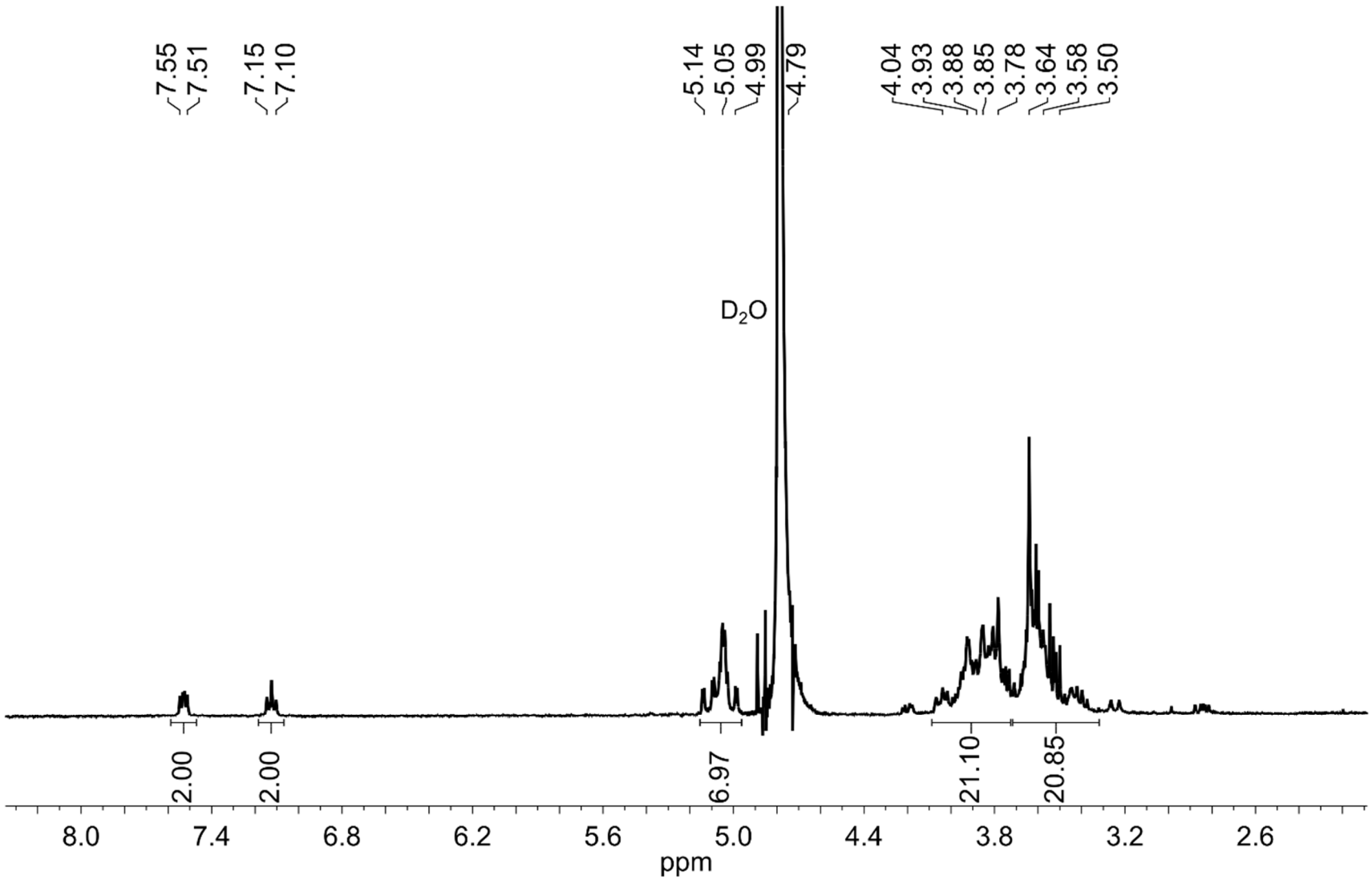

^{1}H NMR spectrum of mono-(6-*S*-(4-fluorophenyl)-6-deoxy)-β-cyclodextrin **5.14**. D_2O, 400 MHz, 25 °C.

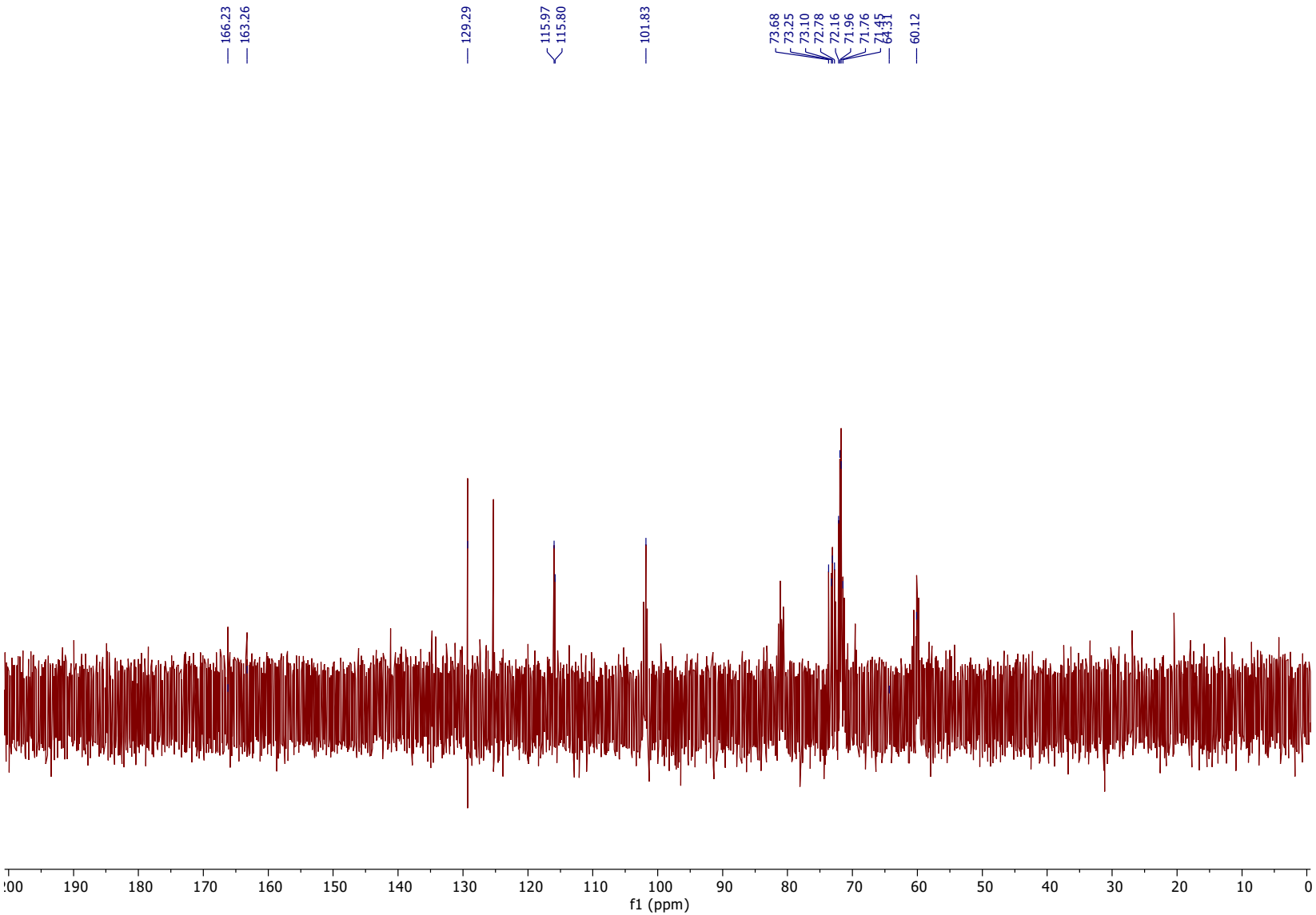

^{13}C NMR spectrum of mono-(6-*S*-(4-fluorophenyl)-6-deoxy)-β-cyclodextrin **5.14**. D_2O, 125 MHz, 25 °C.

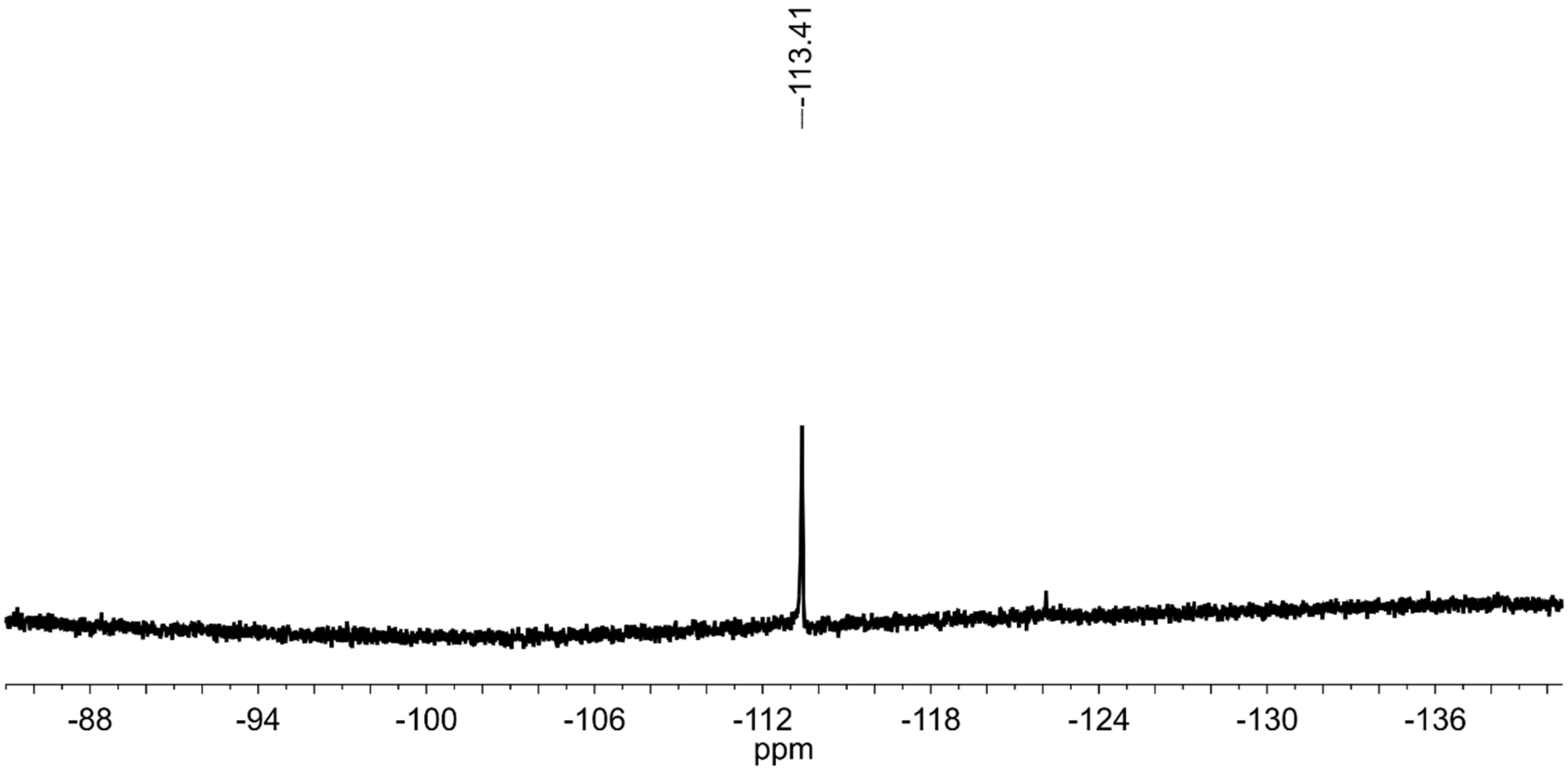

^{19}F NMR spectrum of mono-(6-*S*-(4-fluorophenyl)-6-deoxy)-β-cyclodextrin **5.14**. D_2O, 376 MHz, 25 °C.

5.7. Notes and References

1. Crabtree, R. H., In *The Organometallic Chemistry of the Transition Metals, 6th edn*, Wiley: 2014; pp i-xvi.

2. Diederich, F.; Stang, P. J., Metal-catalyzed cross-coupling reactions. Wiley & Sons: 2008.

3. Halder, R.; Ritter, T., ^{18}F-Fluorination: Challenge and Opportunity for Organic Chemists. *J. Org. Chem.* **2021,** *86* (20), 13873-13884.

4. Sanford, M. S.; Scott, P. J. H., Moving Metal-Mediated ^{18}F-Fluorination from Concept to Clinic. *ACS Central Science* **2016,** *2* (3), 128-130.

5. Brooks, A. F.; Topczewski, J. J.; Ichiishi, N.; Sanford, M. S.; Scott, P. J. H., Late-stage [^{18}F]fluorination: new solutions to old problems. *Chem. Sci.* **2014,** *5* (12), 4545-4553.

6. Brooks, A. F.; Topczewski, J. J.; Ichiishi, N.; Sanford, M. S.; Scott, P. J. H., Late-stage [^{18}F]fluorination: new solutions to old problems. *Chemical Science* **2014,** *5* (12), 4545-4553.

7. Lee, E.; Kamlet, A. S.; Powers, D. C.; Neumann, C. N.; Boursalian, G. B.; Furuya, T.; Choi, D. C.; Hooker, J. M.; Ritter, T., A Fluoride-Derived Electrophilic Late-Stage Fluorination Reagent for PET Imaging. *Science* **2011,** *334* (6056), 639-642.

8. Lee, E.; Hooker, J. M.; Ritter, T., Nickel-Mediated Oxidative Fluorination for PET with Aqueous [^{18}F] Fluoride. *Journal of the American Chemical Society* **2012,** *134* (42), 17456-17458.

9. Tredwell, M.; Preshlock, S. M.; Taylor, N. J.; Gruber, S.; Huiban, M.; Passchier, J.; Mercier, J.; Génicot, C.; Gouverneur, V., A General Copper-Mediated Nucleophilic ^{18}F-Fluorination of Arenes. *Angewandte Chemie International Edition* **2014,** *53* (30), 7751-7755.

10. Ichiishi, N.; Brooks, A. F.; Topczewski, J. J.; Rodnick, M. E.; Sanford, M. S.; Scott, P. J. H., Copper-Catalyzed [^{18}F]Fluorination of (Mesityl)(aryl)iodonium Salts. *Organic Letters* **2014,** *16* (12), 3224-3227.

11. Preshlock, S.; Calderwood, S.; Verhoog, S.; Tredwell, M.; Huiban, M.; Hienzsch, A.; Gruber, S.; Wilson, T. C.; Taylor, N. J.; Cailly, T.; Schedler, M.; Collier, T. L.; Passchier, J.; Smits, R.; Mollitor, J.; Hoepping, A.; Mueller, M.; Genicot, C.; Mercier, J.; Gouverneur, V., Enhanced copper-mediated 18F-fluorination of aryl boronic esters provides eight radiotracers for PET applications. *Chemical Communications* **2016,** *52* (54), 8361-8364.

12. Mossine, A. V.; Brooks, A. F.; Makaravage, K. J.; Miller, J. M.; Ichiishi, N.; Sanford, M. S.; Scott, P. J. H., Synthesis of [^{18}F]Arenes via the Copper-Mediated [^{18}F]Fluorination of Boronic Acids. *Organic Letters* **2015,** *17* (23), 5780-5783.

13. Neumann, C. N.; Hooker, J. M.; Ritter, T., Concerted nucleophilic aromatic substitution with ^{19}F− and ^{18}F−. *Nature* **2016,** *534* (7607), 369-373.

14. Beyzavi, M. H.; Mandal, D.; Strebl, M. G.; Neumann, C. N.; D'Amato, E. M.; Chen, J.; Hooker, J. M.; Ritter, T., ^{18}F-Deoxyfluorination of Phenols via Ru π-Complexes. *ACS Central Science* **2017,** *3* (9), 944-948.

15. McCammant, M. S.; Thompson, S.; Brooks, A. F.; Krska, S. W.; Scott, P. J. H.; Sanford, M. S., Cu-Mediated C–H ^{18}F-Fluorination of Electron-Rich (Hetero)arenes. *Organic Letters* **2017,** *19* (14), 3939-3942.

16. Huang, X.; Liu, W.; Ren, H.; Neelamegam, R.; Hooker, J. M.; Groves, J. T., Late Stage Benzylic C–H Fluorination with [^{18}F]Fluoride for PET Imaging. *Journal of the American Chemical Society* **2014,** *136* (19), 6842-6845.

17. Makaravage, K. J.; Brooks, A. F.; Mossine, A. V.; Sanford, M. S.; Scott, P. J. H., Copper-Mediated Radiofluorination of Arylstannanes with [^{18}F]KF. *Organic Letters* **2016,** *18* (20), 5440-5443.

18. Zhang, M.; Li, S.; Zhang, H.; Xu, H., Research progress of ^{18}F labeled small molecule positron emission tomography (PET) imaging agents. *Eur J Med Chem* **2020,** *205*, 112629.

19. Mossine, A. V.; Tanzey, S. S.; Brooks, A. F.; Makaravage, K. J.; Ichiishi, N.; Miller, J. M.; Henderson, B. D.; Skaddan, M. B.; Sanford, M. S.; Scott, P. J. H., One-pot synthesis of high molar activity 6-[^{18}F]fluoro-l-DOPA by Cu-mediated fluorination of a BPin precursor. *Organic & Biomolecular Chemistry* **2019,** *17* (38), 8701-8705.

20. Wright, J. S.; Kaur, T.; Preshlock, S.; Tanzey, S. S.; Winton, W. P.; Sharninghausen, L. S.; Wiesner, N.; Brooks, A. F.; Sanford, M. S.; Scott, P. J. H., Copper-mediated late-stage radiofluorination: five years of impact on preclinical and clinical PET imaging. *Clinical and Translational Imaging* **2020,** *8* (3), 167-206.

21. Gao, Z.; Gouverneur, V.; Davis, B. G., Enhanced Aqueous Suzuki–Miyaura Coupling Allows Site-Specific Polypeptide 18F-Labeling. *Journal of the American Chemical Society* **2013,** *135* (37), 13612-13615.

22. Way, J. D.; Bergman, C.; Wuest, F., Sonogashira cross-coupling reaction with 4-[^{18}F]fluoroiodobenzene for rapid 18F-labelling of peptides. *Chemical Communications* **2015,** *51* (18), 3838-3841.

23. Gray, E. E.; Nielsen, M. K.; Choquette, K. A.; Kalow, J. A.; Graham, T. J. A.; Doyle, A. G., Nucleophilic (Radio)Fluorination of α-Diazocarbonyl Compounds Enabled by Copper-Catalyzed H–F Insertion. *Journal of the American Chemical Society* **2016,** *138* (34), 10802-10805.

24. Yuan, Z.; Nodwell, M. B.; Yang, H.; Malik, N.; Merkens, H.; Bénard, F.; Martin, R. E.; Schaffer, P.; Britton, R., Site-Selective, Late-Stage C−H ^{18}F-Fluorination on Unprotected Peptides for Positron Emission Tomography Imaging. *Angewandte Chemie International Edition* **2018,** *57* (39), 12733-12736.

25. Verhoog, S.; Kee, C. W.; Wang, Y.; Khotavivattana, T.; Wilson, T. C.; Kersemans, V.; Smart, S.; Tredwell, M.; Davis, B. G.; Gouverneur, V., 18F-Trifluoromethylation of Unmodified Peptides with 5-^{18}F-(Trifluoromethyl)dibenzothiophenium Trifluoromethanesulfonate. *J. Am. Chem. Soc.* **2018,** *140* (5), 1572-1575.

26. Rickmeier, J.; Ritter, T., Site-Specific Deoxyfluorination of Small Peptides with [^{18}F]Fluoride. *Angewandte Chemie International Edition* **2018,** *57* (43), 14207-14211.

27. Kee, C. W.; Tack, O.; Guibbal, F.; Wilson, T. C.; Isenegger, P. G.; Imiołek, M.; Verhoog, S.; Tilby, M.; Boscutti, G.; Ashworth, S.; Chupin, J.; Kashani, R.; Poh, A. W. J.; Sosabowski, J. K.; Macholl, S.; Plisson, C.; Cornelissen, B.; Willis, M. C.; Passchier, J.; Davis, B. G.; Gouverneur, V., 18F-Trifluoromethanesulfinate Enables Direct C–H ^{18}F-Trifluoromethylation of Native Aromatic Residues in Peptides. *Journal of the American Chemical Society* **2020,** *142* (3), 1180-1185.

28. Humpert, S.; Omrane, M. A.; Urusova, E. A.; Gremer, L.; Willbold, D.; Endepols, H.; Krasikova, R. N.; Neumaier, B.; Zlatopolskiy, B. D., Rapid ^{18}F-labeling via Pd-catalyzed S-arylation in aqueous medium. *Chemical Communications* **2021,** *57* (29), 3547-3550.

29. Koniev, O.; Wagner, A., Developments and recent advancements in the field of endogenous amino acid selective bond forming reactions for bioconjugation. *Chemical Society Reviews* **2015,** *44* (15), 5495-5551.

30. Krishnan, H. S.; Ma, L.; Vasdev, N.; Liang, S. H., ^{18}F-Labeling of Sensitive Biomolecules for Positron Emission Tomography. *Chemistry – A European Journal* **2017,** *23* (62), 15553-15577.

31. Vinogradova, E. V.; Zhang, C.; Spokoyny, A. M.; Pentelute, B. L.; Buchwald, S. L., Organometallic palladium reagents for cysteine bioconjugation. *Nature* **2015,** *526* (7575), 687-691.

32. Rojas, A. J.; Pentelute, B. L.; Buchwald, S. L., Water-Soluble Palladium Reagents for Cysteine S-Arylation under Ambient Aqueous Conditions. *Org Lett* **2017,** *19* (16), 4263-4266.

33. Rojas, A. J.; Zhang, C.; Vinogradova, E. V.; Buchwald, N. H.; Reilly, J.; Pentelute, B. L.; Buchwald, S. L., Divergent unprotected peptide macrocyclisation by palladium-mediated cysteine arylation. *Chem Sci* **2017,** *8* (6), 4257-4263.

34. Zhao, W.; Lee, H. G.; Buchwald, S. L.; Hooker, J. M., Direct 11CN-Labeling of Unprotected Peptides via Palladium-Mediated Sequential Cross-Coupling Reactions. *J. Am. Chem. Soc.* **2017,** *139* (21), 7152-7155.

35. Messina, M. S.; Stauber, J. M.; Waddington, M. A.; Rheingold, A. L.; Maynard, H. D.; Spokoyny, A. M., Organometallic Gold(III) Reagents for Cysteine Arylation. *Journal of the American Chemical Society* **2018,** *140* (23), 7065-7069.

36. Stauber, J. M.; Qian, E. A.; Han, Y.; Rheingold, A. L.; Král, P.; Fujita, D.; Spokoyny, A. M., An Organometallic Strategy for Assembling Atomically Precise Hybrid Nanomaterials. *Journal of the American Chemical Society* **2020,** *142* (1), 327-334.

37. Stauber, J. M.; Rheingold, A. L.; Spokoyny, A. M., Gold(III) Aryl Complexes as Reagents for Constructing Hybrid Peptide-Based Assemblies via Cysteine S-Arylation. *Inorg Chem* **2021,** *60* (7), 5054-5062.

38. Zeineddine, A.; Estévez, L.; Mallet-Ladeira, S.; Miqueu, K.; Amgoune, A.; Bourissou, D., Rational development of catalytic Au(I)/Au(III) arylation involving mild oxidative addition of aryl halides. *Nature Communications* **2017,** *8* (1), 565.

39. Way, J. D.; Wuest, F., Automated radiosynthesis of no-carrier-added 4-[^{18}F]fluoroiodobenzene: a versatile building block in ^{18}F radiochemistry. *Journal of Labelled Compounds and Radiopharmaceuticals* **2014,** *57* (2), 104-109.

40. Huang, B.; Hu, M.; Toste, F. D., Homogeneous Gold Redox Chemistry: Organometallics, Catalysis, and Beyond. *Trends in Chemistry* **2020,** *2* (8), 707-720.

41. Rotstein, B. H.; Stephenson, N. A.; Vasdev, N.; Liang, S. H., Spirocyclic hypervalent iodine(III)-mediated radiofluorination of non-activated and hindered aromatics. *Nature Communications* **2014,** *5*, 4365.

42. Rotstein, B. H.; Wang, L.; Liu, R. Y.; Patteson, J.; Kwan, E. E.; Vasdev, N.; Liang, S. H., Mechanistic Studies and Radiofluorination of Structurally Diverse Pharmaceuticals with Spirocyclic Iodonium(III) Ylides. *Chemical science* **2016,** *7* (7), 4407-4417.

43. Koser, G. F.; Wettach, R. H., [Hydroxy(tosyloxy)iodo]benzene, a versatile reagent for the mild oxidation of aryl iodides at the iodine atom by ligand transfer. *The Journal of Organic Chemistry* **1980,** *45* (8), 1542-1543.

44. Jiang, J.; Zeng, W., Synthesis and Crystal Structures of Two New Oxaspirocyclic Compounds. *Crystals* **2016,** *6* (10), 134.

45. Ma, G.; McDaniel, J. W.; Murphy, J. M., One-Step Synthesis of [^{18}F]Fluoro-4-(vinylsulfonyl)benzene: A Thiol Reactive Synthon for Selective Radiofluorination of Peptides. *Org. Lett.* **2021,** *23* (2), 530-534.

46. Chen, H.; Niu, G.; Wu, H.; Chen, X., Clinical Application of Radiolabeled RGD Peptides for PET Imaging of Integrin αvβ3. *Theranostics* **2016,** *6*, 78-92.

47. Chin, F. T.; Shen, B.; Liu, S.; Berganos, R. A.; Chang, E.; Mittra, E.; Chen, X.; Gambhir, S. S., First Experience with Clinical-Grade [^{18}F]FPP(RGD)$_2$: An Automated Multi-step Radiosynthesis for Clinical PET Studies. *Molecular Imaging and Biology* **2012,** *14* (1), 88-95.

48. Vandenberghe, R.; Adamczuk, K.; Dupont, P.; Laere, K. V.; Chételat, G., Amyloid PET in clinical practice: Its place in the multidimensional space of Alzheimer's disease. *NeuroImage: Clinical* **2013,** *2*, 497-511.

49. Lai, W.-F.; Rogach, A. L.; Wong, W.-T., Chemistry and engineering of cyclodextrins for molecular imaging. *Chemical Society Reviews* **2017,** *46* (20), 6379-6419.

50. Shepelytskyi, Y.; Newman, C. J.; Grynko, V.; Seveney, L. E.; DeBoef, B.; Hane, F. T.; Albert, M. S., Cyclodextrin-Based Contrast Agents for Medical Imaging. *Molecules* **2020,** *25* (23), 5576.

51. Bartlett, D. W.; Su, H.; Hildebrandt, I. J.; Weber, W. A.; Davis, M. E., Impact of tumor-specific targeting on the biodistribution and efficacy of siRNA nanoparticles measured by multimodality *in vivo* imaging. *Proceedings of the National Academy of Sciences* **2007,** *104* (39), 15549-15554.

52. Schluep, T.; Hwang, J.; Hildebrandt, I. J.; Czernin, J.; Choi, C. H. J.; Alabi, C. A.; Mack, B. C.; Davis, M. E., Pharmacokinetics and tumor dynamics of the nanoparticle IT-101 from PET imaging and tumor histological measurements. *Proceedings of the National Academy of Sciences* **2009,** *106* (27), 11394-11399.

53. For guidelines of residual metal contents, see: http://www.ema.europa.eu/docs/en_GB/document_library/Scientific_guideline/2009/09/WC500003587.pdf.